THERMAL TREATMENT APPROACH IN IMMOBILIZING SILVER NANOPARTICLES INTO POLYVINYLIDENE FLUORIDE MEMBRANES FOR BIOFOULING MITIGATION DURING WATER TREATMENT

NUR DIYANA AQILAH BINTI KAMARUDIN

FACULTY OF ENGINEERING
UNIVERSITY OF MALAYA
KUALA LUMPUR

2022

THERMAL TREATMENT APPROACH IN IMMOBILIZING SILVER NANOPARTICLES INTO POLYVINYLIDENE FLUORIDE MEMBRANES FOR BIOFOULING MITIGATION DURING WATER TREATMENT

NUR DIYANA AQILAH BINTI KAMARUDIN

THESIS SUBMITTED IN FULFILMENT OF THE REQUIREMENTS FOR THE DEGREE OF DOCTOR OF PHILOSOPHY (PHD)

FACULTY OF ENGINEERING
UNIVERSITY OF MALAYA
KUALA LUMPUR

2022

UNIVERSITY OF MALAYA

ORIGINAL LITERARY WORK DECLARATION

Name of Candidate: NUR DIYANA AQILAH BINTI KAMARUDIN

Registration/Matric No: 17057882/1 / KHA160034

Name of Degree: DOCTOR OF PHILOSOPHY

Title of Project Paper/Research Report/Dissertation/Thesis: THERMAL TREATMENT APPROACH IN IMMOBILIZING SILVER NANOPARTICLES INTO POLYVINYLIDENE FLUORIDE MEMBRANES FOR BIOFOULING MITIGATION DURING WATER TREATMENT

Field of Study: PURIFICATION & SEPARATION PROCESSES

I do solemnly and sincerely declare that:

(1) I am the sole author/writer of this Work;
(2) This Work is original;
(3) Any use of any work in which copyright exists was done by way of fair dealing and for permitted purposes and any excerpt or extract from, or reference to or reproduction of any copyright work has been disclosed expressly and sufficiently and the title of the Work and its authorship have been acknowledged in this Work;
(4) I do not have any actual knowledge nor do I ought reasonably to know that the making of this work constitutes an infringement of any copyright work;
(5) I hereby assign all and every rights in the copyright to this Work to the University of Malaya ("UM"), who henceforth shall be owner of the copyright in this Work and that any reproduction or use in any form or by any means whatsoever is prohibited without the written consent of UM having been first had and obtained;
(6) I am fully aware that if in the course of making this Work I have infringed any copyright whether intentionally or otherwise, I may be subject to legal action or any other action as may be determined by UM.

Candidate's Signature Date:

Subscribed and solemnly declared before,

Witness's Signature Date:

Name:

Designation:

THERMAL TREATMENT APPROACH IN IMMOBILIZING SILVER NANOPARTICLES INTO POLYVINYLIDENE FLUORIDE MEMBRANES FOR BIOFOULING MITIGATION DURING WATER TREATMENT

ABSTRACT

Impregnation of the noble metal, silver nanoparticles (AgNPs) as a disinfectant into the polymeric membrane is one of the empirical modification methods for producing safe drinking water. However, the dispersion and immobilization of AgNPs during membrane fabrication and application are least discussed despite numerous leaching phenomena reported. Moreover, the synthesis method and parameter are crucial factors in determining nanoparticles formation and nucleation process. Additionally, analysis of membrane fouling despite the mitigation approach is vital for an explicit understanding of fouling occurrence. This study presents the effects of precursor concentration and synthesis temperature on AgNPs formation in two distinctive methods. Silver nanoparticles type 1 (AgNPs-1) and type 2 (AgNPs-2) were prepared and incorporated into polyvinylidene fluoride (PVDF) ultrafiltration membranes with the presence of thermal treatment. The effect of thermal treatment was studied at temperatures 25, 40, and 55°C which significantly influenced the physicochemical characteristics of the PVDF membranes. During filtration using lake water as feed, flux decay rate (FDR), and fouling recovery ratio (FRR) analysis of clean and fouled membranes have implied membrane fouling phenomena. Alternatively, the AgNPs incorporated in PVDF membranes were utilized for surface-enhanced Raman spectroscopy (SERS) as an unconventional approach of built-in surface enhance substrate whilst thermogravimetric analysis (TGA)

was employed to quantify foulant as an approach to evaluate the performance of AgNPs. The results have shown a significant variation of AgNPs-1 and AgNPs-2 synthesized with different synthesis parameters for both methods. With respect to particles size determined using a particle size analyzer, the best synthesis condition for AgNPs-1 was at 25°C using 0.255 g $AgNO^3$ while on the other hand the best synthesis condition for AgNPs-2 was at 75°C using 0.03 mol/L $AgNO^3$. Membranes incorporated with selected AgNPs-1 and AgNPs-2, fabricated at the highest temperature portrayed improved mechanical properties and pure water flux. PVDF/PVP/AgNPs-2 membrane released the smallest amount of Ag (3.81%) while PVDF/PVP/AgNPs-1 cast at 40°C released the largest amount of Ag (42.34%) during the phase inversion at fabrication. Notably, no Ag leaching was found in all membranes during the dead-end filtration at 0.5 bar. Membranes with AgNPs-1 and AgNPs-2 showed remarkable bactericidal performance towards *E. coli* with a percentage reduction of 90.38% and 80.77%, respectively. Thus, membranes with AgNPs fabricated at 55°C offered better mechanical properties of the enhanced permeability and excellent stability of AgNPs immobilization which signified the thermal treatment approach. Remarkably, small significant peaks representing biofoulant presence were obtained from normal Raman while total foulant weight indicated reductions of 82.69% and 75.86% with the presence of AgNPs-1 and AgNPs-2, respectively. Hence, the unconventional approach in fouling analysis for AgNPs in PVDF membrane has potentially been earmarked for surface enhancement in normal Raman analysis while foulant quantification provided a profound understanding of fouling occurrences on the membrane which contributes to the development of the fouling mitigation approach.

Keywords: polymeric membrane modification, silver nanoparticles synthesis, thermal treatment approach, fouling analysis, biofouling analysis.

PENDEKATAN RAWATAN HABA DALAM IMOBILISASI NANOPARTIKEL PERAK KE DALAM MEMBRAN POLYVINYLIDENE FLUORIDA UNTUK MITIGASI KOTORAN BIO SEMASA RAWATAN AIR

ABSTRAK

Pengisian logam bernilai, iaitu nanopartikel perak (AgNPs), sebagai disinfektan ke dalam membran polimer adalah salah satu kaedah pengubahsuaian empirikal untuk menghasilkan air minuman yang selamat. Walau bagaimanapun, terdapat perbincangan yang kurang tentang penyebaran dan sifat pegun AgNPs semasa pemfabrikatan membran dan aplikasi, walaupun banyak fenomena larut-lesap telah dilaporkan. Selain itu, kaedah dan parameter sintesis adalah faktor penting dalam menentukan pembentukan nanopartikel dan proses nukleasi. Di samping itu, analisis kotoran membran adalah penting untuk pemahaman yang jelas tentang kejadian kotoran, walaupun terdapat pendekatan pengurangan. Kajian ini mempersembahkan kesan kepekatan prekursor dan suhu sintesis terhadap pembentukan AgNPs dalam dua kaedah yang berbeza. Nanopartikel perak jenis pertama (AgNPs-1) dan jenis kedua (AgNPs-2) telah disediakan dan diperbadankan ke dalam membran polyvinylidene fluorida (PVDF) ultraturasan dengan kehadiran rawatan terma. Kesan rawatan terma yang dikaji pada suhu 25, 40, dan 55°C, telah mempengaruhi ciri-ciri fizikokimia membran PVDF dengan ketara. Semasa penapisan menggunakan air tasik sebagai suapan, kadar kerosakan fluks (FDR) dan nisbah pemulihan kotoran (FRR) analisis membran bersih dan tercemar telah mengisyaratkan fenomena pencemaran membran. Sebagai alternatif, AgNPs yang dimasukkan ke dalam membran PVDF telah digunakan untuk spekroskopi Raman yang dipertingkatkan permukaan (SERS) sebagai pendekatan yang tidak konvensional untuk

substrat peningkatan permukaan terbina dalam, manakala analisis termogravimetrik (TGA) digunakan untuk mengukur bahan kotoran enapan sebagai pendekatan untuk menilai prestasi AgNPs. Dapatan telah menunjukkan variasi ketara dalam AgNPs-1 dan AgNPs-2 yang telah disintesis dengan parameter sintesis yang berbeza untuk kedua-dua kaedah. Dengan mempertimbang saiz partikel yang telah ditentukan menggunakan penganalisa saiz partikel, keadaaan sintesis terbaik bagi AgNPs-1 adalah pada suhu 25°C menggunakan 0.255 g $AgNO_3$ manakala keadaan sintesis terbaik bagi AgNPs-2 adalah pada suhu 75°C menggunakan 0.03 mol/L $AgNO_3$. Membran yang diperbadankan dengan AgNPs-1 dan AgNPs-2 terpilih, disediakan pada suhu tertinggi telah memaparkan sifat mekanikal dan fluks air tulen yang lebih baik. Membran PVDF/PVP/AgNPs-2 membebaskan jumlah Ag paling sedikit (3.81%) sementara membran PVDF/PVP/AgNPs-1 dituang pada suhu 40°C membebaskan jumlah Ag paling tinggi (42.34%) semasa fasa penyongsangan ketika pemfabrikatan. Jelas sekali, tiada larut-lesap Ag ditemui dalam semua membran semasa penapisan buntu pada 0.5 bar. Membran-membran dengan AgNPs-1 dan AgNPs-2 menunjukkan prestasi musnah-bakteria yang luar biasa ke atas *E. coli* dengan pengurangan peratusan masing-masing sebanyak 90.38% dan 80.77%. Oleh itu, membrane dengan AgNPs yang difabrikasi pada suhu 55°C menawarkan ciri mekanikal yang lebih baik iaitu kebolehtelapan yang dipertingkat dan kestabilan pegun AgNPs yang sangat baik yang mana menjadikan pendekatan rawatan terma bererti. Selain itu, puncak penting kecil yang mewakili kehadiran kotoran bio diperolehi daripada Raman biasa, manakala jumlah berat kotoran menunjukkan pengurangan sebanyak 82.69% dan 75.86% masing-masing dengan kehadiran AgNPs-1 dan AgNPs-2. Oleh yang demikian, pendekatan yang tidak konvensional bagi analisis kotoran untuk AgNPs dalam membran PVDF berpotensi diperuntukkan untuk peningkatan permukaan dalam analisis Raman biasa, manakala pengkuantitian kotoran

memberikan pemahaman yang menyeluruh tentang kejadian kotoran pada membran. Ini akan menyumbang kepada pembangunan strategi pengurangan kotoran.

Kata kunci: pengubahsuaian membrane polimer, sintesis nanopartikel perak, pendekatan rawatan terma, analisis kotoran, analisis kotoran bio

ACKNOWLEDGEMENTS

"Verily We have created man into toil and struggle" Quranic version, 90:4

First and foremost, Alhamdulillah for all the strength He had given me in completing my first thesis. He had given me such a wonderful experience with lovely companions of families, lecturers, and friends. Through hardship, He assisted me heaps. There are a lot of things I had gained and learned from the path I was destined to be in. The knowledge I had obtained which I cannot seek from anywhere will always be remembered, InsyaAllah.

Then, I would like to thank all those people who made this thesis possible and an enjoyable experience for me. I wish to express my sincere gratitude to my supervisors, Assoc. Prof. Dr. Nur Awanis Hashim and Assoc. Prof. Dr. Oi Boon Hong @ Ong Boon Hoong for giving me ideas and freedom to express my research and guiding me in completing this research. It enables me to explore the small part of the Chemical Engineering field in very efficient ways. The motivation and courage given will be remembered by heart, always.

On top of all, I am extremely grateful to my family members who always give me support through my thick and thin especially my mother, Noraini Ismail, and my husband, Hasnul Safwan Hassan. The love, hopes, and prays will never be repaid throughout my entire life. Also, to my friends who help me in any way to finish this research, specifically Dr. Fauziyah Ishak, Junaidah Zakaria, Mahirah Ismail, Dr. Wan Adibah, 'The Parias', and 'Lab-Zarah' members. Also, not to forget, to all Universiti Malaya's staff who was kind to assist me to the very end of my study.

TABLE OF CONTENTS

LIST OF FIGURES

LIST OF TABLES

LIST OF SYMBOLS AND ABBREVIATIONS

A	:	Membrane effective area, cm^2
$AgNO_3$	:	Silver nitrate
AgNPs	:	Silver nanoparticles
Ag_L	:	Leaching percent of AgNPs, %
a_f	:	Surface density of fouled membrane, g/m^2
a_m	:	Surface density of membrane, g/m^2
BSA	:	Bovine serum albumin
CA	:	Cellulose acetate
C_{Ag}	:	Concentration of Ag from ICP analysis, ppm
C_p	:	Concentration of permeate, ppm
C_f	:	Concentration of feed, ppm
COD	:	Chemical oxygen demand
DMAc	:	Dimethylacetamide
DOC	:	Dissolved organic carbon
EDX	:	Energy dispersive x-ray analysis
FDR	:	Flux decay rate, %
FESEM	:	Field emission scanning electron microscopy
FRR	:	Flux recovery ratio, %
FR_{NV}	:	Non-volatile fouling rate, %
FTIR	:	Fourier transform infrared spectroscopy
FW	:	Foulant weight, g/m^2
FW_{NV}	:	Non-volatile foulant weight, g/m^2
FW_t	:	Total foulant weight, g/m^2
FW_V	:	Volatile foulant weight, g/m^2

GO	:	Graphene oxide
ICP	:	Inductively Coupled Plasma
J_{av}	:	Average lake water flux, L/m^2.h
J_f	:	Final flux of ultrapure water, L/m^2.h
J_i	:	Initial flux of ultrapure water, L/m^2.h
J_w	:	Distilled water filtration flux, L/m^2.h
L	:	Log reduction
MF	:	Microfiltration
MWCO	:	Molecular weight cut-off
NF	:	Nanofiltration
NOM	:	Natural organic matter
P	:	Percent reduction, %
PA	:	Polyamide
PEEK	:	Polyether ether ketone
PEG	:	Polyethylene glycol
PES	:	Polyether sulfone
PI	:	Polyimide
PP	:	Polypropylene
PS	:	Polysulfone
PVA	:	Poly(vinyl alcohol)
PVC	:	Polyvinyl chloride
PVDF	:	Polyvinylidene fluoride
PVP	:	Polyvinylpyrrolidone
Q	:	Volume of permeated water, ℓ
R	:	Rejection, %
RFR	:	Relative flux reduction, %

RO	:	Reverse osmosis
SERS	:	Surface-enhanced Raman spectroscopy
t	:	Filtration time, h
T	:	Specific temperature in TGA, °C
TDS	:	Total dissolved solids, mg/L
TFR	:	Total fouling ratio, %
TGA	:	Thermogravimetric analysis
TOC	:	Total organic carbon, ppm
TS	:	Total solids
UF	:	Ultrafiltration
W_{Ag}	:	Weight percentage of Ag in casting solution formulation, %
V_{bath}	:	Volume of ultrapure water in coagulation bath, ℓ
W_{cast}	:	Weight of casting solution poured for membrane fabrication, g
W_{Ag}	:	Weight of Ag traces in bath, g
$W_{Ag\ dope}$	:	Weight of Ag in dope, g
W_v	:	Weight of volatile fouling material, g/m^2
W_m	:	Weight of fresh membrane, g/m^2
η_f^T	:	Weight percentage of the remaining portion of the fouled membrane at T, %
η_m^T	:	Weight percentage of the remaining portion of the clean membrane at T, %

LIST OF APPENDICES

CHAPTER 1 : INTRODUCTION

A flood is an example of a water-related natural disaster that affects surface water quality instantly, leaving victims with no safe water supply for domestic use and drinking. In recent decades, membrane technology has offered a favorable solution in providing safe drinking water during an emergency. However, due to the complexity of water composition, some drawbacks need to be overcome to fully utilize membrane technology. Several approaches for synthesizing favorable materials and improving technical methods will enhance the technology regarding the index used for modification performance evaluation. This chapter provides an outlook of the research essentials to clarify the motivation of these ideas.

1.1 Background of the Study

Flood in Asia took the lives of 6,794,304 from 1900 to 2013 and cost up to USD 359 billion in economic loss, according to the webpage of Environmental Issues in Asia (S. E. Kim, Li, & Nam, 2015). Among the countries in South Asia, India is the worst affected by various natural disasters, and the country has the highest number of flood-related deaths (Mohanty, Mudgil, & Karmakar, 2020). The latest major flood event recorded in Malaysia was in December 2014 and January 2015, when Kelantan, Terengganu, and Pahang suffered a great loss of about RM2.9 billion, 25 fatalities, and more than 400,000 people were evacuated (Norizan, Hassan, & Yusoff, 2021).

During emergencies, the affected community will lose their basic needs, such as shelter, food, water, and clothes. Flood spreads through fields and urban areas, potentially transferring various microorganisms, including pathogens of public health concern, such as *Leptospira* sp., *Shigella* sp., and *V. cholera*, which can contaminate water supply systems (Pandey, Kass, Soupir, Biswas, & Singh, 2014). During this period, both tap water and filtered tap water are unfit for daily sanitation and consumption, thus putting

public health at risk (Chaturongkasumrit, Techaruvichit, Takahashi, Kimura, & Keeratipibul, 2013). Therefore, surface water from accessible water bodies must be treated to provide a continuous water supply during emergencies.

Floodwater may contain different types of viruses, bacteria, and microorganisms due to the interaction of several water bodies, including black water. Conventional treatment methods, such as coagulation, flocculation, and sand filtration are less efficient than membrane technology in terms of water effluent quality and precursor removal, whereas chlorination produces halogenated disinfection by-products, which are carcinogenic upon reaction with residual natural organic matter (NOM) in the water (Sengur-Tasdemir et al., 2021). In membrane technology, microfiltration (MF) and ultrafiltration (UF) applications for surface water treatment are the preferred options compared to reverse osmosis (RO) and nanofiltration (NF) as these filtration methods require complex pretreatment procedures and an additional source of energy (L. Li & Visvanathan, 2017).

To date, UF membrane systems are intensively becoming an outstanding alternative for sub-surface and surface water treatment due to the ability to produce high-quality drinking water consistently, which is described as an economically feasible option (W. Yu, Graham, & Fowler, 2016). Membrane technology applications will reduce the possibility of polluting the environment thermally or chemically as no phase change is required and the separation process can be carried out in mild conditions (P. Xiao, Xiao, Wang, Qin, & He, 2012). UF has been identified and suggested as the most promising membrane type for removing microorganisms and providing a reliable water supply during a natural disaster (Loo, Fane, Krantz, & Lim, 2012). This low-pressure membrane is extensively implemented to reject microbial contaminants, bacteria, and waterborne pathogens (Carvajal et al., 2017; ElHadidy, Peldszus, & Van Dyke, 2013; S. Lee, Ihara, Yamashita, & Tanaka, 2017). Figure 1.1 illustrates the general concept of membrane

separation while Figure 1.2 shows the types of membrane separation and their characteristics.

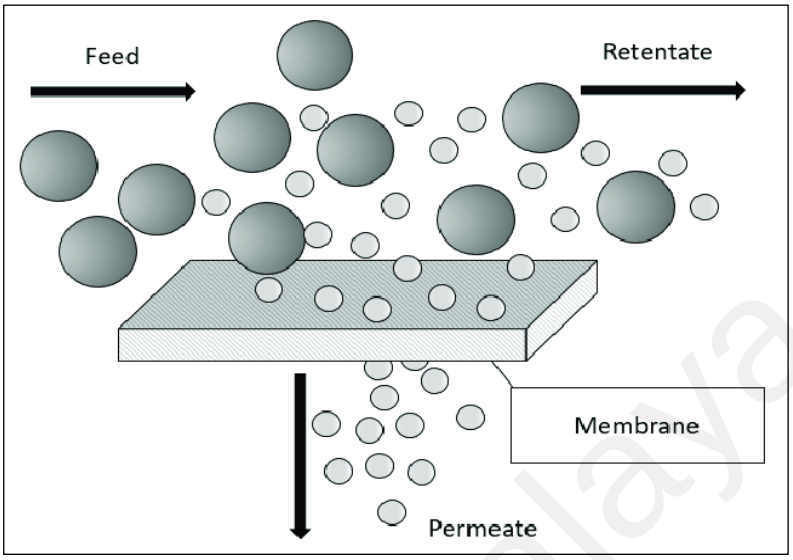

Figure 1.1 The general concept of membrane separation (Yin & Yip, 2017).

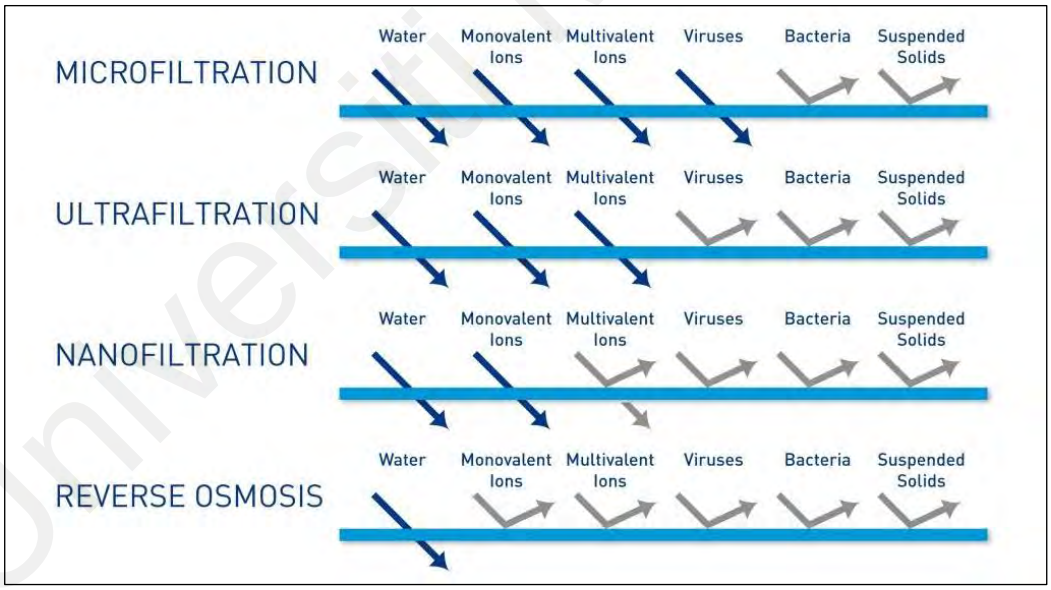

Figure 1.2 Types of membrane separation and the characteristics (Pentair.com, 2022).

However, during microorganism removal, the accumulation of microorganisms on the membrane surface triggers biofouling. According to Vrouwenvelder and colleagues, biofouling can be described as the acquisition of microorganisms, particularly biofilms

on a surface attributed to the growth and deposition of microorganisms, leading to operational problems that are hard to identify (Vrouwenvelder et al., 1998). Therefore, the modification of the UF membrane is essential to improve the performance of the membrane in removing microorganisms typically found in surface water and floodwater during the shortage of drinking water sources. Noble metal nanoparticles have been introduced as a disinfectant to mitigate biofouling and produce better water quality during membrane filtration (Mahmoudi et al., 2019).

One of the modification methods is by impregnating a novel metal (i.e., silver nanoparticles (AgNPs)) as a disinfectant into the membrane. From the literature, it is determined that Ag-based compounds and Ag ions are extremely toxic to microorganisms, which are commonly tested using *E. coli* and *S. aureus* (Y. Chen, Zhang, Zhang, Liu, & Song, 2013; J. Yin, Yang, Hu, & Deng, 2013; Zodrow et al., 2009). The incorporation of AgNPs aims to overcome the limitations of current disinfectants (i.e., chlorine and ozone). Chlorination requires high doses of chlorine and can form dangerous by-products, whereas ozone is claimed to be generally expensive owing to its low efficiency and bromate production during disinfection (Gomes, Matos, Gmurek, Quinta-Ferreira, & Martins, 2019). Additionally, the incorporation resulted in higher hydrophilicity, which significantly improved the membrane permeability of coated membranes; hence, water with better quality and greater quantity can be produced due to high permeability during separation (C. Mecha & V. L. Pillay, 2014).

In recent years, the impressive progress of investigations on nanoparticles immobilization can be found in the literature. As polymer chains contain various functional groups and are flexible, immobilization of nanoparticles is possible via electrostatic, hydrogen, van der Waals, or covalent bonds (Mahouche-Chergui, Guerrouache, Carbonnier, & Chehimi, 2013). It is crucial to apply an improved

modification method for better anchoring AgNPs in the polymeric membrane to fully utilize UF membrane's potential in providing safe drinking water. Thus, to achieve better water treatment performance by mitigating biofouling, the polyvinylidene difluoride (PVDF) membrane was selected to undergo modification by incorporating synthesized AgNPs and applying the thermally induced phase inversion method to enhance the physicochemical properties of the membrane and its filtration performance.

1.2 Problem Statement

The modification of UF membrane is in demand due to the complexity of surface water and floodwater content during the shortage of safe drinking water sources. Filtration of microorganisms in the presence of NOM will develop severe biofouling. Noble metal nanoparticles are introduced as a disinfectant to mitigate biofouling. The application of nanoparticles has currently gained attention due to their defined chemical, optical, and mechanical properties (P. Rai, Rai, Majumdar, DasGupta, & De, 2006).

The impregnation of AgNPs as a disinfectant into membranes is an empirical modification method for drinking water treatment. Although leaching and slow release of nanoparticles have been reported and discussed, the mechanism for the immobilization of nanoparticles in polymeric membranes remains an important issue. The incorporation of nanoparticles in polymeric membranes has been reported in many studies for modification and biofouling mitigation. However, minimal work has been done on altering membrane casting conditions for incorporating nanoparticles and improving the immobilization of nanoparticles in the membrane matrix. Moreover, the information on the synergetic effect of several membrane modification techniques is still lacking, specifically for water treatment during an emergency.

In conjunction with the modification attempt, fouling during surface water filtration should be given attention as an indicator of the effectiveness and reliability of the

mitigation made. Flux and filtration performance have been commonly reported in determining the efficiency of nanoparticles as an antibacterial agent to control biofouling. However, the fouling control strategy has been less analyzed in terms of fouling rate and other quantification methods, which will significantly describe the type of fouling and whether it is attributed to biofouling or other factors. Furthermore, it is vital to analyze the fouling phenomena for better insights into the modification performance and another possible potential of the mitigation approach.

Therefore, the UF PVDF membrane needs to be modified to fully utilize the potential of membrane technology. A practical approach for AgNPs incorporation needs to be deeply considered, where AgNPs are synthesized, tailored, and immobilized in the membrane for application in water treatment. The performance of AgNPs as an antibacterial agent for biofouling mitigation should be carefully analyzed to improve the understanding of the effects and effectiveness of AgNPs incorporation in PVDF membrane, specifically for surface water treatment. In addition, the potentialities of the immobilized AgNPs in the membrane as fouling mitigation agents and a surface enhance substrate in analytical equipment, such as thermogravimetric analysis and Raman spectroscopy will also be examined, respectively.

1.3 Aim and Objectives of the Study

This research aims to develop immobilized AgNPs in the PVDF membrane matrix as an antibacterial filtration membrane for surface water treatment to produce clean water during emergencies. The objectives of this study are:

i. To synthesize AgNPs via two distinctive methods and determine the effects of synthesis conditions on AgNPs characteristics.

ii. To modify the PVDF membrane by incorporating synthesized AgNPs using a thermal treatment approach for the immobilization of AgNPs.

iii. To evaluate the filtration performance of PVDF membrane immobilized with AgNPs during surface water treatment.

iv. To analyze the potentialities of immobilized AgNPs in PVDF membrane as biofouling mitigation agent using thermogravimetric analysis (TGA) and as surface enhance substrate in Raman spectroscopy.

1.4 Research Questions

This research centered upon a few research questions as follows;

i. How do synthesis parameters of precursor concentration and incubation temperature affect the AgNPs size?

ii. How do synthesis methods the incorporation and embedment process of AgNPs in the polymeric membrane?

iii. What are the effects of the thermal treatment approach in immobilizing AgNPs in membranes and how does it affect membrane characteristics and performance?

iv. What are the additional potentials of AgNPs immobilized in PVDF membrane which can be evaluated in certain analyses?

1.5 Research Significance

The findings of this study will benefit society, considering the critical demand for safe drinking water during natural disasters. The state of emergency, putting the vast number of lives in need, justifies the exigency of favorable membrane technology application. Thus, the recommended approach of membrane modification, as discussed in this study, will offer a better application of membrane in water treatment systems. Enhanced filtration performance, safer drinking water quality, and longer membrane lifespan will uncover the critical areas in membrane technology that previously hindered its

implementation. More desirable insights into polymeric membrane modification may promote extensive utilization of membrane technology for the betterment of society.

Throughout this study, the distinguished approach in synthesizing AgNPs altered for membrane technology application for promising antibacterial membrane fabrication is reported. Inventively, thermal treatment is introduced as a facile approach to improving the characteristics of modified PVDF membranes for permeability enhancement and AgNPs immobilization. The performance of AgNPs in membrane formulation as potential colloids for SERS application to examine biofouling from surface water treatment on a PVDF UF membrane is revealed. To the best of our knowledge, little to no similar studies have been reported in the literature. These approaches will provide favorable AgNPs types, alternative fouling analyses, and additional AgNPs function in membrane technology applications which offer better insights into the credibility of AgNPs as biofouling mitigation agents.

1.6 Scope of the Study

The present study embarks on the synthesis of AgNPs, specifically for polymeric membrane incorporation. The AgNPs were prepared based on two distinctive methods, and the resultant AgNPs were denoted as AgNPs-1 and AgNPs-2. Both AgNPs were individually incorporated in PVDF membrane dope composition. The modified PVDF membranes were prepared with thermally induced casting conditions at three different temperatures of 25, 40, and 55°C to enhance the immobilization of AgNPs in the membrane. The membrane with the most immobilized AgNPs was selected for further application in surface water treatment. The lake water quality was analyzed before and after the filtration. During filtration, the membrane flux was monitored to evaluate the antifouling properties of the membrane TGA was performed to quantify fouling weight and Raman spectroscopy was carried out to indicate the presence of biofoulants for precise filtration performance analysis of the membranes. The best membranes were

selected and applied in a crossflow filtration system to evaluate the flux decline in a more extended operation period. The limitations of this research include;

i. Commercial AgNPs selected, denoted as AgNPs-C1 and AgNPs-C2, were chosen based on the nearest size available on market to the size of AgNPs-1 and AgNPs-2.
ii. Characterization of lake water sample only involved pH, turbidity, TDS, DO, and bacteria count (*E. coli* and *S. aureus*).
iii. During ultrafiltration using a dead-end cell, the applied pressure was at 0.5bar using a plastic dead-end filtration set with a capacity of 200 mL feed.
iv. During ultrafiltration using a bench scale separation system, the transmembrane pressure was at 0.5 bar using a crossflow configuration set up with a capacity of 2000 mL feed.
v. Ag leaching phenomena during lake water treatment were examined only up to 4 hours of operation of bench scale crossflow filtration system.

1.7 Research Overview

This study embarks on AgNPs synthesis techniques for modifying polymeric membrane composition. The membrane was fabricated in thermally induced conditions to further attach AgNPs for immobilization. The leaching during fabrication and filtration was studied to provide safe drinking water from the water samples used. Upon the addition of AgNPs in polymeric membrane formulation, the antibacterial properties, filtration performance, and fouling occurrence were thoroughly analyzed to improve biofouling mitigation. The application of the fabricated membrane in a crossflow bench-scale filtration system was also reported. Overall, this study covers the synthesis of AgNPs until the application of the modified membrane in a crossflow filtration system to provide new insights into membrane modification.

1.8 Thesis Outline

This thesis is written in the conventional style format, which consists of five chapters. The description of each chapter is as follows:

Chapter 1: Introduction

This chapter includes a brief background of the research. The problem statement, objectives, significance, overview, and scope of the research are presented in related subsections accordingly.

Chapter 2: Literature Review

In this chapter, recent statistics, and current issues on water treatment during emergencies are first described. Essential information on fundamental theories of polymeric membrane and membrane technology is also discussed. Findings from previous studies related to nanoparticle incorporation and modification techniques, specifically for water treatment application, are reported. Based on all the information gathered, the overall literature is arranged and reviewed for better research design and outcome.

Chapter 3: Methodology

This chapter describes the materials used in performing the research. The methodology in the experimental works is clearly described, including the analysis to characterize the synthesized AgNPs and the modified PVDF membrane fabricated for membrane application in the water treatment system. Analysis of fouling and filtration performance of the membranes are described in detail.

Chapter 4: Results and Discussion

In this chapter, all results are discussed and analyzed to achieve the desired objectives. The results are written in parts according to the objectives, and these characterization and performance studies are used to determine the favorable modified membrane for water treatment application to provide safe drinking water.

Chapter 5: Conclusions and Recommendations

This final chapter expresses the summary of this research findings, and the conclusions are highlighted. Recommendations for future studies relevant to this research are also suggested.

CHAPTER 2 : LITERATURE REVIEW

Various studies have been conducted in the membrane technology field, especially in water treatment applications. This chapter presents a substantial review of the fundamentals, experimental flows, designs, and concepts in membrane technology, including the approaches of modification, characterization, and performance evaluation. A review of the extant literature will provide an extensive reference for this study in modifying UF membrane for water treatment applications with enhanced characteristics and greater performance. An overall review of the subject knowledge is illustrated in the flow diagram in Figure 2.1.

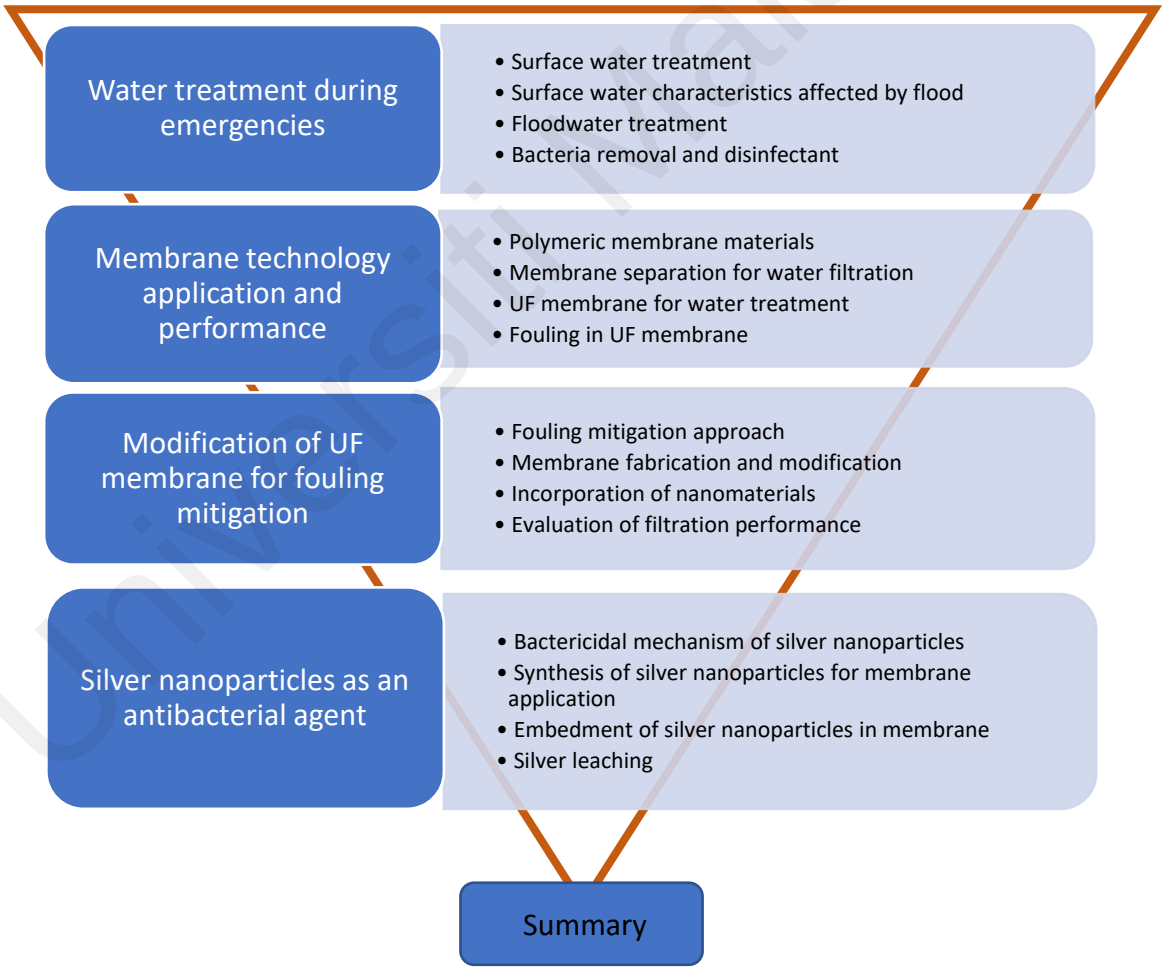

Figure 2.1 The overall flow of reviewed literature

2.1 Water Treatment during Emergencies

Between 1998 and 2017, 7,255 major natural disaster events were recorded, and 91% of the events were climate-related disasters, with 43.4% being caused by the flood. Floods (43.4%) and storms (28.2%) are the two most frequently occurring disasters (Teh & Khan, 2021). The literature on natural disaster occurrence worldwide has highlighted a long-term trend of an increase in the number of natural catastrophes around the globe with ever-growing losses (Hoeppe, 2016). In consequence, emergencies occur when substantial physical loss or damage and social and/or economic disruptions stretch beyond the capacity of society to cope instantly (Loo et al., 2012). Furthermore, this water-related catastrophe can cause public health problems due to the emergence of infectious diseases, such as bacillary dysentery, typhoid fever, cholera, and malaria (Nawfal Dagher, Al-Bayssari, Diene, Azar, & Rolain, 2020).

2.1.1 Surface Water Treatment

According to the United States Geological Survey, surface water is defined as the water on the Earth's surface, such as in a stream, river, lake, or reservoir ("Surface Water Use in the United States," 2018). Surface water is collected at ground level via precipitation and exposed to the atmosphere. The water bodies of surface water are significantly interrelated to each other. The interaction may occur beneath ground level, but it is not considered a surface water interaction. For surface water, the connectivity can be complex, which embarks on the physical topography of a system, as well as dynamic hydraulic gradients that exist during a natural disaster (Trigg, Michaelides, Neal, & Bates, 2013). Figure 2.2 illustrates the connectivity of several water bodies, including surface water.

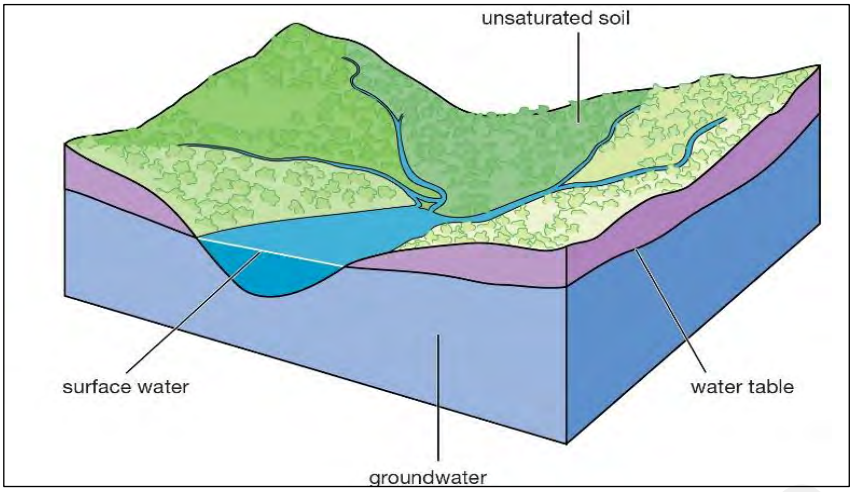

Figure 2.2 Cross-section diagram of a water table including surface water (Britannica, 2011).

An excessive amount of water in an inundation area is generally a combination of several water sources from a river and/or lake with precipitation. The connectivity and interaction of these water sources are complex and hardly quantified (Trigg et al., 2013). Thus, the characteristics of water to be treated vary. Also, limited or no power supply with impermissible access to infrastructure makes surface water treatment during an emergency difficult. Thus, the most favorable and mobile technology is vital to cater to the needs of the unfortunate victims. According to Loo et al., membrane-based water technologies, especially UF, are recognized as the most ideal solution for drinking water emergency response although there is a need to improve existing and emerging technologies in this important area for obtaining easily deployable, versatile, and reliable emergency water technologies for disaster relief (Loo et al., 2012).

2.1.2 Surface Water Characteristics Affected by Flood

Due to flood occurrence, there are changes in river water quality before, during, and after the event. It is influenced by a wide range of organic and inorganic contaminants transported during inundation. Although these organics increased substantially in concentrations, they are more treatable than organics in water before or after the flood period because the river flow rate data can potentially provide early warning of changes

in the character of organics, which can then affect water treatment processing for drinking water supply (Murshed et al., 2014). Thus, it is worth mentioning that water quality impairment and inland flooding are multi-billion dollar problems that are expected to worsen with time (Suttles, Eagle, & McLellan, 2021).

Due to the complex assemblage of multi stressors, managing sustainable water quality in surface water and reservoirs has become a formidable challenge (Mamun, Atique, Kim, & An, 2021; Smith & Schindler, 2009). In a study conducted by Abraham and Sivan (2021), water quality changes prior to flood events consist of five types of parameters: physical, chemical, nutrients, heavy metals, and biological. Various public health concern microorganisms and pathogens, such as V. *cholera*, Shigella *sp*., and Leptospira *sp*. are potentially transferred to the flood, which can contaminate the water supply system as the flood spreads through fields and urban areas (Pandey et al., 2014). Furthermore, a growing number of studies have reported on the sources, composition, and transportation of many other components in floodwater, including dissolved organic matter (DOM) (Bauer et al., 2013); dissolved oxygen (DO) (Gibson et al., 2020); nitrate, ammonium, and phosphate (N. Chen, Krom, Wu, Yu, & Hong, 2018); lead (Gopal et al., 2017); and suspended particulate matter (SPM) (Peraza-Castro, Sauvage, Sánchez-Pérez, & Ruiz-Romera, 2016).

2.1.3 Floodwater Treatment

Flood will bring plenty of dirty water instead of clean water, and it becomes the biggest problem during a disaster. Floodwater is considered dangerous to be used for domestic purposes and sometimes is harmful to the skin as it is contaminated with numerous contaminants, including human and animal waste (N. A. Kamarudin et al., 2018). Over the past decades, many studies have discussed floodwater treatment solutions. The

abundant but unsafe source of water to be used demands an instantaneous treatment approach.

Dorea, Bertrand, and Clarke (2006) reported that possibly effective particle separation approaches for water treatment during emergencies are pressure filtration, clarification, gravel and sand filtration, media filtration, and membrane filtration. Recently, Loo et al. stated that during a flood event, water treatment may ineffectively operate as expected due to the changes in the solution, especially its chemistry. Due to the altered solution chemistry, the water treatment may fail to perform as expected. This is especially true for water treatment processes, such as coagulation/flocculation, adsorption, and high-pressure membrane filtration. Other problems include water quality variability and the absence of onsite toolkits for rapid contaminant screening in emergencies. It is important to choose a purification and filtration system that effectively eliminates the microorganisms in floodwater to be used for drinking and indirectly overcomes the lack of clean water.

2.1.4 Bacterial Removal and Disinfection

The difference between disinfection and sterilization is that disinfection is the partial destruction of pathogenic organisms, whereas sterilization is the process of removing microbial matter in total. Floodwater may contain a certain load of viruses, bacteria, and microorganisms due to the interaction of several water bodies, including black water. The use of various disinfectants creates a potential risk for public health as disinfection by-products (DBP) are formed in conventional treatment techniques. Chlorine, which is the most commonly used treatment, reacts with naturally occurring organic materials to produce numerous by-products, some of which are suspected carcinogens.

Meanwhile, UF can completely remove the microbial load. However, for specific characteristics of surface water, certain parameters of the permeate are beyond the limits

of recommended potable water quality, such as hardness and chemical oxygen demand (COD) (Di Zio, Prisciandaro, & Barba, 2005). Table 2.1 shows the commonly found bacteria and viruses in floodwater, as well as their survival time in the water. Figure 2.3 presents possible disinfection processes for water.

Table 2.1 A literature review on the persistence of pathogens on fomites with survival times for common flood-borne pathogens (Fewtrell & Kay, 2015; Ten Veldhuis, Clemens, Sterk, & Berends, 2010).

	Potential Flood-Borne Pathogens	Total Survival Time
Bacteria	*Campylobacter jejuni*	Up to 6 days
	Salmonella spp	1 day
	Shigella	2 days–5 months
	Leptospira	–
	Enterococci spp.	5 days–4 months
	E. coli	1.5 h–16 months
Viruses	Norovirus	8 h–7 days
	Hepatitis A	2 h–60 days
	Rotavirus	6–60 days
	Adenovirus	7 days–3 months
	Enterovirus	1 day–8 weeks
	Parvovirus	> 1 year
Fungus	*Candida albicans*	1–120 days
	Candida parapsilosis	14 days
	Torulopsis glabrata	102–150 days

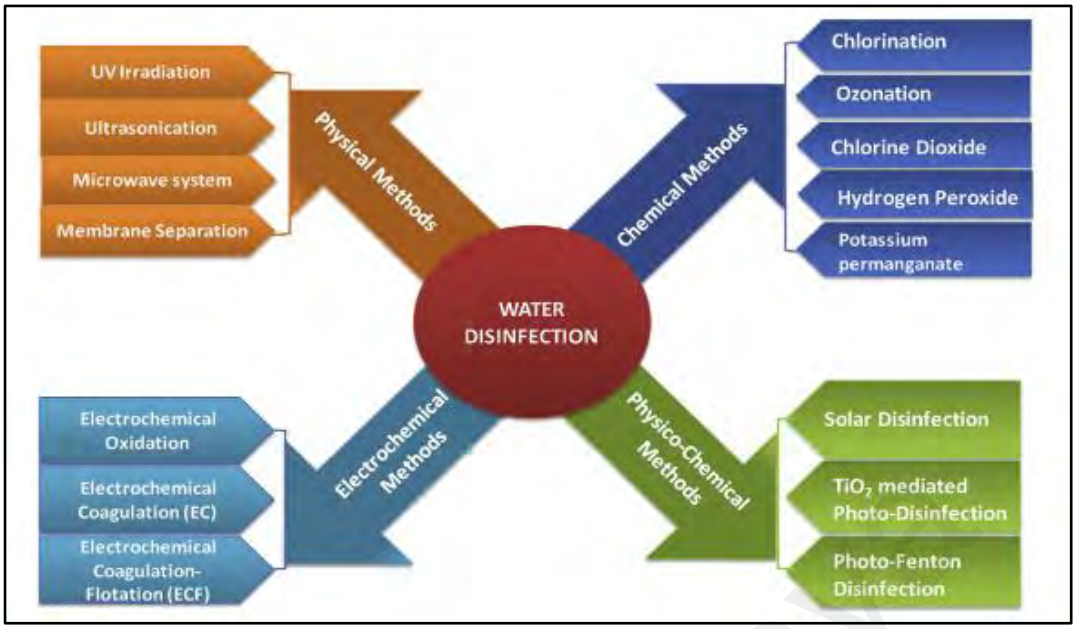

Figure 2.3 Various techniques used for water disinfection (Govindan, Angelin, & Rangarajan, 2018).

2.2 Membrane Technology Application and Performance

The choice of the membrane filter and/or process for a particular application is difficult as the removal of particles, including biological and non-biological colloids by membranes depends on many factors, including pore size and molecular weight cut-off (MWCO), which is the most critical parameter for water disinfection using a membrane (Madaeni, 1999). In addition, various membrane separation processes, such as MF, UF, and reverse osmosis (RO) are capable of moving different sizes of materials, for instance, MF for particle separation, UF for macromolecule separation, and RO for ionic components.

As the membrane can be categorized based on several characteristics, the application of membrane technology is very wide as it can handle many types of feed water with excellent operational reliability (Goh, Wong, Lim, Ismail, & Hilal, 2020). Other advantages of membrane technology reported in the literature include no additional chemicals are needed, the lower energy requirement for UF and MF, and a systematic

process (Padaki et al., 2015). In comparison to a traditional separation process (i.e., absorption), membrane separation offers many advantages, such as lower processing cost, smaller footprint area, easier scale, and ultimately, more environmentally friendly (Z. Dai, Noble, Gin, Zhang, & Deng, 2016). Studies on membrane technology applications from the literature are listed in Table 2.2.

Table 2.2 Studies on membrane technology applications in the literature.

Application	Membrane		Ref
	Materials	Separation Type	
Semiconductor wastewater reclamation and purification.	Polymer	UF/RO	(C. J. Huang, Yang, Chen, Chang, & Kao, 2011)
Crude palm oil biodiesel purification from glycerol and potassium.	Ceramic	UF	(Atadashi, Aroua, Abdul Aziz, & Sulaiman, 2012)
Humic acid removal for water recycling and water treatment.	Polymer	N/A	(L.-L. Hwang, Chen, & Wey, 2013)
Boron removal from aqueous solution	Cellulose	UF	(Palencia, Vera, & Rivas, 2014)
Desalination of brackish water	Polymer	UF	(Thuyavan, Anantharaman, Arthanareeswaran, Ismail, & Mangalaraja, 2015)
Elimination of bacteriophages from whey from raw milk.	Ceramic	MF	(Samtlebe et al., 2015)
Purification of raw sugar beet juice	Polymer, cellulose	UF	(Z. Zhu & Mhemdi, 2016)
Removal of organic micropollutants from RO concentrate	Polymer	MF	(Shanmuganathan, Loganathan, Kazner, Johir, & Vigneswaran, 2017)
Removal of endocrine disrupting compounds from water	Polymer composite	UF	(Y. Zhu et al., 2018)
Direct filtration for coagulated domestic sewage treatment	Ceramic	MF	(Zhao, Li, Li, & Li, 2019)
Arsenic and iron removal for water treatment	Polymeric	MF, UF	(Ahmad et al., 2020)
Removal of ibuprofen for safe water treatment	Polymer nanocomposite	UF	(Rosman et al., 2021)

2.2.1 Polymeric Membrane Materials

In general, membranes can be categorized into organic and inorganic membranes. The majority of industrial membranes consist of synthetic or natural polymers, and membranes with both types of polymers are known as organic membranes. Usually, in the case of membrane separation technology, these polymeric membranes can also be classified as (i) porous and non-porous membranes and (ii) glassy and rubbery membranes based on the interconnected pores like conventional filters and glass transition temperatures, respectively (Mannan et al., 2013). Hence, for membrane technology application, the important elements that need to be considered include good film-forming capability; high mechanical, chemical, and thermal stability; and the trade-off between selectivity and permeability (Z. Cui, Drioli, & Lee, 2014).

For instance, the frequently used polymers for the UF process are polysulfone (PS), poly(ether sulfone) (PES), polyacrylonitrile, cellulose esters, polyimide (PI), polyamide (PA), PVDF, and polyetheretherketone (PEEK). Polymer selection must be based on compatibility with the membrane fabrication technique and the intended application. Furthermore, polymer selection and organic membrane manufacturing need to be factored in based on chain interaction, chain rigidity, functional group polarity, stereoisomerism, contact angle, and other characteristics (K. Wang et al., 2020). Moreover, membrane-solute interaction influences retention performance and consequently plays a significant role in membrane filtration performance (Tsarkov et al., 2012).

The existing literature on PVDF membranes is vast and broadened by numerous attempts to enhance the material with the best performance. High mechanical strength, good thermal stability, outstanding chemical resistance, and great aging resistance are the criteria of PVDF that make it a favorable option for membrane materials in separation applications (G.-d. Kang & Cao, 2014). Besides, PVDF is also robust to withstand organic

compounds, such as acids or oxidants, and also corrosive chemicals (Ji, Liu, Hashim, Abed, & Li, 2015). However, despite these excellent PVDF characteristics, its intrinsic hydrophobicity makes PVDF membranes prone to fouling (G.-d. Kang & Cao, 2014; J. Liu et al., 2016; Shen et al., 2018). Hence, many efforts have been made to overcome such issues and improve membrane filtration performance.

2.2.2 Membrane Separation for Water Filtration

Generally, a membrane can be classified into several different aspects. A membrane can be thin or thick with a heterogeneous or homogeneous structure, active or passive transportation, asymmetric or symmetric, synthetic or natural, and charged or neutral. A semi-permeable membrane permits the selective transport of species from one phase to the other (Murad & Powles, 2019). For a passive transport membrane, it can be driven by external driving forces, such as pressure, thermal, and concentration. Despite the numerous applications reported, a pressure-driven membrane is commonly utilized for water filtration. There are four types of pressure-driven membranes, which are MF, UF, nanofiltration (NF), and RO. Figure 2.4 illustrates the separation principle of pressure-driven membranes.

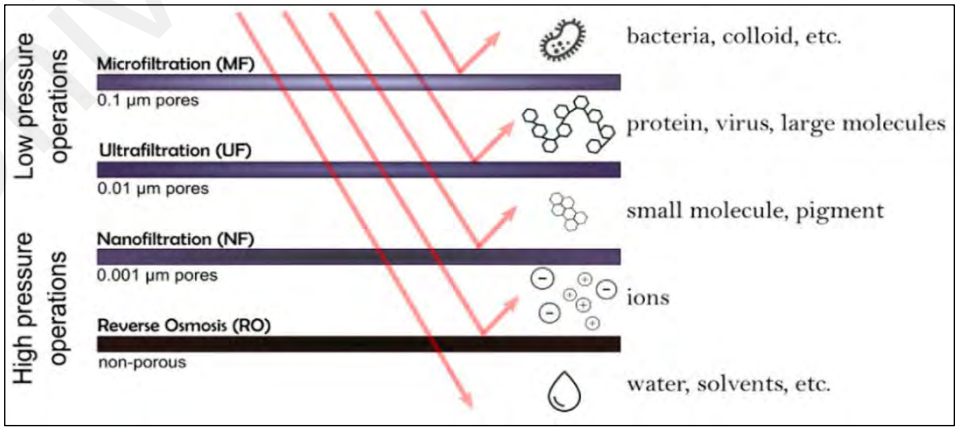

Figure 2.4 Schematic representation of membrane-based separation (García et al., 2021).

The driving force for these membrane processes can be gained mechanically, chemically, thermally, and electrically, which are in the parameters of pressure, concentration, temperature, and voltage, respectively. During separation, the pressure exerted on the solution at one side of the membrane surface has a role as a driving force to separate the feed into permeate and retentate (Van der Bruggen, Vandecasteele, Van Gestel, Doyen, & Leysen, 2003). The retentate is normally a concentrated solution that will be reintroduced as a feed in a system, hence making it a continuous flow system. The retentate also contains molecules that can pass through membrane pores and have better qualities compared to the feed and permeate in terms of the water treatment process. Various membrane characteristics used in water treatment applications are recorded in Table 2.3.

Table 2.3 Membrane characteristics used in various water treatment applications.

Membrane			Application	Solute	Performance	Ref.
Separation Type	*Material*	*Configuration*				
UF, MF	PVDF, PES	Hollow fiber	Drinking water treatment plant	Dissolved organic carbon (DOC)	70% removal	(H. Huang, Cho, Schwab, & Jacangelo, 2012)
UF	PS	Crossflow	River water treatment	Methyl orange dye	Up to 100% retention	(Peiris, Budman, Moresoli, & Legge, 2013)
NF	PP [a]	Hollow fiber	Textile industry wastewater treatment	Textile effluent	91.5% chemical oxygen demand (COD) reduction, 99.3% colour removal rate	(Y. Zheng et al., 2013)
MF	Woven fabric/Ag	Dead-end	Water disinfection	*E.coli* suspension	100% removal	(C. A. Mecha & V. L. Pillay, 2014)
UF	PVDF/PVP [b]	Crossflow	Oily wastewater treatment	Synthetic oily wastewater	More than 95% oil rejection ratio.	(X. Huang et al., 2015)
UF	PVDF/PVP, ZrO_2/Al_2O_3	Hollow fiber	Ground water treatment	synthetic feedwater	Rejection of iron and manganese is higher than 99.5%	(Dashtban Kenari & Barbeau, 2016)
NF	PA/PS/non-woven fabric	Crossflow	Biodiesel wash water effluent treatment	Actual biodiesel wash-water	>98% rejection for TDS [c] and TS [d]	(Mozaffarikhah, Kargari, Tabatabaei, Ghanavati, & Shirazi, 2017)

Table 2.3, continued.

Membrane			Application	Solute	Performance	Ref.
Separation Type	*Material*	*Configuration*				
N/A	Cellulose Acetate	Dead-end	Water treatment	Aqueous sodium alginate (200 ppm)	Maximum rejection is 89% at 7 bar	(H. Y. Kim, Cho, & Kang, 2019)
RO	PA	Dead-end	Industrial zone wastewater reclamation	Actual wastewater treatment plant effluent	Removal efficiencies are upt to 86.3% for COD, 94.9% for Cr ion, 100% for Pb ion, 98.2 for Fe ion, 99.7% for Zn ion, 99.5% for Si ion, and 100% for total phosphorus.	(Ozbey-Unal et al., 2020)
UF	PVDF/GO [f] composite/Ag_2CO_3	Cross flow	Micro-polluted surface water treatment	Lake water	81.58%, 61.10%, and 76.19% removal rate of COD, DOC [e], and aromatic compounds (UV_{254}) respectively.	(L. Wu et al., 2021)

[a] Polypropylene
[b] Polyvinylpyrrolidone
[c] Total dissolved solids
[d] Total solids
[e] Dissolved organic carbon
[f] Graphene oxide

2.2.3 Ultrafiltration for Water Treatment

The membrane separation process is fundamentally based on MWCO. The MWCO in membrane separation is defined as 90% rejection at the smallest molecular weight of a reference compound (Marchetti, Jimenez Solomon, Szekely, & Livingston, 2014; Vandezande, Gevers, & Vankelecom, 2008). Commercial membranes are often characterized based on MWCO to determine the suitable application of the membrane (Boussu et al., 2006). From the literature, it is well understood that UF membranes have the MWCO in the range of l–100 kDa (Winter, Barbeau, & Bérubé, 2017). However, it should be noted that MWCO is unable to provide sufficient details on the separation quality and performance (Marchetti et al., 2014). Membrane pore size and permeability are among the important information for self-fabricated membrane characterization (Calvo, Bottino, Capannelli, & Hernández, 2008; Idris, Zain, & Noordin, 2007). This is because the membrane filtration performance of a porous membrane depends on the morphology and polymer used (De Jong, Lammertink, & Wessling, 2006).

Interestingly, UF membranes with a cut-off within a range of 10–100 kDa are considered to be best implemented for bacteria removal from surface water with different microbiological contents as they showed 100% bacterial rejection (Arnal et al., 2004). UF is considered an effective membrane for disinfection and a suitable alternative for chemical disinfection (Iannelli et al., 2014). Although RO and NF membranes have a finer magnitude of MWCO and pore size compared to UF membranes, RO and NF membranes are physically sensitive to chemical and mechanical conditions and require high operational costs (Habimana, Semião, & Casey, 2014; Ramaswami, Behrendt, & Otterpohl, 2018). Awad et al. comprehensively reviewed the performance and stability of UF membranes and concluded that UF is a versatile process for separation and purification (Awad et al., 2021). Although UF has been utilized and improvised for

drinking water treatment purposes, difficulties persist during its application involving membrane fouling (P. Xiao et al., 2012).

2.2.4 Fouling in Ultrafiltration Membrane

The major drawback of the membrane process is fouling. Generally, fouling is interpreted as permeability loss as a result of substance accumulated within the pores, near the pore opening and on the membrane surface (Alresheedi, Kenari, Barbeau, & Basu, 2022; Chang et al., 2017). According to Kim et al., fouling may be due to one or more of the following mechanisms universally agreed; i. solute surface adsorption or deposition, ii. irreversible change to the polarized layer (such as cake consolidation) gradually, and iii. solute adsorption or deposition within the membrane (Jim, Fane, Fell, & Joy, 1992). Hence, during the filtration process, fouling may take place both on the surface of membranes and inner pores (Lihan Huang & Morrissey, 1998). While during surface water filtration severe membrane fouling can be found due to numerous, naturally existing membrane foulants with various shapes, sizes, and molecular weights (Yuanqing Guo et al., 2020; Xing et al., 2018). Surprisingly, it was reported that biofouling contributed up to 56.0% of total fouling in drinking water treatment applications in the UF process (Hoeppe, 2016).

The membrane fouling phenomenon has raised attention throughout the century since fouling is the utmost hindrance in membrane technology application. Aggregation of small molecules in membrane pores and deposition of retentates on the membrane's top surface are the causes of the fouling phenomenon (Lamsal, Harroun, Brosseau, & Gagnon, 2012). Fouling is normally indicated by flux declination due to the retention of macromolecules on the membrane surface during filtration and the separation process of smaller molecules (Mohammadi, Kohpeyma, & Sadrzadeh, 2005). Deposition of solutes and bacterial growth on membrane surface may lead to the inclination of flux. Physical

observation of the membrane surface will reflect the presence of foulants on the membrane surface, and the types and amount of foulants require exhaustive characterization. Detailed fouling analysis is crucial in better understanding fouling occurrences. An extensive understanding of membrane fouling, including its form, process, and mechanism, would improve the fouling mitigation strategy, which will improve the process period and cost (B. Zhang et al., 2020).

Biofouling is a type of fouling phenomenon attributed to microorganism deposition on the membrane surface, which will initiate biofilm development (Flemming, 2002; Koh, Ashokkumar, & Kentish, 2013; Villeneuve et al., 2021). Numerous studies have reported ways to overcome biofouling issues in the membrane separation process. Researchers have been working on the synthesis and fabrication of membranes with antimicrobial properties to overcome biofouling issues. One of the modification attempts is the idea of immobilizing AgNPs in the polymeric membrane for biofouling mitigation. The attempt shall provide modified membranes with bactericidal properties for *E. coli* and *S. aureus.*

Flux decline in UF in most cases is caused by two main mechanisms: concentration polarization and membrane fouling (Dehaine, Foucaud, Kroll-Rabotin, & Filippov, 2019). Increasing the flow rate over the membrane may worsen the concentration of polarization but rigorous stirring activity near the membrane surface can decrease the concentration of polarization. With a surface deposit as the resultant of fouling occurrence, a dynamic membrane with larger resistance than the clean membrane is formed by membrane selectivity changing and resulting in an increment in rejection due to fouling (Jim et al., 1992). In recent literature, membrane filtration mode or configuration namely dead-end filtration and crossflow filtration was claimed to be responsible for controlling the UF membrane flux (Q. Wang et al., 2022). Figure 2.5 demonstrates the filtration process in different membrane configurations.

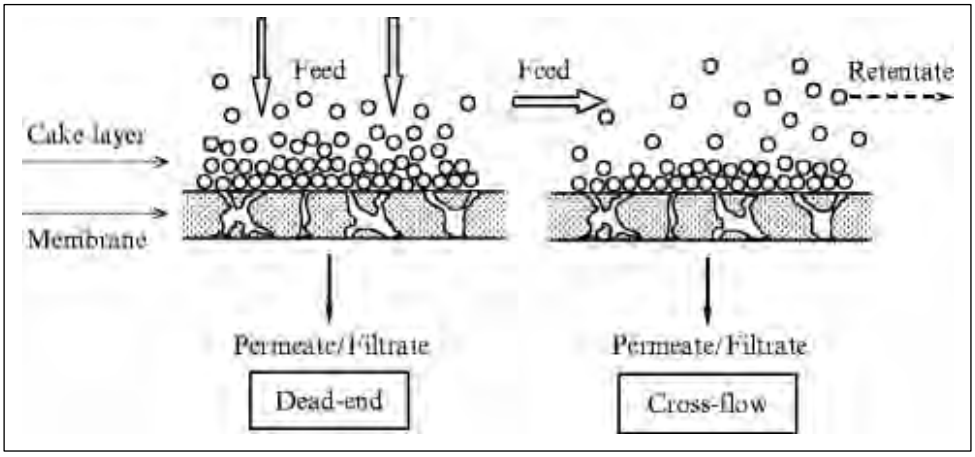

Figure 2.5 Filtration process in dead-end and crossflow membrane configuration (Fane, Wang, & Jia, 2011).

Two types of fouling deposits for UF on the membrane surface are cake (sheets) and aggregates. Therefore, the fouling mechanism relies on the type of membrane and the initial UF flux magnitude (Jim et al., 1992). All factors influencing solute transmission through the membrane need to be considered and properly utilized in order to employ UF as an efficient separation technique (Cheng et al., 2014). This phenomenon corresponds to permeability and selectivity changes. Therefore, the fouling mechanism emerges when deposition begins, which polarized the solute that initially accumulates on the membrane surface (Rudolph, Hermansson, Jönsson, & Lipnizki, 2021).

During fouling, the subsequent deposition can be assumed depending on the initial deposition's extent and nature. Fouling development includes several mechanisms, such as pore blocking, cake formation, concentration polarization, and finally cake layer formation (T. Yang et al., 2019). Fouling can also be classified based on the foulant or solute employed in the feed stream. Colloidal fouling, organic fouling, inorganic fouling, and biofouling are different types of fouling, as illustrated in Figure 2.6.

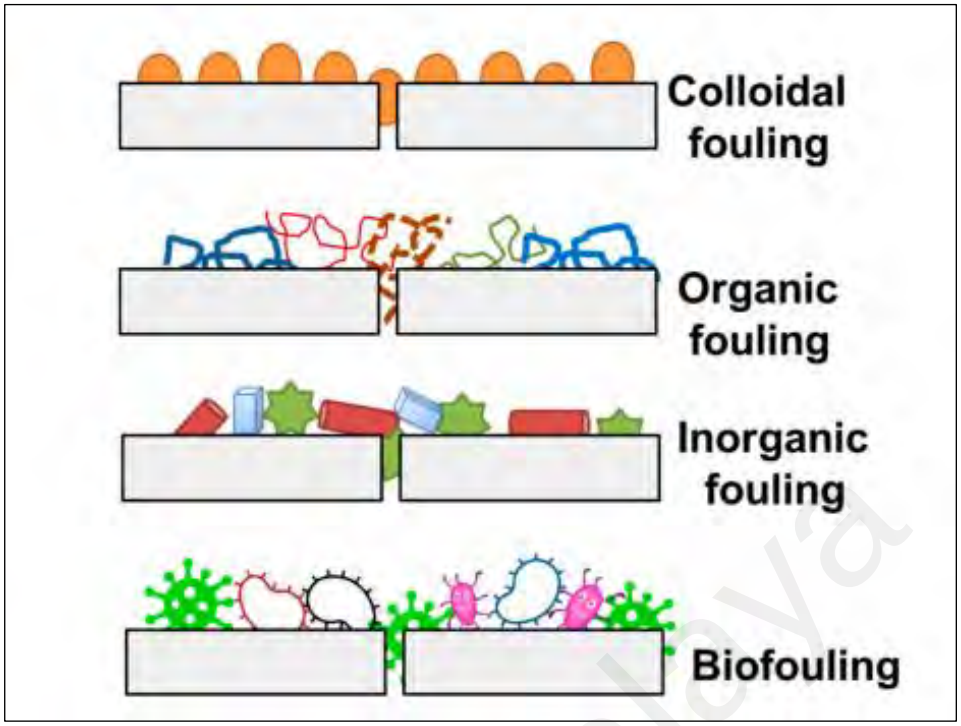

Figure 2.6 Schematic illustration of colloidal fouling, organic fouling, inorganic fouling, and biofouling (Gul, Hruza, & Yalcinkaya, 2021).

As mentioned previously, the UF membrane is an excellent membrane for water disinfection. During surface water filtration, microorganisms cannot pass through the membrane layer, making them inevitably accumulate and attach to the membrane surface before biofilm formation or biofouling (Shao et al., 2020). In an extended period of membrane filtration operation, biofouling develops and causes significant flux decline, which consequently altered the membrane filtration performance (Shao et al., 2018). This explains the growing number of works of literature related to biofouling mitigation via UF membrane modification (Gungormus & Altinkaya, 2021; Khajouei, Najafi, & Jafari, 2019; Nady et al., 2020; Piatkovsky, Acar, Marciel, Tirrell, & Herzberg, 2018). All these studies reported positive outcomes of the modification for biofouling mitigation.

2.3 Modification of Ultrafiltration Membrane for Fouling Mitigation

Modification of the UF membrane is among the most common approach to enhance membrane filtration performance. Modification of polymeric membranes frequently involves hydrophilic additives, macromolecules, and antibacterial agents intended to mitigate fouling (Kanagaraj, Mohamed, Huang, & Liu, 2020; Y. Kim, Rana, Matsuura, & Chung, 2009, 2012; Rana et al., 2012). The inability to control fouling would increase the operational cost of membrane application and hinder the extensive implementation of membrane technology (Yuanqing Guo et al., 2020). Thus, fouling mitigation is crucially needed to overcome this major drawback of membrane technology.

2.3.1 Fouling Mitigation

Fouling mitigation or fouling control strategies have been reported in the literature for the past few decades. These strategies involve feed pre-treatment, membrane composition alteration, operating condition optimization, and cleaning (C. Li, Sun, Lu, Ao, & Li, 2020; Matin, Laoui, Falath, & Farooque, 2021). An overview of fouling control strategies and efforts is presented in Table 2.4. The techniques applied varies from external modification to internal modification of engineering design. Furthermore, modification techniques for UF membranes have been reported to improve the performance of removing organic matter and disinfecting floodwater during the shortage of drinking water sources. A comprehensive review by Mamah et al. (2021) deduced that the materials and techniques for polymeric membrane in water treatment applications should be selected based on the contaminant or compound that needs to be treated in the feed solution.

Table 2.4 Fouling control strategies for UF membranes.

Fouling Control Strategies	Materials	Techniques	Applications	Findings	Ref.
Surface modification via microswelling	PVDF, PS [a]	Post-treatment using solvent	Drinking water treatment	Improved surface properties with higher flux and a slower fouling rate.	(Du, Peldszus, Huck, & Feng, 2015)
Immobilization of polysaccharide-degrading enzyme	CA [b]	Surface immobilization	Municipal and industrial wastewater treatment	Fouling present is non-adherent and removable by simple backwash.	(Meshram et al., 2016)
Surface modification via inorganic nanoparticles embedment	PES	Polymer side chain grafting using TiO_2 nanocluster	Drinking water and municipal wastewater treatment	The membrane exhibited excellent separation, anti-fouling, and self-cleaning properties.	(Geng et al., 2017)
Coupling continuous sand filtration	PVC [c]	External circulation hydraulic sand washing	Pilot plant drinking water treatment	Removal performance was enhanced, dramatically reducing TMP increment and irreversible fouling resistance was minimized.	(Yuanqing Guo et al., 2018)
In-situ surface segregation modification	PVDF	Blending of symmetrical amphiphilic triblock copolymer	Water treatment	The membranes possess enhanced anti-fouling properties with an excellent flux recovery ratio (FRR).	(J. Zhao et al., 2019)

Table 2.4, continued.

Fouling Control Strategies	Materials	Techniques	Applications	Findings	Ref.
Manipulation of surface hydrophilicity and membrane charge	PES	Coating and grafting	Clarification of molasses	Fouling was minimized with improved threshold flux.	(Q. Yang et al., 2019)
Raw water pretreatment	Acetate fiber	Visible light irradiation photocatalysis and coagulation	NOM removal	Cake filtration was reduced to some extent but fouling remained due to pore blocking.	(N. Wang et al., 2020)

[a] Cellulose acetate
[b] Polysulfone
[c] Polyvinyl chloride

2.3.2 Membrane Fabrication and Modification

Phase inversion is one of the most common practices to fabricate membranes. During the process, an initially prepared polymer solution, also known as casting solution, is transformed from the liquid phase to the solid state preceded by liquid-liquid demixing (Hołda & Vankelecom, 2015). This process requires a controlled condition to produce a uniform quality of each membrane. Hołda and Vankelecom (2015) thoroughly reviewed the membrane synthesis conditions affecting membrane morphology and performance. Among them are the type of polymer, evaporation temperature, casting solvent, and casting additive. They compellingly concluded that synthesis parameters are often associated with membrane performance instead of related to morphology studies and certainly not to the synthesis process itself. Thus, thermal treatment approaches are introduced in this study and discussed further in Section 2.4.3.4.

In recent decades, research on membrane modification has drawn the attention of those intended to minimize fouling (Pagidi et al., 2015). Modification of membrane surface chemistry, hydrophilicity, pore structure, surface roughness, and morphology are among the routes for membrane modification (T. Li et al., 2018; Jindan Wu et al., 2018). Several primary protocols in membrane modification methods are tabulated in Table 2.5 considering their advantages and disadvantages. Awad et al. mentioned that surface modification and membrane synthesis significantly improved membrane filtration performance (Awad et al., 2021). Therefore, simultaneous approaches of membrane modification and synthesis technique modification need to be further explored. The multiple effects of these parameters need to be analyzed to develop a full picture of membrane modification efforts and effects.

Table 2.5 Modification methods for polymeric membranes.

Modification method	Merits	Shortcomings
Surface grafting	High control of localized grafting onto the desired surface and relatively higher chemical stability (Kato, Uchida, Kang, Uyama, & Ikada, 2003; X. J. Lee, Show, Katsuda, Chen, & Chang, 2018).	Requires multiple chemical processes to obtain the desired functional groups (Nie et al., 2017).
Surface coatings	Facile and convenient step coating strategy to alter membrane surface chemistry (Meng, Zhang, Ding, Zhang, & Gong, 2018).	Membrane pores blockage consequently decreases water flux and unstable coating layer upon critical conditions (Ma et al., 2015).
Surface plasma treatment	Yield high density of surface functional groups (Nie et al., 2017).	Powerful radiation may induce polymer degradation which will decrease the membrane stability and mechanical properties (Nie et al., 2017).
Blending	Simply method by adding particular modifiers into the casting solution (Nie et al., 2017).	Membrane stability depends on the type of additive/nanoparticles and long-term usage may decrease the membrane stability (Nie et al., 2017).

2.3.3 Incorporation of Nanomaterials

Most research on membrane modification has utilized nanomaterials as a modifier. Inorganic and polymer nanoparticles are often used for membrane modification, which are incorporated via the blending method (Pirsaheb et al., 2019). Reviews on nanoparticles as a modifier in polymeric membranes are presented in Table 2.6. Among numerous metal nanoparticles utilized for their antibacterial properties (i.e., gold, copper, titanium oxide, and zinc oxide), AgNPs have been nominated as the most active antibacterial agent due to their excellent antibacterial property, biocompatibility, and thermal stability (Minh Dat

et al., 2019; Reddy & Pathak, 2018). The application of nanoparticles is capturing stimulus in recent millennials due to established optical, mechanical, and chemical properties (M. Rai, Yadav, & Gade, 2009).

Table 2.6 Types of nanoparticles incorporated in polymeric ultrafiltration membrane.

Type of nanoparticle	Findings	Application	Ref
TiO_2	• Removes *E. Coli* at a very faster rate than neat PVDF membrane with the highest antibacterial property. • 2% TiO2 membrane has the lowest fouling resistance.	Municipal and industrial waste treatment and reuse	(Damodar, You, & Chou, 2009)
O-carboxymethyl chitosan (OCMCS) functionalized Fe_3O_4 nanoparticles (OCMCS-Fe_3O_4)	• A significant increase in hydrophilicity was achieved by the 0.05 wt. % OCMCS-Fe_3O_4 nanoparticles blended membranes. • Excellent antifouling properties	Water recovery and reuse	(Rahimi, Zinatizadeh, & Zinadini, 2019)
CuO/ZnO	• Pure water flux growth to almost 32%. • Improved FRR value during BSA filtration.	Water purification	(Nasrollahi, Vatanpour, Aber, & Mahmoodi, 2018)
Boehmite	• Water flux was significantly enhanced for 0.75 wt.% boehmite • BSA flux growth by 37.2%.	Water treatment	(Farjami, Moghadassi, Vatanpour, Hosseini, & Parvizian, 2019)
GO-ZnO nanocomposite	• Water flux was enhanced by 48%. • Higher flux during activated sludge filtration.	Water and wastewater treatment	(Ayyaru, Dinh, & Ahn, 2020)
Ag/TiO_2	• Inhibition of bacterial growth through disc diffusion method. • Better antifouling with a high FRR value of 64.9%.	N/A	(Haghighat, Vatanpour, Sheydaei, & Nikjavan, 2020)

2.3.4 Evaluation of Filtration Performance

Membrane filtration performance includes the capability of the membrane in terms of permeability, rejection, retention, flux, and fouling behavior. These parameters are often used to analyze the performance of a membrane and to describe the improvement made by the modified membrane. A modification usually aims to reduce the fouling occurrence, which is indicated by flux reduction. The flux data can be used to interpret and postulate the fouling mechanism, as well as to determine the fouling behavior, for example, resistance, reversible and irreversible fouling, and flux decline analysis. Table 2.7 shows the comparison of fouling analysis of modified PVDF membranes for the past decade regarding nanoparticle incorporation. Least found in the literature that the fouling and biofouling analyses were carried out simultaneously in a single study.

Table 2.7 Review on PVDF membranes modified with nanoparticles for fouling/biofouling mitigation.

Membrane Materials	NPs	Model Feed	Analysis		Ref.
			Fouling	Biofouling	
PVDF/PVP	Ag	BSA	Flux recovery percentage	• Antibacterial activity • SEM image	(X. Li et al., 2013)
PVDF/PVP/ PMAA[a]	Silica	• Sodium Alginate • Suwannee River natural organic matter • BSA	• Flux recovery • Cleaning efficiency	-	(Liang et al., 2014)
PVDF/PEG	TiO_2	BSA	FRR	-	(Méricq, Mendret, Brosillon, & Faur, 2015)
PVDF/PVP	GO/TiO_2	BSA	• Resistance-in-series model • FRR • Total fouling ratio (Rt) • Reversible fouling ratio (Rr) • Irreversible fouling ratio (Rir)	-	(Z. Xu et al., 2016)

Table 2.7, continued.

Membrane Materials	NPs	Model Feed	Analysis		Ref.
			Fouling	Biofouling	
• **PVDF/PVP/ PMANa[b]** • **PVDF/PVP/SA[c] PVDF/PVP/EDTA[d]**	SiO_2	Synthetic wastewater	Flux recovery percentage	-	(Liang et al., 2018)
PVDF	• SiO_2 • TiO_2 • Clay	BSA	FRR	-	(Farahani & Vatanpour, 2018)
PVDF/PEG	SiO2-g-PEGMA[e]	• Humic Acid • BSA • oil-in-water emulsion	• FRR • Rt • Rr • Rir	-	(Saini, Sinha, & Dash, 2019)
PVDF	Polyhexanide-CuO	• Humic acid • BSA	FRR	Antibacterial activity (halo-zone method)	(Sri Abirami Saraswathi, Rana, Divya, Gowrishankar, & Nagendran, 2020)
PVDF	Ag-GO	• Salt • BSA • *P. aeruginosa* solution	-	Normalized flux decline	(Y. Yu, Yang, Yu, Koh, & Chen, 2021)

Table 2.7, continued.

Membrane Materials	NPs	Model Feed	Analysis		Ref.
			Fouling	Biofouling	
PVDF/TiO_2	Au	BSA	-	Bactericidal rate	(L. Zhang et al., 2021)
PVDF/PVP	Ag	Varsity Lake water	• FDR • FRR • Foulant weight (TGA)	• Bacteria removal • Raman spectroscopy	*Current study*

[a] Poly(methacrylic acid)
[b] Poly(methacrylic acid sodium)
[c] Sodium alginate
[d] Ethylenediaminetetraacetic acid
[e] Poly(ethylene glycol) methacrylate

2.3.4.1 Fouling Analysis

Fouling is commonly analyzed based on flux during the filtration process. In the past decades, flux decline analysis was commonly reported to indicate fouling phenomena (Bhattacharjee & Bhattacharya, 1993). Later, reversible and irreversible fouling was determined based on the flux decline curve as cleaning actions were introduced at a particular time during the filtration process (Faibish & Cohen, 2001). Meanwhile, a resistance-in-series model can evaluate membrane intrinsic resistance attributed to different fouling factors based on water flux changes during filtration (Palencia, Rivas, & Pereira, 2009). A more recent study involves a simpler approach to evaluate membrane antifouling properties. The antifouling capacities of different a membrane are quantified using the flux recovery ratio (FRR), total fouling ratio (TFR), relative flux reduction (RFR), and flux decay rate (FDR) (Etemadi, Afsharkia, Zinatloo-Ajabshir, & Shokri, 2021; Lau & Yong, 2021; Teow, Chiah, Ho, & Mahmoudi, 2022). Among them, the most frequently found in literature is FRR which indicates the membrane resistivity against fouling (Asadi, Gholami, & Zinatizadeh, 2022).

2.3.4.2 Foulant Quantification

Another interesting yet critical aspect of fouling analysis is fouling quantification. Over the years, several methods have been used to quantitatively assess foulants. Tay, Liu, and Sun (2003) are the first to determine foulants' weight using thermogravimetric analysis (TGA). Schroën, Roosjen, Tang, Norde, and Boom (2010) use laser light reflectometry to quantitatively measure adsorbed amount per foulant unit area at the initial fouling stage. Meanwhile, Marroquin et al. (Marroquin et al., 2014) employ cross-sectional CLSM images to measure foulant amount at different depths. Thus far, the findings of these studies uphold the idea that it is vital to identify and quantify foulants for a deeper understanding of fouling mechanisms and propose an ideal mitigation approach (X. Zheng, Ernst, & Jekel, 2009).

2.3.4.3 Normal Raman and SERS

From the literature, the incorporation of AgNPs in PVDF membrane mainly discusses the ability of AgNPs to reduce fouling occurrences and portray antibacterial properties. There is little to no data concerning the deposited amount of foulants and closely observing the biofouling presence in surface water treatment applications. Cui et al. (L. Cui, Yao, Ren, & Zhang, 2011) reported that surface-enhanced Raman spectroscopy (SERS) has been used to examine the fouling process and evaluate the fouling propensity. Later, Lamsal et al. (Lamsal et al., 2012) demonstrated that SERS was better able to determine organics' functional group related to river water treatment compared to normal Raman. Both studies employed silver colloids as surface enhancers and established that SERS possessed immense potential in detecting organic foulant presence on the membrane surface.

From the literature, SERS substrates can be categorized into two; i. metal colloids and ii. structural solid substrates (Cardinal et al., 2017; Lal et al., 2008). Au or Ag nanostructures are usually prepared in liquid form as metal colloids before being centrifuged for relevant applications (Panneerselvam, Xiao, Waites, Atkinson, & Dluhy, 2018). Particle size, concentration, and species are the indicators that principally reflect SERS enhancement (H. Guo, He, & Xing, 2017). Therefore, the method of preparing and applying AgNPs as surface-enhancing substrates can differentiate the SERS's signal intensity. Additionally, it was reported that the structure of the SERS substrates and the friction direction significantly influenced the enhanced signal (Gao et al., 2019; H. Li, Ma, & Luo, 2021).

Despite these findings, not many attempts have been made to address the possibility of utilizing the embedded AgNPs in the membrane material as a surface-enhancing substance (R. Liu et al., 2019; S. Zhang et al., 2021). Liu et al. have reported that PVDF

sol was decorated with AgNPs to enhance Raman scattering signals upon immersion in multiple dye solutions (R. Liu et al., 2019). Whereas, Zhang et al. have investigated the additional functions of Au @ AgNPs in poly(vinyl alcohol) (PVA) membrane to amplify the Raman signals as the SERS substrate by applying the dye, humic acid, and proteins as foulant (S. Zhang et al., 2021). Figure 2.7 shows the illustration of the modified membrane cross-section in this study with the presence of metal nanoparticles.

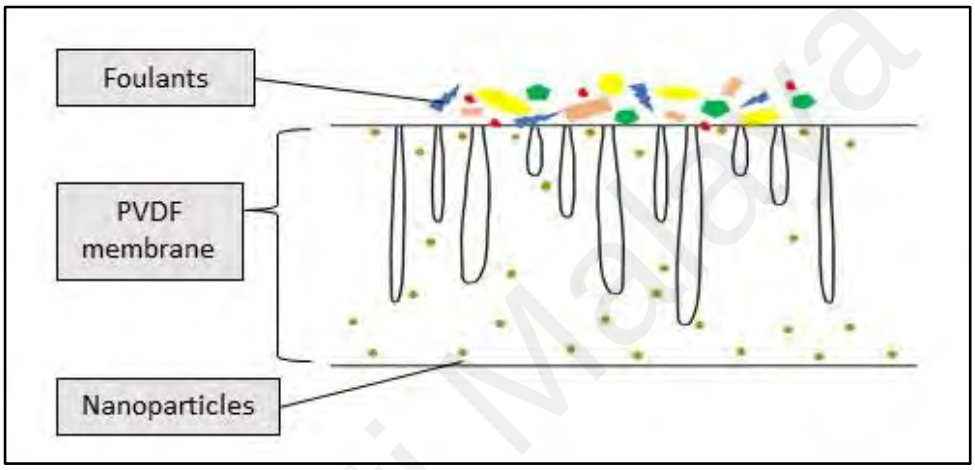

Figure 2.7 Illustration of fouled modified membrane cross-section.

An ideal biofouling mitigation approach should provide an effective hindrance to bacterial adhesion and possible reversible effect of microorganism deposition (Adout, Kang, Asatekin, Mayes, & Elimelech, 2010) making the attachment of biofouling on the membrane surface essential to be identified and examined. Due to the above-discussed limitations, SERS and TGA analyses can be utilized as an alternative approach for fouling analysis. Upon incorporation of AgNPs, the performance of such fouling mitigation approach can be analyzed at a more refined profile.

2.4 Silver Nanoparticles as an Antibacterial Agent

The word silver originates from Gothic meaning shiny white while Argentum means white and shinning which is of Aryan root (Pradeep & Anshup, 2009). For centuries, this noble metal was used in burns and chronic wound treatments (M. Rai et al., 2009). The

silver ions and silver-based substances were claimed to be highly toxic to microorganisms by showing strong biocidal effects on *E.coli* and 15 other species of bacteria (Spadaro, Berger, Barranco, Chapin, & Becker, 1974). An efficient and reliable tool for improving their biocompatibility is by reducing the particle size of materials as nanomaterials so they can be modified for better efficiency to facilitate their applications in different fields such as bioscience and medicine (J. S. Kim et al., 2007).

The nanoparticles possess a large surface area to volume ratio which helps in portraying good antibacterial properties. This supports the claim that the antimicrobial activity of colloidal silver particles is influenced by the dimensions of the particles: the smaller the particles, the greater the antimicrobial effect (L. Zhang et al., 2003). However, the exact mechanism of toxicity is still only partially understood (Guzman, Dille, & Godet, 2012; Q. Li et al., 2008). Figure 2.8 shows various possible mechanisms of antimicrobial activities exerted by nanomaterials.

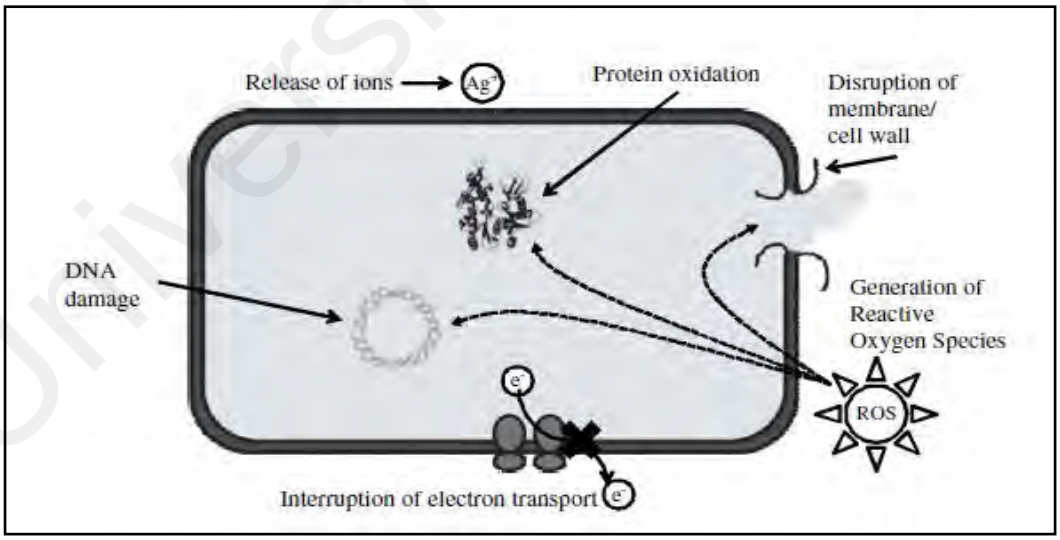

Figure 2.8 Various mechanisms of antimicrobial activities exerted by nanomaterials (Q. Li et al., 2008).

2.4.1 Bactericidal Mechanism of AgNPs

In 1974, Bragg and Rainnie claimed that the antimicrobial action of Ag-NP occurs due to the penetration of nanoparticles inside the bacterial cell membrane, thereby suppressing respiratory enzymes. Recent studies found that silver ions interact with thiol groups in proteins, resulting in the inactivation of respiratory enzymes and leading to the production of ROS (reactive oxygen species) (Matsumura, Yoshikata, Kunisaki, & Tsuchido, 2003). Ag+ ions interfere with DNA components inside the bacterial cell thus preventing DNA replication and transcription which affect the structure and permeability of the cell membrane (Feng et al., 2000; W.-R. Li et al., 2010; Pal, Tak, & Song, 2007).

This supported the finding in a study assessing the mechanism of toxicity induced by Ag nanoparticles that deduce Ag nanoparticles toxicity is mainly dependent on the presence of Ag ions (De Matteis et al., 2015). Since the underlying cellular and molecular mechanisms remain unclear, there is a report that fully reduced Ag nanoparticles have no antibacterial effect when the experiment is conducted in a condition that precludes the formation of Ag ions – anaerobic conditions (De Matteis et al., 2015). Also, there is a study suggesting that Ag nanoparticles are independent of free Ag ions which the mechanism of toxicity action may be different from those Ag ions (S. Kim et al., 2009). However, in the study, it was not excluded that Ag nanoparticles intracellularly released Ag ions in culture media. In a case study of *E.coli* as a model for gram-negative bacteria, negatively charged Ag nanoparticles interact with bacterial membrane material causing structural changes and degradation before the death of the cell (Sondi & Salopek-Sondi, 2004). In addition, a study conducted by Kawata et al. (2009) concluded that both Ag nanoparticles and Ag ions caused the toxicology effects of overall Ag nanoparticles (Kawata, Osawa, & Okabe, 2009).

Hence, in recent years several mechanisms have been postulated for the antimicrobial property of silver nanoparticles (Q. Li et al., 2008): (1) adhesion of nanoparticles to the surface alters the membrane properties. Ag nanoparticles have been reported to degrade lipopolysaccharide molecules, accumulate inside the membrane by forming ‘‘pits’’, and cause large increases in membrane permeability (Spadaro et al., 1974); (2) Ag nanoparticles penetrating inside the bacterial cell, resulting in DNA damage; (3) dissolution of Ag nanoparticles release antimicrobial Ag+ ions (Jose Ruben et al., 2005). On top of that, electrostatic attraction between negatively charged bacterial cells and positively charged nanoparticles is crucial for the activity of nanoparticles as bactericidal materials (Hamouda & Baker Jr, 2000).

2.4.2 AgNPs Synthesis for Membrane Application

To synthesize silver nanoparticles with well-defined shapes, several methods can be applied which the majority involved silver nitrate reduction (Moradi, Akhbari, Phuruangrat, & Costantino, 2017). During the synthesis, particle growth can be stabilized when a surfactant is present. Surfactant consists of different functional group for example; alcohols, amines, and thiols, which interact to stabilize growth, preserve its surface property, and prevent particles from agglomeration and sedimentation (Iravani, Korbekandi, Mirmohammadi, & Zolfaghari, 2014). Primitively, metal nanoparticles are likely to agglomerate and experience a coalescent process without the presence of a stabilizing agent. Gallic acid, sodium dodecyl sulfate, ethylene glycol, and polyvinyl alcohol are among the reported stabilizer used in nanometals synthesis (López-Miranda, López-Valdivieso, & Viramontes-Gamboa, 2012; Malina, Sobczak-Kupiec, Wzorek, & Kowalski, 2012; Pimpang, Sutham, Mangkorntong, Mangkorntong, & Choopun, 2008).

Upon definite material composition and synthetic conditions, polyvinyl pyrrolidone (PVP) can be utilized as a nanoparticle dispersant, surface stabilizer, reducing agent, and

growth modifier (Koczkur, Mourdikoudis, Polavarapu, & Skrabalak, 2015). PVP offered greater stability than citrate or tannic acid as it is strongly attached to AgNPs' surface (Mavani & Shah, 2013a). Therefore, stable and high concentration silver nanocolloids solutions can be directly synthesized involving chemical reduction by dissolving Ag/PVP nanocomposites in water or organic solvent (Mavani & Shah, 2013b). Significantly, in membrane fabrication PVP is used to initially increase casting solution viscosity and enhance membrane morphology by reducing macrovoids (J. S. Kang & Lee, 2002). However, the application of AgNPs stabilized by PVP specifically for the polymeric membrane is scarcely reported up till now.

Previous studies had demonstrated the effect of synthesis parameters mostly temperature towards the shape and size of AgNPs (Fleitas-Salazar et al., 2017; Pimpang et al., 2008; Piñero, Camero, & Blanco, 2017). Nevertheless, the least information was found about controlled synthesis with the presence of PVP. Instead, earlier works have focussed on the effect of PVP size and concentration used on the nucleation growth of AgNPs without manipulating other related synthesis parameters (J. S. Kang & Lee, 2002; Koczkur et al., 2015). Worth mentioning that there is no simultaneous study on the effects of synthesis temperature and precursor amount on AgNPs size which means for polymeric membrane incorporation. It is significant to emphasize that there is no detailed comparison of in-house synthesized AgNPs with commercial AgNPs performance as an antibacterial agent.

2.4.3 Embedment of AgNPs in Membranes

Water treatment for safe water supply especially during emergencies i.e natural disasters is crucial. A portable water treatment system, with a single step of producing drinkable water, is needed. Over the recent decades, the introduction of metallic nanoparticles in the filtration process for disinfectant effect has captured the interest of

researchers in the water treatment field. One of the many attempts made in utilizing the antibacterial properties of AgNPs is incorporating the AgNPs in polymeric membranes for water treatment application. However, over recent years, the performance of AgNPs was analyzed and evaluated at different depths of study. Consequently, the roles of AgNPs with their full potential were not utilized at the utmost. The ability to unveil the performance of AgNPs in many approaches is crucial, especially for an effective fouling mitigation approach.

It is well understood that Ag ions and Ag-based compounds are highly toxic to microorganisms which are commonly tested using *E.coli* and *S. aureus* (Y. Chen et al., 2013). As the mechanism of toxicity is still only partially understood, several mechanisms have been postulated for the antimicrobial property of silver nanoparticles – (1) adhesion of nanoparticles to the surface altering the membrane properties by degrading the lipopolysaccharide molecules, before accumulating inside the membrane and forming pits which cause a huge increment in membrane permeability (Sondi & Salopek-Sondi, 2004). Membrane modified or induced with silver nanoparticles can be carried out by applying several different methods. Among them, immersion is typically used in studying the antibacterial effects of the nanoparticles coated on the membrane surface.

2.4.3.1 Surface Modification of Polymeric Membranes

Yang et al. used a simple nanosilver-coating method in modifying the surface of the RO membrane and spacer to mitigate biofouling (Yang, Lin, & Huang, 2009). The RO membrane and spacer were then applied in seawater desalination. Using a modified chemical reduction method, woven fabric microfiltration membranes were soaked in $AgNO_3$ solution to coat the membrane surface with silver nanoparticles (C. A. Mecha & V. L. Pillay, 2014). The membrane was physically changed in color, yet it was claimed

that there is no significant difference in the morphology of the membranes after the impregnation.

In order to test the anti-bacterial properties of the modified membrane, water spiked with bacteria was filtered and removal efficiency of 100% was achieved. A hybrid membrane was prepared using polyethersulfone with sulfonated polyethersulfone before the membrane was immersed in excess $AgNO_3$ solution followed by reducing the silver nanoparticles with vitamin C (Cao, Tang, Liu, Nie, & Zhao, 2010). In this work, the advantage of the ion adsorption capacity of the sulfonated polyethersulfone was utilized to prepare silver nanoparticles on the surface of the sulfonated polyethersulfone by adsorbing the silver ions through the sulfonic group first before reducing them. This was to immobilize silver nanoparticles onto the membrane. In addition, a study on imparting antimicrobial and anti-adhesive properties was carried out (Tang, Huynh, Fleming, Larronde-Larretche, & Chen, 2015).

In a work reported by Tang et al., a microfiltration polysulfone membrane that was commercially purchased was modified by filtering silver nanoparticles suspension on the desired concentration through the membrane under dead-end filtration mode. Following that, a polyelectrolyte multilayer was assembled on the modified membrane surface under crossflow mode through the layer-by-layer adsorption technique. Using *E. coli*, the anti-biofouling properties of the membranes were found to be diminished with time-demanding further studies on methods to improve the robustness and longevity of the nanocomposites layers on the membranes (Tang et al., 2015).

Pan et al. have modified PVDF membrane for biofouling and organic fouling mitigation using Ag/SiO2 nanocomposites. In-situ formed AgNPs were synthesized via in-situ technique in solvent and immobilized with SiO2 nanoparticles which were then chemically bound onto a PVDF UF membrane surface to provide effective fouling control

strategies (Pan et al., 2017). In other ways, Samree et al, have modified commercial flat sheet PVDF membrane by dipped-coating approach in AgNPs suspension. However, a longer coating time reported results in membrane pores blockage by the aggregation of nanoparticles (Samree et al., 2020).

2.4.3.2 Chemical Bonding

The use of cysteamine as a bridging agent for attachment of AgNPs on the surface of PA thin-film composite membrane via covalent bond reduced biofouling effectively (J. Yin et al., 2013). In the study, a covalent bonding method was developed to immobilize AgNPs due to their stability in maintaining good water flux and salt rejection apart from reducing biofouling. As leaching is a common phenomenon in adding silver into membranes by physical blending, an attempt has been made to decrease the rapid depletion of silver, which slowly releases silver. On the other hand, chitosan has been used to bind silver on different materials through the coordination between silver ions and amino groups (nitrogen atoms) chitosan (Y. Chen et al., 2013). By creating covalent bonding interaction, acrylamide can be grafted onto the polymeric membrane surface and AgNPs formed within the grafted layer (Sawada et al., 2012).

2.4.3.3 In-Situ Method

An in-situ method is a method used to add silver into the casting solution. In a study on novel biogenic silver, the synthesized biogenic silver was introduced into the dope solution of PES membranes (M. Zhang, Field, & Zhang, 2014). The anti-bacterial properties of the modified membrane were evaluated by conducting experiments in an activated sludge tank for up to 9 weeks and also underwent bacterial suspension filtration of *E. coli*. Meanwhile, a study was conducted to determine bacterial deposition and detachment kinetics of a nanocomposite membrane where AgNPs were added to the polysulfone casting solution (Y. Liu, Rosenfield, Hu, & Mi, 2013). It was observed from

this study that the leaching of silver ions from the nanocomposite membrane was continuous with time but significantly slowed down within the first few hours. Meanwhile, the silver ions enhanced the anti-adhesive property of the nanocomposite membrane by decreasing the capability of bacteria to permanently attach to the membrane surface.

2.4.3.4 Other Types of Approaches

Another approach was reported in a study of wastewater treatment using a membrane bioreactor, where the prepared nanosilver stock was pumped into an anoxic chamber (M. Zhang et al., 2014). However, this action can be considered less effective in controlling biofouling as it does not significantly reduce fouling that was contributed by soluble microbial products, yet the biofilm formation on the hollow fiber PVDF membrane was reduced. To improve membrane performance, a study prepared nanoparticle-stacked membranes with a very thin active separation layer (Kawada, Saeki, & Matsuyama, 2014).

AgNPs with opposite charges were prepared using ionic polyelectrolytes as a stabilizing agent before the nanoparticles were stacked onto an inorganic supporting membrane through layer-by-layer dipping. The UF membrane performance was evaluated using a crossflow membrane filtration system with Mili-Q water as a feed solution. Among different synthesis options, the most favorable potential technique for the extensive and cost-worthy method of AgNPs preparation is by using the wet chemical synthesis technique (Sarkar et al., 2009).

2.4.4 Silver Leaching Phenomena

In a study on novel biogenic silver, an in-situ method was applied in which synthesized biogenic silver was introduced into a dope solution of PES membranes (M. Zhang et al., 2014). However, there is a study of observation on bacterial deposition and detachment

kinetics of a nanocomposite membrane where silver nanoparticles were added to the polysulfone casting solution (Y. Liu et al., 2013). From this study, the leaching of silver ions from the nanocomposite membrane was continuous with time but significantly slowed down within the first few hours while silver also enhances the anti-adhesive property of the nanocomposite membrane by decreasing the capability of bacteria to permanently attach to the membrane surface.

Since leaching is a common phenomenon in adding silver into membranes by physical blending, an attempt has been made to decrease the rapid depletion of silver which releases silver slowly. In creating covalent bonding interaction, acrylamide was grafted onto a polyethersulfone membrane surface and silver nanoparticles were formed within the grafted layer (Sawada et al., 2012). Commercially purchased polyethersulfone hollow fiber membranes were used and BSA protein solution was filtered to investigate the organic antifouling properties during the study which was later considered as successfully prepared a membrane with both antifouling and antibacterial properties. Using cysteamine as a bridging agent, attachment of AgNPs on the surface of polyamide (PA) thin-film composite membrane via covalent bond also effectively reduced biofouling (J. Yin et al., 2013).

Over the recent decades, the introduction of metallic nanoparticles in the filtration process for disinfectant effect has captured the interest of researchers in the water treatment field. One of the many attempts made in utilizing the antibacterial properties of AgNPs is incorporating the AgNPs in polymeric membranes for water treatment application. However, over recent years, it was reported that AgNPs embedded in polymeric membrane leached out and some may undergo a prolonged release. Consequently, many approaches have been carried out to immobilize AgNPs to sustain the antibacterial properties of the membrane which is crucial, especially for biofouling

mitigation. Table 2.8 shows the comparison of leaching analysis of AgNPs in sequence since 2013 related to PVDF membranes. Various impregnation methods were reported yet the leaching analysis was still scarcely reported even in the immobilization study.

Table 2.8 Comparison of leaching analysis of PVDF membrane impregnated with AgNPs concerning impregnation method.

Membrane Materials	Impregnation Method	Leaching Analysis			Ref.
		Condition	Period	Min. Ag Trace	
Ag/PVDF-g-PAA [a]	Grafting	N/A			(J.-H. Li, Shao, Zhou, Li, & Zhang, 2013)
Ag/PVDF	In situ formation	Dead-end filtration, 0.1Mpa	After 8hours	Less than 100 µg/l	(X. Li et al., 2013)
GO-Ag/PVDF	*Blending	Ultrasonic	10 hours	3.0 ppm	(J. Li et al., 2016)
Ag/PVDF-HFP [b]	*Mixing AgNPs	Vacuum filtration	2 hours	0.0275 ± 0.016 mg/L	(Macevele, Moganedi, & Magadzu, 2017)
PVDF/PVP/Ag	Blending $AgNO_3$	Dead-end filtration, 0.2Mpa	At 8^{th} hours	20 µg/l	(A. Abdul-Majeed, 2018)
PVDF/Ag	*Blending $AgNO_3$	N/A			(Nasir, Mataram, & Pujiono, 2019)
PVDF/Ag	*Mixing electrospinning	N/A			(Nthunya et al., 2019)
Ag/TiO2 /PVDF@TiO2	Coating	N/A			(Y.-X. Wang et al., 2019)
PVDF/AgNPs	*Coating	N/A			(Samree et al., 2020)
PVDF/Ag-SiO2	Dispersion	Dry membrane (EDX)	15days immersion	No leaching	(Ahsani, Hazrati, Javadi, Ulbricht, & Yegani, 2020)

Table 2.8, continued.

Membrane Materials	Impregnation Method	Leaching Analysis			Ref.
		Condition	Period	Min. Ag Trace	
PVDF-PVA/GO	Imprinted	N/A			(L. Yu, Yang, Zhang, & Yu, 2020)
Ag/EGCG [c] -PVDF	Soaking	Dead-end filtration, 0.2Mpa	After 1.5L filtration	1.2 µg/L	(N. Zhang et al., 2020)
PVDF/PVP/Ag	Mixing and thermal treatment	• Phase inversion • Dead-end filtration, 0.5 bar	• 96 hours • After 3.0L	-	*Current study*

[a] Poly(acrylic acid)
[b] Hexafluoropropylene
[c] Epigallocatechin gallate
* Not mentioned as immobilization attempt

2.5 Summary

Thus far, previous studies have revealed much information on surface water treatment using membrane technology. In short, a UF membrane is the most suitable membrane to be used for surface water treatment during a flood. However, to satisfy the needs during emergencies, which is a lack of infrastructure access and power supply, a one-step filtration process that is portable, reliable, and requires the least energy is needed. UF membrane needs to be further improvised to meet all the requirements. Also, the water quality profile needs to be considered for the filtration process that will disinfect and improve water quality. Impregnation of AgNPs in the membrane is promising but the immobilization and dispersion of the nanoparticles need to be extensively studied. Although the incorporation of nanoparticles in polymeric membranes has been previously reported for modification and biofouling mitigation, minimal work has been done on altering membrane casting conditions for incorporating nanoparticles and improving the immobilization of nanoparticles in the membrane matrix. The available literature discussing on AgNPs leaching phenomena in depth is very scarce. It is important to determine leaching phenomena as soon as it takes place to prevent contamination, sustain the antibacterial effect and provide better insights into enhancing the immobilization approach. In this regard, this study is able to determine leaching phenomena at the very beginning of membrane fabrication and immobilized AgNPs even before the filtration process was performed.

Furthermore, fouling and biofouling were simply investigated via flux decline analysis upon filtration for water treatment application. Minimal work was found to analyze the capability of AgNPs thoroughly in fouling and biofouling mitigation including other possible functions of AgNPs. Due to the above-discussed problems and limitations, SERS and TGA analyses can be utilized as an alternative approach for fouling analysis. Upon incorporation of AgNPs, the performance of such fouling mitigation approach can be

analyzed at a more refined profile. Therefore, this research aims to produce a membrane with immobilized well-dispersed AgNPs suitable for surface water treatment application with improved filtration performance. The mentioned bottlenecks inspired the author to carry out a study to achieve the objectives mentioned in Chapter 1.

CHAPTER 3 : METHODOLOGY

In this chapter, experimental setup and procedures are described in detail including the materials and equations involved. The experimental works comprise the chronology of experiments from the synthesis of AgNPs, characterization of the AgNPs and the modified membranes, followed by fouling analysis and possible use of AgNPs for Raman spectroscope, and lastly filtration performance of the membranes during its application in the bench-scale system.

3.1 Overall methodology

The overall research framework was written in a flow diagram in Figure 3.1. Sub-flow diagram of parameters, characterization, and analysis involved were also included to achieve all the objectives of this research.

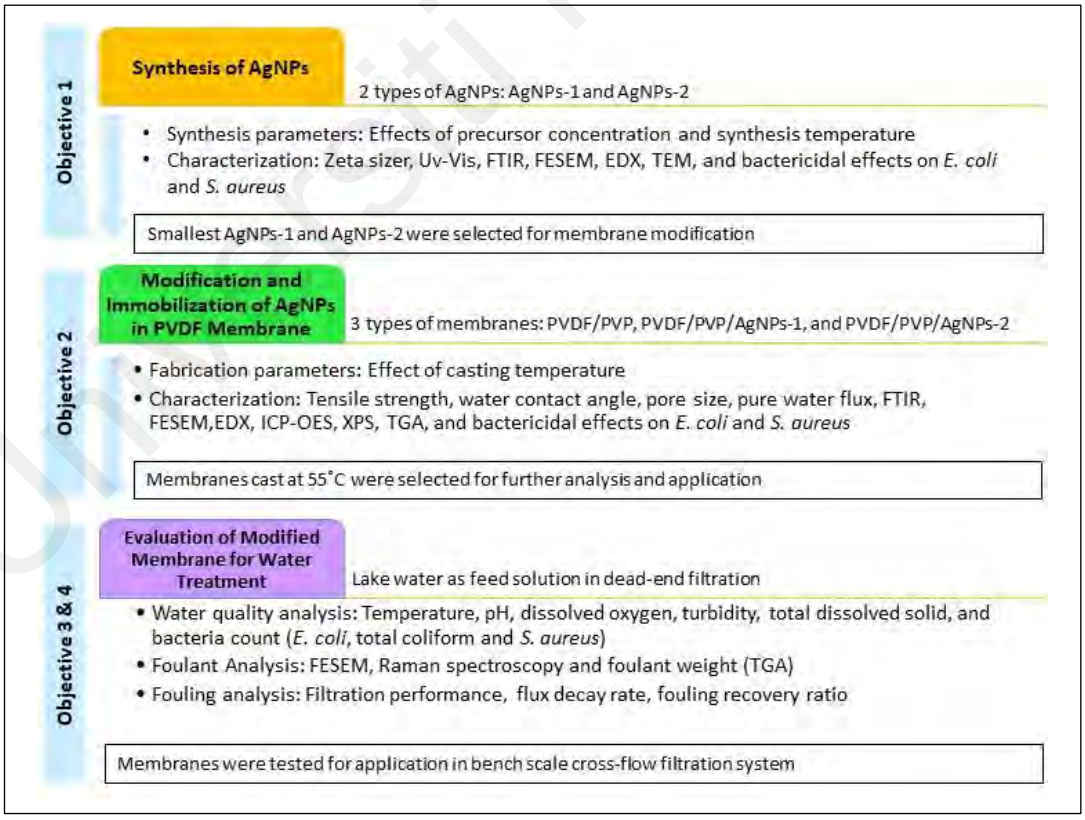

Figure 3.1 Overall research flow diagram.

3.2 Materials

All materials and chemicals used in this study were of analytical grade and used without any further purification. Polyvinylidene fluoride (PVDF) powder of 99.99% purity was obtained from Kynar, Arkema Group, China. Polyvinylpyrrolidone (PVP) powder with a molecular weight of ~40,000 g mol^{-1} was purchased from Bendosen. Silver nitrate ($AgNO_3$) powder of 99% purity, silver was obtained from Sigma Chemical Co., Western Australia. Commercial AgNPs of 30 nm and 100 nm for comparison of bactericidal properties were purchased from GetNanoMaterials, Oocap Inc., France. Sodium hydroxide (NaOH) granule 99% purity and Dimethylacetamide (DMAc) 99.98% purity were purchased from Merck, Germany.

Meanwhile, glucose powder, citrate stabilized AgNPs, PEG 100 KDa, bovine serum albumin (BSA), ovalbumin, azocasein, and lysozyme were obtained from Sigma Aldrich, USA. Dipotassium hydrogen phosphate (K_2HPO_4), potassium dihydrogen phosphate (KH_2PO_4), Coomassie® Brilliant blue G 250, AND phosphoric acid (H_3PO_4, 85%) were purchased from Merck, Germany. All these chemicals were needed for total protein determination. Ultrapure water was used throughout the study including as nonsolvent during the phase inversion technique. Count plate for *E. coli*, total coliform, and *S. aureus* was obtained from 3M, Petrifilm, United States. Ethanol absolute 99.8% was obtained from R&M Chemicals, Malaysia.

3.3 Synthesis of AgNPs

Two different methods were used to synthesize AgNPs. The first method was based on an in-situ approach while the second method was based on an ex-situ approach before being incorporated in membrane dope composition respectively. Throughout the synthesis process, skin and eye contact with all chemicals should be avoided. The experiments were all carried out in a laminar airflow fume hood to avoid inhalation.

3.3.1 Preparation of AgNPs Synthesized in DMAc

The method described by He et al. (He, Li, & Wen, 2015), was modified in this study whereby the amount of $AgNO_3$ and synthesis temperature were varied. 0.75 g PVP and different amounts of $AgNO_3$ (0.255, 0.510, or 0.765 g) were put in a 300 mL conical flask and 30 mL DMAc was added to dissolve the $AgNO_3$ salt completely. The mixture was stirred with a magnetic stirrer without any presence of light at a few different temperatures (25, 50, or 75°C). The reaction time at these temperatures was set to 10 minutes. Typically, a series of colour changes were observed during the synthesis before a specific colour scheme, dark brown was found unchanged. The AgNPs synthesized were denoted as AgNPs-1.

3.3.2 Preparation of AgNPs Powder Dispersed in DMAc

The method described by Andrade et al (Andrade, de Faria, Oliveira, Arruda, & Gonçalves, 2015) was modified in this study as the synthesis temperature and $AgNO_3$ concentration were varied. AgNPs were synthesized using an aqueous silver nitrate solution. Glucose was used as a reducing agent, sodium hydroxide as a reaction catalyst, and PVP as a stabilizer. 15 mL glucose (0.013 mol L^{-1}), 15 ml NaOH (0.01 mol L^{-1}), and 30 mL PVP (0.015 mol L^{-1}) aqueous solutions were combined and heated using a water bath at a constant speed. Once the above solution reached the temperature of interest (25, 50, or 75°C), at 1drop/s rate, 20 mL of $AgNO_3$ aqueous solution at different concentrations (0.01, 0.03, or 0.05 mol L^{-1}) was added and stirred for 10 minutes of reaction time. The solution was centrifuged (Centurion CR4000R, UK) at 10000 rpm for 30 min. Lastly, to remove nitrate ions and excess reactants, the reaction products were washed with DI water thrice. The AgNPs obtained were let dry at 60°C for 3 days to remove all moisture. The powder was then weighted and dispersed in DMAc for further characterization. DMAc was chosen as a solvent for dispersion as it is the common solvent used in polymeric membrane fabrication. During the study, the synthesized

AgNPs were denoted as AgNPs-2. Simplified methods of AgNPs synthesis were illustrated as in Figure 3.2.

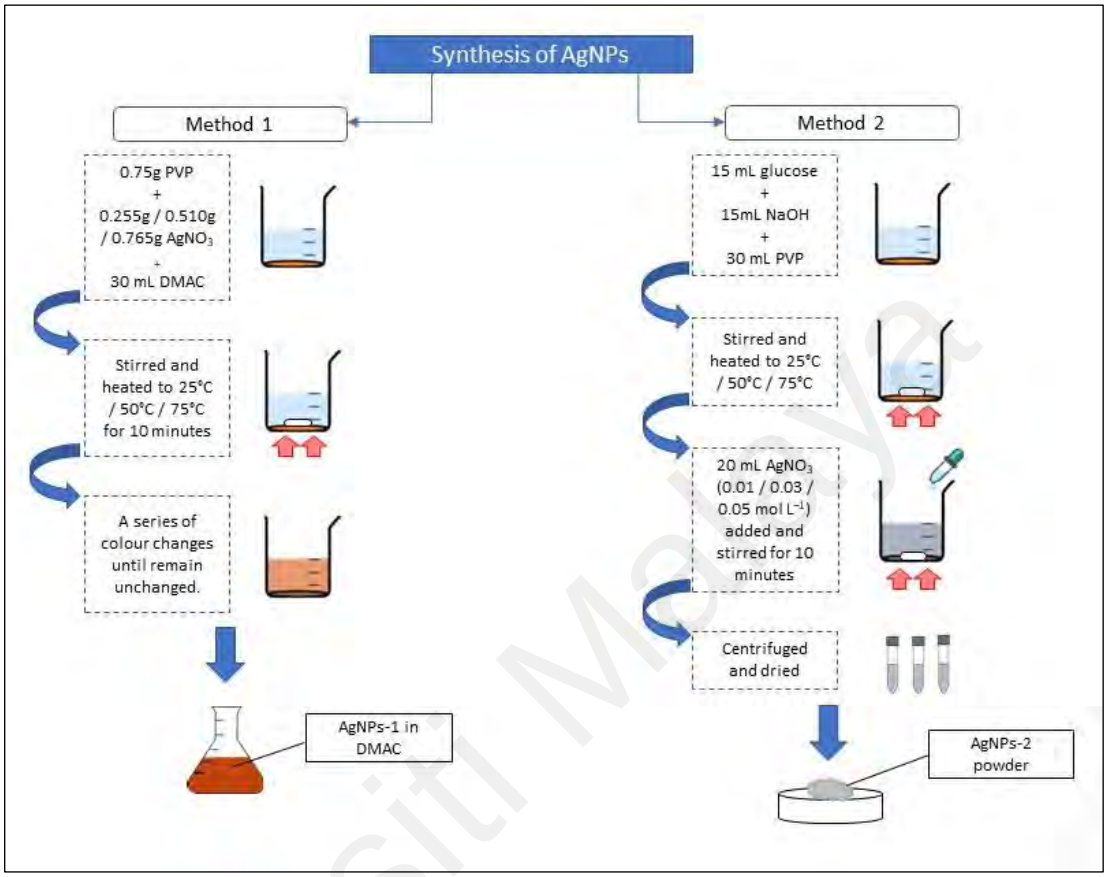

Figure 3.2 The methods of AgNPs-1 and AgNPs-2 preparation.

3.3.3 AgNPs Synthesis Parameters

During the synthesis of AgNPs for both methods, temperature effects on AgNPs size were studied at 25, 50, and 75°C. Different amounts of $AgNO_3$ powder of 0.255, 0.510, and 0.765 g were used during the synthesis of AgNP-1 while the different concentrations of $AgNO_3$ namely 0.01, 0.03, and 0.05 mol L^{-1} for the synthesis of AgNPs-2 powder were used to study the effects of precursor amount.

3.4 Characterization of AgNPs

Size, absorbance, elemental composition, and morphology of the synthesized AgNPs were characterized. The size of the AgNPs was measured using a particle size analyzer,

Zetasizer (Malvern, UK) at 25°C in terms of nm and set for three replicates for an average reading. The particle size distribution was also recorded. The absorption bands present in the samples were characterized via Ultraviolet-visible (Uv-vis) absorption spectroscopy (UV-1800, Shimadzu, Japan). Fourier transform infrared spectroscopy (FT-IR Spectrum 400, ATR, Perkin Elmer Inc., USA) aimed to observe the molecular bond of the AgNPs prepared. The size and morphology of AgNPs were analyzed using Field Emission Scanning Electron Microscope (Quanta FEG 450) at an operating voltage of 1.00 kV. Besides, the prepared AgNPs were characterized using Energy Dispersive X-ray Spectroscopy (EDX-OXFORD). Further characterization was carried out using Transmission Electron Microscopy (HR-TEM 120 KV, Hitachi HT7700). Samples were prepared by dropping the liquid mixture on copper-coated grids.

3.5 Bactericidal Performance of AgNPs

Two different sizes of commercial AgNPs were used to compare the bactericidal performance of commercially available silver and synthesized silver in this study. Commercial AgNPs with a size of 30 nm were denoted as AgNPs-C1 and commercial AgNPs with a size of 100 nm were denoted as AgNPs-C2. Lake water was chosen as a model water sample in the application of surface water treatment using the modified PVDF membranes. Lake water is used to simulate the composition of the surface water quality affected during a flood. A sample of Universiti Malaya's Lake was taken and tested for the presence of *E. coli* and *S. aureus* bacteria and triplicate for the average number of bacteria. The test was carried out using a commercial purchase count plate (3M, USA). This method was chosen as the count plate portrays the number of living bacteria indicating approximate antibacterial effects of the samples tested. Each AgNPs were placed on a filter paper in the uniform size of 0.8 cm^2 before placing it on the count plate. All AgNPs were quantified at an equal amount before being tested. The log and

percentage reduction of bacteria were calculated based on Eq. (3.1) and Eq. (3.2) as follows;

$$Log\ reduction, L = \log_{10} \frac{A}{B} \quad \text{Eq. (3.1)}$$

$$Percent\ reduction, P = (1 - 10^{-L}) \times 100 \quad \text{Eq. (3.2)}$$

Where;

A = number of living microorganisms in the lake water sample

B = number of living microorganisms in the lake water sample with the presence of AgNPs

Note that, commercial AgNPs selected, denoted as AgNPs-C1 and AgNPs-C2, were chosen based on the nearest size available on market to the size of the smallest selected AgNPs-1 and AgNPs-2 which was tabulated as Table 3.1.

Table 3.1 The size of commercial and synthesized AgNPs.

Nanoparticles	***Size, nm***
AgNPs-1	30.88
AgNPs-2	109.50
AgNPs-C1	30
AgNPs-C2	100

3.6 Preparation of Membrane Casting Solution

To prepare the casting solution, 2 g PVP as pore former was dissolved in 79.55 g DMAc at a constant speed and heated up to 60°C. 18 g of polymer powder was added to the solution and stirred for up to 8 hours to ensure a homogeneous solution was obtained. The solution was degassed to remove bubbles and preserved overnight before being fabricated as a flat sheet membrane. AgNPs-1 was firstly synthesis in DMAc according to the method described in section 3.3.1. For casting solution containing AgNPs-2, 0.45 g of AgNPs-2 powder were first dispersed into DMAc before PVP and PVDF were added

as previously described. The weight percentage of casting solution composition for DMAc, PVDF, PVP, and Ag was computed based on the method in sections (3.3.1), (3.3.2), and (3.3.3) tabulated as in Table 3.2. The prepared membrane casting solutions have a different physical appearance as shown in Figure 3.3.

Table 3.2 The weight percentage of each casting solution composition.

	Weight percent, %			
Casting solution formulation	**DMAc**	**PVDF**	**PVP**	**Ag**
PVDF/PVP	80	18	2	0
PVDF/PVP/AgNPs-1	79.18	18	2.11	0.45
PVDF/PVP/AgNPs-2	79.55	18	2	0.45

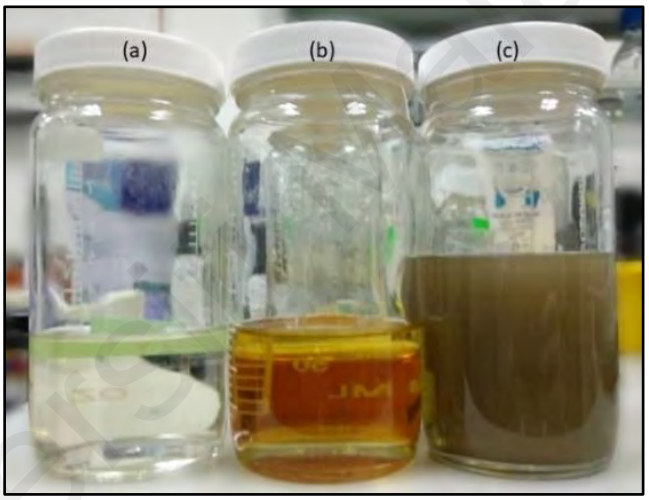

Figure 3.3 Casting solution of (a) PVDF/PVP, (b) PVDF/PVP/AgNPs-1, and (c) PVDF/PVP/AgNPs-2.

3.7 Fabrication of Ultrafiltration PVDF Membranes

The plate was heated up to a few different temperatures as stated below to investigate the effect of thermal treatment. Concerning common dissolution temperature of PVDF starts at 55°C and the flash point of DMAc is 63°C while the ambient temperature is 25°C, the elevated temperature for membrane fabrication was carried out at 25, 40, 55°C respectively. Then, the casting solution was cast onto the heated glass plate. With an aid of an automatic film applicator, Elcometer 4340 Motorised, the solution was uniformly

spread at 250 μm gate height at a 30 mm/s shear rate. Approximately, the time between casting the solution and transferring it into the ultrapure water coagulation bath was 10s. The membrane then naturally peeled off from the glass plate and was further immersed in ultrapure water for 96 hours before dried at ambient temperature for further characterization. The ultrapure water of the coagulation bath was changed every 24 hours. The setup for membrane fabrication and phase inversion was illustrated in Figure 3.4.

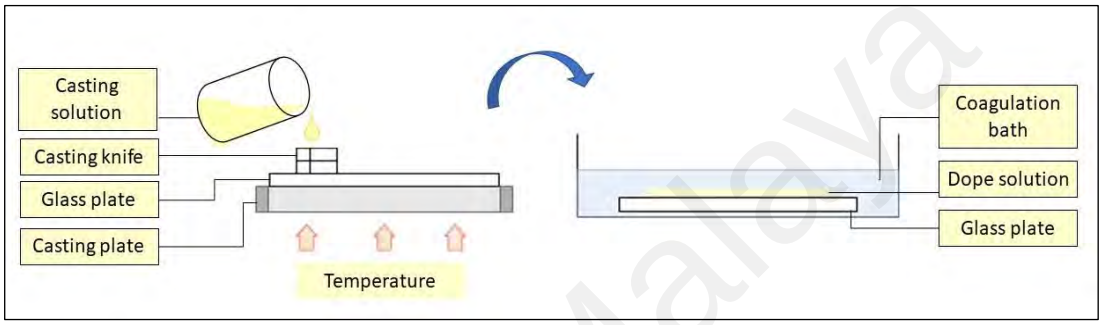

Figure 3.4 Thermal treatment approach during membrane casting and phase inversion setup.

3.8 Characterization of PVDF Membranes

Membrane characterization was carried out after the phase inversion process was completed and the flat sheet membranes were let dry at ambient temperature for 48 hours. Tensile strength measurement was carried out to study the mechanical properties of the membranes using Instron 5569, Instron, USA. The contact angle measurement was carried out based on the sessile drop method. 5 μL of ultrapure water was dropped on top of the dried membrane surface and the contact angle between the water droplet and membrane surface was measured. At least five different locations of water contact angle were measured and averaged. The permeability of ultrapure water across the membrane was recorded at the pressure of 0.5 bar using dead-end filtration set at room temperature to study the membrane filtration performance. Pure water flux for all fabricated membranes was determined using ultrapure water only after compaction. The pure water flux, J was calculated based on Eq. (3.3) where filtration time to filter 3.0 L of ultrapure

water as feed was taken into account. The pore size distributions of the membranes were identified using Porometer from Beneflux Scientific, Belgium. The prepared membranes with a diameter of 2 cm were immersed in porefil (surface tension of 16 dynes/cm) before being analyzed using nitrogen gas with increasing pressure. The membranes morphology was analyzed using Fourier transform infrared spectroscopy (FTIR), FT-IR Spectrum 400, ATR, Perkin Elmer Inc., USA. The pore distribution and morphology of the membranes were investigated using Field Emission Scanning Electron Microscope (FESEM), Quanta FEG 450 at an operating voltage of 2.00 kV with the magnification of 300x to 3.00Kx accordingly. The prepared membranes were also characterized using Energy Dispersive X-ray Spectroscopy (EDX), Oxford EDX system to identify silver elements present in the membrane matrices.

$$J = \frac{Q}{A \times t} \qquad \text{Eq. (3.3)}$$

Where;

Q = volume of permeated water, L

A = effective membrane area of filtration, m^2

t = filtration time, h

3.9 Leaching Analysis of AgNPs from Membranes

Herein, leaching phenomena refer to the amount of Ag released during the fabrication of the membranes known as the phase inversion process. During phase inversion, the flat sheet membrane was immersed in ultrapure water for up to 96 hours to investigate any silver leaching traces in the coagulation bath. Ag traces were examined instantaneously when the glass plate was placed in the coagulation bath and denoted as t=0. For every 24 hours of immersion, the sample of coagulation bath ultrapure water was taken to determine the presence of Ag as leaching phenomena happened. The volume of ultrapure water in the coagulation bath was controlled at 5.0 L with a known weight of casting

solution immersed to quantify the leaching percentage. Samples of ultrapure water in the coagulation bath were taken in three replicates and analyzed using Inductively Coupled Plasma Atomic Emission Spectroscopy (ICP) Optima 7000 DV ICP-OES, Perkin Elmer, USA with a detection limit of 1ppm. The leaching percentage of AgNPs was determined based on Eq. (3.4) to Eq. (3.6). The calibration curve for AgNPs concentration was attached in Appendix A. To further analyze the composition of the flat sheet membrane, X-ray photoelectron spectroscopy (XPS) from K-Alpha Surface Analysis, Thermo Scientific was used to closely examine the embedment of Ag element in the membrane morphology at the top and bottom surface of the dried membrane. Dried membranes with the least leached AgNPs were characterized using Thermal Gravimetric Analysis (TGA), TA Instrument Q500, England under nitrogen flow, and the weight loss of membranes was monitored over the temperature of 50 to 600°C to analyze the residual silver in the membranes' composition after the 96 hours immersion.

$$Weight\ of\ Ag\ traces\ in\ bath, W_{Ag\ bath} = C_{Ag} \times V_{bath} \quad \text{Eq. (3.4)}$$

$$Weight\ of\ Ag\ in\ dope, W_{Ag\ dope} = W_{Ag} \times W_{dope} \quad \text{Eq. (3.5)}$$

$$Leaching\ Percent, Ag_L = \frac{W_{Ag\ bath}}{W_{Ag\ dope}} \times 100 \quad \text{Eq. (3.6)}$$

Where;

C_{Ag} = Concentration of Ag from ICP analysis, ppm

V_{bath} = Volume of ultrapure water in coagulation bath, L

W_{Ag} = Weight percentage of Ag in casting solution formulation, %

W_{cast} = Weight of casting solution poured for membrane fabrication, g

3.10 Determination of Molecular Weight Cut-Off

To determine the MWCO of the selected membrane, several types of protein and PEG with known molecular weight were filtered. Protein presence was tested using Bradford reagent and the concentration was quantified. Protein with a concentration of 1000 ppm was prepared in a buffer solution and filtered at a pressure of 0.5 bar. Meanwhile, PEG concentration was determined using total organic carbon (TOC) analysis (Shimadzu TOC-VCPH, Japan). The detailed procedure of total protein concentration analysis was explained in Appendix B including the calibration curve. The calibration curve for TOC analysis of PEG concentration was attached in Appendix C. The protein and PEG used for this experiment and their molecular weights were listed as in Table 3.3.

Table 3.3 Proteins and PEG with their molecular weight and average solute radius.

Protein	Molecular weight (kDa)	Average solute radius (nm)
Bovine serum albumin (BSA)	66	4.5
Egg albumin / Ovalbumin	45	3.3
Azocasein	23.6	2.15
Lysozyme	14.3	1.9
PEG	100	-

3.11 Membranes Bactericidal Performance

Membranes containing AgNPs-1 and AgNPs-2 with the least leaching phenomena were selected for bactericidal performance analysis. The lake water sample was taken and tested for the presence of *E. coli* and *S. aureus* bacteria as these bacteria were commonly used in water treatment studies representing the gram-negative and gram-positive bacteria (Y. Chen et al., 2013). Using the count plate method, only viable bacteria including total coliform are counted with this method as the method excludes dead bacteria and debris (Hazan, Que, Maura, & Rahme, 2012). Bacteria count for lake water samples before in contact with the membrane was measured. Bacteria count for lake water samples in the

presence of PVDF/PVP, PVDF/PVP/AgNPs-1, and PVDF/PVP/AgNPs-2 membrane were carried out for further analysis and comparison. The dried membrane was cut to the same size of 0.28 cm^2 and placed on the count plate. 1 mL of lake water sample was carefully pipetted and evenly speared on the count plate in contact with the membrane. As the count plate portrays the number of living bacteria in a sample, the bactericidal capability of the membranes was measured based on the reduced number of living bacteria in the sample. The log and percentage reduction of bacteria were calculated based on Eq. (3.1) and Eq. (3.2).

3.12 Characterization of Lake Water

Varsity Lake located in Universiti Malaya was selected to represent surface water as feed during the filtration process. The lake water sample was taken and used on the same day as the experiments and characterizations. The lake water was characterized based on several water quality parameters. Dissolved oxygen (DO), pH, temperature, and total dissolved solids (TDS) were determined using Professional Plus Multiparameter Water Quality Meter, YSI Inc., USA. Turbidity of the lake water was measured using 2100Q Portable Turbidimeter, Hach, USA. Then, presence of *S. aureus* bacteria and *E. coli*. bacteria were tested using a commercial count plate (3M, USA). 1 mL of the sample was placed on the count plate and let sit in a dry dark container for 48 hours before being ready for colony count.

3.13 Filtration of Lake Water in Dead-end Cell

A dead-end filtration setup was used to employ the fabricated membranes for the filtration of surface water. The lake water was filtered by using nitrogen gas at 0.5 bar as the driving force with an effective area of 15.91 cm^2. The feed temperature was kept at 25 ± 1°C. The flux of ultrapure water was first determined and known as initial flux, J_i. Then, the flux of lake water was computed for every 1.0 L feed. The total amount of feed

filtered was 3.0 L and the flux was consecutively denoted as J_1, J_2, and J_3. The average flux of the feed was denoted as J_{av}. Next, ultrapure water was filtered, and the final flux was denoted as J_f. FDR and FRR were computed using Eq. (3.9), and (3.10), respectively:

$$FDR = \left(1 - \frac{J_{av}}{J_i}\right) \times 100 \quad \text{Eq. (3.9)}$$

$$FRR = \frac{J_f}{J_i} \times 100 \quad \text{Eq. (3.10)}$$

Where;

J_{av} = average lake water flux of J_1, J_2, and J_3

J_i = initial flux of ultrapure water

J_f = final flux of ultrapure water

3.14 Determination of foulant weight (FW) using TGA

Fresh membranes, as well as fouled membranes, were desiccated at room temperature for 3 days. The dried membranes were then analyzed under nitrogen flow by a thermogravimetric analyzer (TA Instrument Q500, England). The membrane's weight loss was examined at the temperature ranges of 100 to 700°C. Non-volatile foulant weight (FW_{NV}) was calculated from the data obtained from TGA by using Eq. (3.11) (Tay et al., 2003).

$$FW_{NV} = a_m \frac{\eta_f^T - \eta_m^T}{1 - \eta_f^T} \quad \text{Eq. (3.11)}$$

Where;

a_m = surface density of membrane (weight per unit surface area of membrane)

η_f^T = weight percentage of the remaining portion of the fouled membrane at T

η_m^T= weight percentage of the remaining portion of the clean membrane at T

On the other hand, the non-volatile fouling rate (FR_{NV}) was determined based on Eq. (3.12). FR_{NV} was computed in this study to compare the rate of fouling occurrence in modified membrane to the native membrane as a significant indication of the fouling mitigation approach's effectiveness.

$$FR_{NV} = \frac{FW_{NV}^{m}}{FW_{NV}^{n}} \times 100 \qquad \text{Eq. (3.12)}$$

Where;

FW_{NV}^{m} = foulant weight of the modified membrane

FW_{NV}^{n} = foulant weight of the native membrane

Based on the study of BSA as a foulant with known thermogravimetric properties, volatile foulant weight was expressed as Eq. (3.13) (Tay et al., 2003).

$$FW_V = \mathrm{a_m} \frac{\eta_m^T - \eta_f^T}{\eta_f^T - \eta_v^T} = \mathrm{a_m} \frac{\mathrm{W_v}}{\mathrm{W_m}} \qquad \text{Eq. (3.13)}$$

Where T in Eq. (3.13) is in the range of 105˚C < T < 500°C, which is considered as the low temperate range. Temperature-scan curves of the clean membrane, feed volatile component, and fouled membrane should be determined to compute the sum of FW (Tay et al., 2003). However, since the lake water is considered as a feed solution of unknown composition and the temperature-scan curve of total solids in the lake water is hardly carried out, total foulant weight (FW_t) can be computed using Eq. (3.14) by assuming FW_{NV} from equation (3.11) at lowest remaining percent was already the sum of FW_{NV} of the membrane.

$$FW_t = \mathrm{a_f} - \mathrm{a_m} \qquad \text{Eq. (3.14)}$$

Where;

$\mathrm{a_f}$ = surface density of fouled membrane

Based on equation (3.14) the FW_V of the membrane can be calculated as Eq. (3.15).

$$FW_V = FW_t - FW_{NV} \quad \text{Eq. (3.15)}$$

Throughout the experiments, a few assumptions and postulation have been taken into consideration as follow;

i. Physical appearance, weight, and thermogravimetric properties of clean and fouled membranes were different due to foulant or fouling materials.

ii. The foulant was evenly distributed across the membrane effective area despite only a small piece of the membrane being sampled for SEM, Raman, and TGA analysis.

iii. No further chemical reaction occurs upon contact with foulant and membrane surface; foulant was physically attached to the membrane surface and pores after the filtration process.

iv. "The fouling material can be categorized as 'volatile' and 'non-volatile' components. In practice, it is assumed that the volatile component undergoes decomposition in the temperature range of 105–500°C and loses weight completely beyond 500°C; whereas the non-volatile component does not lose weight even up to a high temperature beyond 500°C. In fact, volatile fouling material is mainly composed of organic substances, whereas non-volatile fouling material is made up of inorganic substances. It is known that the loss of organic matter by volatilization usually is minimal less than 103°C; mainly occurs in the higher temperature range up to 500°C" (Eaton et al., 1995, as cited in Tay et al., 2003).

v. Total foulant weight was determined based on the difference between clean and fouled membrane weight only.

vi. As TGA gives numerous readings of residual weight percentage with the increase of temperature, reasonable temperature ranges were selected along with 5 other different

points before and after the specific temperature for computation, and the average values were calculated to minimize the bias.

3.15 Normal Raman and SERS analysis

A confocal Raman microscope (LabRAM HR-800, Horiba, Japan) was used to collect all normal Raman and SERS spectra. The 532 nm excitation was obtained using YAG laser of 100 mW. A 20X objective lens was employed for laser beam focus. A small piece of clean and fouled membranes was cut into approximately 1x1 cm square and placed under the laser directly before the spectra of normal Raman were collected. On the other hand, 5 μL of citrate stabilized AgNPs (10 nm) colloids was placed onto the membrane coupon surface for SERS. After the suspension had dried, the spectra were recorded. Spectra for each sample were measured three times at different spots and all the spectra reported here were measured within an accumulation time of 20 s.

3.16 Filtration of lake water in bench-scale system

Despite the use of a dead-end cell filtration system to analyze the filtration performance of the modified membranes, filtration of lake water in a bench-scale crossflow system was carried out to investigate the filtration performance at a longer period which is commonly designed for large scale applications. The image of the bench scale filtration system used is as in Figure 3.5. The layout set-up for the bench scale crossflow filtration system is illustrated as in the schematic diagram in Figure 3.6 below.

Figure 3.5 Bench scale crossflow filtration system.

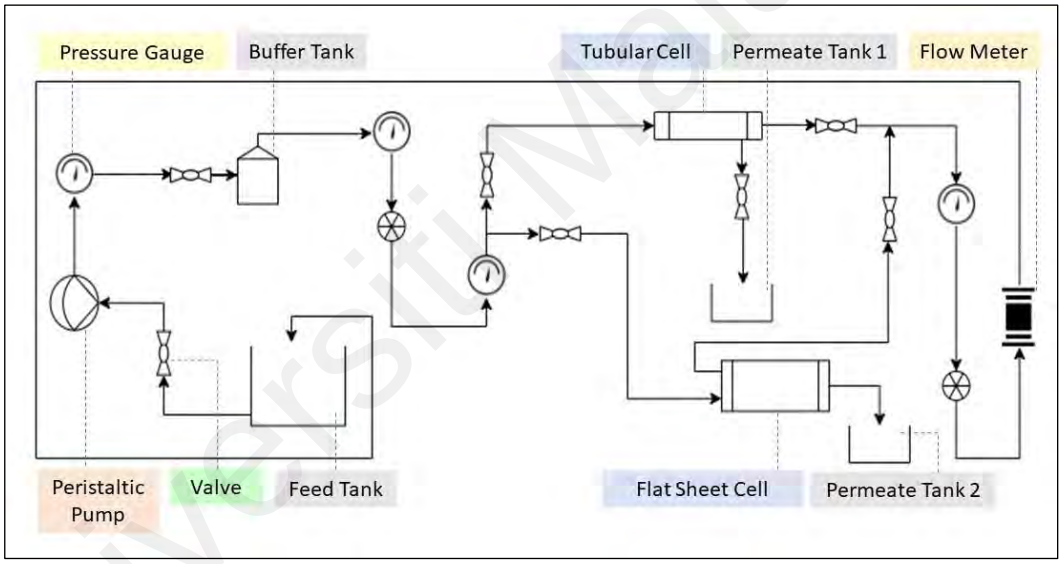

Figure 3.6 Schematic diagram of bench scale crossflow filtration system.

The transmembrane pressure was controlled at 0.5 bar using a crossflow configuration set up with a capacity of 2000 ml feed and effective membrane area of 41.0 cm^2. Similar to the procedure using dead-end cell, the flux of ultrapure water was first determined and known as initial flux, J_w. Then, the flux of lake water was computed for 3 hours operation time. The total amount of feed filtered was measured and the flux was denoted as J_{lake}. The normalized flux was computed using Eq. (3.16) and denoted as J_N. At the end of the

filtration period, ultrapure water was filtered, and the final flux was denoted as J_w'. FDR and FRR were computed using Eq. (3.9), (3.10) as previously mentioned.

$$J_N = \frac{J_{lake}}{J_w} \quad \text{Eq. (3.16)}$$

Where;

J_N = normalized flux

J_{lake} = flux of lake water filtration

J_w = initial flux of ultrapure water

CHAPTER 4 : RESULTS AND DISCUSSIONS

All results obtained from the experiment were gathered and discussed. From the experiment, the size of AgNPs synthesized were determined before further characterized and selected for incorporation into membrane formulation. During membrane fabrication, a thermal treatment approach was applied to immobilize AgNPs. Selected membranes were implemented in a crossflow system for water treatment application.

4.1 Effect of Synthesis Parameters on AgNPs Size

Effect of synthesis parameters – precursor amount and synthesis temperature were investigated. The effect of synthesis parameters on AgNPs sizes which were determined based on hydrodynamic size will be further discussed based on Figure 4.1 and Figure 4.2 for AgNPs-1 and AgNPs-2 accordingly. All synthesized AgNPs-1 and AgNPs-2 sizes were tabulated and provided in Appendix D.

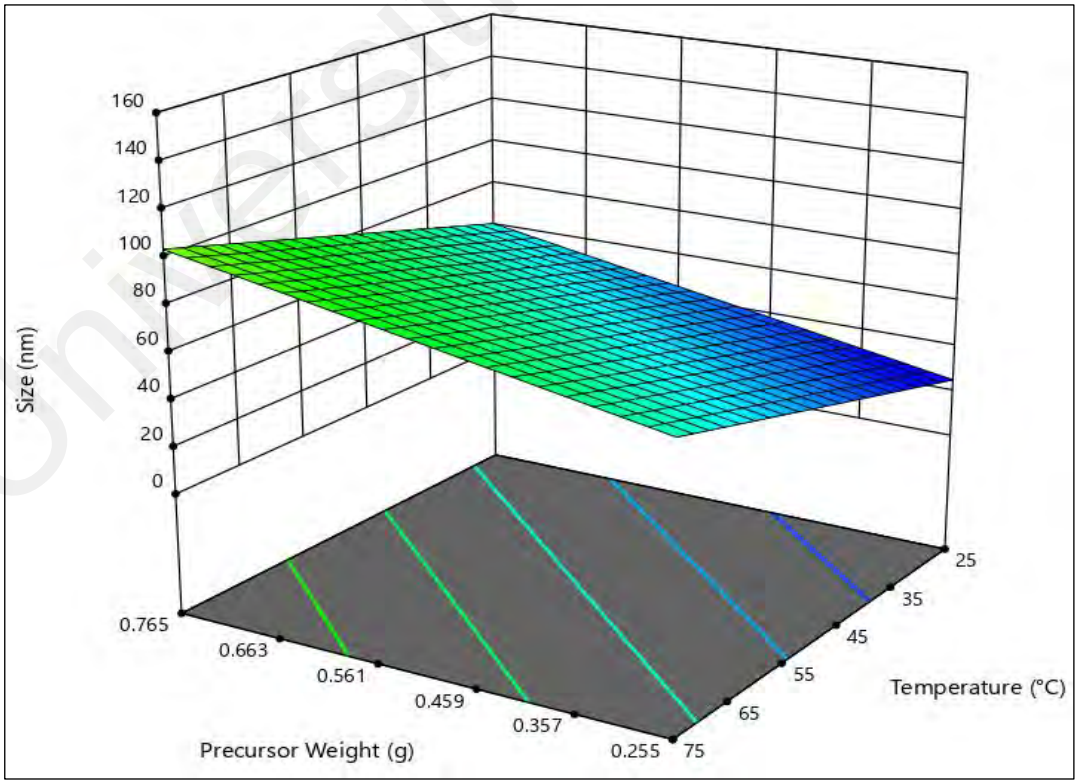

Figure 4.1 3D graph of precursor weight and temperature versus nanoparticles sizes for AgNPs-1.

Figure 4.1 shows the various sizes of AgNPs-1 that were obtained from the synthesis of AgNPs in DMAc solvent. For 25 °C synthesis temperature, the AgNPs size obtained was in a range of 30.88 nm to 99.16 nm. The smallest size was obtained when using 0.255 g $AgNO_3$ while the largest AgNPs were obtained during this temperature when using 0.765 g $AgNO_3$. It is believed that at the smallest amount and lowest temperature, the reduction rate was very minimal producing smaller AgNPs in terms of size and amount. However, with the addition of precursors which was thrice of 0.255 g, the largest AgNPs was formed. This excessive amount of precursor offered a surfeit free radical from metal salts which result in coalescence and nanoparticles aggregation (Fleitas-Salazar et al., 2017).

For 50°C synthesis temperature, the smallest size of 34.69 nm was obtained when using 0.255 g $AgNO_3$ while the largest AgNPs of 68.73 nm was obtained when using 0.510 g AgNO. While for 75°C synthesis temperature, the AgNPs size obtained was in a range of 53.72 nm to 130.70 nm. The significant difference in size at 75°C synthesis temperature was due to the accelerated reduction process at higher temperature causing an extended nucleation process to take place (J. Polte, 2015). The reduction process rapidly happened, and this was in good agreement with research done by Pinero et al. (Piñero et al., 2017). The reaction kinetic, the aggregative mechanisms of the nanoparticles, and the movement of atoms on the solution (Brownian movement) were all changed by the increment of the temperature (Piñero et al., 2017).

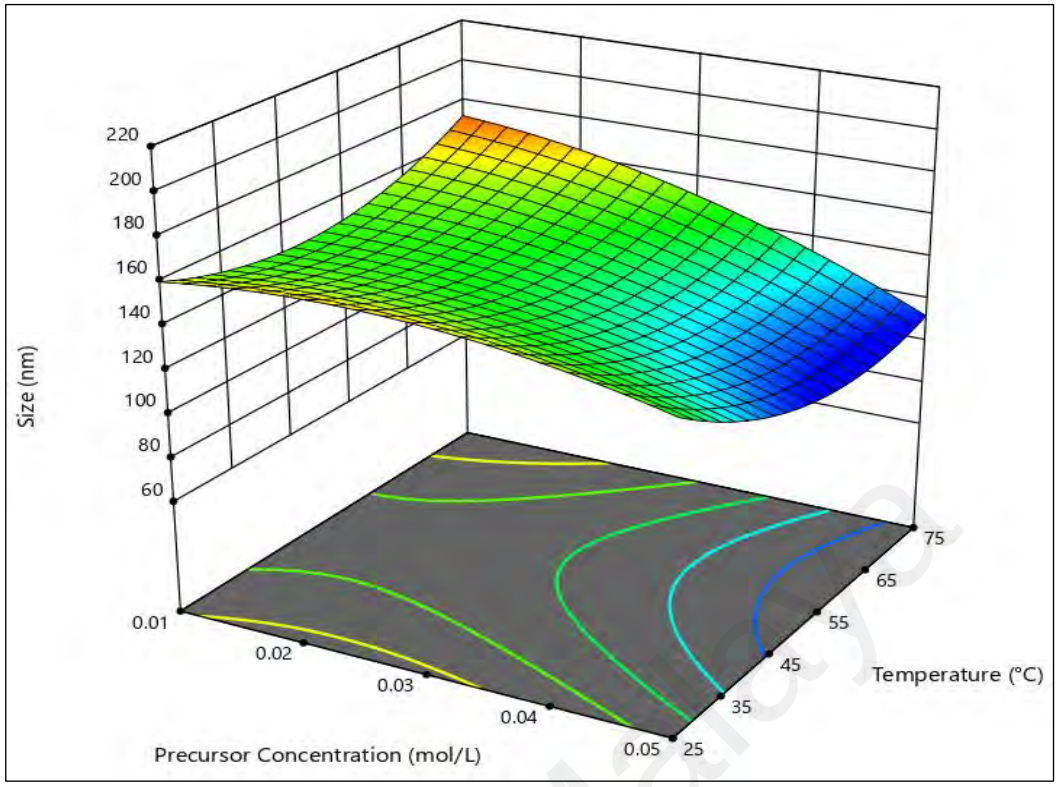

Figure 4.2 3D graph of precursor weight and temperature versus nanoparticles size for AgNPs-2.

As for AgNPs-2, Figure 4.2 portrays various sizes of AgNPs obtained from the synthesis of AgNPs powder. For 25°C synthesis temperature, the AgNPs size obtained was in a range of 153.2 nm to 175.5 nm. For 50°C synthesis temperature, the AgNPs size obtained was in a range of 115.2 nm to 164.5 nm. The smallest size was obtained when using 0.01 mol/L $AgNO_3$ while the largest AgNPs was obtained when using 0.05 mol/L $AgNO_3$. In addition, for 75°C synthesis temperature, the AgNPs size obtained was in a range of 109.5 nm to 179.4 nm. The smallest size was obtained when using 0.03 mol/L $AgNO_3$ while the largest AgNPs was obtained when using 0.01 mol/L $AgNO_3$.

In the event in which the reduction process was eventuated, other elements that are present during the reduction process are least discussed. AgNPs-2 growth was faster at a temperature of 25°C compared to 50°C. This event remarked by the heat introduced during the synthesis process actually reacted on DMAc and PVP making the reduction of

AgNPs decreased (Piñero et al., 2017). In correlation, the precursor underwent complete reduction making the nucleation rate increase throughout time proportionally to its size. In addition, it was reported that the synthesis process carried out at higher temperature will increase the reaction rate and consequently accelerate the process of ions to nanoparticles conversion (Majeed et al., 2018) which explained the smallest AgNP-2 obtained at 75℃.

As illustrated in Figure 4.1 and 4.2, the synthesis method played important role in the formation of AgNPs. AgNPs-2 has wider size range compared to AgNPs-1. The flat area projected in relation to temperature and precursor weight portrays the statistical importance values of these parameters is the same as discussed by Quintero-Quiroz et al. (Quintero-Quiroz et al., 2019). This may be associated with the fact that the higher amount of precursor present in the synthesis process, the more AgNPs can be obtained and the higher the temperature, the more rapid the nucleation process takes place in which both parameters played their role simultaneously at significance.

Nonetheless, the elliptical or saddle shape of a three-dimensional graph depicted a specific level of interaction significance and can be drawn upon perfect interaction among the independent variables of the parameters studied (Reddivari, Chirumamila, Marchant, & Nigam, 2001). Non-planar relation of AgNPs-2 synthesis indicates higher importance value of precursor concentration compared to temperature magnitude as each parameter produces a different gradient of interaction towards AgNPs size. From literature, it is known that the morphology, size, stability, physical properties, and chemical properties of metal nanoparticles are extremely affected by the interaction kinetics of metal ions with reducing agents, experimental conditions and adsorption processes of stabilizing agents with metal nanoparticles (Bagur et al., 2022).

Therefore, the size and morphology of the synthesized AgNPs can be restrained by implementing specific synthesis conditions (Anbu, Gopinath, Yun, & Lee, 2019). González, Noguez, Beránek, and Barnard (2014) claimed that there are two options possible to govern AgNPs formation – (i) specify the temperature and differing the size, and (ii) specify the size and varying the temperature in which the size of AgNPs can be controlled or varied based on the amount of silver salt involved during the chemical reaction. Besides, since the growth process of nanocrystalline is controlled by stabilizers or protective agents, the size and shape of AgNPs can possibly be altered by selecting different stabilizers to prevent agglomeration of the nanoparticle (Konował, Sybis, Modrzejewska-Sikorska, & Milczarek, 2017; López-Miranda, López-Valdivieso, & Viramontes-Gamboa, 2012). It was reported that PVP as stabilizing agent affects the duration of each step in La Mer´s model for nucleation and growth and is able to reduce polydispersity by up to 20% (Mer & Dinegar, 1950; Pacioni, Borsarelli, Rey, & Veglia, 2015; J. r. Polte et al., 2012).

4.1.1 Characterization of AgNPs-1and AgNPs-2

AgNPs synthesized in DMAc, AgNPs-1 was dark brown in colour while AgNPs powder dispersed in DMAc, AgNPs-2 was dark grey in colour. Figure 4.3 shows the two conditions of AgNPs in DMAc.

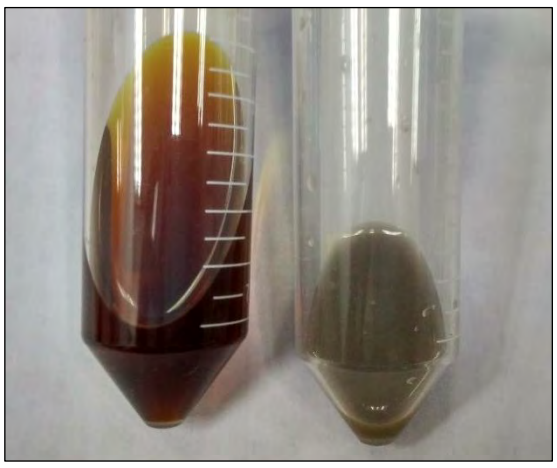

Figure 4.3 AgNPs synthesized in DMAc (AgNPs-1) on the left while AgNPs powder dispersed in DMAc (AgNPs-2) on the right.

Figure 4.3 shows the physical appearance of DMAc solvent containing AgNPs-1 and AgNPs-2. $AgNO_3$ was used as a precursor during the synthesis of both, AgNps-1 and AgNPs-2. According to Konował et al. (2017), $AgNO_3$ is typically used as a precursor for AgNPs formation compared to other soluble salts such as silver perchlorate ($AgClO_4$) and silver sulphate (Ag_2SO_4). It was important to choose the same initial precursor since it is able to directly influent the morphology, size, agglomeration, and dispersion of the nanoparticles synthesized (Moradi et al., 2017). The distinguished appearance of both synthesized products significantly portrayed different characteristics of synthesis products. According to El-Naggar, Mohamedin, Hamza, and Sherief (2016), the dark brown colour of AgNPs is an explicit indicator of AgNPs formation from Ag^+ ions reduction.

The synthesized AgNPs were also characterized using ultraviolet-visible spectroscopy. Based on Figure 4.4, similarly, in both types of silver, strong plasmon bands were found around 410-450 nm which denoted that the silver ions were reduced to Ag. Wide shoulder peaks in Uv-vis indicate broad particle size distribution and in some cases due to not only spherical particles present in the sample (Bousalem, Benmansour, & Ziani Cherif, 2017; Graf et al., 2009) which will be further examined using TEM analysis. Abbas, Atwan, Abdulhussein, and Mahdi (2019) prepared AgNPs using the electrochemical method reported an absorption spectrum at 421nm and discussed that the particle size and shape influenced the absorption peak values. According to Konował et al. (2017), silver metals portrayed a characteristic absorption band at around 420 nm due to the presence of plasmonic nanoparticles of silver. The peak at 410 nm was reported as the peak of silver metal Ag^0 (Sundar & Deevi, 2006). A maximum absorbance peak at around 313 nm for AgNPs-1 was observed and a similar phenomenon was reported by Chen et al. (2019) in a study of AgNPs synthesis due to the high concentration of $AgNO_3$ presence. This also

indicates the presence of silver colloid of Ag ions, Ag^{+} (Sundar & Deevi, 2006; D. Zhang, Liu, Wang, Yang, & Lu, 2011).

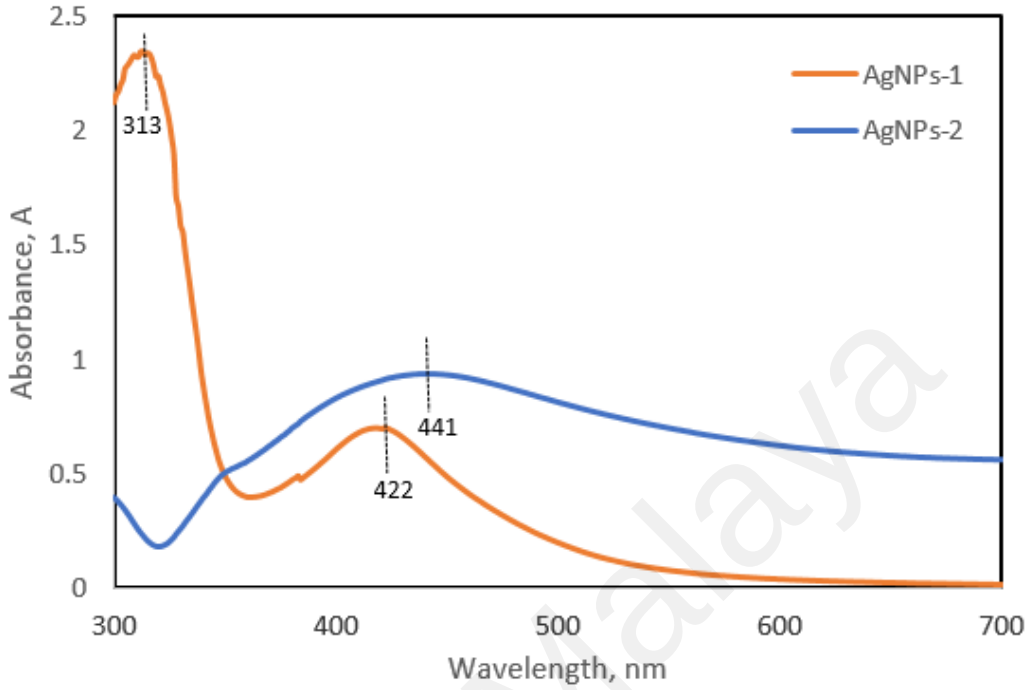

Figure 4.4 Uv-vis spectra of AgNPs-1 synthesized in DMAc and AgNPs-2 dispersed in DMAc.

Both AgNPs types were characterized using FTIR in which several peaks were identified, and various functional groups were signified. The chemical structure of both types of AgNPs in DMAc is shown in Figure 4.5. For AgNPs-1, the FTIR results showed a broad band at 3485 cm^{-1}. It was attributed to the hydroxyl group (- OH). During the synthesis of AgNPs-1 in DMAc, reducing agent and catalyst solutions were all mixed. The phenomenon of hetero-associated hydrogen bonds is able to facilitate the interconnection between polymer and nanoparticles (Yee, Ching, Rozali, Awanis Hashim, & Singh, 2016).

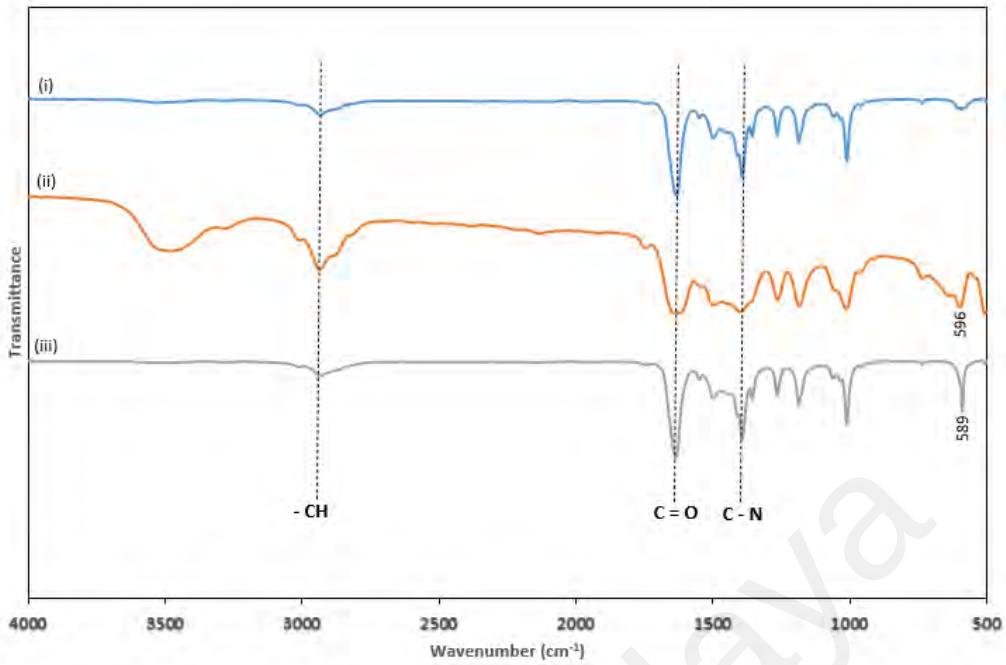

Figure 4.5 FTIR of (i) PVP and DMAc; (ii) AgNPs-1; and (iii) AgNPs-2 dispersed in DMAc.

These solutions contained water which portrayed at the broad medium peak in AgNPs-1 solution resulted from water stretching vibration. PVP alkyl chain was indicated by the peak at 2935 cm^{-1} which assigned the methylene (- CH) stretching for all samples since all the samples contained PVP as a stabilizer. The vibration peak at 1630 cm^{-1} was a functional of carbonyls (C=O) in which a carbon atom double-bonded to an oxygen atom and all samples contained this same peak. The peak at 1395 cm^{-1} was related to C-N bond vibration. This peak is deduced from the typical bond in PVP (Manikprabhu & Lingappa, 2013b). Significantly, more intense peaks at 596 cm^{-1} and 589 cm^{-1} were found in AgNPs-1 and AgNPs-2 corresponded to the Ag metal presence in the solution tested (Waghmode, Chavan, Kalyankar, & Dagade, 2013). A similar phenomenon was also observed by Vijayan et al. (Vijayan et al., 2014) during the synthesis of Ag using the reduction method due to the presence of a reducing agent.

AgNPs-1 and AgNPs-2 morphology were studied along with the size of the particles. The physical characteristic of both types of AgNPs was observed after withdrawing both samples from their solvent or dispersion medium – DMAc. The FESEM images of both

AgNPs are presented in Figure 4.6. Consecutively, EDX was also carried out to identify the presence of silver (Ag) and the results are portrayed in Figure 4.7.

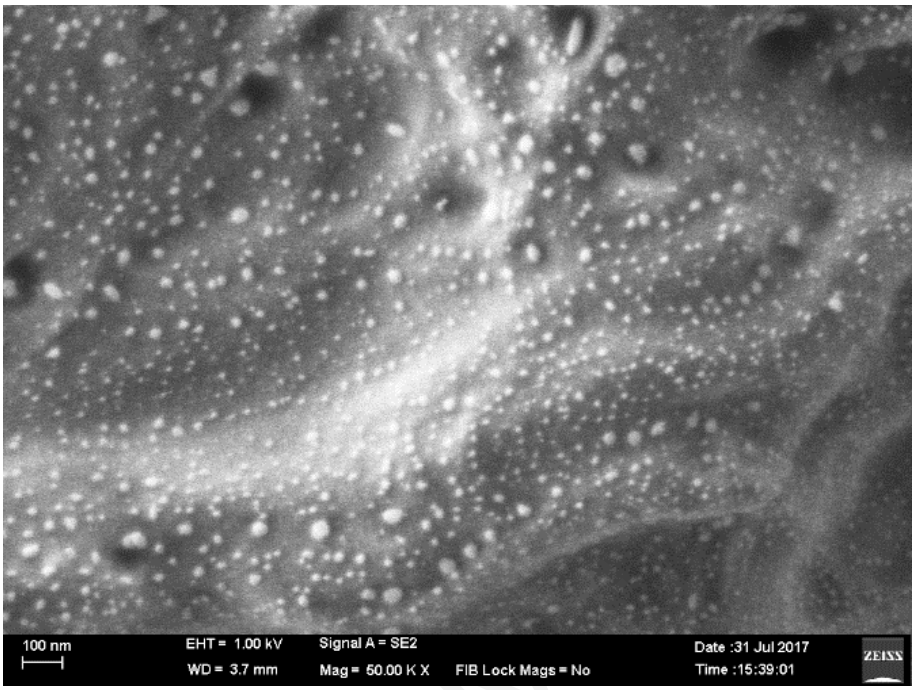

(a)

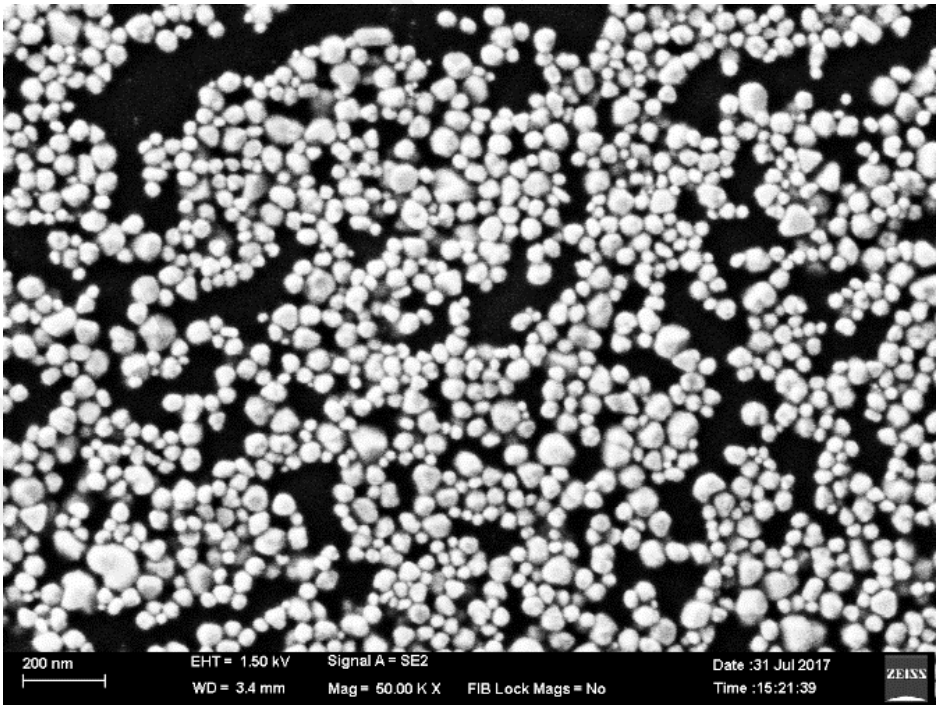

(b)

Figure 4.6 FESEM images of (a) AgNPs-1 and (b) AgNPs-2.

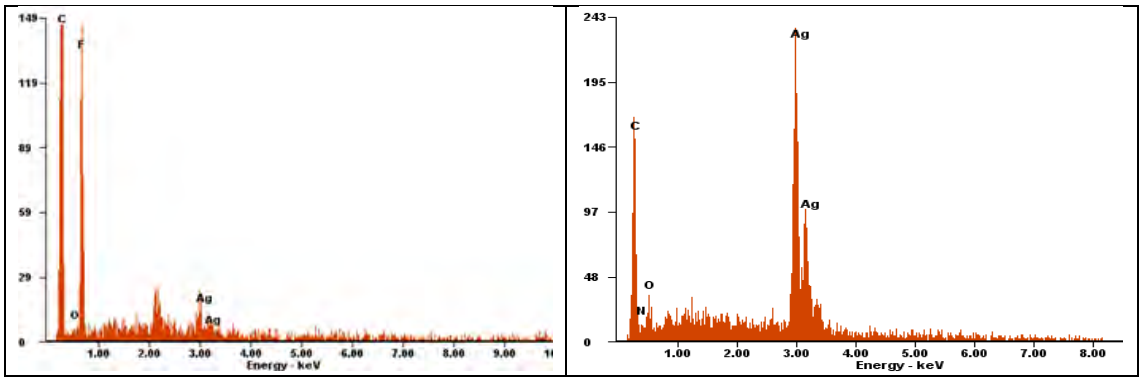

(a) (b)

Figure 4.7 EDX spectrum that showed the chemical composition of (a) AgNPs-1 and (b) AgNPs-2.

Based on the figure, AgNPs-1 produced a spherical shape of AgNPs. The irregular size of the spheres was in a range of 14 nm to 47 nm in diameter. The AgNPs is evenly distributed on the filter paper surface as the composite material did not contain aggregates or particles sintered together. In contrast, AgNPs-2 has a wider size range of 18 nm to 112 nm with a uniform spherical shape. For both types of AgNPs, EDX analysis as in Figure 4.7 has established Ag as one of the elements in the sample. Carbon is the major constituent element for AgNPs-1 possibly due to the presence of PVP. Since AgNPs-2 originated from AgNPs powder redispersed in DMAc, it is a good agreement that the major element identified from EDX analysis for AgNPs-2 was Ag. Also, the characteristic of nanosized metallic silver was indicated by the strong signal of the spectrum at 3 keV (Magudapathy, Gangopadhyay, Panigrahi, Nair, & Dhara, 2001).

Based on particle size analyzer measurement, the particle size results were analyzed to investigate the possible aggregation of AgNPs-1 and AgNPs-2 in DMAc. Figure 4.8 showed the size range of the smallest AgNPs-1 and AgNPs-2 synthesized.

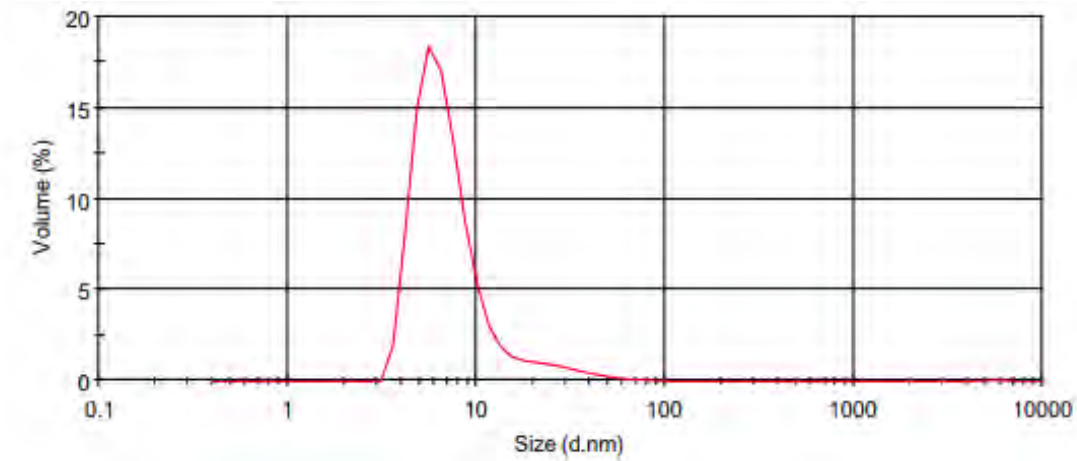

(a)

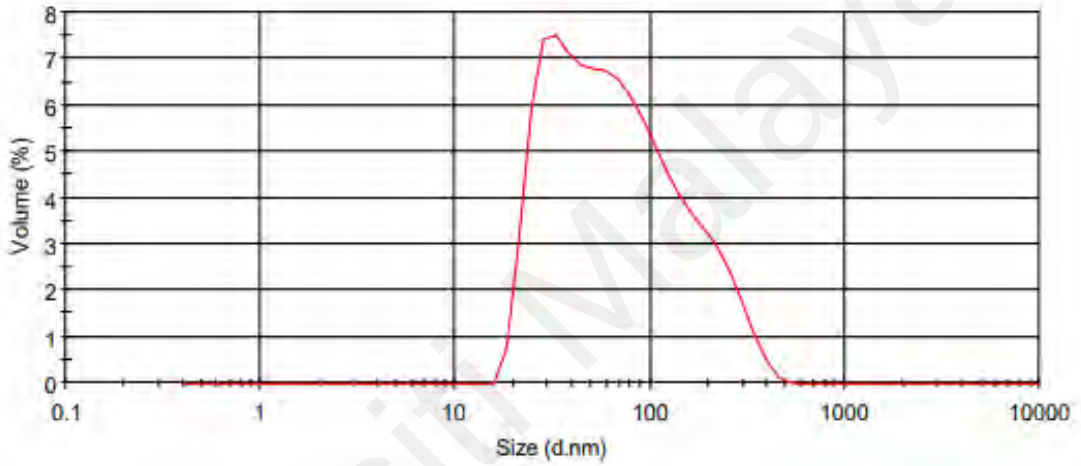

(b)

Figure 4.8 Volume versus size of (a) AgNPs-1 and (b) AgNPs-2 dispersed in DMAc generated from particle size analyzer.

The poly-dispersity index (PDI) value for smallest AgNPs-1 is 0.574 while for smallest AgNPs-2 the PDI value is 0.223. From the literature, it was reported that a lower PDI value demonstrated more evenly sized nanoparticles based on their hydrodynamic diameter (Anbu, Gopinath, Yun, & Lee, 2019). A higher PDI value was attributed to AgNPs-1 while AgNPs-2 has a wider nanoparticles' sizes range and thus the PDI value was used to indicate the uniformity and stability of particles formation (Masarudin, Cutts, Evison, Phillips, & Pigram, 2015). Both particles were considered monodispersed as in literature stated particle with PDI >0.7 is polydisperse with a very broad size range (Honary, Barabadi, Gharaei, & Naghibi, 2013).

From the volume, % versus size,d.nm graph, AgNPs-1 formed a peak at 8.208 nm (diameter). This indicated that significantly smaller nanoparticles were synthesized in DMAC solvent, yet the remaining nanoparticles possessed relatively larger sizes making the average diameter bigger which is 30.88 nm. AgNPs-2 form a slightly wider peak at 87.25 nm. Concerning AgNPs-2 PDI value, the volume affirmatively supports that AgNPs-2 was less aggregated when dispersed in DMAc. The average size of AgNPs-2 was 109.5 nm which is slightly bigger compared to the size at its peak.

To further examine the size, shape, and distribution of AgNPs, TEM images of AgNPs-1 and AgNPs-2 were captured. The size range for AgNPs-1 was found to be 14.2-21.9 nm while AgNPs-2 was 82-127 nm. From the images, it is noticeable that AgNPs-1 dispersed evenly as the distance of each particle is almost uniform while AgNPs-2 assemble close to each other. This condition is in good agreement with the SEM images in Figure 4.6. Even so, AgNPs-1 portrayed two peaks in Uv-vis analysis, the narrow peaks of each signify that only identical almost spherical shape particles were observed. As different shape particles were observed in Figure 4.9 (b), this finding is proportional to AgNPs-2 spectroscopy characteristic and the wider range of size from TEM images corresponded well with the results obtained from Uv-vis, SEM and particle size distribution.

However, a slight difference in particles' sizes were recorded when using a scaled particle size measurer attached to SEM or TEM instrument due to the hydrodynamic condition during measurement in Zetasizer. Hydrodynamic size is measured based on the particle size in the presence of a solvent layer absorbed over the particles' surface in liquid suspension while during TEM analysis the particles were measured after drying considering only its metallic core (Bagur et al., 2020). In essence, it was well understood that different synthesis parameters lead to different particles shape, average size, diameter, dispersion, and size range.

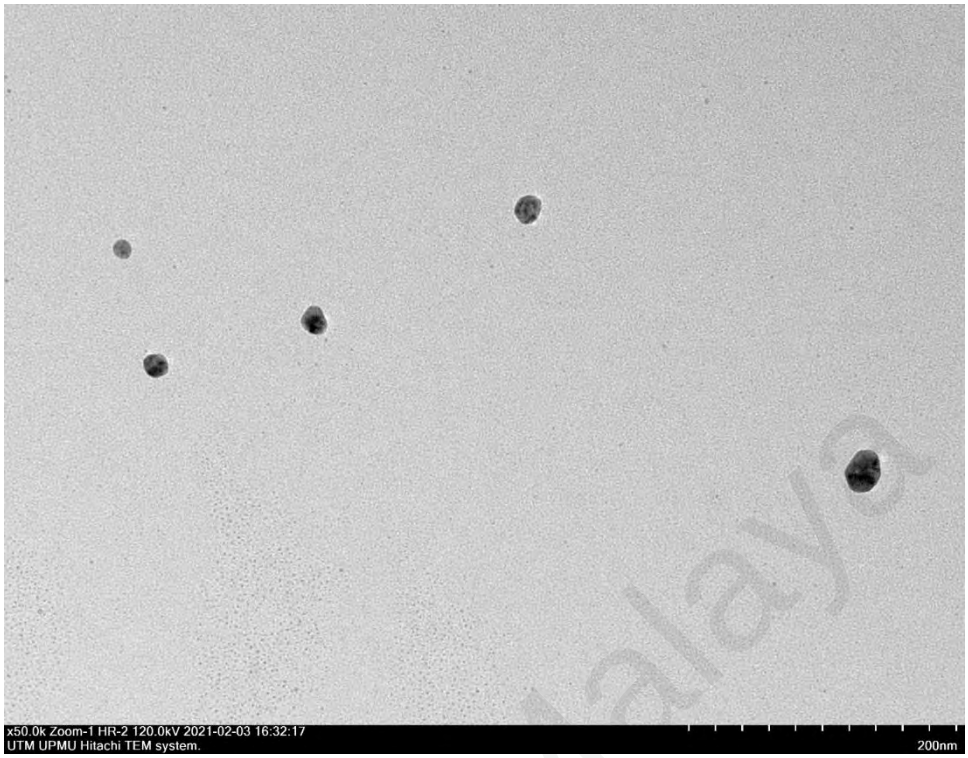

(a)

(b)

Figure 4.9 HR-TEM images of (a) AgNPs-1 and (b) AgNPs-2.

4.1.2 Bactericidal Performance of AgNPs-1 and AgNPs-2

As reported, the size of noble metals nanoparticles played a crucial role in determining the antibacterial performances of the nanoparticles, in which smaller size consists of a larger effective surface area which consequently ceded higher magnitude of toxicity (Chernousova & Epple, 2013; Vimbela, Ngo, Fraze, Yang, & Stout, 2017). Thus, the smallest sizes of AgNPs-1 and AgNPs-2 were selected for a further antibacterial performance test. Bacteria are classified into two groups which are gram-positive and gram-negative based on their various membranes and peptidoglycan layer (Dehghan, Mardanpour, Kamali, & Alirezaei, 2020). The images of the bacteria count plates for antibacterial analysis were captured in Figure 4.10 to Figure 4.12. Briefly, the average colony number of *E. coli* (gram-negative), total coliform, and *S. aureus* (gram-positive) were plotted as in Figure 4.13 with the presence of AgNPs-C1, AgNPs-1, AgNPs-C2, and AgNPs-2.

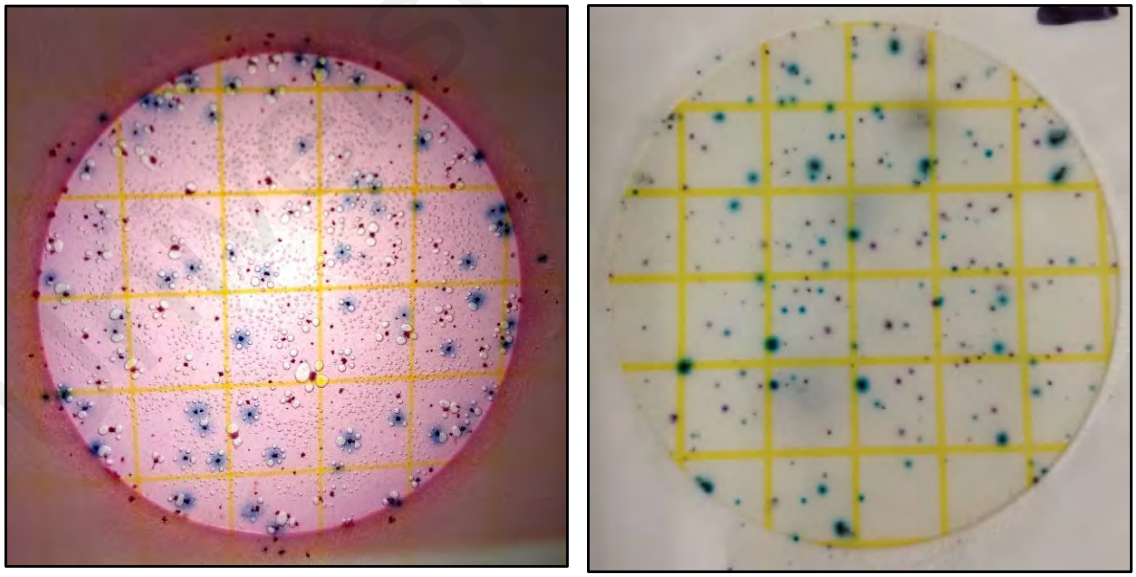

(a) (b)

Figure 4.10 Bacteria count for lake water sample without any presence of AgNPs – (a) *E. coli* bacteria count and (b) *S. aureus* bacteria count.

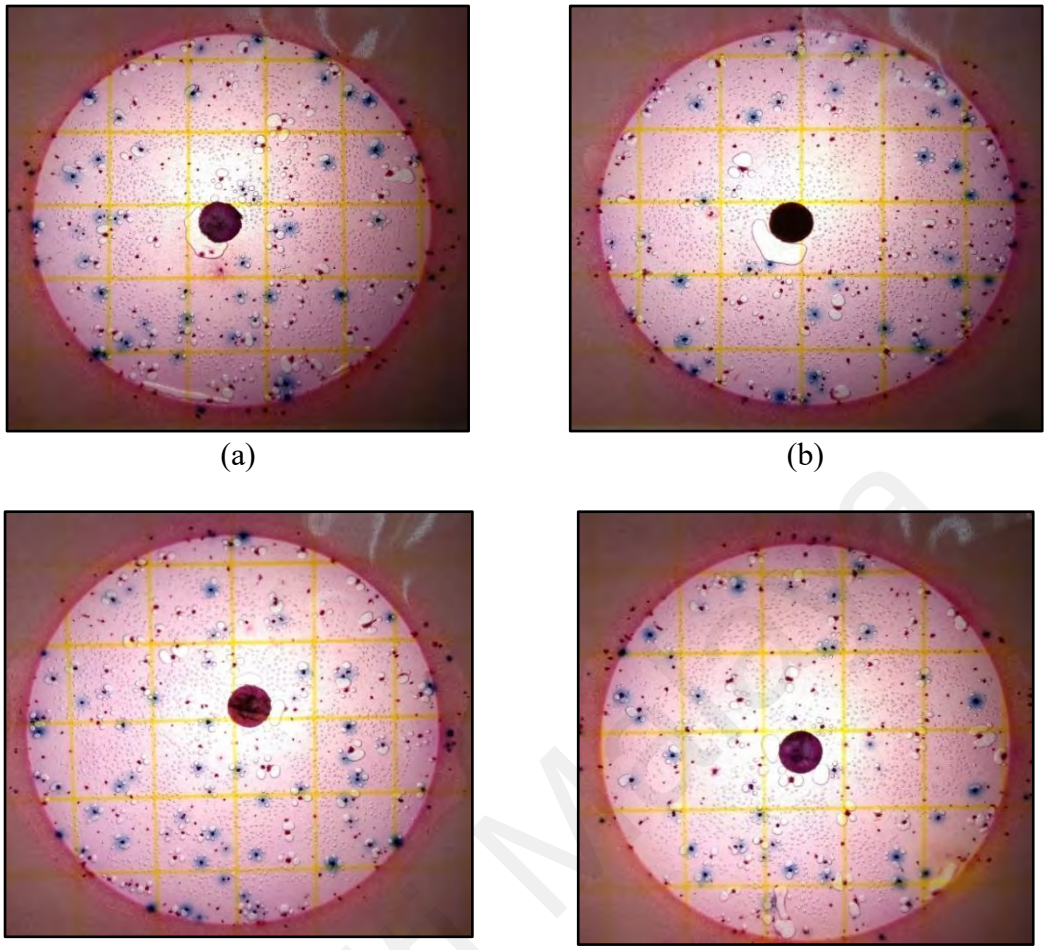

Figure 4.11 Bacteria count for lake water sample with the presence of (a)AgNPs-C1, (b)AgNPs-1, (c)AgNPs-C2, and (d)AgNPs-2 for *E. coli* bacteria and total coliform.

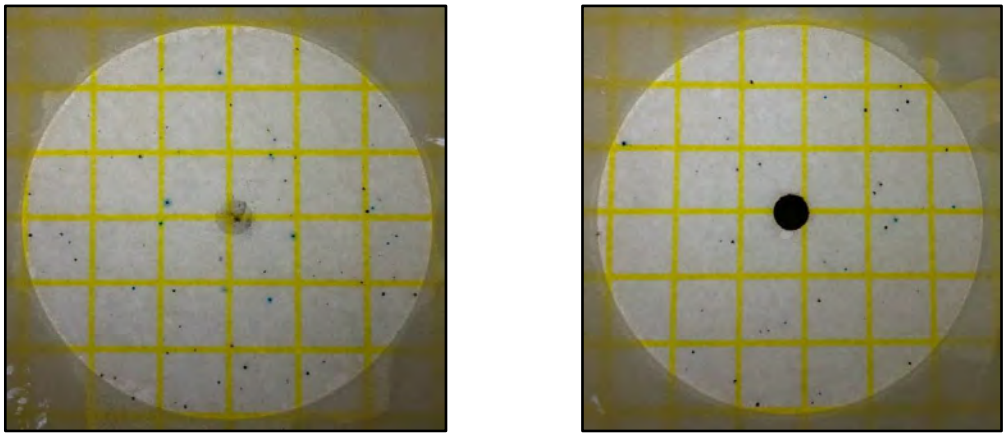

(a)

(b)

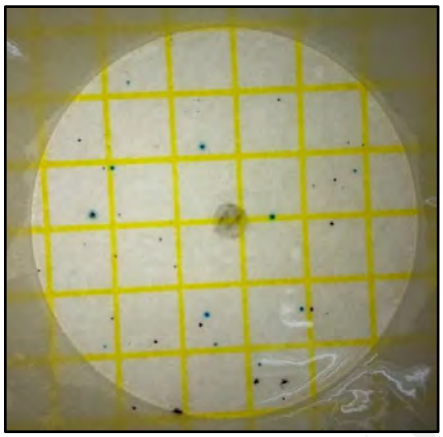

(c)

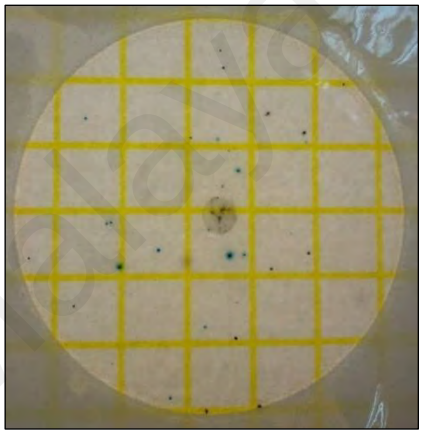

(d)

Figure 4.12 Bacteria count for lake water sample with the presence of (a)AgNPs-C1, (b)AgNPs-1, (c)AgNPs-C2, and (d)AgNPs-2 for *S. aureus*.

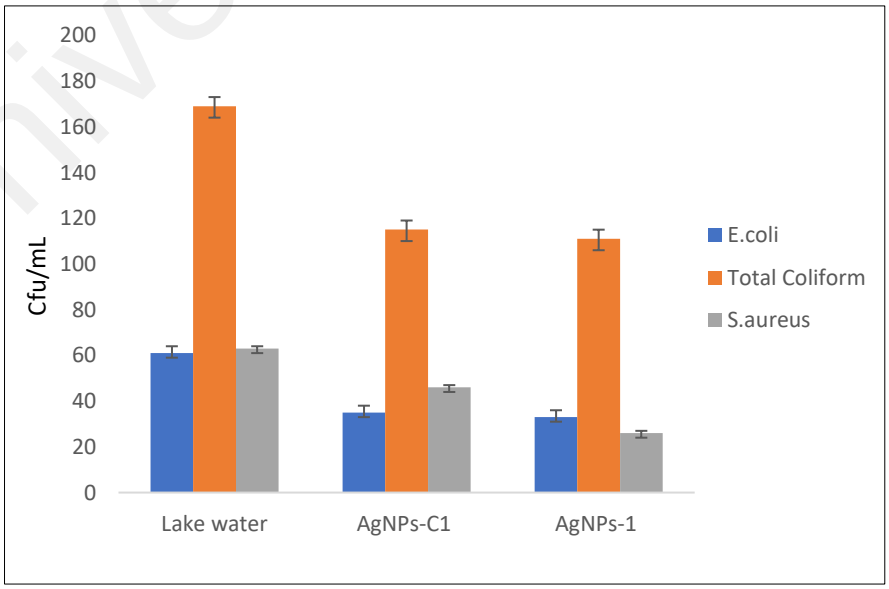

(a)

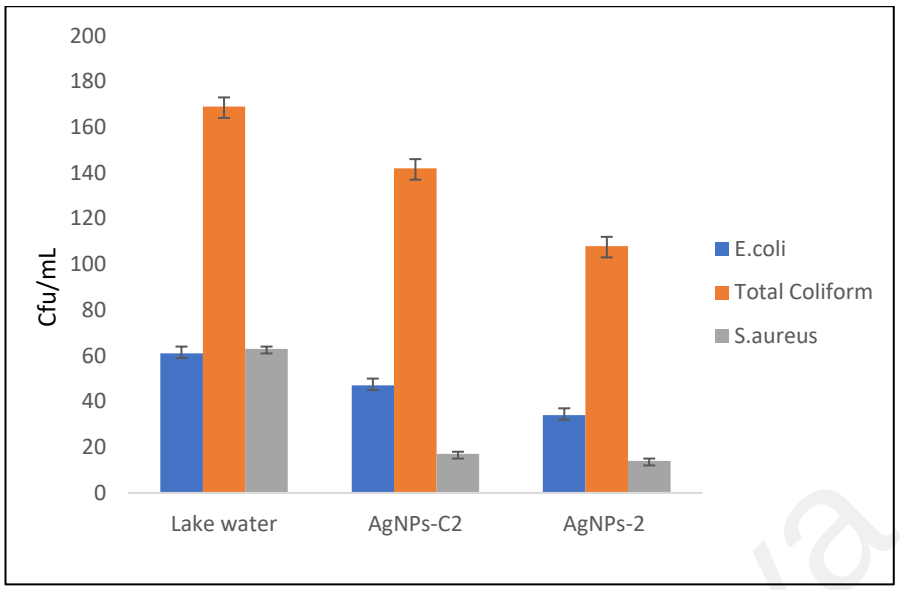

(b)

Figure 4.13 Bacteria count for lake water sample and lake water sample with presence of (a) AgNPs-C1 and AgNPs-1; and (b) AgNPs-C2 and AgNPs-2.

Many had reported the antibacterial effects of AgNPs against *E. coli* and *S. aureus* using the disc diffusion method, measuring the inhibition zone as an indication of antibacterial activity (Bagur et al., 2020; Foroutan Koudehi, Imani Fooladi, Aghozbeni, & Nourani, 2019; Reddy & Pathak, 2018; Taghavizadeh Yazdi et al., 2019). Despite the common employment of the disk diffusion method, the colony count method is significant in providing a quantitative estimation of the bactericidal effects of AgNPs (Abbas et al., 2019; Bagur et al., 2020). Figure 4.13 indicates that the synthesized AgNPs-1 potentially has better antibacterial properties compared to AgNPs-C1. The significant difference in reduction indicated that the synthesized silver potentially has better antibacterial properties towards the gram-positive bacteria compared to commercialized silver. For AgNPs-2, although only a slightly different reduction was quantified, still, AgNPs-2 offered better antibacterial properties compared to the commercialized AgNPs. The log reduction and percentage reduction were calculated based on Eq (3.1) and Eq. (3.2), and the values were summarized in Table 4.1.

Table 4.1 Log reduction and percentage reduction of *E. coli*, total coliform and *S. aureus*.

		AgNPs-C1	AgNPs-1	AgNPs-C2	AgNPs-2
Log reduction, L	*E. coli*	0.24	0.27	0.11	0.25
	Total Coliform	0.17	0.18	0.08	0.19
	S. aureus	0.14	0.38	0.57	0.65
Percentage reduction, P (%)	*E. coli*	42.62	45.90	22.95	44.26
	Total Coliform	31.95	34.32	15.98	36.09
	S. aureus	26.98	58.73	56.89	65.32

Since the test was initially conducted using the filter paper method which was conducted by many in these recent years (Liang et al., 2018), it is possible that agglomeration of AgNPs occurred on the filter paper surface that hindered the antibacterial properties of the AgNPs (Ravindran, Chandran, & Khan, 2013; Tankhiwale & Bajpai, 2009) and AgNPs synthesized potentially portray better antibacterial performance when incorporated in polymeric membrane fabrication. The smaller size allowed a wider surface area to interact with bacteria which later altered their performance as an antibacterial agent (Agnihotri, Mukherji, & Mukherji, 2014; Raza et al., 2016). In conjunction, these nanoparticles possess a large surface area to volume ratio which helps in portraying good antibacterial properties. For better application in the targeted field, nanoparticles size and shape are vital efficacy for their biocompatibility enhancement and further alteration (Jian Wu, Du, Wang, & Chen, 2020).

4.2 Effects of Thermal Treatment Approach during Modified PVDF Membrane Fabrication

Upon selection of favorable AgNPs, PVDF membrane was incorporated with AgNPs-1 and AgNPs-2 respectively. During the membrane fabrication, a thermal treatment approach was introduced as a novel method to combat the leaching phenomena of AgNPs. Since the heat was introduced, the characteristics of the membranes were consequently

changed physico-chemically. The effects of the thermal treatment approach were discussed in this section.

4.2.1 Modified PVDF Membrane Mechanical Properties

Mechanical properties and pure water flux of the membranes were analyzed for tensile strength, contact angle measurement, and pure water permeability. The mechanical strength of the membrane is one of the properties to be determined especially in considering membrane technology for large-scale applications. The results were tabulated in Table 4.2. as follows.

Table 4.2 Mechanical properties of PVDF membranes.

Membranes	*Casting temperature (ºC)*	*Tensile Strength (MPa)*	*Water Contact Angle (°)*
PVDF/PVP	25	5.220 ± 0.4	63.6 ± 2.1
	40	5.126 ± 0.4	62.8 ± 1.8
	55	4.837 ± 0.2	60.4 ± 1.9
PVDF/PVP/AgNPs-1	25	5.464 ± 0.3	66.3 ± 1.2
	40	5.341 ± 0.2	64.4 ± 1.5
	55	5.220 ± 0.3	62.1± 2.2
PVDF/PVP/AgNPs-2	25	5.360 ± 0.2	67.2 ± 1.6
	40	5.232 ± 0.3	64.9 ± 2.1
	55	5.145 ± 0.5	63.2 ± 1.5

From the experiment, it was found that the mechanical strength of the membrane decreases with the increase in temperature. The decrement of tensile strength can be related to pore enlargement and changes in pore architecture (Kotsilkova et al., 2018). In relation to this, membranes pore size was determined and tabulated in Table 4.3. During the thermal treatment method, heat is introduced at the bottom surface of the membrane casting glass. The heat had induced the evaporation of solvent instantaneously which result in a more porous structure of the membrane. Morphologically, membrane porous structure is attributed to pore size, pore length, skin structure thickness, cellular structure thickness, and finger-like voids number (Guillen, Farrell, Kaner, & Hoek, 2010; H. Zhang

et al., 2018). Besides, it is worth mentioning that for large-scale applications, the minimum requirement for mechanical strength is 2 MPa (J. F. Kim, Kim, Lee, & Drioli, 2016) and the smallest mechanical strength fabricated in this study is 4.837 MPa making all the membranes possible to be up scaled for further application.

Water contact angle measurement was taken to assess the effect of temperature on the surface hydrophilicity of the porous PVDF/PVP membranes. The contact angle of the PVDF membranes samples decreases as the temperature increase. The pristine PVDF/PVP membrane shows the smallest contact angle even though PVDF is hydrophobic by nature. With the presence of PVP, the hydrophilicity of the membrane increased as PVP is a polar polymer that contains multiple carbonyl groups in its molecular chain. In a study of PVDF/PVP membrane flat sheet fabrication, it was reported that the membrane contact angle obtained was 65.1˚ which is in the same range as the current study (X.-h. Liu et al., 2015). It was reported that Ag nanoparticles with the presence of PVP is more hydrophilic as a result of the amphiphilic properties of PVP (P. Xiao et al., 2012).

Nonetheless, it was reported that a certain concentration of Ag in polymeric membrane had proportionally increased the membrane contact angle as the concentration increased (Filip et al., 2014; Maheswari, Prasannadevi, & Mohan, 2013). Thus, this explains the increasing contact angle at 25℃ with the incorporation of AgNPs-1 and AgNPs-2 as compared to the pristine membrane. Maziya et al. recently (2020) also observed the same trend upon grafted AgNPs onto the PES membrane (Maziya, Dlamini, & Malinga, 2020). This finding is in good agreement with the previously reported result in several studies which is the incorporation of AgNPs onto polymeric membrane increased the membrane contact angle attributed to AgNPs hydrophobicity (D. Y. Zhang et al., 2018; D. Y. Zhang et al., 2016).

Meanwhile, as the temperature increases, the contact angle of the membranes all decreases. This phenomenon may be caused by the mechanical structure of the membrane that changed upon the thermal treatment approach. For membrane with AgNPs, the hydrophilicity increased further as the contact angle reduced more as compared to the pristine membrane. This may result from the presence of AgNPs in membrane morphology (Lichuan Huang et al., 2016) and consequently indicates a different amount of AgNPs content in each membrane at each temperature as an effect of immobilization attempt. The membranes pore size was computed based on a single peak diameter and tabulated as in Table 4.3.

Table 4.3 Pore size diameter of all membranes.

Membranes	***Casting temperature, °C***		
	25	*40*	*55*
	Pore size, nm		
PVDF/PVP	59.40	60.53	61.45
PVDF/PVP/AgNPs-1	63.48	66.55	69.93
PVDF/PVP/AgNPs-2	54.63	58.16	60.60

For each type of membrane, the pore size increases as the temperature increases. This is in good correlation with the membranes' mechanical strength aforementioned. In comparison with a study reported by Ghasem et al. (Ghasem, Al-Marzouqi, & Duaidar, 2011), the effect of temperature in thermally induced phase separation (TIPS) on the microporous structure of PVDF membrane resulted in an increment of pore size and weaken mechanical strength which is in good agreement with the current study. As the pore size of all membranes is in a range of 54.63 nm to 69.93 nm, the membrane is a UF membrane that is suitable for bacteria removal from a liquid stream (Lichuan Huang et al., 2016). Upon incorporation of AgNPs-1, membrane pore size has increased. This finding is in good agreement with what was reported by Li et al (2013) in which the membrane pores enlarged as AgNPs was introduced to membrane casting solution

formulation due to altered demixing process kinetics during membrane fabrication (X. Li et al., 2013). In contrast, membrane pore size decreased as AgNPs-2 was added possibly due to the blockage of the pore by AgNPs. This can be postulated as our findings on AgNPs hydrodynamic diameters are 30.88 nm and 109.5 nm for AgNPs-1 and AgNPs-2, respectively.

As reported in the literature, hydrophilicity which is measured as water contact angle normally portrays an inversely proportional trend with permeability (Zuo et al., 2020) which is measured as pure water flux in this study and shown in Figure 4.14. The flux showed higher values as the casting temperature increased. This might be associated with increasing temperature during membrane fabrication that promotes rapid evaporation of solvent which increases the porosity of the membrane. During the phase inversion process, the polymeric membrane solidifies once the membrane casting solution is immersed into nonsolvent coagulant through the exchange of the solvent and nonsolvent (T. Xiao, Wang, Yang, Cai, & Lu, 2015).

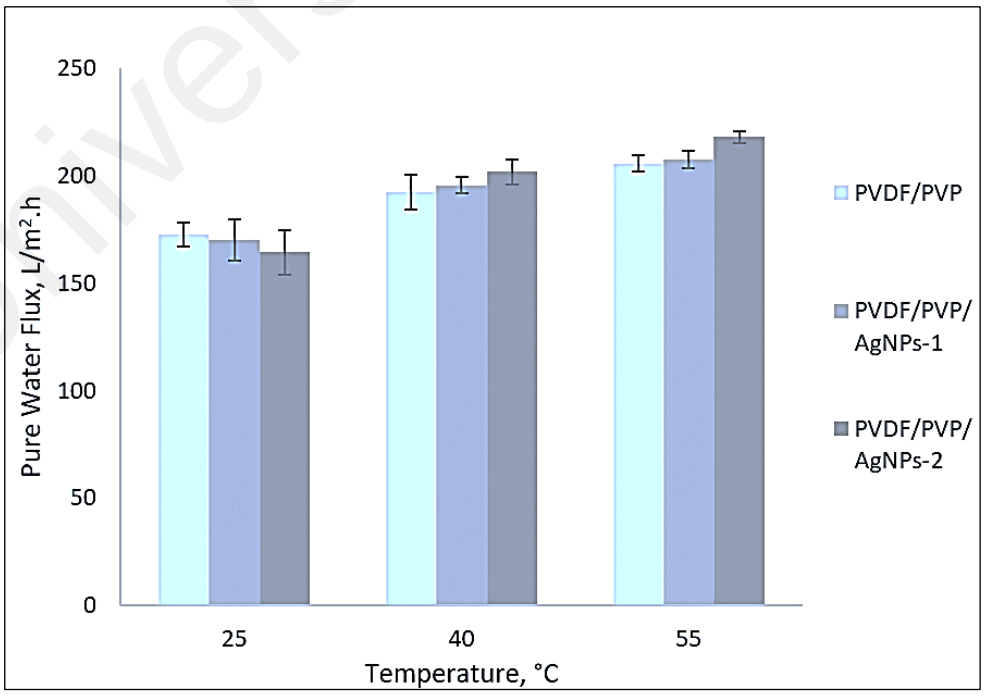

Figure 4.14 The pure water flux of PVDF/PVP, PVDF/PVP/AgNPs-1, and PVDF/PVP/AgNPs-2 during dead-end filtration at 0.5bar.

According to Tiron, Pintilie, Vlad, Birsan, and Baltă (2017), the formation of the denser skin layer of the membrane took place upon the application of reduced temperature using the thermally induced phase separation technique. It was claimed that without solvent evaporation, the asymmetric membrane's skin formed on top of the membrane porous structure usually is less dense as compared to the membrane prepared during the dry/wet method which allows solvent to first evaporate before being immersed in the nonsolvent bath for phase inversion process (D.-M. Wang & Lai, 2013). Denser skin will generally result in lower water flux, thus this explains the trend of the membranes fabricated in this work. In addition, the lower contact angle indicated more hydrophobic characteristics of the PVDF membrane. Consequently, it provides higher pure water flux which signifies improved permeability of the membranes cast at the higher temperature. Notably, different amounts of AgNPs in membrane composition will also affect the membrane flux (X. Li et al., 2013).

4.2.2 Characterization of Modified PVDF Membranes

To investigate the effect of casting temperatures, FTIR-ATR analysis was carried out to determine the structure of the PVDF and AgNPs in fabricated membranes, as well as to study the effect of temperature on structural changes in the elemental functional group. The chemical structures of PVDF membranes containing AgNPs were shown in Figure 4.15 to 4.17.

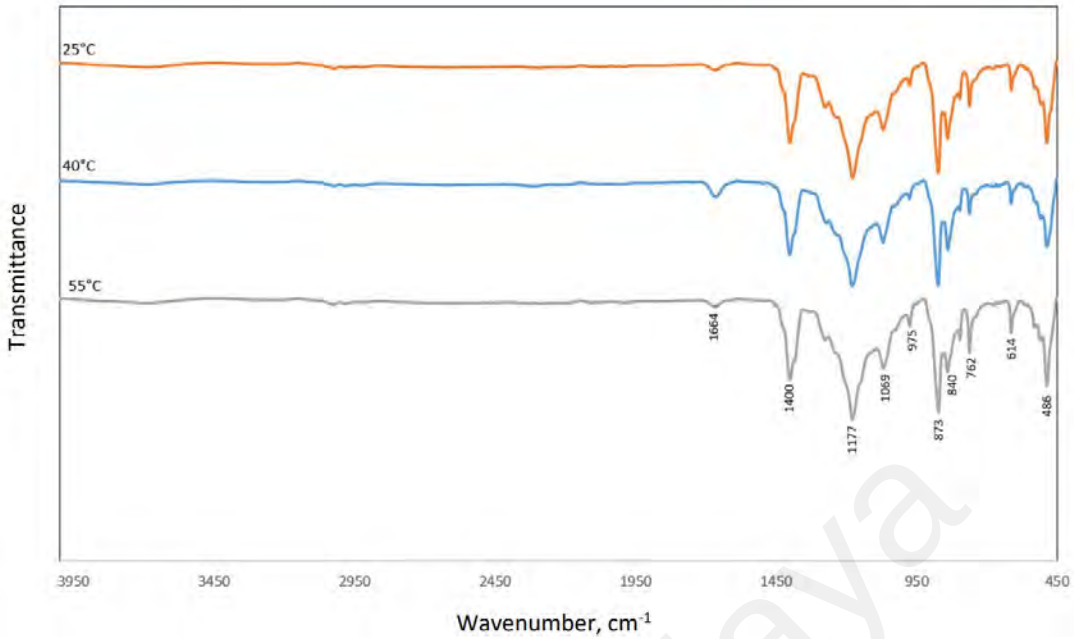

Figure 4.15 Characterization of pristine PVDF/PVP membrane cast at temperature 25, 40, and 55°C using FTIR-ATR.

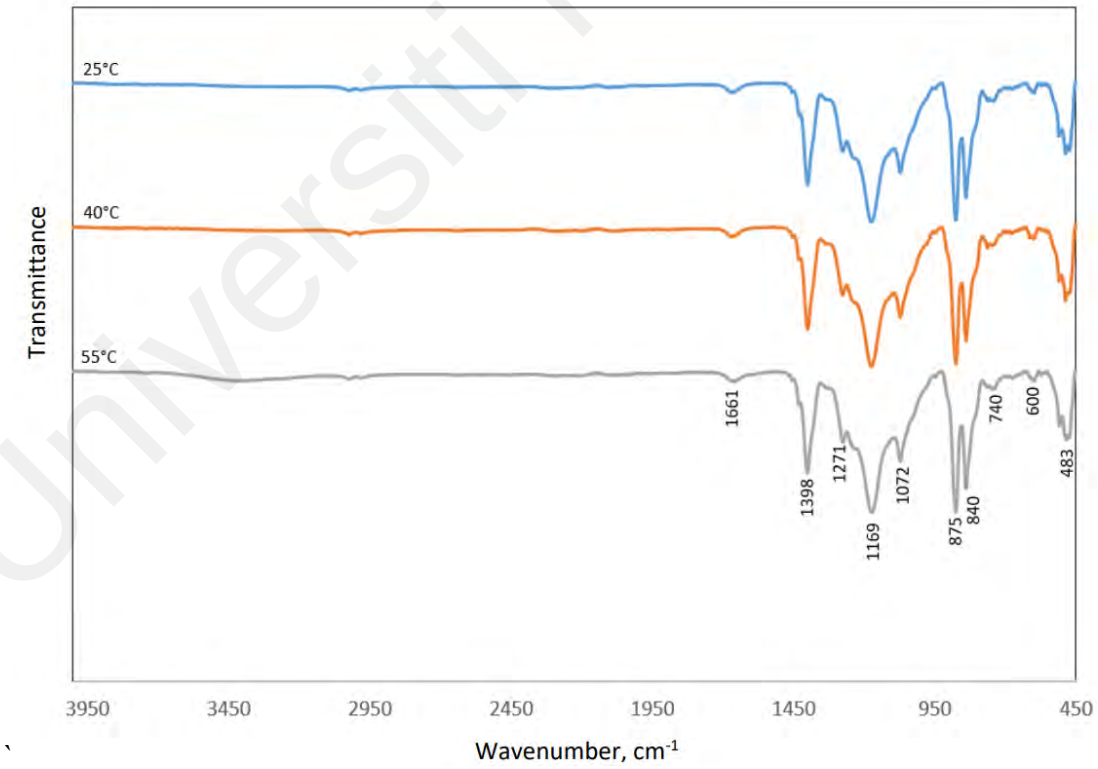

Figure 4.16 Characterization of PVDF/PVP/AgNPs-1 membranes cast at temperature 25, 40, and 55°C using FTIR-ATR.

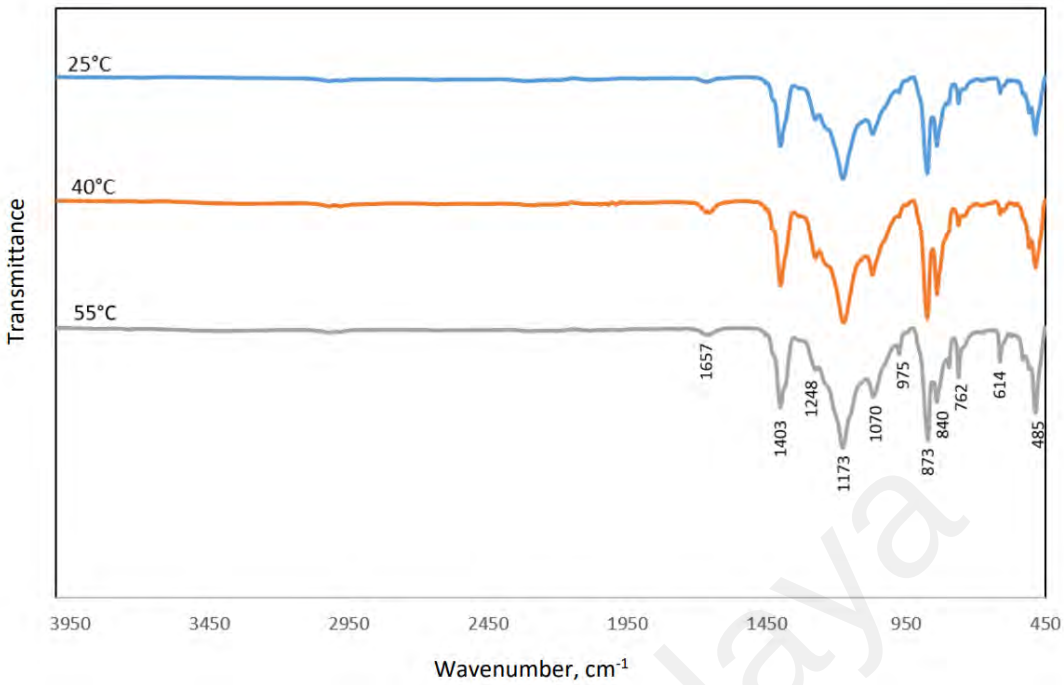

Figure 4.17 Characterization of PVDF/PVP/AgNPs-2 membranes cast at temperature 25, 40, and 55°C using FTIR-ATR.

Generally, carbonyl stretching absorption bands of PVP were indicated in all membranes at peaks 1664, 1661, and 1657 cm^{-1}. C-H bending vibrations in PVP were found at 1400, 1398, and 1403 cm^{-1} (Anilkumar, Jinisha, Manoj, & Jayalekshmi, 2017; Kumar et al., 2014). Peaks at 1271 and 1248 cm^{-1} were related to C-N stretching vibration upon the presence of PVP as a reducing agent (Y. Dai & Zhu, 2018; Manikprabhu & Lingappa, 2013a). The absorption peaks at 873 and 875 cm^{-1} indicated the presence of C-H bond vibration. The peaks at 614 and 600 cm^{-1} indicated the visibility of α-form PVDF while the peaks at 486, 483, and 485 cm^{-1} were PVDF in β-form (Koseki, Aimi, & Ando, 2012; Peng & Wu, 2004; F. Wang et al., 2018). The phenomena caused by the interaction between carbonyl group, C=O of PVP and fluorine group of PVDF transformed PVDF from α-phase to β-phase. The crystallinity of PVDF decreased as an effect of the weakened entanglement and hydrogen bond when PVDF was blended with PVP (F. Wang et al., 2018).

Vibration modes at 765 and 616 cm^{-1} at temperature 25°C in the spectrum of PVDF/PVP/AgNPs-2 membranes are shifted to a lower wavenumber with higher intensity with increasing temperature. This shift is attributed to the interaction in the carbonyl group which increased the crystallinity of PVDF and PVP (Cai, Lei, Sun, & Lin, 2017). The increasing intensity of the peaks indicated the increasing amount of the carbonyl group associated with the molecular bond per unit volume. This clearly signified PVDF and PVP structure had chemically changed during the fabrication of the membrane with the presence of AgNPs in the membrane matrix (Safo, Werheid, Dosche, & Oezaslan, 2019).

In order to examine the effect of thermal treatment on the morphological alteration of polymeric membranes, FESEM images of the top, bottom, and cross-sectional of the membranes were obtained and are shown in Figure 4.18, 4.19, and 4.20.

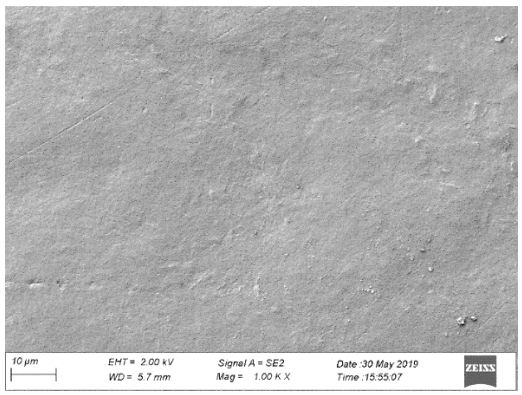

(a)

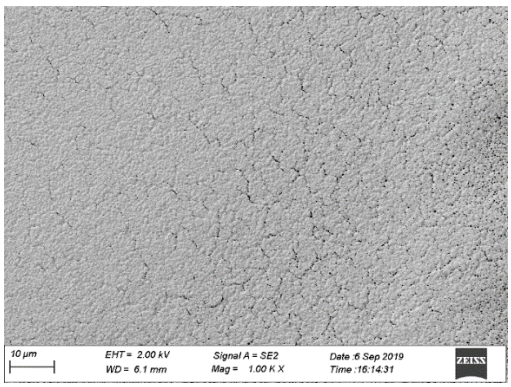

(b)

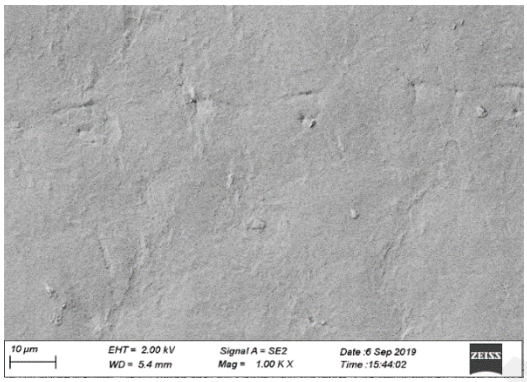

(c)

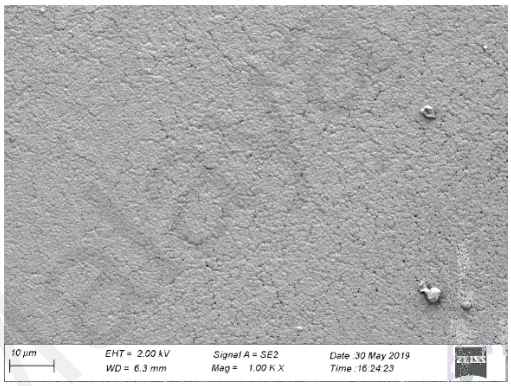

(d)

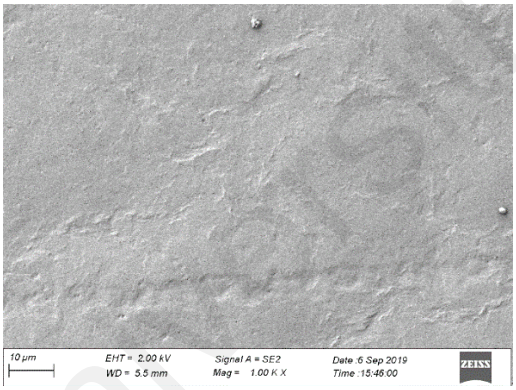

(e)

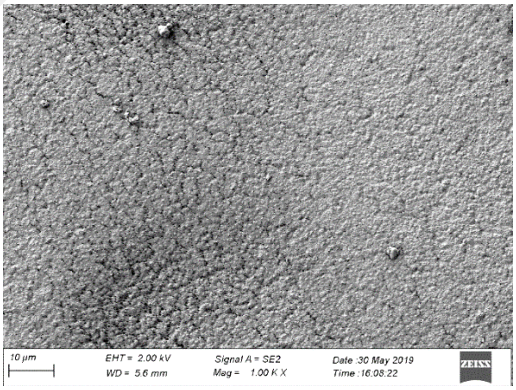

(f)

Figure 4.17 FESEM images of PVDF/PVP membranes (a) top, (b) bottom; PVDF/PVP/AgNPs-1 membranes (c) top, (d) bottom; and PVDF/PVP/AgNPs-2 (e) top, (f) bottom cast at 25℃.

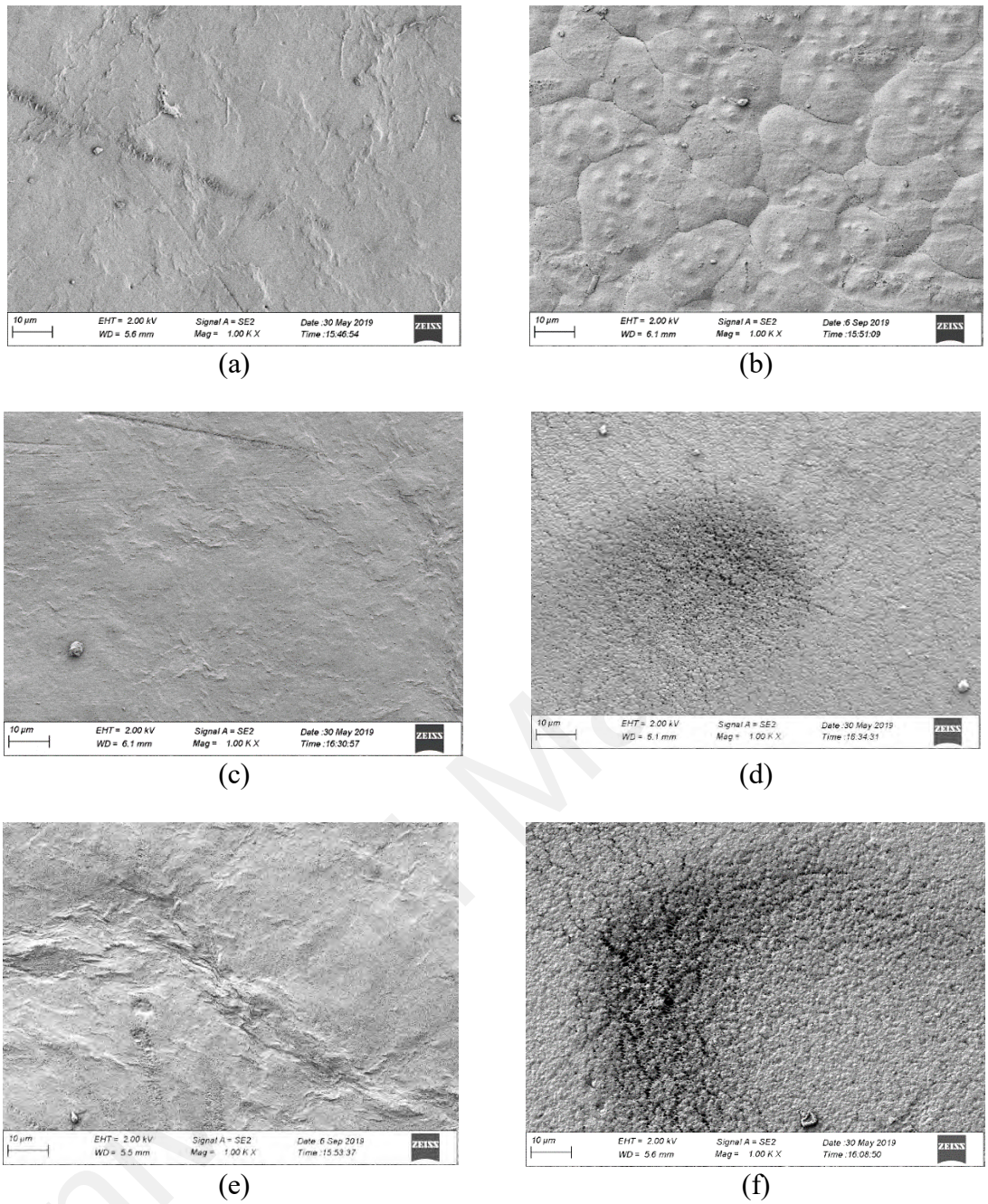

Figure 4.18 FESEM images of PVDF/PVP membranes (a) top, (b) bottom; PVDF/PVP/AgNPs-1 membranes (c) top, (d) bottom; and PVDF/PVP/AgNPs-2 (e) top, (f) bottom cast at 40℃.

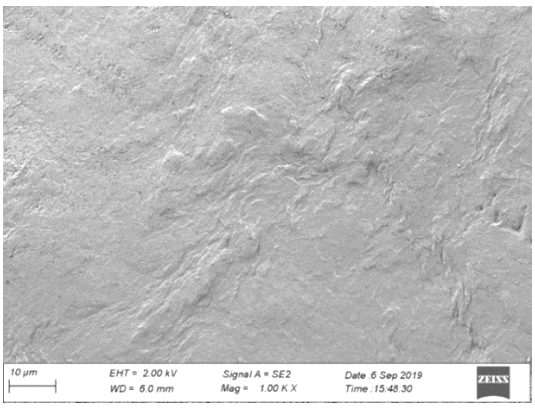

(a)

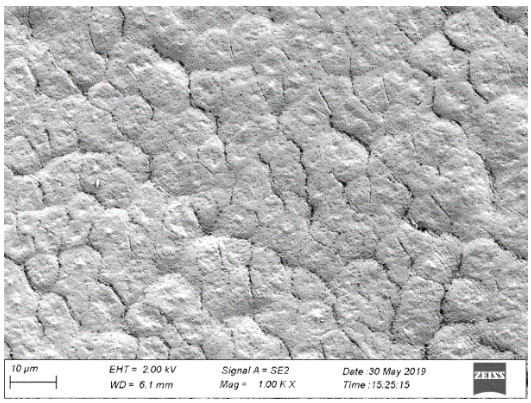

(b)

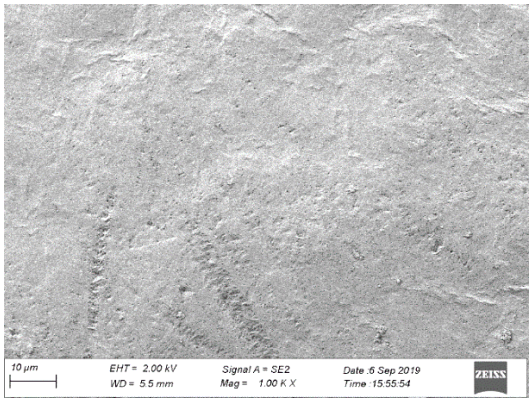

(c)

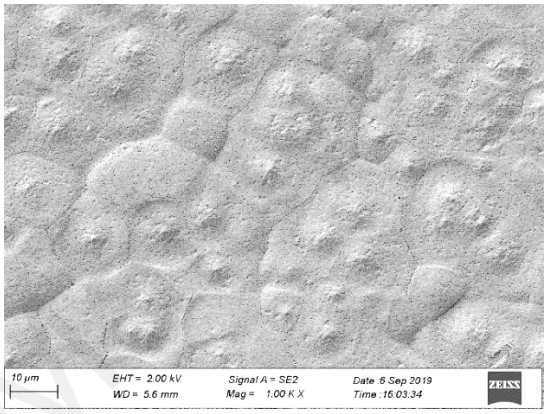

(d)

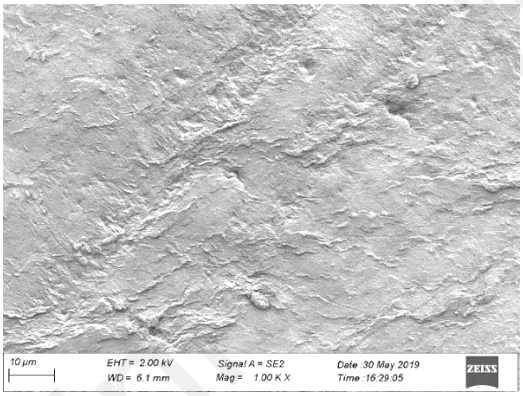

(e)

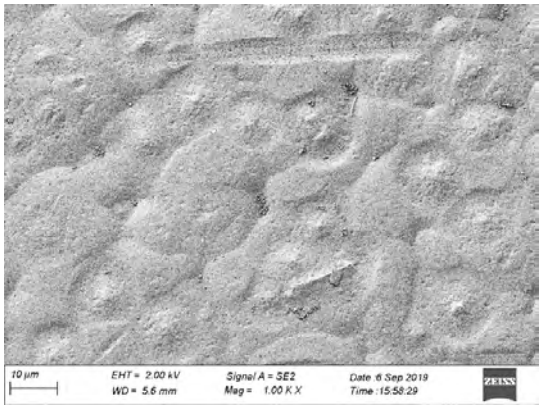

(f)

Figure 4.19 FESEM images of PVDF/PVP membranes (a) top, (b) bottom; PVDF/PVP/AgNPs-1 membranes (c) top, (d) bottom; and PVDF/PVP/AgNPs-2 (e) top, (f) bottom cast at 55℃.

Membrane cast at 25°C has a smooth top surface and visible small pores at the bottom surface. However, as temperature increases, there were significant changes observed particularly at the bottom surface. As the membranes were thermally induced, the rate of solvent evaporation also increased way before the membrane underwent phase inversion in the coagulation bath. From Figure 4.19 and 4.20, it can be observed that there is an

uneven surface with larger pores exist the bottom surface of the membrane. As the heat was introduced to the casting glass, the heat was first exerted at the bottom surface of the membrane. This explains the significant difference between the bottom membranes' surfaces.

Furthermore, as the temperature was induced at the bottom of the membrane thin film surface, the rate of solvent evaporation increases as temperature increases. Horibe et al. (Horibe et al., 2014) reported that the DMAC evaporation rate during PVDF crystalline structure production increased drastically from 0.00058 and 0.03 g min^{-1} when the temperature increased from 25 to 60°C. This hypothesized that the thermal treatment approach significantly affects membrane morphology as the evaporation rate induced altered the membrane solidification process. As the evaporation process during membrane fabrication is able to change the active layer thickness of the membrane (Kusworo et al., 2017), the cross-sections of the membranes were examined and portrayed in Figure 4.21.

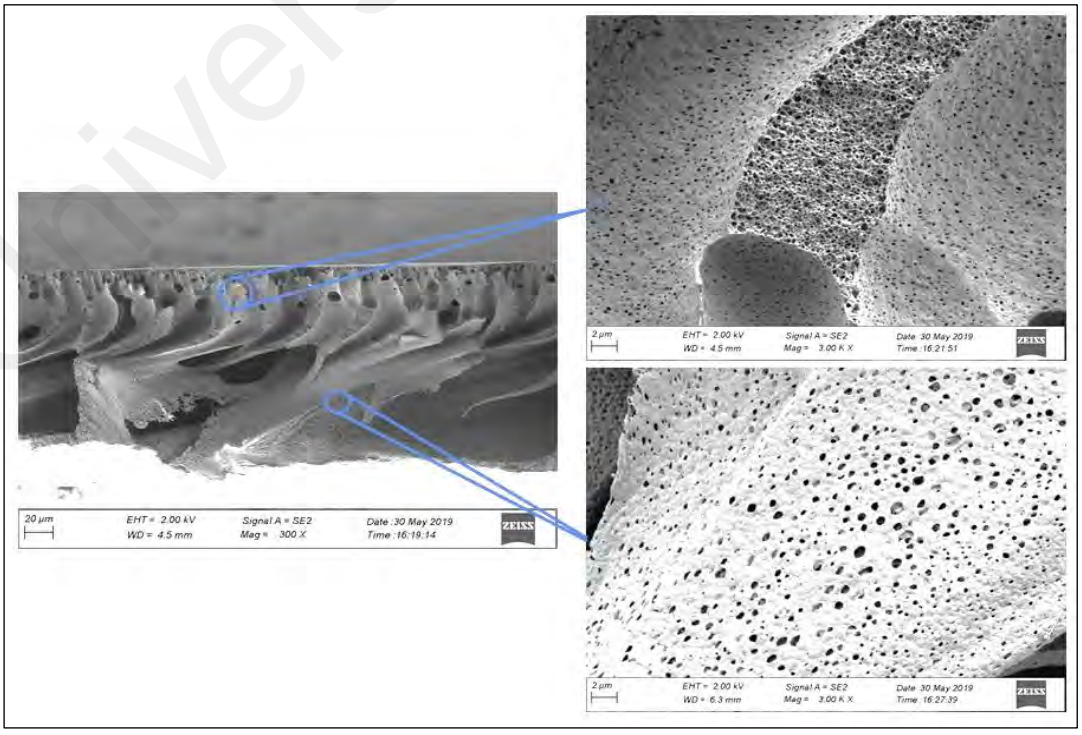

(a)

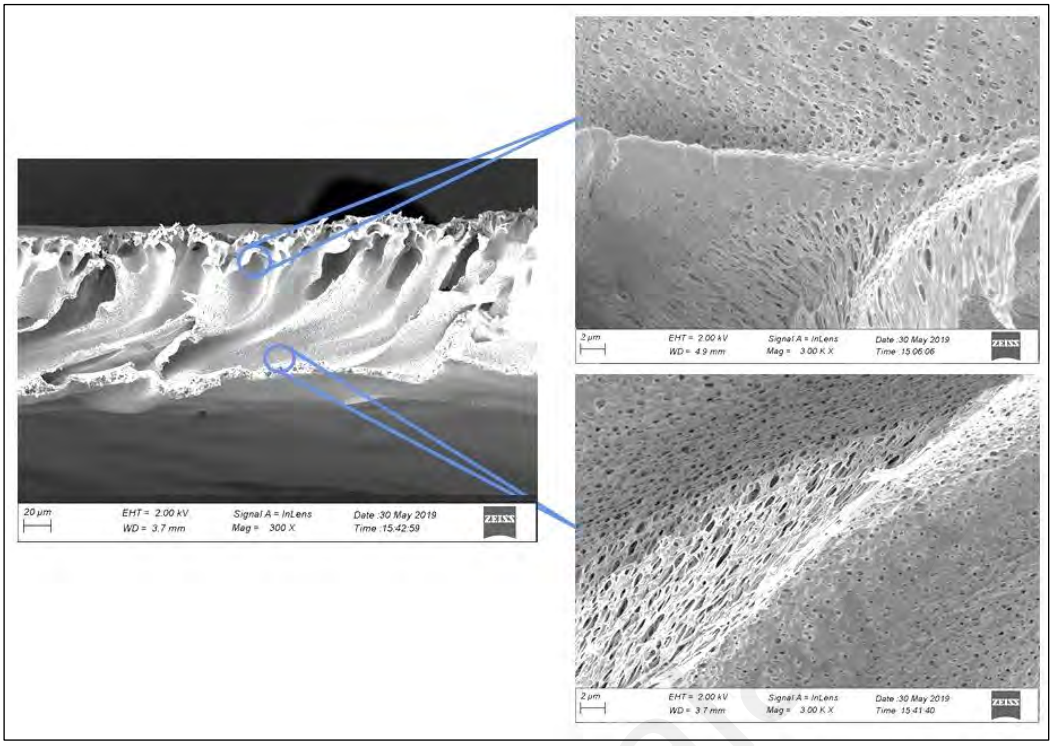

(b)

Figure 4.20 Cross-section FESEM images of membranes contained (a) AgNPs-1 at 55°C and (b) AgNPs-2 at 55°C.

Cross-sectional FESEM images provided more detailed information about the structure of the PVDF membrane when thermal treatment was applied. It was found that bottom surfaces significantly changed as compared to the top surfaces of the membranes. The efficiency of the UF process depends on the physicochemical characteristics of the polymeric membrane including its pore structure (Ismail, Ali, Kamarudin, & Yatim, 2021). Generally, both membranes have an almost identical morphological structure which consists of finger-like structures in sub-layer under the dense top surface of the common asymmetric membrane (Khan, Haider, Khurram, Wang, & Wang, 2020). In the comparison of the membrane with AgNPs-1 and AgNPs-2, PVDF/PVP/AgNPs-1 membrane had a more porous structure with the presence of evenly distributed pores on its wall. For PVDF/PVP/AgNPs-1 membrane, the walls of the membrane had larger pores but were unevenly distributed. Some regions of the membrane's wall were denser as compared to the others. The larger finger-like structure of the PVDF/PVP/AgNPs-2

membrane is possibly due to the larger surface area of thermal conductivity. Thermal conductivity increase as Ag content in PVDF increases (Chae et al., 2007). The thermal conductivity of Ag will facilitate the flow of heat upon solidification of the membrane casting solution. In relation to thermal conductivity, with respect to the finger-like structure of both membranes, the content of AgNPs in the membrane significantly differs although initial casting solution formulations were controlled at 0.45%. Furthermore, as AgNPs-1 and AgNPs-2 were synthesized via a distinctive method, the size and morphology of the AgNPs its selves were different. Therefore, the embedment location and response to the thermal treatment approach are unique for each type of membrane containing AgNPs-1 and AgNPs-2.

To capture the image of AgNPs embedded onto the bottom surface of the membrane, FESEM imaging was used with the presence of a mapping marker and EDX analysis. However, the only membrane with AgNPs-2 cast at 55°C able to be mapped and marked with the presence of Ag elements was detected via EDX analysis. The EDX mapping is shown in Figure 4.22.

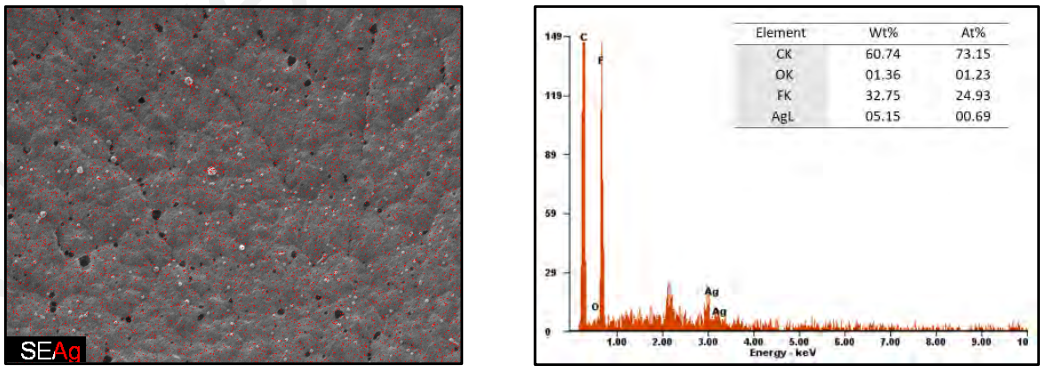

Figure 4. 21 EDX analysis for bottom surface of membrane containing AgNPs-2 cast at 55°C.

EDX analysis was carried out for both membranes containing AgNPs-1 and AgNPs-2 However, there was only one membrane with AgNPs-2 that was able to show the presence of Ag element on EDX analysis. The Ag traces were mapped in the FESEM images with

red dots. It was observed that the AgNPs-2 were evenly distributed at the bottom surface of the membrane. From the literature, it was mentioned that EDX is not favourable to be used to quantify polymeric membrane as the polymeric membrane is an organic material consisting of hydrogen, carbon, nitrogen, and oxygen which produce weak X-ray signals resulting inaccurate composition of the sample quantitatively (Alqaheem & Alomair, 2020). It is mentioned that the standard detection limit for EDX is 1000ppm or 0.1 wt% (Alqaheem & Alomair, 2020) which is considered a high detection limit for such elemental analysis (Hector, Olivero, Orange, Duñach, & Gal, 2019). Nevertheless, XPS offered a lower detection limit of up to 0.1 at% (Shard, 2014) and approximately 0.2 at% in a general solid sample (Korin, Froumin, & Cohen, 2017). Thus, XPS analysis was carried out and discussed in the following section (3.2.2).

4.2.3 AgNPs Leaching Analysis

Several analyses were carried out to determine the leaching phenomena of AgNPs within the membrane mainly during the fabrication process as a result of the thermal treatment approach. The feasibility of the thermal treatment approach in combating leaching was closely investigated.

4.2.3.1 Inductively Coupled Plasma Atomic Emission Spectroscopy (ICP-OES) Analysis

To investigate the leaching behaviour of the membrane incorporated with AgNPs, ICP-OES analysis was used to determine the Ag traces in water during the phase inversion process. Figure 4.23 shows the percentage of Ag traces concerning total Ag content in membrane casting solution formulation for (a) AgNPs-1 and (b) AgNPs-2 versus time at various casting temperatures.

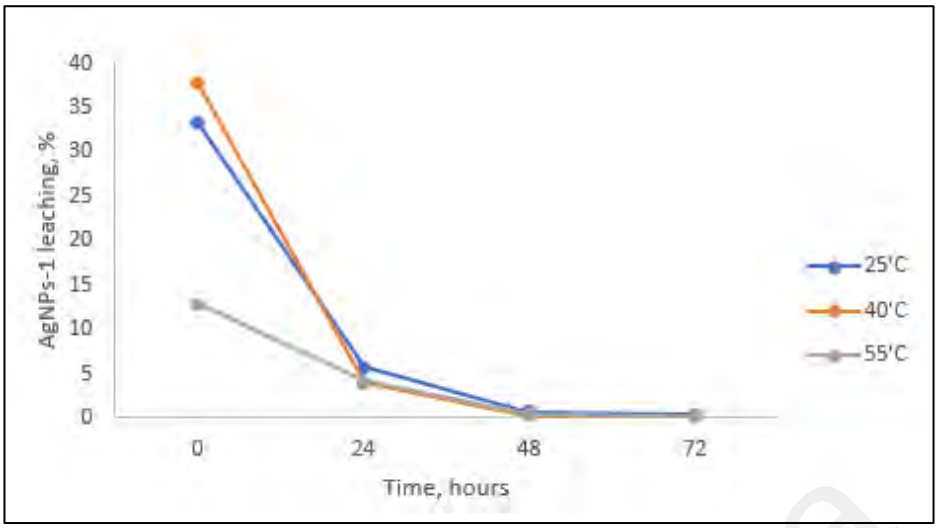

(a)

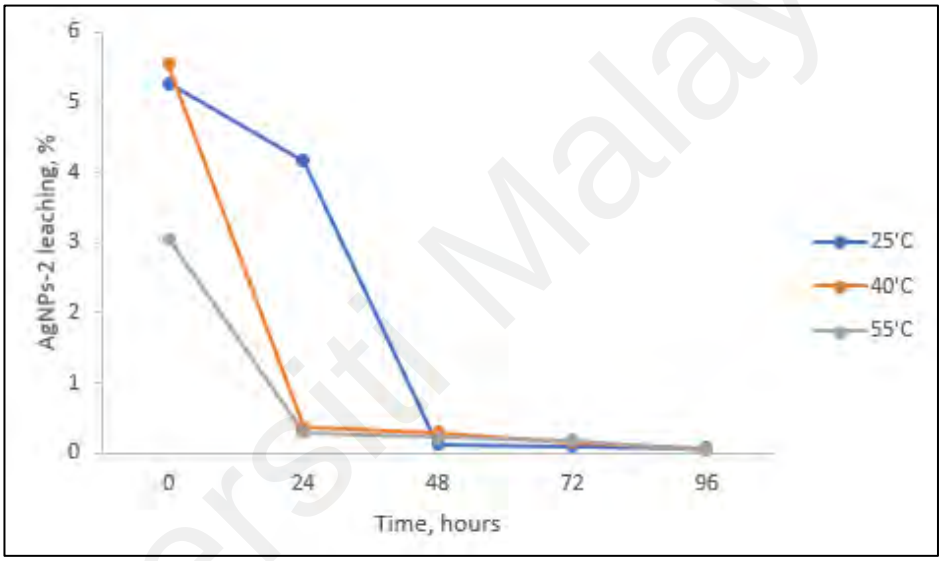

(b)

Figure 4.22 Leaching percentage of (a) AgNPs-1 and (b) AgNPs-2 versus time at various casting temperatures.

From the figure, it was found that AgNPs leached the most during the phase inversion process at t=0 when instantaneous demixing happened. Comparing the two AgNPs, a significant amount of AgNPs-1 leached more than AgNPs-2 and this portrayed that the incorporation method played an important role in determining the extent of AgNPS immobilization in the membrane matrix. Although AgNPs-1 was synthesized in DMAc, AgNPs-2 which was synthesized as a powder before being dispersed in DMAc formed a better attachment in the membrane matrix. For the PVDF/PVP/AgNPs-1 membrane, no further trace of leaching was found after 72 hours of immersion while for the

PVDF/PVP/AgNPs-2 membrane Ag trace was further identified until 96 hours of immersion.

Membranes cast at temperature 40°C have the highest leaching percentage at t = 0. A possible explanation for this is the less intense peak of alpha and beta-phase of PVDF at a particular temperature for membranes with AgNPs-1 and AgNPs-2. To further investigate the leaching of AgNPs from the flat sheet membrane fabricated, a sample of permeate during pure water filtration at 0.5 bar was tested and none of the AgNPs traces was found based on ICP analysis. The summary of leaching phenomena during phase inversion and filtration process was tabulated in Table 4.4.

Table 4.4 Leaching percentage of Ag during phase inversion and filtration**.**

Membranes	***Casting temperature, ˚C***	***Total Ag leaching, %***	
		Phase inversion (up to 96 hours)	**Filtration Process** (at 0.5 bar for 3L feed)
PVDF/PVP/ AgNPs-1	25	40.17	0
	40	42.34	0
	55	17.65	0
PVDF/PVP/ AgNPs-2	25	9.74	0
	40	6.39	0
	55	3.81	0

After the leaching phenomena was quantified, it is clear that the residual Ag is still entrapped in the membrane matrix and this finding was supported with XPS, TGA analyses, as well as bactericidal performance testing. As an attempt for biofouling mitigation, the bactericidal performance was attributed to the AgNPs residue entrapped in the membrane matrix.

4.2.3.2 X-ray Photoelectron Spectroscopy (XPS) Analysis

In this study, the XPS analysis was used to analyze the elemental composition of the top and bottom surfaces of the AgNPs incorporated membranes.

Table 4.5 Elemental composition of PVDF membrane.

Membranes	*Casting temp., °C*	*Side*	*Atomic %*				
			C	**N**	**O**	**F**	**Ag3d**
PVDF/PVP	25	T	33.53	2.13	2.02	45.53	-
		B	31.56	2.12	2.14	45.92	-
	55	T	35.82	2.05	2.27	43.56	-
		B	35.64	2.09	2.15	43.58	-
PVDF/PVP/	25	T	32.69	1.87	1.90	44.60	0.05
		B	32.7	1.91	1.92	44.35	0.05
AgNPs-1	55	T	48.43	1.69	3.78	34.51	0.04
		B	52.99	2.01	2.92	42.00	0.08
PVDF/PVP/	25	T	33.97	1.84	2.04	44.67	0.13
		B	33.94	1.86	1.93	43.68	0.13
AgNPs-2	55	T	56.50	2.36	3.16	37.38	0.60
		B	37.52	1.93	2.09	41.63	0.69

T = Top
B = Bottom

Table 4.5 shows the elemental composition of the modified PVDF membranes from XPS analysis. Carbon and fluorine were the main elements detected since the membrane polymer used is PVDF. Membrane cast at 55°C contained a higher Ag atomic percentage as compared to membrane fabricated at 25°C. This can be postulated as an effect of casting temperature whereby thermally induced conditions will speed up the evaporation of solvent making the membrane solidified faster. Consequently, the AgNPs incorporated were rapidly entrapped in the membrane matrix. In addition, concerning the FTIR-ATR result, the shifted carbonyl group vibration mode has indicated increasing intensity within the molecular bond. Thus, the elevated temperature during membrane casting significantly improved the embedment of AgNPs into the polymer matrix.

For both AgNPs, a higher Ag atomic percentage was detected at the bottom surface as compared to the top surface. Since the bottom surface is the surface that is in contact with thermally induced casting glass, it is possible the bottom surface of the membrane initially solidify before the membrane was placed in the coagulation bath for phase inversion due to solvent evaporation. During phase inversion, casting glass was instantaneously placed in a coagulation bath. In such an event, hydraulic turbulence was created around the

membrane dope when concurrently the dope underwent solidification as a flat sheet membrane. The presence of hydraulic abrasion promoted AgNPs to scour out of the membrane matrix which facilitated AgNPs release and detachment from the membrane formulation during the unsettled state of the liquid-solid phase. This finding portrays physical evidence that AgNPs is possible to leach out from membrane due to hydraulic abrasion as investigated by Bi et al., for polyamide membrane using a water jetting test (Bi et al., 2018).

In comparison between AgNPs-1 with AgNPs-2, AgNPs-2 have higher Ag percentage at any temperature. This is possibly due to the different incorporation methods of both AgNPs into the PVDF membrane. As AgNPs-1 leached significantly lower as compared to AgNPs-2, thus XPS result showed a good agreement as to the Ag element in AgNPs-1, which is significantly higher than AgNPs-2. For membrane containing AgNPs-2 cast at 25°C, the top surface consists of slightly higher Ag elements giving a contradicting result to the ICP analysis made earlier. However, higher Ag concentration was found at the bottom surface which deduces that the rapid solidification favoured at the bottom surface of the membrane when thermally induced. For both membranes cast at 25°C, the percentage of Ag found at the top and the bottom surface was identical. Since no thermal treatment was applied, it was postulated the solidification during phase inversion occurred at the same rate.

4.2.3.3 Thermogravimetric analysis (TGA)

To determine the presence of AgNPs in the membrane formation, TGA analysis was carried out for membranes with most AgNPs remaining in the composition. Figure 4.24 shows the TGA profile for all membranes fabricated at 55°C.

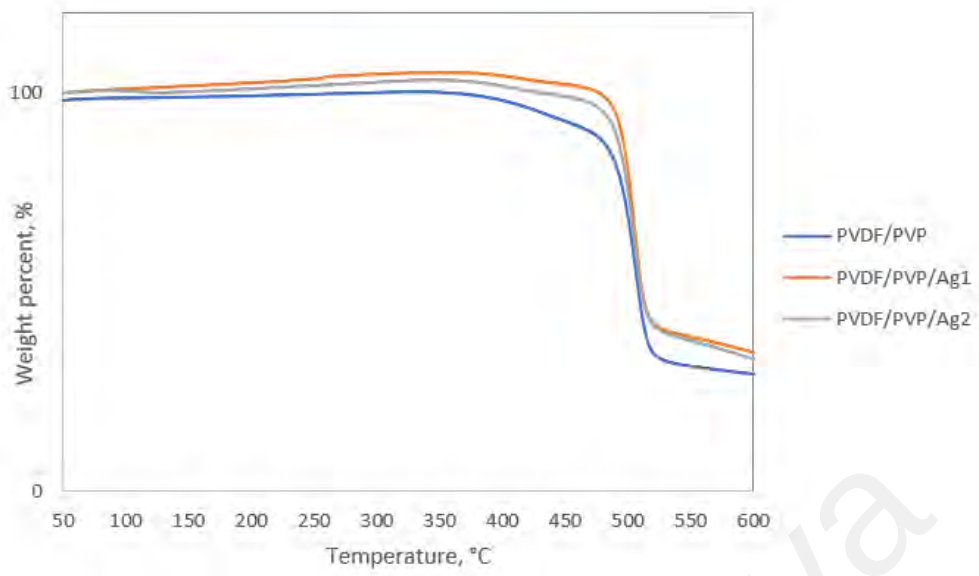

Figure 4.23 TGA profile for PVDF/PVP membrane, PVDF/PVP/AgNPs-1 and PVDF/PVP/AgNPs-2 fabricated at 55°C.

Based on Figure 4.24, all membranes underwent single-step degradation between 370 to 510°C. In such a case, the temperature in the range of 300 to 600°C is the main decomposition temperature which is suitable to be evaluated for thermal properties and stability performance for polymer composites (Ng, Ching, Awanis, Ishenny, & Rahman, 2014). Initial degradation occurred to PVDF pristine membrane and the degradation temperature shifted to 465°C as AgNPs-1 and AgNPs-2 were introduced into the membrane formulation. These show that the thermal stability of the modified membranes was significantly enhanced. It was reported that the thermal stability of PVDF and AgNPs composites related to (i) the immobilization of chains of polymer and free radical due to interaction with AgNPs and (ii) the degradation of interacted volatiles and AgNPs, which result in hampering the diffusion of this volatiles from polymer (Issa, Al-Maadeed, Luyt, Ponnamma, & Hassan, 2017).

Based on the results from ICP and XPS analysis, significant leaching of AgNPs was found in PVDF/PVP/AgNPs-1. However, at the end of the degradation curve at 600°C, the residual weight of PVDF/PVP/AgNPs-1 was higher than the PVDF/PVP/AgNPs-2

membrane which was 36.82% and 35.16% respectively while PVDF/PVP membrane was 31.44%. As there was more AgNPs content in PVDF/PVP/AgNPs-2 membrane, it was hypothesized that AgNPs had facilitated the thermal decomposition process of PVDF as AgNPs has higher thermal conductivity (Chae et al., 2007). The introduction of AgNPs delayed the decomposition of the composite phase change as the thermal weight loss was improved for both membranes containing AgNPs. This TGA result supports the finding in XPS analysis when the weight and degradation temperature of the membrane portrayed the atomic presence of Ag.

4.2.4 Bactericidal Performance of Modified PVDF Membranes towards *E. coli* and *S. aureus*

Bactericidal performance of PVDF/PVP/AgNPs-1 and PVDF/PVP/AgNPs-2 membranes were analyzed using a bacteria count plate method and shown in Figure 4.25. Figure 4.26 shows the bacteria count for the lake water sample with the presence of membranes cast at 55°C and without any presence of the membrane.

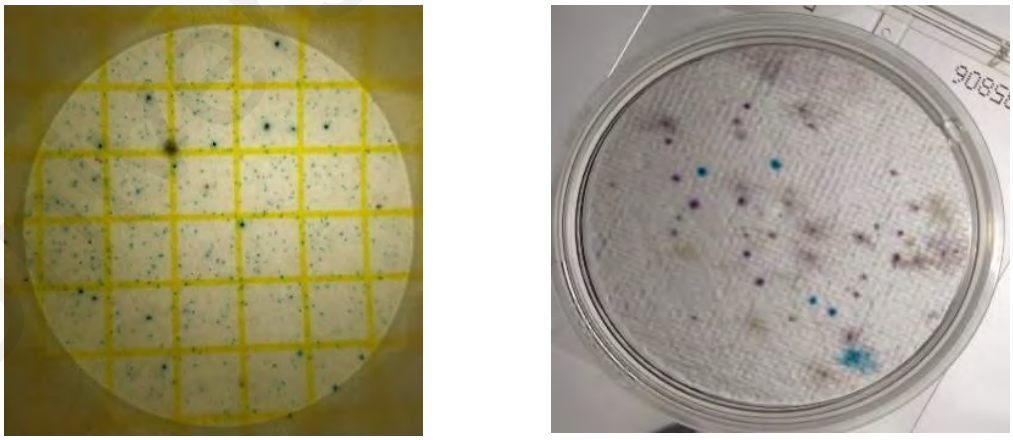

(a) (b)

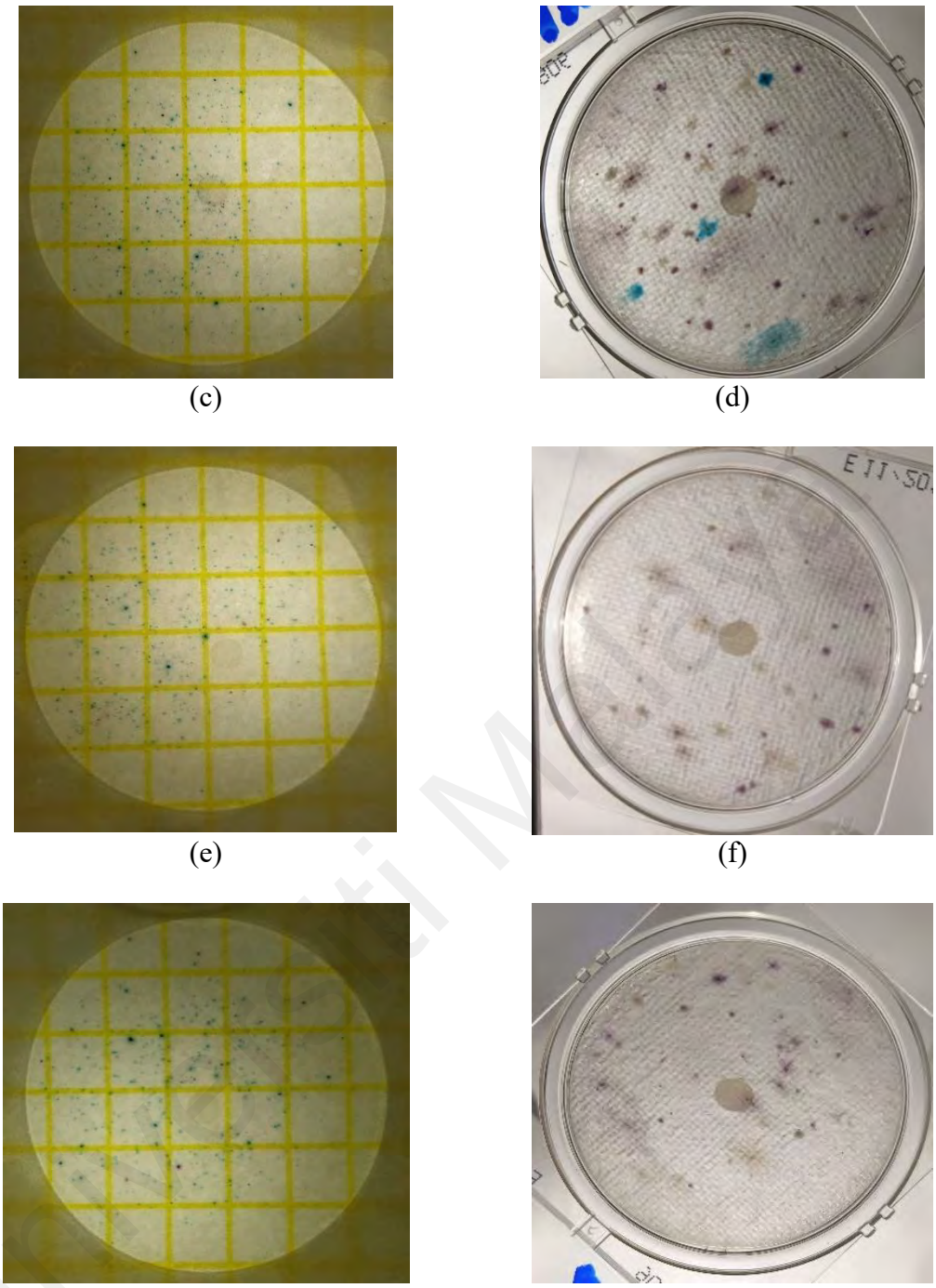

Figure 4.24 Bacteria count plate for *S. aureus* (yellow, left) and *E. coli* (white, right) tested for (a,b) lake water, (c,d) lake water with the presence of PVDF/PVP membrane, (e,f) lake water with the presence of PVDF/PVP/AgNPs-1 membrane, (g,h) lake water with the presence of PVDF/PVP/AgNPs-2 membrane.

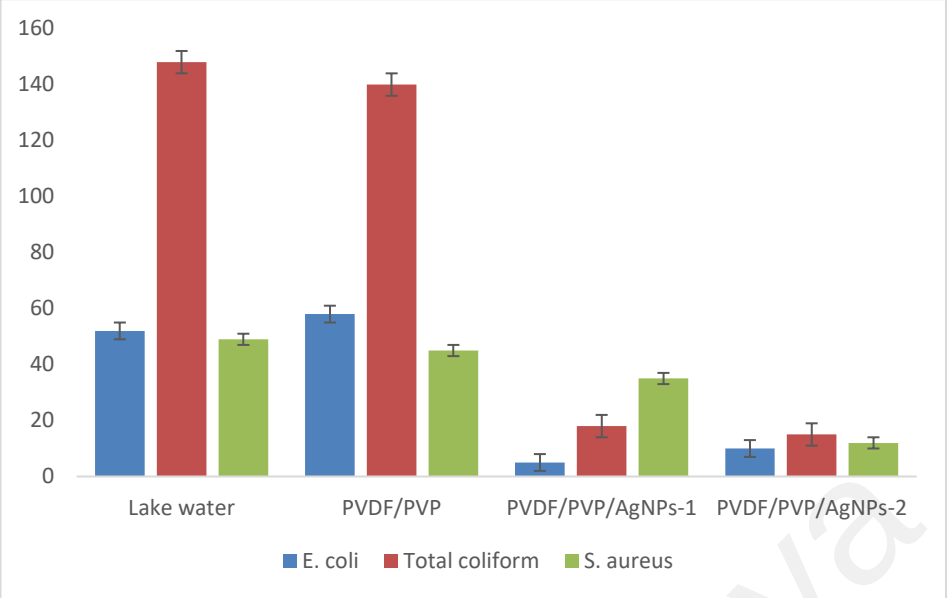

Figure 4.25 Lake water bacteria count of total coliform, *S. aureus* and *E. coli* in contact with different type of membranes.

The antibacterial performance of both membranes selected was carried out using the bacteria count plate method as the method portrayed the actual number of living bacteria in the sample. The lake water sample was pipetted onto the surface of the membranes which was placed in the middle of the count plate. Upon the entrance of the Ag ion inside the bacteria cell, the bacterial respiratory chain was disturbed as the thiol group bound to the involved enzyme which signifies the bactericidal properties of AgNPs (Hasan, Waibhaw, Saxena, & Pandey, 2018). The log reduction and percentage reduction were calculated based on Eq (3.1) and Eq. (3.2), and the values were summarized as depicted in Table 4.6.

Table 4.6 Log reduction and percentage reduction of *E. coli,* total coliform and *S. aureus.*

Membranes		*PVDF/PVP/AgNPs-1*	*PVDF/PVP/AgNPs-2*
Log reduction, L	*E. coli*	1.02	0.72
	Total Coliform	0.91	0.99
	S. aureus	0.15	0.61
Percentage reduction, P (%)	*E. coli*	90.38	80.77
	Total Coliform	87.84	89.86
	S. aureus	28.57	75.51

4.2.5 Membranes Molecular Weight Cut-Off

Commonly, MWCO measurements were used to characterize the membrane solute transport properties (Cheryan, 1998; Ju et al., 2008) while MWCO specified by the manufacturer was used to select the suitable application of the membrane at first (Razdan, Joshi, & Shah, 2003). The solute rejections versus the multiple molecular weight of a single solute were plotted in Figure 4.27.

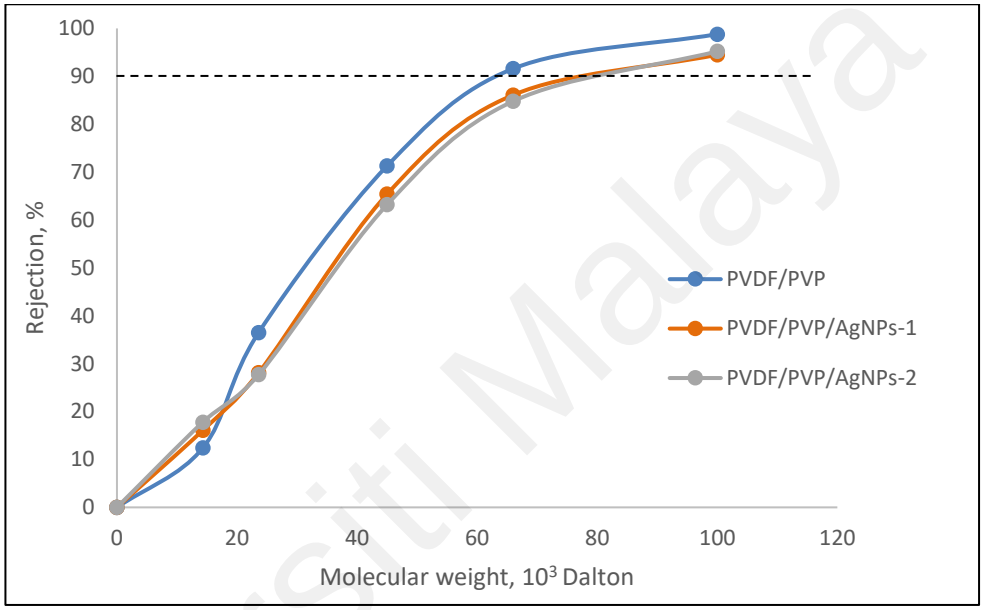

Figure 4.26 Percentage of rejection values versus multiple molecular weight of tested protein solutes for MWCO determination.

The MWCO of the native PVDF membrane was estimated to be 64 kDa while PVDF/PVP/AgNPs-1 was 72 kDa and PVDF/PVP/AgNPs-2 was 78 kDa. The MWCO was increased upon the addition of AgNPs with PVDF/PVP/AgNPs-2 having the highest MWCO. This could be featured to the change during the fabrication process due to the presence of heat as a thermal treatment approach and AgNPs as a bactericidal agent. As compared to the results in (4.2.3) the amount of AgNPs-2 is higher than AgNPs-1 in the membranes following the leaching phenomena in the modified membranes which reflect the different characteristics of the membranes including MWCO. Interestingly, these findings match the expectation upon observation of FESEM images.

Obviously, all membranes were considered as UF membranes based on the MWCO computed. The MWCO obtained for all membranes upheld the literature of which PWP increased as nominal MWCO increased (Peeva, Million, & Ulbricht, 2012). Besides, the PVDF/PVP and PVDF/PVP/AgNPs-1 membranes were consistent with pore size results and reflect well on the MWCO obtained. Conversely, PVDF/PVP/AgNPs-2 have the smallest pore size, which was discussed earlier and believed to be caused by the blockage of AgNPs in the membrane matrix. The trade-off behaviour observed is likely associated with the transport process and rejection mechanism (Ren, Li, & Wong, 2006). Additionally, fouling and adsorption during the filtration process may result in overestimation and underestimation of MWCO (T.-Y. Liu, Zhang, Li, Van der Bruggen, & Wang, 2014). Whereas the difference in predicted retention is commonly reported and justified upon the presence of abnormal pores (Arkhangelsky, Duek, & Gitis, 2012; Urase, Yamamoto, & Ohgaki, 1994, 1996). In spite of the various empirical relationships, the 90% retention capability was achieved within 100kDa.

4.3 Surface Water Filtration Performance

The filtration performances of all membranes were examined upon the filtration of an actual surface water sample. A lake water sample from Varsity Lake in Universiti Malaya was used in this study without any pre-treatment. The lake water characteristics were first determined before the filtration process.

4.3.1 Lake Water Characteristics

To assess the purification effect of the modified membranes on surface water, characteristics of the feed and permeated were recorded with reference to water quality standards as in Table 4.7.

Table 4.7 Characteristics of lake water used as feed and the permeate after filtration.

Characteristics	*Feed*	*Permeate*			*Drinking Water Quality Standards**
		PVDF/ PVP	**PVDF/PVP/ AgNPs-1**	**PVDF/PVP /AgNPs-2**	
Temperature (°C)	25.33	25.0	24.8	24.8	-
pH	6.73	7.03	6.98	7.02	6.5 - 9
Dissolved Oxygen (mg/L)	6.3	7.8	8.7	8.2	-
Turbidity (NTU)	22.0	4.92	4.63	4.71	5
Total Dissolved Solid (mg/L)	45.6	43.7	43.2	42.9	1000
*E. coli (*Cfu)	25	0	0	0	0 in 100ml
Total Coliform (Cfu)	6	0	0	0	0 in 100ml
*S. aureus (*Cfu)	28	0	0	0	-

** Maximum acceptable value (mg/liter (unless otherwise stated)) (Ministry of Health Malaysia, 2004).*

The water quality of the feed was significantly improved after the membrane filtration process. Turbidity of the permeate water was reduced to less than 5 NTU which complies with national drinking water guidelines. Total coliform, *E. coli*, and *S. aureus* was removed entirely based on the bacteria count plate test carried out is comparable with previous literature, which also described the capability of ultrafiltration membranes to remove bacteria effectively (Hoslett et al., 2018). Membrane-based water technologies, especially UF, are the most modular option to remove bacteria (Loo et al., 2012). Significantly, this indicates the presence of bacteria on the membrane surface as biofouling due to its inability to pass through membrane filtration. In relation to dissolved oxygen (DO) concentration, permeate of the unmodified membrane has less DO compared to modified membranes which might be caused by higher microorganism presence at the membrane surface forming the biofouling layer (Q. Wang et al., 2022).

In contrast, the increment of DO in all permeates flux is related to the air flow rate as it is one of the influencing operating parameters in membrane filtration set-up (Iritani et al., 2007). During filtration, the feed was continuously stirred in the dead-end cell creating

turbulence in the water flow (Kimura, Nakamura, & Watanabe, 2002). Additionally, the permeate was collected at an elevated level from the collection beaker resulting indirect aeration process (Alturki et al., 2010). In all water bodies, including surface and groundwater, natural organic matter (NOM) does exist. It consists of largely aliphatic, highly colored and aromatic, and uncharged to highly charged chemical compositions with a wide range of molecular sizes (Matilainen & Sillanpää, 2010). Based on these criteria of NOM, MF and UF are barely feasible for the removal of the dissolved contaminants, principally NOM in surface water, as it adversely affects the filtration performance of both membranes due to fouling (Zularisam, Ismail, & Salim, 2006). This justified the minimal removal of total dissolved solid upon filtration of the membrane.

4.3.2 Dead-End Cell Filtration Performance

The lake water was filtered through the membranes to develop a fouling layer. Fouling can be simply indicated by flux reduction, and it was concluded that the fouling mechanism relies on the type of membrane and initial UF flux magnitude (Jim et al., 1992). Therefore, the initial flux for ultrapure water for each membrane, followed by the flux of 1L lake water filtration consecutively three times and the flux for ultrapure water after the filtration process, were plotted in Figure 4.28.

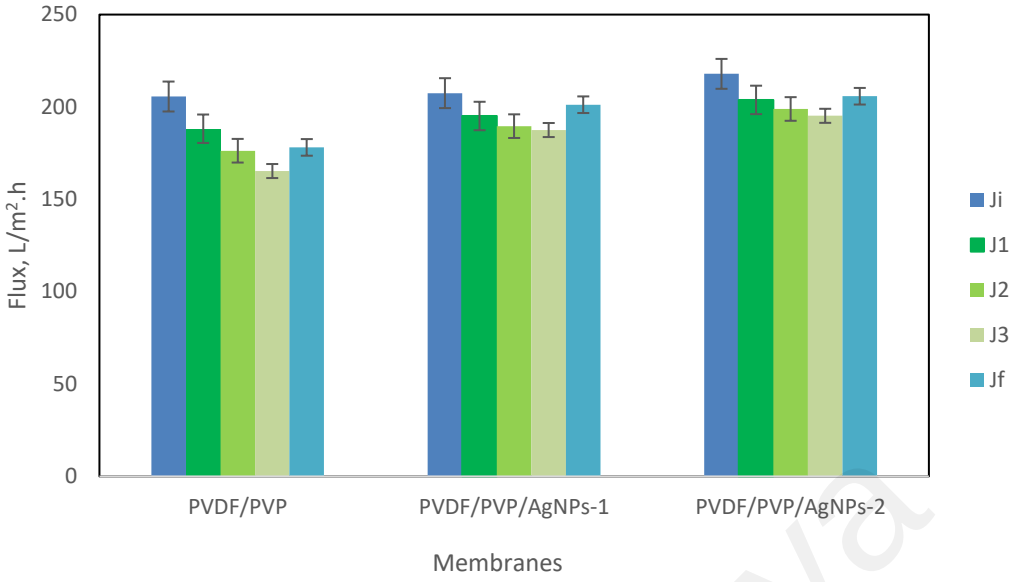

Figure 4.27 Flux declines for all membranes upon filtration of lake water.

Based on the figure, it is found that the flux of water at the end of the filtration process is not the same as the initial flux before any filtration takes place. Originally, the initial flux of pure water permeation for all modified membranes is improved as reported in section 4.2.1. Along the filtration period, the flux of all membranes has declined yet the overall filtration performance of both PVDF/PVP/AgNPs-1 and PVDF/PVP/AgNPs-2 membranes are enhanced compared to PVDF/PVP membrane. Such declines during filtration are a clear indication of fouling occurrence whereby any particles in the lake water which unable to pass through the membrane barrier are deposited onto the membrane surface. Accumulation of this material as foulant drastically reduces the lake water flux and the pure water flux at the end of experiments. Even so, the flux recorded was unable to return to its initial state, which is likely related to unreversible fouling. Thus far, prior studies have established that fouling can be classified into reversible and irreversible fouling which the reversible one can be scoured out depending on the reversibility rate and extent (Kanani, Sun, & Ghosh, 2008).

In our context, the filtration of pure water at the end of the experiment is to remark the presence of foulant onto the membrane surface relatively. Earlier on, it was reported that flux decay during filtration was attributed to the combination of a few fouling mechanisms throughout time (Lim & Bai, 2003). Since the flux of each division of lake water filtration is declining throughout time, it is proportional to the previous literature reported that each fouling mechanism changes with time (D. Kamarudin, Ismail, & Othman, 2015; Lim & Bai, 2003). AgNPs incorporation method and casting temperature also played important roles in determining the final composition of AgNPs in the membrane before and during the filtration application. Notably, different amounts of AgNPs in membrane composition will also affect the membrane flux (Li et al., 2013). To further analyze the fouling occurrence on the membrane surface, fouling analysis was carried out and reported in Section 4.4 ahead based on the dead-end filtration system.

4.3.3 Filtration Performance in a Bench-Scale System

To examine the performance of lake water filtration in a more advanced condition of a longer filtration period and higher feed load, the same flat sheet membranes fabricated were employed in a crossflow filtration system and used for a longer period of 180 minutes at 0.5 bar. The flux decline curves were recorded in Figure 4.29.

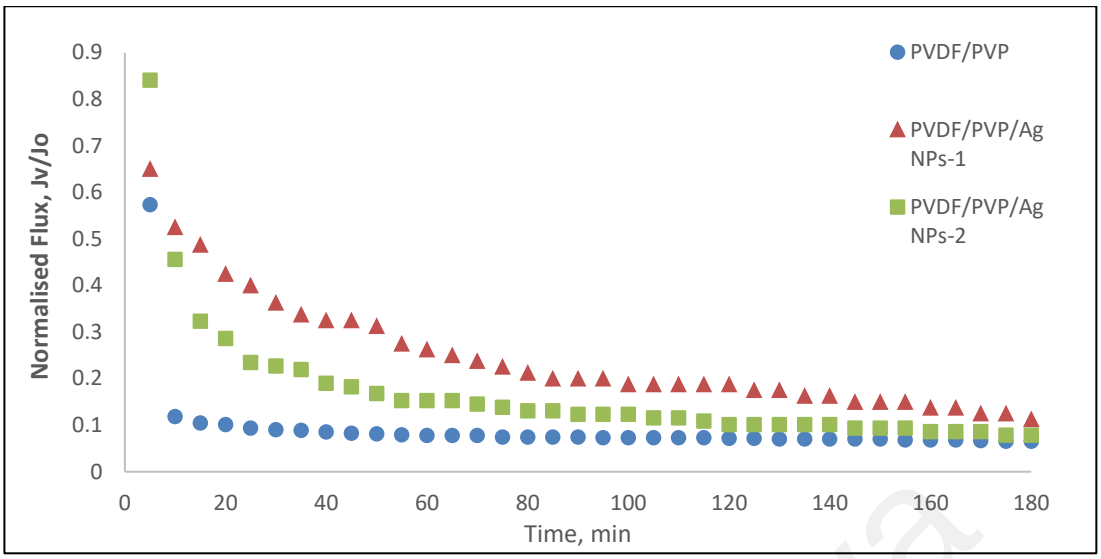

Figure 4.28 Flux decline curves of normalized flux for all membranes.

Figure 4.29 shows the declination of normalized flux curves during the filtration of the lake water using the three different membranes. The initial minutes of the filtration process recorded a very rapid declination of flux in all membranes. This is commonly discussed as the effects of the accumulation of rejected solutes on the membrane surface (Ariono, Aryanti, Subagjo, & Wenten, 2017; Braghetta, DiGiano, & Ball, 1998; Jarusutthirak, Mattaraj, & Jiraratananon, 2007). As the filtration continues, on the 10th and 30th minutes of modified membranes, the flux gradually declines while the native membrane already declined at a steady state before the major flux decline at the beginning of the filtration process. Even at constant pressure, the flux decline during operation due to fouling was frequently reported in literature yet the mechanism was only partially unraveled (Yu Guo, Li, Xiao, Wang, & Xie, 2020; K.-J. Hwang & Wu, 2008; Rezaei, Ashtiani, & Fouladitajar, 2011; Tolkach & Kulozik, 2006).

After the 100th minute of operation, the flux decline of the PVDF/PVP membrane reached a pseudo-steady state in which the flux was maintained almost unchanged. Both modified membranes continue to have a minimal declination of flux as the filtration continues. This indicates that fouling compacted over time as the filtration pursue over a

long period (Tsai et al., 2019). Deposition of solutes onto membrane surface and pores, and cake layer formation were all possible especially when filtering complex solutes from the actual sample as in this study. This condition eventually reduces the permeability of the membrane and leads to performance and lifespan reduction (Peters, Rantissi, Gitis, & Hankins, 2021). Taken together, the overall filtration performance suggests that the fouling occurrence in the modified membrane is significantly less severe compared to the native membrane. Nevertheless, upon the comparison of AgNPs-1 and AgNPs-2 as modification agents, PVDF/PVP/AgNPs-1 membrane offered enhanced filtration performance compared to PVDF/PVP/AgNPs-2 membrane in crossflow system application for a longer period. Rapid declination of flux in less than 20 minutes filtration period using PVDF/PVP membrane portrays that PVDF membrane immobilized with AgNPs is vital for sustainable application of membrane technology.

4.4 Fouling Analysis of Modified PVDF Membranes

FDR and FRR were claimed to be vital indexes in portraying membrane antifouling capabilities (Wu et al., 2021). Thus, these two parameters were calculated based on the flux obtained in Figure 4.28 and represented in Figure 4.30.

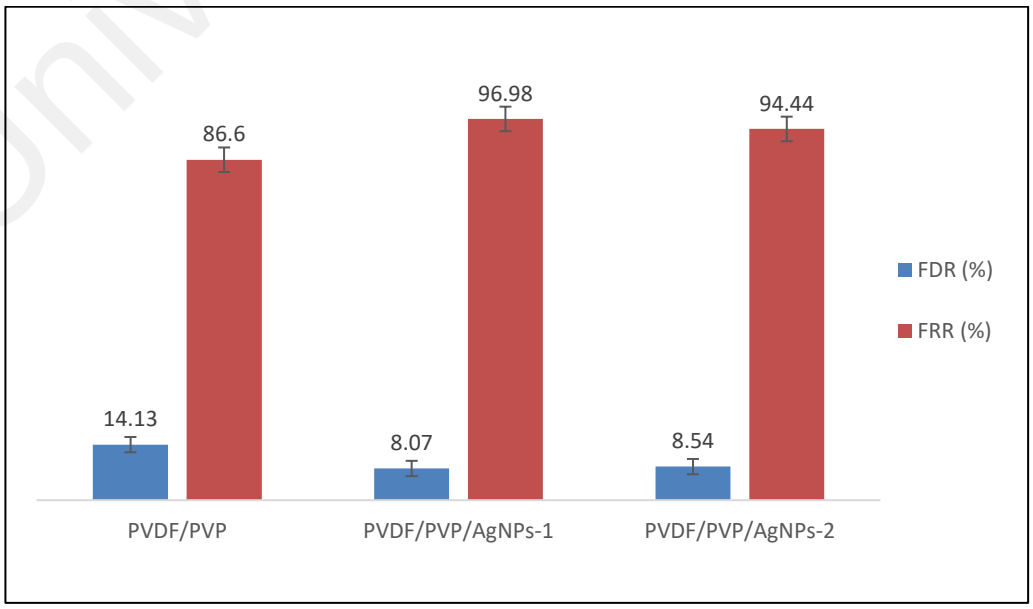

Figure 4.29 FDR and FRR for all membranes.

The maximum FDR value was obtained from the native membrane which is 14.13%. Upon incorporation of AgNPs in PVDF/PVP/AgNPs-1 and PVDF/PVP/AgNPs-2, the FDR values were significantly reduced to 8.07% and 8.54% indicating that the AgNPs have served as fouling mitigation agents. Meanwhile, the highest FRR value was obtained from PVDF/PVP/AgNPs-1 membrane which is 96.98% followed by PVDF/PVP/AgNPs-2 membrane at 94.44% and PVDF/PVP membrane at 86.6%. The previous study has demonstrated that flux recovery depends on the initial flux of the membrane and the feed composition (Nguyen, Adha, Field, & Kim, 2021).

Even so, the applications of metal nanoparticles rely on their physicochemical properties namely composition, size, shape, crystallinity, and structure (Mdluli et al., 2011). Within our context, the impregnation of AgNP as a disinfectant into polymeric membranes for water filtration is one of many attempts made to utilize the antibacterial property of AgNPs. Despite the total leaching percentage of AgNPs-1 and AgNPs-2 being 17.65% and 3.81% respectively, it is noteworthy that leaching phenomena were significantly improved from 40.17% and 9.74% without the application of thermal treatment. Amazingly, a smaller amount of AgNPs-1 compared to AgNPs-2 is able to deliver better performance in bactericidal effects towards *E. coli*, dead-end filtration, and crossflow filtration.

In relation to the results in Figure 4.28, the initial flux for the modified membranes was slightly higher as compared to the native membrane. This explains the modification via adding AgNPs in the membrane composition had altered the membrane's permeability as previously discussed. Moreover, physical observations of the changes in surface morphology of the clean and fouled membrane were captured using FESEM as in Figure 4.31.

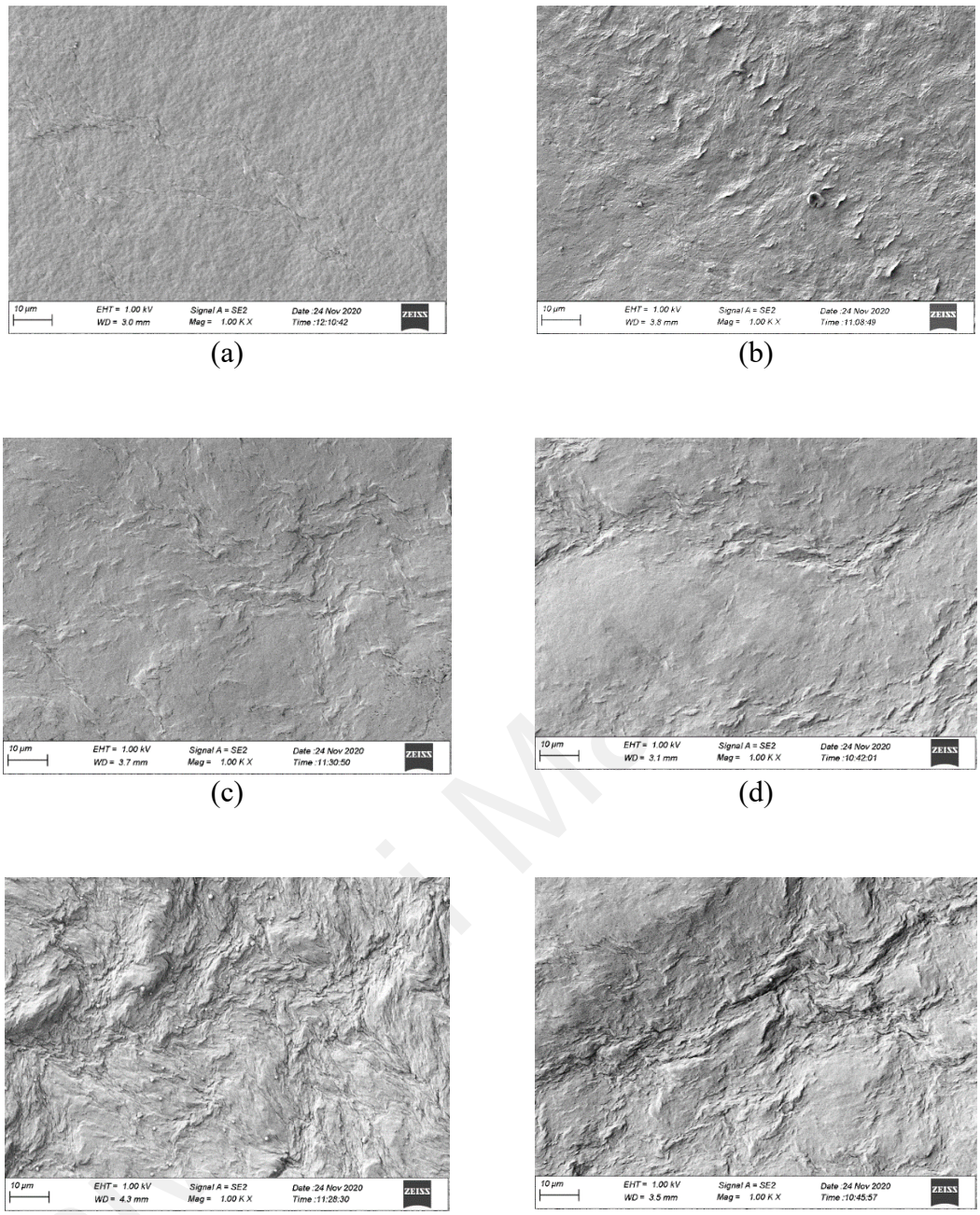

Figure 4.30 FESEM images of the (a) clean and (b) fouled PVDF/PVP membrane; (c) clean and (d) fouled PVDF/PVP/AgNPs-1 membrane; (e) clean and (f) fouled PVDF/PVP/AgNPs-2 membrane.

From the images, it is empirically apparent that foulant has accumulated onto the membrane surface. The wrinkles that appeared on the surface of the clean membranes are attributed to the thermal treatment at 55˚C exerted during the membranes fabrication as previously discussed. This approach of elevating the fabrication temperature is designated to anchor more AgNPs and minimize leaching phenomena during the fabrication, and the remarkable success of this approach was also reported. Consequently, this approach

creates ‘hill’ and ‘valley’, which were also reported in works of literature with multiple different methods applied (Szczygiełda, Krajewska, Zheng, Nghiem, & Prochaska, 2021; Toh, Oh, Chew, & Ahmad, 2020; H. Xu et al., 2020).

With the presence of AgNPs, the height and depth of the hill and valley were noticeably observed, and this can be related to the thermal conductivity of the AgNPs aforementioned. As foulant is embedded on the membrane surface, it is likely to fill the valleys during the filtration process. Thus, it is speculated that the fouled membranes have a smoother surface as the foulant built up and formed a layer. Yet, fouled membrane PVDF/PVP possesses flakier topology due to the accumulation of much more foulants which were the rejected solutes (Mondal & Wickramasinghe, 2008). A flaky fouled membrane surface was also reported by Szczygiełda, Krajewska, Zheng, Nghiem, and Prochaska (2021) suggesting the probable of insufficient applied pressure and a relatively short filtration period. Also, it is worth mentioning that the foulant was not evenly distributed on the membrane surface (Amigo, Urtubia, & Suárez, 2018; Szczygiełda et al., 2021). By way of benefiting the wrinkles, Liu et al. had reported that such topography of membrane surface is less susceptible to fouling occurrence owing to the less shelter for foulant attachment (T. Liu et al., 2021).

4.4.1 Foulant Weight Quantification using TGA

Commonly, the physical and thermal properties of polymeric membranes are investigated using TGA (Montaser, Wassel, & Al-Shaye'a, 2019). Previously, the enhancement of the modified PVDF membranes' thermal stability was reported as an indication of AgNPs in the composition of the membranes supported with X-ray photoelectron spectroscopy (XPS) and inductively coupled plasma atomic emission spectroscopy (ICP-OES) analysis. Yet, the current analysis of TGA remains underutilized since it was first reported for fouling quantification by Tay et al. in 2003 (Tay et al., 2003).

This section will investigate the use of TGA as a tool for the quantification of fouling weight (FW) of AgNPs modified membranes. Figure 4.32 shows the thermal degradation for all clean and fouled membranes.

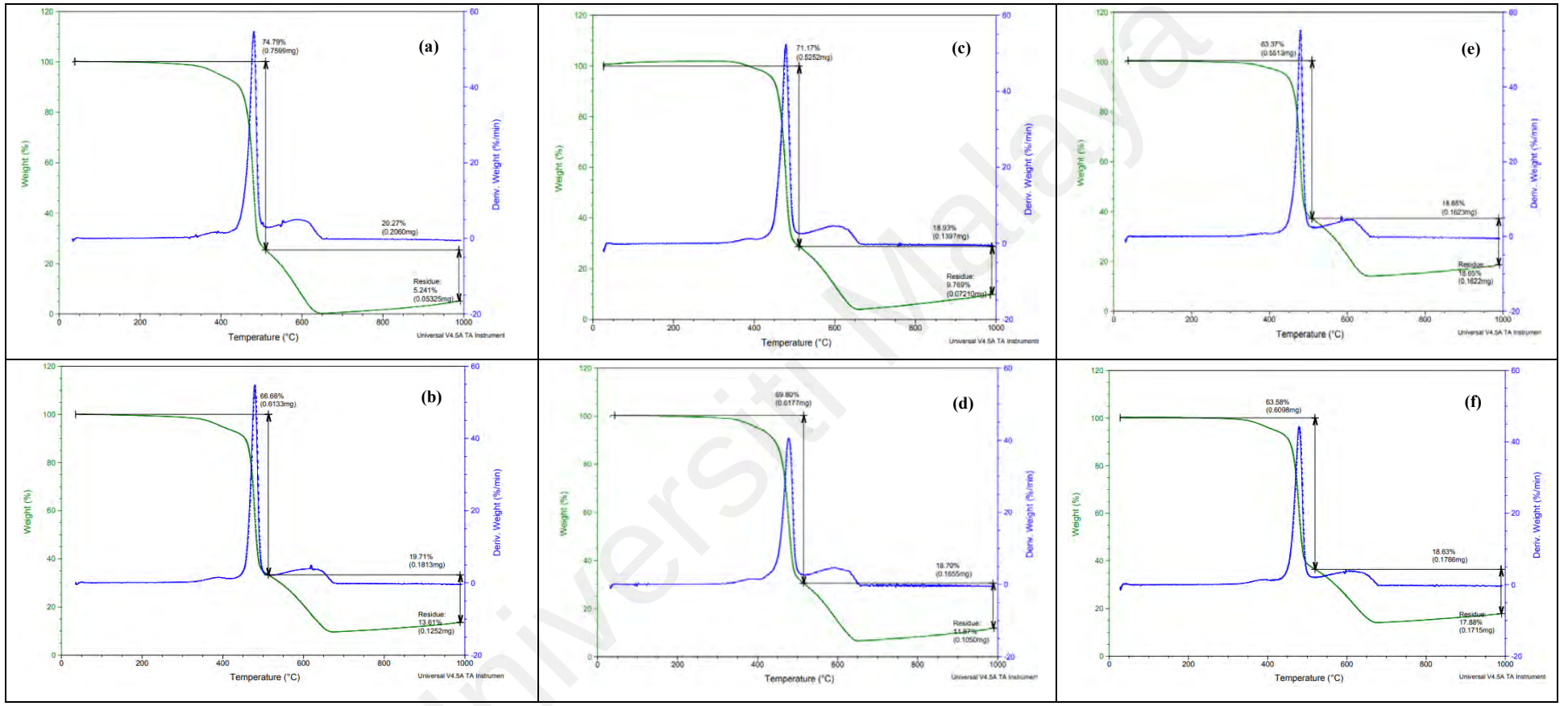

Figure 4.31 Thermogravimetric properties of (a) clean and (b) fouled PVDF/PVP membrane; (c) clean and (d) fouled PVDF/PVP/AgNPs-1 membrane; (e) clean and (f) fouled PVDF/PVP/AgNPs-2 membrane.

It could be observed from the curves that all fouled membranes possessed more residual at the end of the degradation temperature. The lowest weight percent of fouled membranes are higher compared to clean membranes indicating there is the presence of other materials in the sample, which is assumed as foulant, entirely. Slight weight gain at the end of the TGA curves was described to be the effect of buoyancy, oxidation, absorption, adsorption, decomposition, or reduction (Banerjee; Potter, Cotts, & Wiebke, 2017). This phenomenon can be observed in a few other studies related to the polymeric membrane at a temperature higher than 700°C (Abedini, 2019; Bousbih et al., 2021; Jayalakshmi, Kim, & Kwon, 2015; Kancherla, Kumar, Prabhaker Reddy, & Sridhar, 2020). It is also possible that at such temperature further thermal degradation of polymer and metal nanoparticles phase change occurred (Nicolais & Carotenuto, 2013).

The thermogravimetric analysis approach provides a mean weight loss at a certain temperature concerning volatile and non-volatile solid decomposition. Theoretically, volatile component undergoes decomposition in the temperature range of 105 to 500°C (Tay et al., 2003) and some considered complete degradation of volatile components at 500 to 600°C (Ismail, Ali, Kamarudin, & Yatim, 2020; Languer et al., 2020; Vuppaladadiyam, Antunes, Sanchez, Duan, & Zhao, 2021). In the present study, the minimum remaining weight was considered in determining the non-volatile FW which was different for every sample. Thus, five different points of temperature in the minimal region located before and after the lowest point of the remaining residual were taken into consideration and computed to determine non-volatile FW.

4.4.1.1 Non-volatile FW

Non-volatile FW was first determined using Equation (3.11). The lowest weight remaining portion occurred at temperature >500°C making the temperature suitable to be selected for non-volatile FW determination as all volatile compound was fully vaporized

at a temperature beyond 500°C. Table 4.8-4.10 shows data derived from the temperature scan curve calculated to determine the non-volatile FW of each membrane.

Table 4.8 Non-volatile FW for PVDF/PVP membrane.

Temp., °C	***Weight percentage of remaining portions, %***		***Foulant deposited*** *(coefficient, no unit)*	***FW_{NV}, g/m²***
	Clean membrane	*Fouled membrane*		
644	0.3366	12.1251	0.1342	106.2333
645	0.3176	11.9535	0.1322	104.6543
646	0.2964	11.7894	0.1303	103.1767
647	0.2954	11.6405	0.1284	101.6761
648	0.2903	11.4839	0.1265	100.1417
*649***	0.2878	11.3354	0.1246	98.6702
650	0.2949	11.1950	0.1227	97.1991
651	0.3085	11.0541	0.1208	95.6696
652	0.3259	10.9202	0.1189	94.1803
653	0.3372	10.7983	0.1173	92.8692
654	0.3498	10.6855	0.1157	91.6397
Average:			0.1246	98.6930

** a_m is 791.8936 g/m²*
*** temperature at the lowest remaining portion.*

Table 4.9 Non-volatile FW for PVDF/PVP/AgNPs-1 membrane.

Temp., °C	***Weight percentage of remaining portions, %***		***Foulant deposited*** *(coefficient, no unit)*	***FW_{NV}, g/m²***
	Clean membrane	*Fouled membrane*		
654	4.0216	6.5757	0.0273	23.6653
655	3.9917	6.6003	0.0279	24.1773
656	3.9679	6.6251	0.0285	24.6329
657	3.9482	6.6323	0.0287	24.8848
658	3.9339	6.6687	0.0293	25.3649
*659***	3.9322	6.6737	0.0294	25.4285
660	3.9350	6.6897	0.0295	25.5556
661	3.9314	6.6879	0.0295	25.5722
662	3.9367	6.7040	0.0297	25.6761
663	3.9461	6.7024	0.0295	25.5736
664	3.9490	6.7133	0.0296	25.6508
Average:			0.0290	25.1075

** a_m is 865.6363 g/m²*
*** temperature at the lowest remaining portion.*

Table 4.10 Non-volatile FW for PVDF/PVP/AgNPs-2.

Temp., °C	***Weight percentage of remaining portions, %***		***Foulant deposited*** *(coefficient, no unit)*	***FW_{NV}, g/m^2***
	Clean membrane	*Fouled membrane*		
651	14.1972	15.8841	0.0201	17.1187
652	14.1621	15.7373	0.0187	15.9573
653	14.1272	15.6134	0.0176	15.0340
654	14.1098	15.5059	0.0165	14.1048
655	14.1052	15.3730	0.0150	12.7882
*656***	14.0919	15.2459	0.0136	11.6219
657	14.0930	15.1400	0.0123	10.5319
658	14.1016	15.0299	0.0109	9.3259
659	14.1062	14.9335	0.0097	8.3023
660	14.1123	14.8479	0.0086	7.3741
661	14.1020	14.7679	0.0078	6.6691
Average:			0.0137	11.7116

** a_m is 853.6111 g/m^2*
*** temperature at the lowest remaining portion.*

The versatility of TGA data which can generate multiple readings in a small temperature range has made the data possible to be used for FW determination at any given temperature. Nonetheless, a large error could be obtained as the difference between fouled and clean membrane weight was relatively very small at a certain temperature. In such a case, the range of temperature selected was reasonably considered and the average of the range was computed to reduce any bias (Tay et al., 2003). The standard deviation and confidence level of the calculated values were also computed to determine the dispersion of the data values and tabulated as in Table 4.11.

From Table 4.11, it was found that the non-volatile FW of the native PVDF membrane was the highest with a value of 98.6930 g/m^2. With the addition of AgNP-1 and AgNPs-2 into the native membrane, the amount was significantly reduced by 74.56% and 88.13 % respectively. Obtaining those values proved that the fouling occurrence was mitigated by incorporating AgNPs into PVDF membranes. Nevertheless, since both AgNPs were incorporated with a different approach and possessed different characteristics, their performance as fouling mitigation agents was notably different. PVDF/PVP shows the

highest value of standard deviation due to the magnitude of FW being the highest, while the relative standard deviation of PVDF/PVP/AgNPs-2 is significantly high portraying the value of each data spread widely from the mean data.

Table 4.11 Summary of FW_{NV} and FR_{NV} values for all membranes and their descriptive statistics.

Membranes	***PVDF/PVP***	***PVDF/PVP/ AgNPs-1***	***PVDF/PVP/ AgNPs-2***
FW_{NV}, g/m²	98.6930	25.1075	11.7116
FR_{NV}, %	100	25.44	11.87
Standard Deviation, g/m²	4.8875	0.6813	3.5797
Relative Standard Deviation, %	4.95	2.71	30.57
Confidence Level (95.0%), g/m²	3.2835	0.4577	2.4048

It was mentioned that relative standard deviation can be deceptive in some cases when involving a small mean number (Coleman & Vanatta, 2012). This is compelling when considering that the smallest amount of non-volatile FW was found in PVDF/PVP/AgNPs-2. A possible issue that emerges from this finding is to reduce the value of relative standard deviation by selecting a narrower range of temperature for a smaller mean value with the same size set of samples. Thus the results of standard deviation should be further associated with a confidence level (Coleman & Vanatta, 2012). The high confidence level of 95% was computed to reduce the risk of falsely categorizing a good result as not being significant while determining the possible values of data lying within the range of confidence interval (Stone & Ellis, 2008).

4.4.1.2 Total FW and Volatile FW

As aforementioned, total FW was determined using Equation (3.14). The difference in surface density of fouled and clean membrane gives the value of FW_t. Consequently, the

value of volatile FW can be computed by subtracting the value of total FW from non-volatile FW. The values calculated were all tabulated as in Table 4.12.

Table 4.12 a_m, a_f, and other computed values for all membranes.

Membranes	PVDF/PVP	PVDF/PVP/AgNPs-1	PVDF/PVP/AgNPs-2
a_m (g/m^2)	791.8936	865.6363	853.6111
a_f (g/m^2)	1054.5020	911.2612	917.0050
FW_t (g/m^2)	262.6084	45.6249	63.3939
FR_t (%)	100	17.37	24.14
FW_V (g/m^2)	163.9154	20.5174	51.6823
FR_V (%)	100	12.52	31.53

As expected, the amount of foulant in the modified membranes was significantly low compared to PVDF/PVP membrane. This indicates that AgNPs incorporated had efficiently mitigated fouling occurrence. The total fouling rate was reduced by 82.69% and 75.86% while volatile FW was reduced by 87.48% and 68.47% for membrane PVDF/PVP/AgNPs-1 and PVDF/PVP/AgNPs-2 simultaneously. In a comparison of AgNPs-1 and AgNPs-2, it is clearly shown that AgNPs-1 has portrayed better anti-fouling properties. Further discussions on the findings of the TGA analysis are in the following subsections.

4.4.1.3 FW and Other Fouling Analysis

The correlation between FW and other fouling analysis approaches was depicted in Figure 4.33. FDR and FRR were selected to further assess the performance of AgNPs as fouling mitigation agents towards the enhancement of membrane filtration performance.

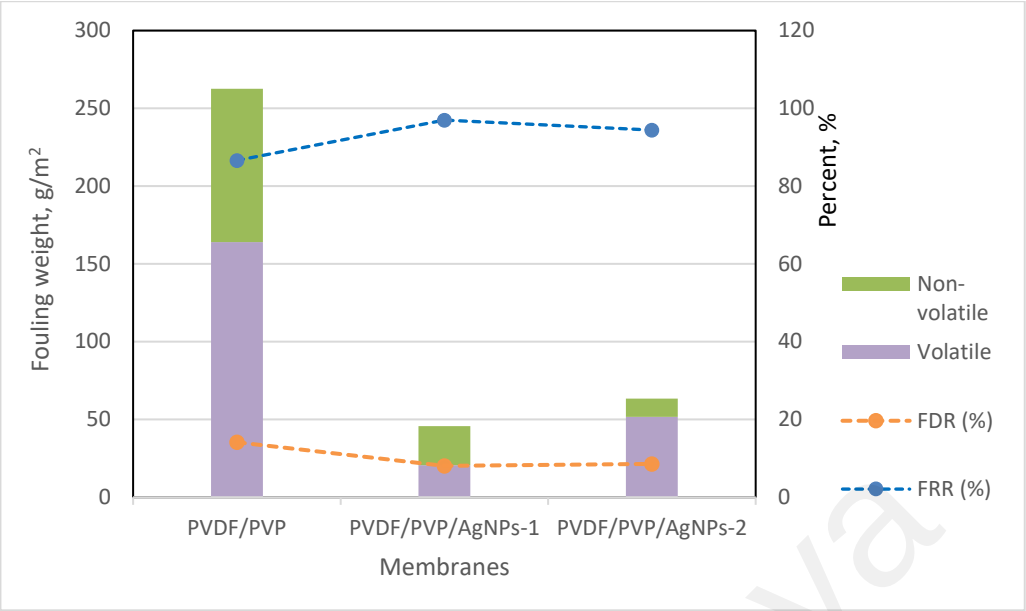

Figure 4.32 FW for all membranes in the fraction of volatile and non-volatile.

A very positive correlation was found between FW with FDR and FRR. From the figure, it is clearly shown that PVDF/PVP/AgNPs-1 membrane possessed the lowest foulant which reflects the lowest FDR recorded. The highest FRR obtained from PVDF/PVP/AgNPs-1 membrane reveals that the fouling phenomenon in PVDF/PVP/AgNPs-1 membrane was highly reversible compared to PVDF/PVP membrane and PVDF/PVP/AgNPs-2 membrane. Membrane fouling includes reversible and irreversible fouling which is important in determining the best cleaning practice for flux recovery (Mi & Elimelech, 2010; Y.-q. Wang et al., 2005). The results of total FW with FDR are in good agreement for all membranes. However, the fraction of volatile and non-volatile FW was significantly different for all membranes. Volatile FW contributed 62.42%, 44.97%, and 81.53% from total FW for PVDF/PVP, PVDF/PVP/AgNPs-1, and PVDF/PVP/AgNPs-2 respectively. This result is partially similar to the previously reported literature that the fouling evaluated is mainly composed of volatile solids up to 85% (Salazar-Peláez, Morgan-Sagastume, & Noyola, 2017). Contrary, FW of PVDF/PVP/AgNPs-1 membrane is mainly composed of non-volatile solids which are likely due to various components of solutes that are hardly controlled when using actual

lake water samples. Nonetheless, FW determination using TGA to evaluate fouling phenomena is plausible for all types and configurations of membranes as TGA requires a very small size sample regardless of its shape. Provided that the sample has different thermogravimetric properties from the foulants and does not chemically react with the foulants at any temperature (Tay et al., 2003).

4.4.2 Normal Raman Spectroscopy and SERS Analysis

As the membrane fabricated in this study contains two types of AgNPs, the possibility of these AgNPs acting as SERS substrates is evaluated to trace the presence of bacteria in the deposited foulant on the membrane surface. Therefore, this study reports the performance of AgNPs in membrane formulation as potential colloids for SERS application to examine biofouling from surface water treatment on a PVDF UF membrane. This provides alternative AgNPs functions and fouling analyses of the membrane which offer better insights into the credibility of AgNPs as biofouling mitigation agents. Figure 4.34 shows the normal Raman spectra and Figure 4.35 shows the SERS spectra.

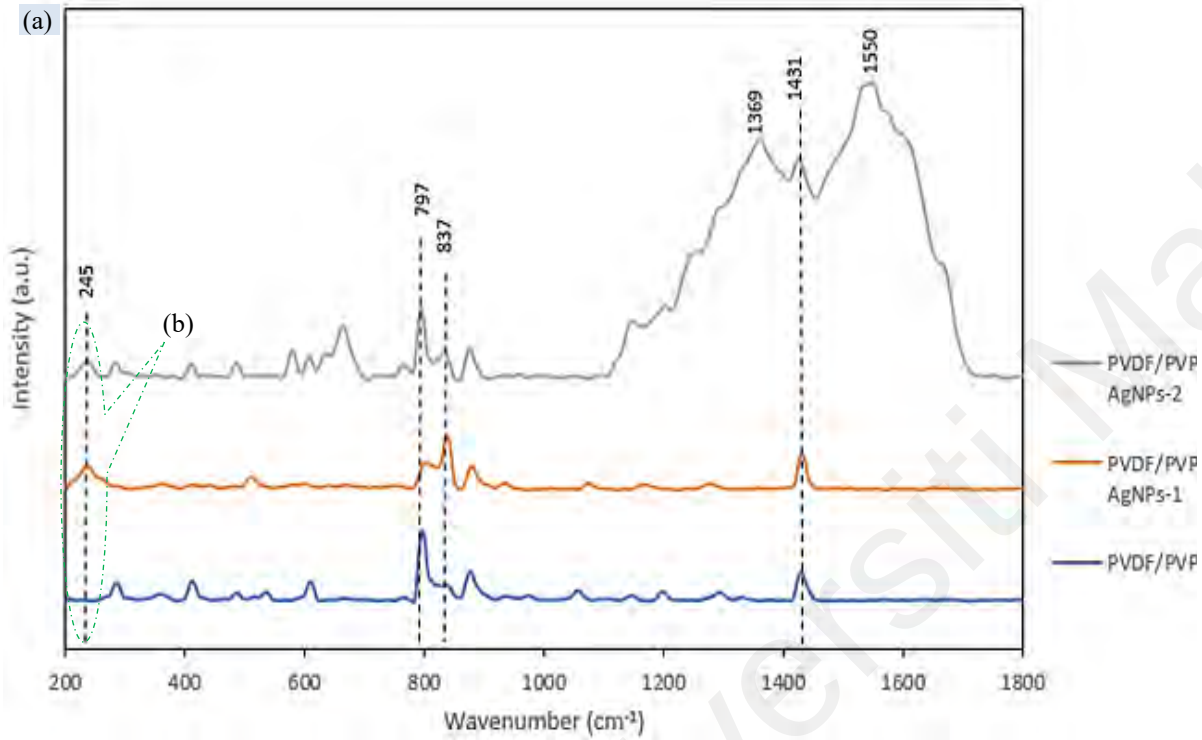

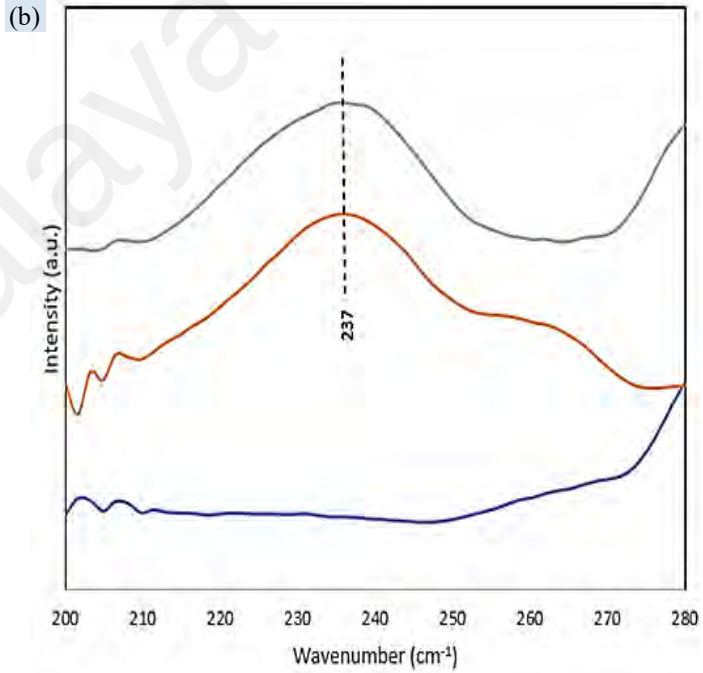

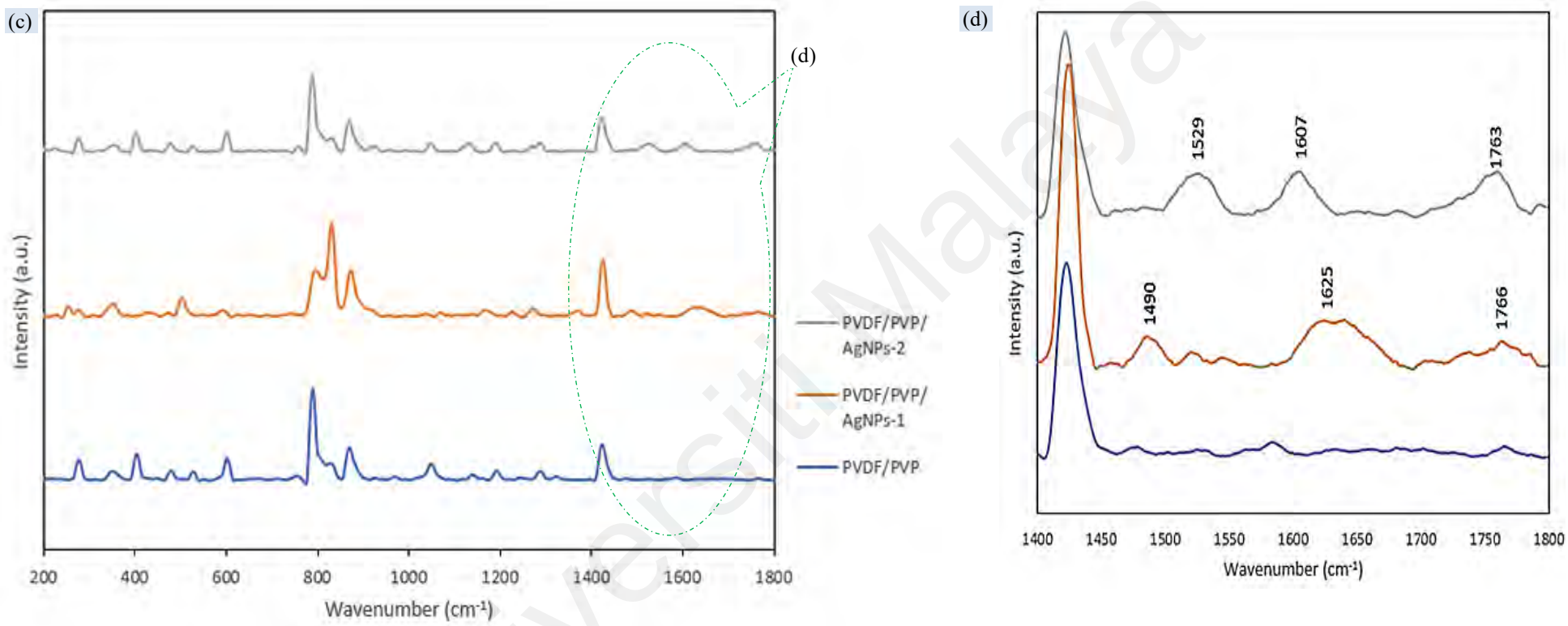

Figure 4.33 Normal Raman spectra of (a) clean membrane, (b) close-up spectra in the range of 200-280cm-1, (c) fouled membranes and (d) close-up spectra in the range of 1400-1800cm-1.

From Figure 4.34(a), normal Raman spectra of clean PVDF/PVP/AgNPs-1 and PVDF/PVP/AgNPs-2 membranes show the presence of an Ag-O band located at 245 cm^{-1}. However, the band is stronger in PVDF/PVP/AgNPs-1 membrane compared to PVDF/PVP/AgNPs-2 membrane as PVDF/PVP/AgNPs-2 membrane possesses two vibration modes at 1369 and 1550 cm^{-1}. This happens due to a higher amount of AgNPs that facilitates the breaking of the Ag-O bond and the degradation of PVP molecules adsorbed on AgNPs surfaces (Dhafer, Mezni, & Smiri, 2017). Initially, PVP was involved as a stabilizer during syntheses of both types of AgNPs. Even though the composition of AgNPs in membrane formulation is identical for PVDF/PVP/AgNPs-1 and PVDF/PVP/AgNPs-2 membranes, the leaching phenomenon during fabrication of the membrane, as reported in our previous study, alters the final amount of AgNPs in PVDF/PVP/AgNPs-1 and PVDF/PVP/AgNPs-2 membranes. The existence of the two vibration modes is in good agreement with the previous analysis which portrays the higher amount of AgNPs in the PVDF/PVP/AgNPs-2 membrane compared to the PVDF/PVP/AgNPs-1 membrane.

The aggregation of particles changes the particle size distribution and shifts the plasmon resonance conditions toward a longer wavelength (Moskovits, 1985). This is relatable to the TEM images in Figure 4.9 which explain the size and particle distribution of synthesized AgNPs upon incorporation into polymeric membrane matrix portrayed by the significant differences of spectrum for clean PVDF/PVP/AgNPs-1 and PVDF/PVP/AgNPs-2 membranes. Raman scattering of around 797 cm^{-1} in all membranes is attributed to CH2 rocking vibration (Nallasamy & Mohan, 2005) while 837 cm^{-1} shows the γ-phase of PVDF, which gives a high frequency for the liberation lattice mode due to the strong molecular force (Jabbarnia & Asmatulu, 2015; Kobayashi, Tashiro, & Tadokoro, 1975). The strong band at the area of 1431 cm^{-1} in all membranes is a mixture

of α-phase and γ-phase crystals (Boccaccio, Bottino, Capannelli, & Piaggio, 2002). These show that AgNPs-2 has the potential to be utilized as a surface-enhancing substrate.

However, Figure 4.34 (c) shows that the normal Raman spectra of all fouled membranes are almost identical with small spectra differences. Comparing PVDF/PVP membrane to PVDF/PVP/AgNPs-1 and PVDF/PVP/AgNPs-2 membranes, the only small bands that appear as surface-enhancing effects are 1490, 1625, and 1768 cm^{-1} for PVDF/PVP/AgNPs-1 membrane while 1529, 1607, and 1768 cm^{-1} are for PVDF/PVP/AgNPs-2 membrane as in Figure 4(d). These peaks are all connected to the vibration of amide, proteins, and DNA of *E. coli* (Sengupta, Laucks, & Davis, 2005) and *S. aureus* (X. Chen et al., 2019; Gonchukov et al., 2016). Normal Raman produces low signals from different biological samples due to its limited sensitivity hence needing a SERS substrate to enhance the signals and possible identification of different biological systems (Knauer, Ivleva, Liu, Niessner, & Haisch, 2010).

Previous research has reported that the optimization of SERS colloids is fabricated using a modified procedure of Leopold and Lendl (Leopold & Lendl, 2003) which can obtain high enhancement factors for microorganism detection (Knauer, Ivleva, Niessner, & Haisch, 2010). This suggests that the amount of AgNPs in the membrane is not adequate to yield notably enhanced spectra. Likewise, this indicates that the observed peaks mainly represent PVDF membrane structure and reveal some information concerning the foulant layer, which is present on the surface at low concentrations (Lamsal et al., 2012). Additionally, Sengupta et al. reported a low concentration of Ag suspension to produce low enhancement due to inadequate silver particles in contact with relevant groups on the bacterial surface (Sengupta et al., 2005). This reflects the fact that the amount of AgNPs-1 and AgNPs-2 in the membrane is relatively small and located

mostly at the bottom of the membrane matrix observed from XPS analysis which makes them minimally in contact with *E. coli* and *S. aureus* in the lake water.

Since only small significant peaks representing foulant presence were obtained from normal Raman, the membranes were further characterized using SERS to compare the additional possible peak to gather any information on the foulant layer. Figure 4.35 shows the SERS spectra of fouled PVDF/PVP, PVDF/PVP/AgNPs-1, and PVDF/PVP/AgNPs-2 membranes.

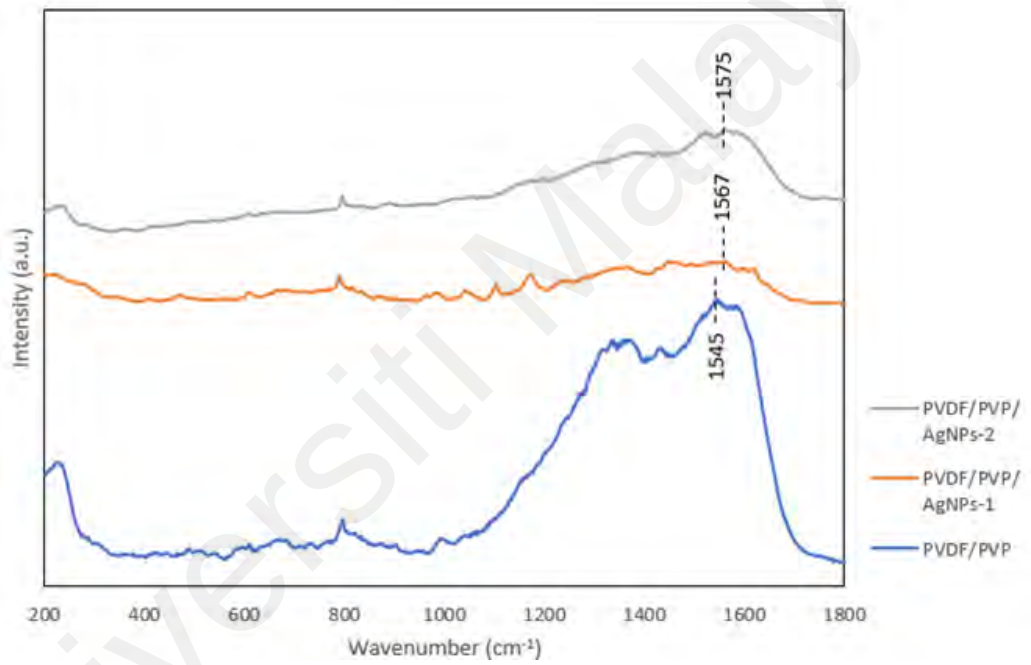

Figure 4.34 SERS spectra of all fouled membranes.

Based on Figure 4.35, new peaks are found at 1545, 1567, and 1575 cm^{-1} in PVDF/PVP, PVDF/PVP/AgNPs-1, and PVDF/PVP/AgNPs-2 membranes, respectively, possibly due to the foulant layer (Lamsal et al., 2012). This peak area may be associated with amide-II vibrations which is the characteristic of proteinaceous substances in NOM foulant layers (Campion & Kambhampati, 1998). Raman frequencies in the range of 1200–1600 cm^{-1} region may be due to the amide I–III vibrations associated with the protein backbones of DNA/RNA and carboxylic stretches which are likely to dominate

the SERS vibrational signatures in this region (Lin et al., 2014; Premasiri et al., 2005; H.-H. Wang et al., 2006). The lack of such information limits the information of the foulant layer.

Surprisingly, SERS spectra of fouled PVDF/PVP membrane are almost similar to Raman spectra of clean PVDF/PVP/AgNPs-2 membrane. This may deduce the fact that AgNPs-2 in PVDF/PVP/AgNPs-2 membrane is sufficient to provide surface enhancement but the very small peaks detected at fouled PVDF/PVP/AgNPs-2 membrane in Figure 4.34 (c) and (d) is due to the very minimal presence of foulant. On the contrary, Figure 4.34 (a) shows Raman spectra for a clean PVDF/PVP/AgNPs-1 membrane which is comparable to a clean PVDF/PVP membrane which signifies that the AgNPs-1 is insufficiently or excessively present as a surface-enhancing substance. This was reported by Liu et al. upon the addition of AgNPs for in-situ SERS activity, concluding that surface-enhancing effects were achieved at the optimal amount of AgNPs (R. Liu et al., 2019). An identical phenomenon was also recorded when the intensity of the Raman peaks increased and decreased with the increase of Ag content which was closely related to the number, size, and shape of Ag particles (Lian, Lv, Sun, Hui, & Wang, 2020). Moreover, The complexity of the actual lake water sample used as foulant may result in no to less specific enhancement toward the resultant spectra (Butler et al., 2016).

In addition, Figure 4.35 shows that the addition of Ag colloids for SERS on PVDF/PVP/AgNPs-1 and PVDF/PVP/AgNPs-2 membranes reduces the enhancement. This is possibly due to the amount of Ag colloid on top of existing AgNPs and the overall distribution of the substance which affects the performance and sensitivity detection (Ngo, Li, Simon, & Garnier, 2012). A notable challenge known in the SERS community is spectral reproducibility (Haynes, McFarland, & Van Duyne, 2005) which is attributed to several variables including the geometry of the SERS substrate concerning the analyte

(Jarvis, Brooker, & Goodacre, 2004). Thus, the present study raises the possibility that the incorporation of AgNPs in the membrane as a surface enhancer in Raman is more favorable compared to the conventional use of Ag colloids. This also upholds the additional function of AgNPs in polymeric membrane modification.

Although the incorporation of AgNPs can offer abundant hot spots for SERS detection (R. Liu et al., 2019), Chen et al. summarized that the dosage of SERS substrates may affect the permeability, pore size, and morphology of membranes compared to raw membranes because SERS substrates may cause fouling by themselves. This type of membrane modification may affect fouling mechanisms (W. Chen, Qian, Zhou, & Yu, 2018). Hence, it is suggested that the optimum amount of AgNPs-1 and AgNPs-2 should be considered to be added into the membrane along an ample amount of foulant layer.

CHAPTER 5: CONCLUSIONS AND RECOMMENDATIONS FOR FUTURE STUDIES

In this final chapter, conclusions and recommendations are outlined based on the research findings reported in the previous chapter. The aim of developing immobilized AgNPs in the PVDF membrane matrix as an antibacterial filtration membrane for surface water treatment was achieved along with the outlined objectives, which are believed to contribute to the membrane technology field significantly.

5.1 Conclusions

In this study, the smallest AgNPs were chosen for the membrane modification due to the larger surface area, which is crucial in determining the performance as an antibacterial agent. For AgNPs-1, the smallest AgNPs hydrodynamic diameter was in the range of 30.88–130.70 nm. For AgNPs-2, the range of hydrodynamic diameter was 109.5–179.4 nm. The method applied in forming AgNPs-1 is suitable to be used to synthesize smaller AgNPs, with the specific synthesis parameters studied. Meanwhile, the AgNPs-2 method can be applied to synthesize bigger but more uniform AgNPs. It is clearly indicated that the synthesized AgNPs exhibit immense potential as antibacterial elements, which offer an alternative and promising option to commercial AgNPs.

The membrane fabricated at higher temperatures demonstrated significantly improved embedment of both AgNPs-1 and AgNPs-2. The incorporation of AgNPs and the increase of casting temperature resulted in a significant increase in the water permeability of the membranes. When the PVDF membrane was cast at 55°C, AgNPs-2 offered a more feasible option for nanometal immobilization as only 3.81% AgNPs was lost throughout the fabrication process as compared to AgNPs-1, which leached 17.65% of its total Ag. However, AgNPs in both membranes were found to be completely immobilized during filtration. From the study, leaching phenomena was successfully controlled as the thermal

treatment approach was introduced during membrane fabrication and the incorporation of AgNPs-2 exhibits immense potential for PVDF membrane modification based on its immobilization, permeability, and bactericidal performance. The study has shown that the AgNPs incorporation method and casting temperature are vital in determining the final composition of AgNPs in the membrane before and during filtration.

AgNPs significantly improve membrane filtration performance based on FDR and FRR. As the lake water sample contains *E. coli* and *S. aureus* while all membranes recorded 100% removal of these bacteria, foulant on the membrane surface is plausible to be partially attributed to biofouling. Biofouling presence is indicated with normal Raman with enhanced spectra and fouling mitigation of AgNPs is indicated with FDR, FRR, and FW. This study suggests that the embedment of AgNPs can be a useful technique for surface enhancement in Raman in detecting bacteria presence in foulant from lake water considering the amount of AgNPs and foulant on the membrane. Herein, the systematic investigation of two different species of AgNPs in the PVDF membrane has shown that PVDF/PVP/AgNPs-1 membrane possesses better antifouling properties while PVDF/PVP/AgNPs-2 membrane possesses better surface enhancement of Raman intensity.

It is worth mentioning that the actual lake water used as solutes in this study contains a combination of various species of foulant, which eventually gives a more complex fouling mechanism and phenomenon compared to other reported studies. Conversely, this may provide a pivotal concept and idea of fouling mitigation approach with profound insights into the modification agent used. There is abundant room for improvement as the surface-enhancing substance, upon optimization of several parameters, generates a more significant peak in Raman spectra. Besides, the analysis made based on foulant

quantification can be expanded in various membrane technology applications especially when information needed is related to volatile and non-volatile foulants.

For future investigation, the application of this approach is plausible for different types of membranes and solutes. SERS requires a small size of flat sample making it possible for other types of membrane applications from microfiltration to reverse osmosis, while TGA analysis requires a small amount of sample regardless of the shape and size which can be extended for other membrane configuration characterization including tubular, hollow-fiber, and spiral wound. To best utilize AgNPs for fouling mitigation and fouling analysis, it is possible to optimally incorporate both AgNPs in a membrane formulation. Understanding the credibility of AgNPs may eventually lead to a more sustainable application of AgNPs in membrane technology.

5.2 Recommendations for Future Studies

Based on the analysis and findings obtained from the present study, several recommendations are suggested for future work as follows:

1. Further research may utilize other analyses for AgNPs and membrane characterization to establish the chemical interaction between these components so that the mechanism beyond the immobilization can be improvised.
2. Extensive work can be done using various solutes during filtration to determine the retention and separation characteristics of the fabricated membrane; thus, the applications of the membranes can be expanded.
3. A good progression of this work is to combine both species of AgNPs for PVDF membrane modification simultaneously to have a profound insight into the synergetic effects of this approach.

4. The issue of AgNPs utilization as a surface-enhanced substance in Raman analysis can be explored in future research related to optimization of the substrate and foulant amount.
5. Alternative analysis on fouling and biofouling using other analysis instruments such as X-Ray diffraction analysis (XRD) and Brunauer-Emmett-Teller (BET) analysis can be carried out to produce interesting findings that evaluate the credibility of the modification method applied.

REFERENCES

A. Abdul-Majeed, M. (2018). Preparation and Characterization of AgNp/PVDF Cmposite Ultrafiltration Membrane. *Journal of Engineering, 24*, 50. doi:10.31026/j.eng.2018.07.04

Abbas, W. S., Atwan, Z. W., Abdulhussein, Z. R., & Mahdi, M. (2019). Preparation of silver nanoparticles as antibacterial agents through DNA damage. *Materials Technology, 34*(14), 867-879.

Abedini, R. (2019). Enhanced antifouling properties of poly(ethersulfone) nano-composite membrane filled with nano-clay particles. *Polymer Bulletin, 76*(4), 1737-1753. doi:10.1007/s00289-018-2464-1

Abraham, K., & Sivan, A. (2021). Pre-and Post-Flood Water Quality of National Water Way 3, Near Industrial Effluent Discharge Zone, Kollam, Kerala. *Journal of Aquatic Biology & Fisheries, 9*, 60-67.

Adout, A., Kang, S., Asatekin, A., Mayes, A. M., & Elimelech, M. (2010). Ultrafiltration Membranes Incorporating Amphiphilic Comb Copolymer Additives Prevent Irreversible Adhesion of Bacteria. *Environmental science & technology, 44*(7), 2406-2411. doi:10.1021/es902908g

Agnihotri, S., Mukherji, S., & Mukherji, S. (2014). Size-controlled silver nanoparticles synthesized over the range 5–100 nm using the same protocol and their antibacterial efficacy. *RSC Advances, 4*(8), 3974-3983.

Ahmad, A., Rutten, S., de Waal, L., Vollaard, P., van Genuchten, C., Bruning, H., . . . van der Wal, A. (2020). Mechanisms of arsenate removal and membrane fouling in ferric based coprecipitation–low pressure membrane filtration systems. *Separation and Purification Technology, 241*, 116644. doi:https://doi.org/10.1016/j.seppur.2020.116644

Ahsani, M., Hazrati, H., Javadi, M., Ulbricht, M., & Yegani, R. (2020). Preparation of antibiofouling nanocomposite PVDF/Ag-SiO2 membrane and long-term performance evaluation in the MBR system fed by real pharmaceutical wastewater. *Separation and Purification Technology, 249*, 116938. doi:https://doi.org/10.1016/j.seppur.2020.116938

Alqaheem, Y., & Alomair, A. A. (2020). Microscopy and Spectroscopy Techniques for Characterization of Polymeric Membranes. *Membranes, 10*(2), 33.

Alresheedi, M. T., Kenari, S. L. D., Barbeau, B., & Basu, O. D. (2022). Flux modulation: A novel approach for ultrafiltration fouling control. *Journal of Water Process Engineering, 46*, 102551.

Alturki, A. A., Tadkaew, N., McDonald, J. A., Khan, S. J., Price, W. E., & Nghiem, L. D. (2010). Combining MBR and NF/RO membrane filtration for the removal of trace organics in indirect potable water reuse applications. *Journal of Membrane Science, 365*(1-2), 206-215.

Amigo, J., Urtubia, R., & Suárez, F. (2018). Exploring the interactions between hydrodynamics and fouling in membrane distillation systems – A multiscale approach using CFD. *Desalination, 444*, 63-74. doi:https://doi.org/10.1016/j.desal.2018.07.009

Anbu, P., Gopinath, S. C. B., Yun, H. S., & Lee, C.-G. (2019). Temperature-dependent green biosynthesis and characterization of silver nanoparticles using balloon flower plants and their antibacterial potential. *Journal of Molecular Structure, 1177*, 302-309. doi:https://doi.org/10.1016/j.molstruc.2018.09.075

Andrade, P. F., de Faria, A. F., Oliveira, S. R., Arruda, M. A. Z., & Gonçalves, M. d. C. (2015). Improved antibacterial activity of nanofiltration polysulfone membranes modified with silver nanoparticles. *Water Research, 81*, 333-342. doi:http://dx.doi.org/10.1016/j.watres.2015.05.006

Anilkumar, K. M., Jinisha, B., Manoj, M., & Jayalekshmi, S. (2017). Poly(ethylene oxide) (PEO) – Poly(vinyl pyrrolidone) (PVP) blend polymer based solid electrolyte membranes for developing solid state magnesium ion cells. *European Polymer Journal, 89*, 249-262. doi:https://doi.org/10.1016/j.eurpolymj.2017.02.004

Ariono, D., Aryanti, P., Subagjo, S., & Wenten, I. (2017). *The effect of polymer concentration on flux stability of polysulfone membrane.* Paper presented at the AIP Conference Proceedings.

Arkhangelsky, E., Duek, A., & Gitis, V. (2012). Maximal pore size in UF membranes. *Journal of Membrane Science, 394*, 89-97.

Arnal, J. M., Sancho, M., Verdú, G., Lora, J., Marín, J. F., & Cháfer, J. (2004). Selection of the most suitable ultrafiltration membrane for water disinfection in developing countries. *Desalination, 168*, 265-270. doi:http://dx.doi.org/10.1016/j.desal.2004.07.007

Asadi, A., Gholami, F., & Zinatizadeh, A. A. (2022). Enhanced oil removal from a real polymer production plant by cellulose nanocrystals-serine incorporated polyethersulfone ultrafiltration membrane. *Environmental Science and Pollution Research*. doi:10.1007/s11356-021-18055-4

Atadashi, I. M., Aroua, M. K., Abdul Aziz, A. R., & Sulaiman, N. M. N. (2012). High quality biodiesel obtained through membrane technology. *Journal of Membrane Science, 421-422*, 154-164. doi:https://doi.org/10.1016/j.memsci.2012.07.006

Awad, E. S., Sabirova, T. M., Tretyakova, N. A., Alsalhy, Q. F., Figoli, A., & Salih, I. K. (2021). A mini-review of enhancing ultrafiltration membranes (UF) for wastewater treatment: Performance and stability. *ChemEngineering, 5*(3), 34.

Ayyaru, S., Dinh, T. T. L., & Ahn, Y.-H. (2020). Enhanced antifouling performance of PVDF ultrafiltration membrane by blending zinc oxide with support of graphene oxide nanoparticle. *Chemosphere, 241*, 125068. doi:https://doi.org/10.1016/j.chemosphere.2019.125068

Bagur, H., Medidi, R. S., Somu, P., Choudhury, P. J., Karua, C. S., Guttula, P. K., . . . Poojari, C. C. (2020). Endophyte fungal isolate mediated biogenic synthesis and evaluation of biomedical applications of silver nanoparticles. *Materials Technology*, 1-12.

Bagur, H., Medidi, R. S., Somu, P., Choudhury, P. J., Karua, C. S., Guttula, P. K., . . . Poojari, C. C. (2022). Endophyte fungal isolate mediated biogenic synthesis and evaluation of biomedical applications of silver nanoparticles. *Materials Technology, 37*(3), 167-178.

Banerjee, D. Experimental Techniques in Thermal Analysis Thermogravimetry (TG) & Differential Scanning Calorimetry (DSC). *Instrumentation facilities.* Retrieved from https://www.iitk.ac.in/che/pdf/resources/TGA-DSC-reading-material.pdf

Bauer, J. E., Cai, W.-J., Raymond, P. A., Bianchi, T. S., Hopkinson, C. S., & Regnier, P. A. (2013). The changing carbon cycle of the coastal ocean. *Nature, 504*(7478), 61-70.

Bhattacharjee, C., & Bhattacharya, P. (1993). Flux decline analysis in ultrafiltration of kraft black liquor. *Journal of Membrane Science, 82*(1-2), 1-14.

Bi, Y., Han, B., Zimmerman, S., Perreault, F., Sinha, S., & Westerhoff, P. (2018). Four release tests exhibit variable silver stability from nanoparticle-modified reverse osmosis membranes. *Water Research, 143*, 77-86. doi:https://doi.org/10.1016/j.watres.2018.06.036

Boccaccio, T., Bottino, A., Capannelli, G., & Piaggio, P. (2002). Characterization of PVDF membranes by vibrational spectroscopy. *Journal of Membrane Science, 210*(2), 315-329.

Bousalem, N., Benmansour, K., & Ziani Cherif, H. (2017). Synthesis and characterization of antibacterial silver-alginate - chitosan bionanocomposite films using UV irradiation method. *Materials Technology, 32*(6), 367-377. doi:10.1080/10667857.2016.1241856

Bousbih, S., Belhadj Ammar, R., Ben Amar, R., Dammak, L., Darragi, F., & Selmane, E. (2021). Synthesis and Evaluation of Asymmetric Mesoporous PTFE/Clay Composite Membranes for Textile Wastewater Treatment. *Membranes, 11*(11). doi:10.3390/membranes11110850

Boussu, K., Van der Bruggen, B., Volodin, A., Van Haesendonck, C., Delcour, J., Van der Meeren, P., & Vandecasteele, C. (2006). Characterization of commercial nanofiltration membranes and comparison with self-made polyethersulfone membranes. *Desalination, 191*(1-3), 245-253.

Braghetta, A., DiGiano, F. A., & Ball, W. P. (1998). NOM accumulation at NF membrane surface: impact of chemistry and shear. *Journal of Environmental Engineering, 124*(11), 1087-1098.

Britannica, E. (2011). diagram illustrating the water table. Encyclopædia Britannica: Encyclopædia Britannica.

Butler, H. J., Ashton, L., Bird, B., Cinque, G., Curtis, K., Dorney, J., . . . Martin-Hirsch, P. L. (2016). Using Raman spectroscopy to characterize biological materials. *Nature protocols, 11*(4), 664-687.

Cai, X., Lei, T., Sun, D., & Lin, L. (2017). A critical analysis of the α, β and γ phases in poly(vinylidene fluoride) using FTIR. *RSC Advances, 7*(25), 15382-15389. doi:10.1039/C7RA01267E

Calvo, J. I., Bottino, A., Capannelli, G., & Hernández, A. (2008). Pore size distribution of ceramic UF membranes by liquid–liquid displacement porosimetry. *Journal of Membrane Science, 310*(1-2), 531-538.

Campion, A., & Kambhampati, P. (1998). Surface-enhanced Raman scattering. *Chemical Society Reviews, 27*(4), 241-250.

Cao, X., Tang, M., Liu, F., Nie, Y., & Zhao, C. (2010). Immobilization of silver nanoparticles onto sulfonated polyethersulfone membranes as antibacterial materials. *Colloids and Surfaces B: Biointerfaces, 81*(2), 555-562. doi:http://dx.doi.org/10.1016/j.colsurfb.2010.07.057

Cardinal, M. F., Vander Ende, E., Hackler, R. A., McAnally, M. O., Stair, P. C., Schatz, G. C., & Van Duyne, R. P. (2017). Expanding applications of SERS through versatile nanomaterials engineering. *Chemical Society Reviews, 46*(13), 3886-3903.

Carvajal, G., Branch, A., Sisson, S. A., Roser, D. J., van den Akker, B., Monis, P., . . . Khan, S. J. (2017). Virus removal by ultrafiltration: Understanding long-term performance change by application of Bayesian analysis. *Water Research, 122*, 269-279. doi:https://doi.org/10.1016/j.watres.2017.05.057

Chae, D., Hwang, S., Hong, S., Hong, S., Cho, B., & Kim, B. (2007). Influence of High Contents of Silver Nanoparticles on the Physical Properties of Poly(Vinylidene Fluoride). *Molecular Crystals and Liquid Crystals - MOL CRYST LIQUID CRYST, 464*. doi:10.1080/15421400601031140

Chang, H., Liang, H., Qu, F., Liu, B., Yu, H., Du, X., . . . Snyder, S. A. (2017). Hydraulic backwashing for low-pressure membranes in drinking water treatment: A review. *Journal of Membrane Science, 540*, 362-380.

Chaturongkasumrit, Y., Techaruvichit, P., Takahashi, H., Kimura, B., & Keeratipibul, S. (2013). Microbiological evaluation of water during the 2011 flood crisis in Thailand. *The Science of the total environment, 463-464*, 959-967. doi:10.1016/j.scitotenv.2013.06.071

Chen, M.-T., Zhang, W. K., Liang, W.-L., Li, Y.-S., Li, X.-J., Zhu, L.-H., & Tang, H.-B. (2019). Controllable and extra-fast synthesis of bio-applicable silver nanoparticles with Lycium Barbarum L. aqueous extract and visible light. *Materials Technology, 34*(10), 581-591.

Chen, N., Krom, M. D., Wu, Y., Yu, D., & Hong, H. (2018). Storm induced estuarine turbidity maxima and controls on nutrient fluxes across river-estuary-coast continuum. *Science of the Total Environment, 628*, 1108-1120.

Chen, W., Qian, C., Zhou, K.-G., & Yu, H.-Q. (2018). Molecular spectroscopic characterization of membrane fouling: a critical review. *Chem, 4*(7), 1492-1509.

Chen, X., Tang, M., Liu, Y., Huang, J., Liu, Z., Tian, H., . . . Fu, W. (2019). Surface-enhanced Raman scattering method for the identification of methicillin-resistant *Staphylococcus aureus* using positively charged silver nanoparticles. *Microchimica Acta, 186*(2), 102.

Chen, Y., Zhang, Y., Zhang, H., Liu, J., & Song, C. (2013). Biofouling control of halloysite nanotubes-decorated polyethersulfone ultrafiltration membrane modified with chitosan-silver nanoparticles. *Chemical Engineering Journal, 228*, 12-20. doi:https://doi.org/10.1016/j.cej.2013.05.015

Cheng, X. Q., Zhang, Y. L., Wang, Z. X., Guo, Z. H., Bai, Y. P., & Shao, L. (2014). Recent advances in polymeric solvent‐resistant nanofiltration membranes. *Advances in Polymer Technology, 33*(S1).

Chernousova, S., & Epple, M. (2013). Silver as antibacterial agent: ion, nanoparticle, and metal. *Angewandte Chemie International Edition, 52*(6), 1636-1653.

Cheryan, M. (1998). *Ultrafiltration and microfiltration handbook*: CRC press.

Coleman, D., & Vanatta, L. (2012). Part 48 - Relative Standard Deviations (RSDs). *Statistics in Analytical Chemistry.* Retrieved from https://www.americanlaboratory.com/913-Technical-Articles/114240-Part-48-Relative-Standard-Deviations-RSDs/

Cui, L., Yao, M., Ren, B., & Zhang, K.-S. (2011). Sensitive and versatile detection of the fouling process and fouling propensity of proteins on polyvinylidene fluoride membranes via surface-enhanced Raman spectroscopy. *Analytical chemistry, 83*(5), 1709-1716.

Cui, Z., Drioli, E., & Lee, Y. M. (2014). Recent progress in fluoropolymers for membranes. *Progress in Polymer Science, 39*(1), 164-198.

Dai, Y., & Zhu, X. (2018). Improved dielectric properties and energy density of PVDF composites using PVP engineered BaTiO3 nanoparticles. *Korean Journal of Chemical Engineering, 35*(7), 1570-1576. doi:10.1007/s11814-018-0047-3

Dai, Z., Noble, R. D., Gin, D. L., Zhang, X., & Deng, L. (2016). Combination of ionic liquids with membrane technology: A new approach for CO2 separation. *Journal of Membrane Science, 497*, 1-20.

Damodar, R. A., You, S.-J., & Chou, H.-H. (2009). Study the self cleaning, antibacterial and photocatalytic properties of TiO2 entrapped PVDF membranes. *Journal of Hazardous Materials, 172*(2), 1321-1328. doi:https://doi.org/10.1016/j.jhazmat.2009.07.139

Dashtban Kenari, S. L., & Barbeau, B. (2016). Understanding ultrafiltration fouling of ceramic and polymeric membranes caused by oxidized iron and manganese in water treatment. *Journal of Membrane Science, 516*, 1-12. doi:https://doi.org/10.1016/j.memsci.2016.06.003

De Jong, J., Lammertink, R. G., & Wessling, M. (2006). Membranes and microfluidics: a review. *Lab on a Chip, 6*(9), 1125-1139.

De Matteis, V., Malvindi, M. A., Galeone, A., Brunetti, V., De Luca, E., Kote, S., . . . Pompa, P. P. (2015). Negligible particle-specific toxicity mechanism of silver nanoparticles: The role of Ag+ ion release in the cytosol. *Nanomedicine: Nanotechnology, Biology and Medicine, 11*(3), 731-739. doi:http://dx.doi.org/10.1016/j.nano.2014.11.002

Dehaine, Q., Foucaud, Y., Kroll-Rabotin, J., & Filippov, L. (2019). Experimental investigation into the kinetics of Falcon UF concentration: Implications for fluid dynamic-based modelling. *Separation and Purification Technology, 215*, 590-601.

Dehghan, F., Mardanpour, H., Kamali, S., & Alirezaei, S. (2020). Synthesis and antibacterial properties of novel Al2O3-Ag anodised composite coating. *Materials Technology*, 1-10. doi:10.1080/10667857.2020.1794276

Dhafer, C. E. B., Mezni, A., & Smiri, L. (2017). Surface-enhanced Raman scattering study of Ag-PVP interactions in the biocompatible Ag@PVP nanoparticles. *Journal of the Tunisian Chemical Society, 19*, 152.

Di Zio, A., Prisciandaro, M., & Barba, D. (2005). Disinfection of surface waters with UF membranes. *Desalination, 179*(1), 297-305. doi:http://dx.doi.org/10.1016/j.desal.2004.11.075

Division, E. S. (2004). *NATIONAL STANDARD FOR DRINKING WATER QUALITY*. Ministry of Health Malaysia Retrieved from http://extwprlegs1.fao.org/docs/pdf/mal189903.pdf.

Dorea, C., Bertrand, S., & Clarke, B. (2006). Particle separation options for emergency water treatment. *Water Science and Technology, 53*(7), 253-260.

Du, J. R., Peldszus, S., Huck, P. M., & Feng, X. (2015). Modification of membrane surfaces via microswelling for fouling control in drinking water treatment. *Journal of Membrane Science, 475*, 488-495. doi:https://doi.org/10.1016/j.memsci.2014.10.040

El-Naggar, N. E.-A., Mohamedin, A., Hamza, S. S., & Sherief, A.-D. (2016). Extracellular Biofabrication, Characterization, and Antimicrobial Efficacy of Silver Nanoparticles Loaded on Cotton Fabrics Using Newly Isolated Streptomyces sp. SSHH-1E. *Journal of Nanomaterials, 2016*, 17. doi:10.1155/2016/3257359

ElHadidy, A. M., Peldszus, S., & Van Dyke, M. I. (2013). An evaluation of virus removal mechanisms by ultrafiltration membranes using MS2 and φX174 bacteriophage. *Separation and Purification Technology, 120*, 215-223. doi:https://doi.org/10.1016/j.seppur.2013.09.026

Etemadi, H., Afsharkia, S., Zinatloo‐Ajabshir, S., & Shokri, E. (2021). Effect of alumina nanoparticles on the antifouling properties of polycarbonate‐polyurethane blend

ultrafiltration membrane for water treatment. *Polymer Engineering & Science, 61*(9), 2364-2375.

Faibish, R. S., & Cohen, Y. (2001). Fouling and rejection behavior of ceramic and polymer-modified ceramic membranes for ultrafiltration of oil-in-water emulsions and microemulsions. *Colloids and Surfaces A: Physicochemical and Engineering Aspects, 191*(1), 27-40. doi:https://doi.org/10.1016/S0927-7757(01)00761-0

Fane, A. G., Wang, R., & Jia, Y. (2011). Membrane Technology: Past, Present and Future. In L. K. Wang, J. P. Chen, Y.-T. Hung, & N. K. Shammas (Eds.), *Membrane and Desalination Technologies* (pp. 1-45). Totowa, NJ: Humana Press.

Farahani, M. H. D. A., & Vatanpour, V. (2018). A comprehensive study on the performance and antifouling enhancement of the PVDF mixed matrix membranes by embedding different nanoparticulates: Clay, functionalized carbon nanotube, SiO2 and TiO2. *Separation and Purification Technology, 197*, 372-381. doi:https://doi.org/10.1016/j.seppur.2018.01.031

Farjami, M., Moghadassi, A., Vatanpour, V., Hosseini, S. M., & Parvizian, F. (2019). Preparation and characterization of a novel high-flux emulsion polyvinyl chloride (EPVC) ultrafiltration membrane incorporated with boehmite nanoparticles. *Journal of Industrial and Engineering Chemistry, 72*, 144-156. doi:https://doi.org/10.1016/j.jiec.2018.12.014

Feng, Q. L., Wu, J., Chen, G. Q., Cui, F., Kim, T., & Kim, J. (2000). A mechanistic study of the antibacterial effect of silver ions on *Escherichia coli* and *Staphylococcus aureus*. *Journal of Biomedical Materials Research, 52*(4), 662-668.

Fewtrell, L., & Kay, D. (2015). Recreational water and infection: a review of recent findings. *Current environmental health reports, 2*(1), 85-94.

Filip, D., Macocinschi, D., Stoleru, E., Munteanu, B., Dumitriu, R., Lungu, M., & Vasile, C. (2014). Polyurethane biocompatible silver bionanocomposites for biomedical applications DOI: 10.1007/s11051-014-2710-x. *Journal of Nanoparticle Research, 16*, 2710. doi:10.1007/s11051-014-2710-x

Fleitas-Salazar, N., Silva-Campa, E., Pedroso-Santana, S., Tanori, J., Pedroza-Montero, M. R., & Riera, R. (2017). Effect of temperature on the synthesis of silver nanoparticles with polyethylene glycol: new insights into the reduction mechanism. *Journal of Nanoparticle Research, 19*(3), 113. doi:10.1007/s11051-017-3780-3

Flemming, H.-C. (2002). Biofouling in water systems–cases, causes and countermeasures. *Applied microbiology and biotechnology, 59*(6), 629-640.

Foroutan Koudehi, M., Imani Fooladi, A. A., Aghozbeni, E. A. H., & Nourani, M. R. (2019). Nano bioglass/gelatin scaffold enhanced by nanosilver as an antibacterial conduit for peripheral nerve regeneration. *Materials Technology, 34*(13), 776-784.

Gao, M., Li, H., Ma, L., Gao, Y., Ma, L., & Luo, J. (2019). Molecular behaviors in thin film lubrication—Part two: Direct observation of the molecular orientation near the solid surface. *Friction, 7*(5), 479-488.

García, A., Rodríguez, B., Giraldo, H., Quintero, Y., Quezada, R., Hassan, N., & Estay, H. (2021). Copper-Modified Polymeric Membranes for Water Treatment: A Comprehensive Review. *Membranes, 11*(2), 93.

Geng, Z., Yang, X., Boo, C., Zhu, S., Lu, Y., Fan, W., . . . Yang, X. (2017). Self-cleaning anti-fouling hybrid ultrafiltration membranes via side chain grafting of poly(aryl ether sulfone) and titanium dioxide. *Journal of Membrane Science, 529*, 1-10. doi:https://doi.org/10.1016/j.memsci.2017.01.043

Ghasem, N., Al-Marzouqi, M., & Duaidar, A. (2011). Effect of quenching temperature on the performance of poly(vinylidene fluoride) microporous hollow fiber membranes fabricated via thermally induced phase separation technique on the removal of CO2 from CO2-gas mixture. *International Journal of Greenhouse Gas Control, 5*(6), 1550-1558. doi:https://doi.org/10.1016/j.ijggc.2011.08.012

Gibson, P. B., Waliser, D. E., Guan, B., DeFlorio, M. J., Ralph, F. M., & Swain, D. L. (2020). Ridging associated with drought across the western and southwestern United States: characteristics, trends, and predictability sources. *Journal of Climate, 33*(7), 2485-2508.

Goh, P. S., Wong, T. W., Lim, J. W., Ismail, A. F., & Hilal, N. (2020). Innovative and sustainable membrane technology for wastewater treatment and desalination application *Innovation strategies in environmental science* (pp. 291-319): Elsevier.

Gomes, J., Matos, A., Gmurek, M., Quinta-Ferreira, R. M., & Martins, R. C. (2019). Ozone and photocatalytic processes for pathogens removal from water: a review. *Catalysts, 9*(1), 46.

Gonchukov, S., Baikova, T., Alushin, M., Svistunova, T., Minaeva, S., Ionin, A., . . . Zayarny, D. (2016). *Single bacterium detection using SERS.* Paper presented at the Journal of Physics: Conference Series.

González, A., Noguez, C., Beránek, J., & Barnard, A. (2014). Size, shape, stability, and color of plasmonic silver nanoparticles. *The Journal of Physical Chemistry C, 118*(17), 9128-9136.

Gopal, V., Krishnakumar, S., Peter, T. S., Nethaji, S., Kumar, K. S., Jayaprakash, M., & Magesh, N. (2017). Assessment of trace element accumulation in surface sediments off Chennai coast after a major flood event. *Marine pollution bulletin, 114*(2), 1063-1071.

Govindan, K., Angelin, A., & Rangarajan, M. (2018). Critical evaluation of mechanism responsible for biomass abatement during electrochemical coagulation (EC) process: A critical review. *Journal of Environmental Management, 227*, 335-353.

Graf, P., Mantion, A., Foelske, A., Shkilnyy, A., Mašić, A., Thünemann, A. F., & Taubert, A. (2009). Peptide-Coated Silver Nanoparticles: Synthesis, Surface Chemistry,

and pH-Triggered, Reversible Assembly into Particle Assemblies. *Chemistry – A European Journal, 15*(23), 5831-5844. doi:10.1002/chem.200802329

Guillen, G. R., Farrell, T. P., Kaner, R. B., & Hoek, E. M. V. (2010). Pore-structure, hydrophilicity, and particle filtration characteristics of polyaniline–polysulfone ultrafiltration membranes. *Journal of Materials Chemistry, 20*(22), 4621-4628. doi:10.1039/B925269J

Gul, A., Hruza, J., & Yalcinkaya, F. (2021). Fouling and Chemical Cleaning of Microfiltration Membranes: A Mini-Review. *Polymers, 13*(6), 846.

Gungormus, E., & Altinkaya, S. A. (2021). Facile fabrication of Anti-biofouling polyaniline ultrafiltration membrane by green citric acid doping process. *Separation and Purification Technology, 279*, 119756.

Guo, H., He, L., & Xing, B. (2017). Applications of surface-enhanced Raman spectroscopy in the analysis of nanoparticles in the environment. *Environmental Science: Nano, 4*(11), 2093-2107.

Guo, Y., Bai, L., Tang, X., Huang, Q., Xie, B., Wang, T., . . . Liang, H. (2018). Coupling continuous sand filtration to ultrafiltration for drinking water treatment: Improved performance and membrane fouling control. *Journal of Membrane Science, 567*, 18-27. doi:https://doi.org/10.1016/j.memsci.2018.09.034

Guo, Y., Li, T.-y., Xiao, K., Wang, X.-m., & Xie, Y. F. (2020). Key foulants and their interactive effect in organic fouling of nanofiltration membranes. *Journal of Membrane Science, 610*, 118252. doi:https://doi.org/10.1016/j.memsci.2020.118252

Guo, Y., Liang, H., Bai, L., Huang, K., Xie, B., Xu, D., . . . Tang, X. (2020). Application of heat-activated peroxydisulfate pre-oxidation for degrading contaminants and mitigating ultrafiltration membrane fouling in the natural surface water treatment. *Water research, 179*, 115905. doi:https://doi.org/10.1016/j.watres.2020.115905

Guzman, M., Dille, J., & Godet, S. (2012). Synthesis and antibacterial activity of silver nanoparticles against gram-positive and gram-negative bacteria. *Nanomedicine: Nanotechnology, Biology and Medicine, 8*(1), 37-45. doi:http://dx.doi.org/10.1016/j.nano.2011.05.007

Habimana, O., Semião, A. J. C., & Casey, E. (2014). The role of cell-surface interactions in bacterial initial adhesion and consequent biofilm formation on nanofiltration/reverse osmosis membranes. *Journal of Membrane Science, 454*, 82-96. doi:https://doi.org/10.1016/j.memsci.2013.11.043

Haghighat, N., Vatanpour, V., Sheydaei, M., & Nikjavan, Z. (2020). Preparation of a novel polyvinyl chloride (PVC) ultrafiltration membrane modified with Ag/TiO2 nanoparticle with enhanced hydrophilicity and antibacterial activities. *Separation and Purification Technology, 237*, 116374. doi:https://doi.org/10.1016/j.seppur.2019.116374

Hamouda, T., & Baker Jr, J. (2000). Antimicrobial mechanism of action of surfactant lipid preparations in enteric Gram‐negative bacilli. *Journal of applied microbiology, 89*(3), 397-403.

Hasan, A., Waibhaw, G., Saxena, V., & Pandey, L. M. (2018). Nano-biocomposite scaffolds of chitosan, carboxymethyl cellulose and silver nanoparticle modified cellulose nanowhiskers for bone tissue engineering applications. *International Journal of Biological Macromolecules, 111*, 923-934. doi:https://doi.org/10.1016/j.ijbiomac.2018.01.089

Haynes, C. L., McFarland, A. D., & Van Duyne, R. P. (2005). Surface-Enhanced Raman Spectroscopy. *Analytical chemistry, 77*(17), 338 A-346 A. doi:10.1021/ac053456d

Hazan, R., Que, Y.-A., Maura, D., & Rahme, L. G. (2012). A method for high throughput determination of viable bacteria cell counts in 96-well plates. *BMC Microbiology, 12*(1), 259. doi:10.1186/1471-2180-12-259

He, G.-w., Li, F.-f., & Wen, J.-b. (2015). DMAc used as a reducer for preparation of spherical silver nanoparticles with high dispersion. *Journal of Central South University, 22*(2), 445-449. doi:10.1007/s11771-015-2541-7

Hector, D., Olivero, S., Orange, F., Duñach, E., & Gal, J.-F. (2019). Quality Control of a Functionalized Polymer Catalyst by Energy Dispersive X-ray Spectrometry (EDX or EDS). *Analytical Chemistry, 91*(3), 1773-1778. doi:10.1021/acs.analchem.8b04170

Hoeppe, P. (2016). Trends in weather related disasters – Consequences for insurers and society. *Weather and Climate Extremes, 11*, 70-79. doi:https://doi.org/10.1016/j.wace.2015.10.002

Hołda, A. K., & Vankelecom, I. F. J. (2015). Understanding and guiding the phase inversion process for synthesis of solvent resistant nanofiltration membranes. *Journal of Applied Polymer Science, 132*(27). doi:https://doi.org/10.1002/app.42130

Honary, S., Barabadi, H., Gharaei, E., & Naghibi, F. (2013). Green Synthesis of Silver Nanoparticles Induced by theFungus Penicillium citrinum. *Tropical Journal of Pharmaceutical Research, 12*, 7-11. doi:10.4314/tjpr.v12i1.2

Horibe, H., Sasaki, Y., Oshiro, H., Hosokawa, Y., Kono, A., Takahashi, S., & Nishiyama, T. (2014). Quantification of the solvent evaporation rate during the production of three PVDF crystalline structure types by solvent casting. *Polymer journal, 46*(2), 104-110. doi:10.1038/pj.2013.75

Hoslett, J., Massara, T. M., Malamis, S., Ahmad, D., van den Boogaert, I., Katsou, E., . . . Jouhara, H. (2018). Surface water filtration using granular media and membranes: A review. *Science of The Total Environment, 639*, 1268-1282. doi:https://doi.org/10.1016/j.scitotenv.2018.05.247

Huang, C. J., Yang, B. M., Chen, K. S., Chang, C. C., & Kao, C. M. (2011). Application of membrane technology on semiconductor wastewater reclamation: A pilot-scale

study. *Desalination, 278*(1), 203-210. doi:https://doi.org/10.1016/j.desal.2011.05.032

Huang, H., Cho, H.-H., Schwab, K. J., & Jacangelo, J. G. (2012). Effects of magnetic ion exchange pretreatment on low pressure membrane filtration of natural surface water. *Water research, 46*(17), 5483-5490. doi:https://doi.org/10.1016/j.watres.2012.07.003

Huang, L., & Morrissey, M. T. (1998). Fouling of membranes during microfiltration of surimi wash water: Roles of pore blocking and surface cake formation. *Journal of membrane science, 144*(1), 113-123. doi:https://doi.org/10.1016/S0376-7388(98)00038-6

Huang, L., Zhao, S., Wang, Z., Wu, J., Wang, J., & Wang, S. (2016). In situ immobilization of silver nanoparticles for improving permeability, antifouling and anti-bacterial properties of ultrafiltration membrane. *Journal of Membrane Science, 499*, 269-281. doi:https://doi.org/10.1016/j.memsci.2015.10.055

Huang, X., Wang, W., Liu, Y., Wang, H., Zhang, Z., Fan, W., & Li, L. (2015). Treatment of oily waste water by PVP grafted PVDF ultrafiltration membranes. *Chemical Engineering Journal, 273*, 421-429. doi:https://doi.org/10.1016/j.cej.2015.03.086

Hwang, K.-J., & Wu, Y.-J. (2008). Flux enhancement and cake formation in air-sparged crossflow microfiltration. *Chemical Engineering Journal, 139*(2), 296-303.

Hwang, L.-L., Chen, J.-C., & Wey, M.-Y. (2013). The properties and filtration efficiency of activated carbon polymer composite membranes for the removal of humic acid. *Desalination, 313*, 166-175. doi:https://doi.org/10.1016/j.desal.2012.12.019

Iannelli, R., Ripari, S., Casini, B., Buzzigoli, A., Privitera, G., Verani, M., & Carducci, A. (2014). Feasibility assessment of surface water disinfection by ultrafiltration. *Water Supply, 14*(4), 522-531. doi:10.2166/ws.2014.003

Idris, A., Zain, N. M., & Noordin, M. (2007). Synthesis, characterization and performance of asymmetric polyethersulfone (PES) ultrafiltration membranes with polyethylene glycol of different molecular weights as additives. *Desalination, 207*(1-3), 324-339.

Iravani, S., Korbekandi, H., Mirmohammadi, S. V., & Zolfaghari, B. (2014). Synthesis of silver nanoparticles: chemical, physical and biological methods. *Research in Pharmaceutical Sciences, 9*(6), 385-406.

Ismail, N. M., Ali, N. a., Kamarudin, D., & Yatim, N. I. (2020). Fouling Weight Quantification in Antibacterial Polymeric Membrane During Protein Washwater Ultrafiltration– Synergetic Effects of Silver Nanoparticles and Chitosan. *Biointerface Research in Applied Chemistry, 11*(3), 10. doi:10.33263/BRIAC113.1037110380

Issa, A. A., Al-Maadeed, M. A., Luyt, A. S., Ponnamma, D., & Hassan, M. K. (2017). Physico-mechanical, dielectric, and piezoelectric properties of PVDF electrospun mats containing silver nanoparticles. *C—Journal of Carbon Research, 3*(4), 30.

Jabbarnia, A., & Asmatulu, R. (2015). Synthesis and characterization of PVdF/PVP-based electrospun membranes as separators for supercapacitor applications. *J. Mater. Sci. Technol. Res, 2*, 43-51.

Jarusutthirak, C., Mattaraj, S., & Jiraratananon, R. (2007). Factors affecting nanofiltration performances in natural organic matter rejection and flux decline. *Separation and Purification Technology, 58*(1), 68-75.

Jarvis, R. M., Brooker, A., & Goodacre, R. (2004). Surface-enhanced Raman spectroscopy for bacterial discrimination utilizing a scanning electron microscope with a Raman spectroscopy interface. *Analytical chemistry, 76*(17), 5198-5202.

Jayalakshmi, A., Kim, I.-C., & Kwon, Y.-N. (2015). Cellulose acetate graft-(glycidylmethacrylate-g-PEG) for modification of AMC ultrafiltration membranes to mitigate organic fouling. *RSC Advances, 5*(60), 48290-48300. doi:10.1039/C5RA03499J

Ji, J., Liu, F., Hashim, N. A., Abed, M. R. M., & Li, K. (2015). Poly(vinylidene fluoride) (PVDF) membranes for fluid separation. *Reactive and Functional Polymers, 86*, 134-153. doi:https://doi.org/10.1016/j.reactfunctpolym.2014.09.023

Jim, K. J., Fane, A. G., Fell, C. J. D., & Joy, D. C. (1992).]Fouling mechanisms of membranes during protein ultrafiltration. *Journal of Membrane Science, 68*(1), 79-91. doi:http://dx.doi.org/10.1016/0376-7388(92)80151-9

Jose Ruben, M., Jose Luis, E., Alejandra, C., Katherine, H., Juan, B. K., Jose Tapia, R., & Miguel Jose, Y. (2005). The bactericidal effect of silver nanoparticles. *Nanotechnology, 16*(10), 2346.

Ju, H., McCloskey, B. D., Sagle, A. C., Wu, Y.-H., Kusuma, V. A., & Freeman, B. D. (2008). Crosslinked poly (ethylene oxide) fouling resistant coating materials for oil/water separation. *Journal of Membrane Science, 307*(2), 260-267.

Kamarudin, D., Ismail, M., & Othman, N. (2015). Fouling Evaluation for Ultrafiltration of Protein-based Washwater: A Resistance-in-series Model Approach. *Jurnal Teknologi, 74*(7).

Kamarudin, N. A., Kamarudin, M. K. A., Umar, R., Hassan, A., Lananan, F., & Sunardi, S. (2018). Determination of filtration and purification system for flood water filter. *International Journal of Engineering & Technology, 7*(2.15), 8-12.

Kanagaraj, P., Mohamed, I. M. A., Huang, W., & Liu, C. (2020). Membrane fouling mitigation for enhanced water flux and high separation of humic acid and copper ion using hydrophilic polyurethane modified cellulose acetate ultrafiltration membranes. *Reactive and Functional Polymers, 150*, 104538. doi:https://doi.org/10.1016/j.reactfunctpolym.2020.104538

Kanani, D. M., Sun, X., & Ghosh, R. (2008). Reversible and irreversible membrane fouling during in-line microfiltration of concentrated protein solutions. *Journal of Membrane Science, 315*(1), 1-10. doi:https://doi.org/10.1016/j.memsci.2008.01.053

Kancherla, R., Kumar, V. R., Prabhaker Reddy, G., & Sridhar, S. (2020). Nitrate removal studies on polyurea membrane using nanofiltration system – membrane characterization and model development. *Chemical Product and Process Modeling*. doi:doi:10.1515/cppm-2020-0041

Kang, G.-d., & Cao, Y.-m. (2014). Application and modification of poly(vinylidene fluoride) (PVDF) membranes – A review. *Journal of Membrane Science, 463*, 145-165. doi:https://doi.org/10.1016/j.memsci.2014.03.055

Kang, J. S., & Lee, Y. M. (2002). Effects of molecular weight of polyvinylpyrrolidone on precipitation kinetics during the formation of asymmetric polyacrylonitrile membrane. *Journal of Applied Polymer Science, 85*(1), 57-68. doi:doi:10.1002/app.10569

Kato, K., Uchida, E., Kang, E.-T., Uyama, Y., & Ikada, Y. (2003). Polymer surface with graft chains. *Progress in Polymer Science, 28*(2), 209-259.

Kawada, S., Saeki, D., & Matsuyama, H. (2014). Development of ultrafiltration membrane by stacking of silver nanoparticles stabilized with oppositely charged polyelectrolytes. *Colloids and Surfaces A: Physicochemical and Engineering Aspects, 451*, 33-37. doi:http://dx.doi.org/10.1016/j.colsurfa.2014.03.043

Kawata, K., Osawa, M., & Okabe, S. (2009). In vitro toxicity of silver nanoparticles at noncytotoxic doses to HepG2 human hepatoma cells. *Environmental science & technology, 43*(15), 6046-6051.

Khajouei, M., Najafi, M., & Jafari, S. A. (2019). Development of ultrafiltration membrane via in-situ grafting of nano-GO/PSF with anti-biofouling properties. *Chemical Engineering Research and Design, 142*, 34-43.

Khan, B., Haider, S., Khurram, R., Wang, Z., & Wang, X. (2020). Preparation of an Ultrafiltration (UF) Membrane with Narrow and Uniform Pore Size Distribution via Etching of SiO2 Nano-Particles in a Membrane Matrix. *Membranes, 10*(7), 150.

Kim, H. Y., Cho, Y., & Kang, S. W. (2019). Porous cellulose acetate membranes prepared by water pressure-assisted process for water-treatment. *Journal of Industrial and Engineering Chemistry, 78*, 421-424. doi:https://doi.org/10.1016/j.jiec.2019.05.027

Kim, J. F., Kim, J. H., Lee, Y. M., & Drioli, E. (2016). Thermally induced phase separation and electrospinning methods for emerging membrane applications: A review. *AIChE Journal, 62*(2), 461-490.

Kim, J. S., Kuk, E., Yu, K. N., Kim, J.-H., Park, S. J., Lee, H. J., . . . Cho, M.-H. (2007). Antimicrobial effects of silver nanoparticles. *Nanomedicine: Nanotechnology, Biology and Medicine, 3*(1), 95-101. doi:http://dx.doi.org/10.1016/j.nano.2006.12.001

Kim, S., Choi, J. E., Choi, J., Chung, K.-H., Park, K., Yi, J., & Ryu, D.-Y. (2009). Oxidative stress-dependent toxicity of silver nanoparticles in human hepatoma

cells. *Toxicology in Vitro, 23*(6), 1076-1084. doi:http://dx.doi.org/10.1016/j.tiv.2009.06.001

Kim, S. E., Li, H. M. D., & Nam, J. (2015). *Overview of Natural Disasters and their Impacts in Asia and the Pacific, 1970 - 2014* Retrieved from

Kim, Y., Rana, D., Matsuura, T., & Chung, W.-J. (2009). Influence of surface modifying macromolecules on the surface properties of poly (ether sulfone) ultra-filtration membranes. *Journal of Membrane Science, 338*(1-2), 84-91.

Kim, Y., Rana, D., Matsuura, T., & Chung, W.-J. (2012). Towards antibiofouling ultrafiltration membranes by blending silver containing surface modifying macromolecules. *Chemical Communications, 48*(5), 693-695.

Kimura, K., Nakamura, M., & Watanabe, Y. (2002). Nitrate removal by a combination of elemental sulfur-based denitrification and membrane filtration. *Water research, 36*(7), 1758-1766.

Knauer, M., Ivleva, N. P., Liu, X., Niessner, R., & Haisch, C. (2010). Surface-enhanced Raman scattering-based label-free microarray readout for the detection of microorganisms. *Analytical chemistry, 82*(7), 2766-2772.

Knauer, M., Ivleva, N. P., Niessner, R., & Haisch, C. (2010). Optimized surface-enhanced Raman scattering (SERS) colloids for the characterization of microorganisms. *Analytical Sciences, 26*(7), 761-766.

Kobayashi, M., Tashiro, K., & Tadokoro, H. (1975). Molecular vibrations of three crystal forms of poly (vinylidene fluoride). *Macromolecules, 8*(2), 158-171.

Koczkur, K. M., Mourdikoudis, S., Polavarapu, L., & Skrabalak, S. E. (2015). Polyvinylpyrrolidone (PVP) in nanoparticle synthesis. *Dalton Transactions, 44*(41), 17883-17905.

Koh, L., Ashokkumar, M., & Kentish, S. (2013). Membrane fouling, cleaning and disinfection. *Membrane Processing: Dairy and Beverage Applications*, 73-106.

Konował, E., Sybis, M., Modrzejewska-Sikorska, A., & Milczarek, G. (2017). Synthesis of dextrin-stabilized colloidal silver nanoparticles and their application as modifiers of cement mortar. *International Journal of Biological Macromolecules*.

Korin, E., Froumin, N., & Cohen, S. (2017). Surface Analysis of Nanocomplexes by X-ray Photoelectron Spectroscopy (XPS). *ACS Biomaterials Science & Engineering, 3*(6), 882-889. doi:10.1021/acsbiomaterials.7b00040

Koseki, Y., Aimi, K., & Ando, S. (2012). Supplement of encyclopedia nuclear magnetic resonance Supplement of encyclopedia nuclear magnetic resonance, 2002. *Polymer journal, 44*(8), 757-763.

Kotsilkova, R., Borovanska, I., Todorov, P., Ivanov, E., Menseidov, D., Chakraborty, S., & Bhattacharjee, C. (2018). Tensile and Surface Mechanical Properties of Polyethersulphone (PES) and Polyvinylidene Fluoride (PVDF) Membranes.

Journal of Theoretical and Applied Mechanics, 48, 85-99. doi:10.2478/jtam-2018-0018

Kumar, K. K., Ravi, M., Pavani, Y., Bhavani, S., Sharma, A. K., & Narasimha Rao, V. V. R. (2014). Investigations on PEO/PVP/NaBr complexed polymer blend electrolytes for electrochemical cell applications. *Journal of Membrane Science, 454*, 200-211. doi:https://doi.org/10.1016/j.memsci.2013.12.022

Kusworo, T. D., Ikhsan, D., Rokhati, N., Prasetyaningrum, A., Mutiara, F., & Sofiana, N. (2017). *Effect of combination dope composition and evaporation time on the separation performance of cellulose acetate membrane for demak brackish water treatment.* Paper presented at the MATEC Web of Conferences.

Lal, S., Grady, N. K., Kundu, J., Levin, C. S., Lassiter, J. B., & Halas, N. J. (2008). Tailoring plasmonic substrates for surface enhanced spectroscopies. *Chemical Society Reviews, 37*(5), 898-911.

Lamsal, R., Harroun, S. G., Brosseau, C. L., & Gagnon, G. A. (2012). Use of surface enhanced Raman spectroscopy for studying fouling on nanofiltration membrane. *Separation and Purification Technology, 96*, 7-11. doi:https://doi.org/10.1016/j.seppur.2012.05.019

Languer, M. P., Batistella, L., Alves, J. L. F., Da Silva, J. C. G., da Silva Filho, V. F., Di Domenico, M., . . . José, H. J. (2020). Insights into pyrolysis characteristics of Brazilian high-ash sewage sludges using thermogravimetric analysis and bench-scale experiments with GC-MS to evaluate their bioenergy potential. *Biomass and Bioenergy, 138*, 105614. doi:https://doi.org/10.1016/j.biombioe.2020.105614

Lau, S. K., & Yong, W. F. (2021). Recent Progress of Zwitterionic Materials as Antifouling Membranes for Ultrafiltration, Nanofiltration, and Reverse Osmosis. *ACS Applied Polymer Materials, 3*(9), 4390-4412.

Lee, S., Ihara, M., Yamashita, N., & Tanaka, H. (2017). Improvement of virus removal by pilot-scale coagulation-ultrafiltration process for wastewater reclamation: Effect of optimization of pH in secondary effluent. *Water Research, 114*, 23-30. doi:https://doi.org/10.1016/j.watres.2017.02.017

Lee, X. J., Show, P. L., Katsuda, T., Chen, W.-H., & Chang, J.-S. (2018). Surface grafting techniques on the improvement of membrane bioreactor: State-of-the-art advances. *Bioresource Technology, 269*, 489-502. doi:https://doi.org/10.1016/j.biortech.2018.08.090

Leopold, N., & Lendl, B. (2003). A new method for fast preparation of highly surface-enhanced Raman scattering (SERS) active silver colloids at room temperature by reduction of silver nitrate with hydroxylamine hydrochloride. *The Journal of Physical Chemistry B, 107*(24), 5723-5727.

Li, C., Sun, W., Lu, Z., Ao, X., & Li, S. (2020). Ceramic nanocomposite membranes and membrane fouling: A review. *Water research, 175*, 115674. doi:https://doi.org/10.1016/j.watres.2020.115674

Li, H., Ma, L., & Luo, J. (2021). A simple method to understand molecular conformation on surface-enhanced Raman scattering substrate. *Journal of Molecular Structure, 1223*, 128908. doi:https://doi.org/10.1016/j.molstruc.2020.128908

Li, J.-H., Shao, X.-S., Zhou, Q., Li, M.-Z., & Zhang, Q.-Q. (2013). The double effects of silver nanoparticles on the PVDF membrane: Surface hydrophilicity and antifouling performance. *Applied Surface Science, 265*, 663-670. doi:https://doi.org/10.1016/j.apsusc.2012.11.072

Li, J., Liu, X., Lu, J., Wang, Y., Li, G., & Zhao, F. (2016). Anti-bacterial properties of ultrafiltration membrane modified by graphene oxide with nano-silver particles. *Journal of Colloid and Interface Science, 484*, 107-115. doi:https://doi.org/10.1016/j.jcis.2016.08.063

Li, L., & Visvanathan, C. (2017). Membrane technology for surface water treatment: advancement from microfiltration to membrane bioreactor. *Reviews in Environmental Science and Bio/Technology, 16*(4), 737-760. doi:10.1007/s11157-017-9442-1

Li, Q., Mahendra, S., Lyon, D. Y., Brunet, L., Liga, M. V., Li, D., & Alvarez, P. J. J. (2008). Antimicrobial nanomaterials for water disinfection and microbial control: Potential applications and implications. *Water Research, 42*(18), 4591-4602. doi:https://doi.org/10.1016/j.watres.2008.08.015

Li, T., Liu, F., Lin, H., Xiong, Z., Wang, H., Zhong, Y., . . . Wu, A. (2018). Fabrication of anti-fouling, anti-bacterial and non-clotting PVDF membranes through one step "outside-in" interface segregation strategy. *Journal of colloid and interface science, 517*, 93-103.

Li, W.-R., Xie, X.-B., Shi, Q.-S., Zeng, H.-Y., You-Sheng, O.-Y., & Chen, Y.-B. (2010). Antibacterial activity and mechanism of silver nanoparticles on *Escherichia coli*. *Applied microbiology and biotechnology, 85*(4), 1115-1122.

Li, X., Pang, R., Li, J., Sun, X., Shen, J., Han, W., & Wang, L. (2013). In situ formation of Ag nanoparticles in PVDF ultrafiltration membrane to mitigate organic and bacterial fouling. *Desalination, 324*, 48-56. doi:https://doi.org/10.1016/j.desal.2013.05.021

Lian, X., Lv, Y., Sun, H., Hui, D., & Wang, G. (2020). Effects of Ag contents on the microstructure and SERS performance of self-grown Ag nanoparticles/Mo–Ag alloy films. *Nanotechnology Reviews, 9*(1), 751-759.

Liang, S., Qi, G., Xiao, K., Sun, J., Giannelis, E. P., Huang, X., & Elimelech, M. (2014). Organic fouling behavior of superhydrophilic polyvinylidene fluoride (PVDF) ultrafiltration membranes functionalized with surface-tailored nanoparticles: Implications for organic fouling in membrane bioreactors. *Journal of Membrane Science, 463*, 94-101. doi:https://doi.org/10.1016/j.memsci.2014.03.037

Liang, S., Xiao, K., Zhang, S., Ma, Z., Lu, P., Wang, H., & Huang, X. (2018). A facile approach to fabrication of superhydrophilic ultrafiltration membranes with surface-tailored nanoparticles. *Separation and Purification Technology, 203*, 251-259. doi:https://doi.org/10.1016/j.seppur.2018.04.051

Lim, A., & Bai, R. (2003). Membrane fouling and cleaning in microfiltration of activated sludge wastewater. *Journal of Membrane Science, 216*(1-2), 279-290.

Lin, C.-C., Yang, Y.-M., Liao, P.-H., Chen, D.-W., Lin, H.-P., & Chang, H.-C. (2014). A filter-like AuNPs@MS SERS substrate for *Staphylococcus aureus* detection. *Biosensors and Bioelectronics, 53*, 519-527. doi:https://doi.org/10.1016/j.bios.2013.10.017

Liu, J., Ma, Y., Gao, B., Meng, H., Yu, L., & Wang, L. (2016). Ammonium persulphate as novel additive for filtration performance improvement of PVDF microporous membrane. *Separation and Purification Technology, 165*, 78-85.

Liu, R., Tang, J., Yang, H., Jin, W., Liu, M., Liu, S., & Hu, J. (2019). In situ decoration of plasmonic silver nanoparticles on poly (vinylidene fluoride) membrane for versatile SERS detection. *New Journal of Chemistry, 43*(18), 6965-6972.

Liu, T.-Y., Zhang, R.-X., Li, Q., Van der Bruggen, B., & Wang, X.-L. (2014). Fabrication of a novel dual-layer (PES/PVDF) hollow fiber ultrafiltration membrane for wastewater treatment. *Journal of Membrane Science, 472*, 119-132.

Liu, T., Chen, D., Cao, Y., Yang, F., Chen, J., Kang, J., . . . Xiang, M. (2021). Construction of a composite microporous polyethylene membrane with enhanced fouling resistance for water treatment. *Journal of Membrane Science, 618*, 118679. doi:https://doi.org/10.1016/j.memsci.2020.118679

Liu, X.-h., Duan, J., Yang, J.-h., Huang, T., Zhang, N., Wang, Y., & Zhou, Z. (2015). Hydrophilicity, morphology and excellent adsorption ability of poly(vinylidene fluoride) membranes induced by graphene oxide and polyvinylpyrrolidone. *Colloids and Surfaces A: Physicochemical and Engineering Aspects, 486*, 172-184. doi:10.1016/j.colsurfa.2015.09.036

Liu, Y., Rosenfield, E., Hu, M., & Mi, B. (2013). Direct observation of bacterial deposition on and detachment from nanocomposite membranes embedded with silver nanoparticles. *Water Research, 47*(9), 2949-2958. doi:http://dx.doi.org/10.1016/j.watres.2013.03.005

Loo, S.-L., Fane, A. G., Krantz, W. B., & Lim, T.-T. (2012). Emergency water supply: a review of potential technologies and selection criteria. *Water Research, 46*(10), 3125-3151. doi:10.1016/j.watres.2012.03.030

López-Miranda, A., López-Valdivieso, A., & Viramontes-Gamboa, G. (2012). Silver nanoparticles synthesis in aqueous solutions using sulfite as reducing agent and sodium dodecyl sulfate as stabilizer. *Journal of Nanoparticle Research, 14*(9), 1101. doi:10.1007/s11051-012-1101-4

Ma, L., Cheng, C., He, C., Nie, C., Deng, J., Sun, S., & Zhao, C. (2015). Substrate-independent robust and heparin-mimetic hydrogel thin film coating via combined LbL self-assembly and mussel-inspired post-cross-linking. *ACS applied materials & interfaces, 7*(47), 26050-26062.

Macevele, L. E., Moganedi, K. L., & Magadzu, T. (2017). Investigation of antibacterial and fouling resistance of silver and multi-walled carbon nanotubes doped poly

(vinylidene fluoride-co-hexafluoropropylene) composite membrane. *Membranes, 7*(3), 35.

Madaeni, S. S. (1999). The application of membrane technology for water disinfection. *Water Research, 33*(2), 301-308. doi:http://dx.doi.org/10.1016/S0043-1354(98)00212-7

Magudapathy, P., Gangopadhyay, P., Panigrahi, B. K., Nair, K. G. M., & Dhara, S. (2001). Electrical transport studies of Ag nanoclusters embedded in glass matrix. *Physica B: Condensed Matter, 299*(1), 142-146. doi:https://doi.org/10.1016/S0921-4526(00)00580-9

Maheswari, P., Prasannadevi, D., & Mohan, D. (2013). Preparation and performance of silver nanoparticle incorporated polyetherethersulfone nanofiltration membranes. *High Performance Polymers, 25*(2), 174-187. doi:10.1177/0954008312459865

Mahmoudi, E., Ng, L. Y., Ang, W. L., Chung, Y. T., Rohani, R., & Mohammad, A. W. (2019). Enhancing Morphology and Separation Performance of Polyamide 6,6 Membranes By Minimal Incorporation of Silver Decorated Graphene Oxide Nanoparticles. *Scientific Reports, 9*(1), 1216. doi:10.1038/s41598-018-38060-x

Mahouche-Chergui, S., Guerrouache, M., Carbonnier, B., & Chehimi, M. M. (2013). Polymer-immobilized nanoparticles. *Colloids and Surfaces A: Physicochemical and Engineering Aspects, 439*, 43-68. doi:https://doi.org/10.1016/j.colsurfa.2013.04.013

Majeed, A., Ullah, W., Anwar, A. W., Shuaib, A., Ilyas, U., Khalid, P., . . . Ali, S. (2018). Cost-effective biosynthesis of silver nanoparticles using different organs of plants and their antimicrobial applications: A review. *Materials Technology, 33*(5), 313-320. doi:10.1080/10667857.2015.1108065

Malina, D., Sobczak-Kupiec, A., Wzorek, Z., & Kowalski, Z. (2012). Silver Nanoparticles Synthesis With Different Concentrations Of Polyvinylpyrrolidone. *Digest Journal of Nanomaterials & Biostructures (DJNB), 7*(4), 1527-1534.

Mamah, S. C., Goh, P. S., Ismail, A. F., Suzaimi, N. D., Yogarathinam, L. T., Raji, Y. O., & El-badawy, T. H. (2021). Recent development in modification of polysulfone membrane for water treatment application. *Journal of Water Process Engineering, 40*, 101835. doi:https://doi.org/10.1016/j.jwpe.2020.101835

Mamun, M., Atique, U., Kim, J. Y., & An, K.-G. (2021). Seasonal Water Quality and Algal Responses to Monsoon-Mediated Nutrient Enrichment, Flow Regime, Drought, and Flood in a Drinking Water Reservoir. *International Journal of Environmental Research and Public Health, 18*(20), 10714.

Manikprabhu, D., & Lingappa, K. (2013a). Microwave Assisted Rapid and Green Synthesis of Silver Nanoparticles Using a Pigment Produced by Streptomyces coelicolor klmp33. *Bioinorganic Chemistry and Applications, 2013*. doi:10.1155/2013/341798

Manikprabhu, D., & Lingappa, K. (2013b). *Microwave Assisted Rapid and Green Synthesis of Silver Nanoparticles Using a Pigment Produced by Streptomyces coelicolor klmp33* (Vol. 2013).

Mannan, H. A., Mukhtar, H., Murugesan, T., Nasir, R., Mohshim, D. F., & Mushtaq, A. (2013). Recent Applications of Polymer Blends in Gas Separation Membranes. *Chemical Engineering & Technology, 36*(11), 1838-1846. doi:https://doi.org/10.1002/ceat.201300342

Marchetti, P., Jimenez Solomon, M. F., Szekely, G., & Livingston, A. G. (2014). Molecular Separation with Organic Solvent Nanofiltration: A Critical Review. *Chemical Reviews, 114*(21), 10735-10806. doi:10.1021/cr500006j

Marroquin, M., Vu, A., Bruce, T., Powell, R., Wickramasinghe, S. R., & Husson, S. M. (2014). Location and quantification of biological foulants in a wet membrane structure by cross-sectional confocal laser scanning microscopy. *Journal of Membrane Science, 453*, 282-291. doi:https://doi.org/10.1016/j.memsci.2013.11.011

Masarudin, M. J., Cutts, S. M., Evison, B. J., Phillips, D. R., & Pigram, P. J. (2015). Factors determining the stability, size distribution, and cellular accumulation of small, monodisperse chitosan nanoparticles as candidate vectors for anticancer drug delivery: application to the passive encapsulation of [(14)C]-doxorubicin. *Nanotechnology, science and applications, 8*, 67-80. doi:10.2147/NSA.S91785

Matilainen, A., & Sillanpää, M. (2010). Removal of natural organic matter from drinking water by advanced oxidation processes. *Chemosphere, 80*(4), 351-365. doi:http://dx.doi.org/10.1016/j.chemosphere.2010.04.067

Matin, A., Laoui, T., Falath, W., & Farooque, M. (2021). Fouling control in reverse osmosis for water desalination & reuse: Current practices & emerging environment-friendly technologies. *Science of the Total Environment, 765*, 142721. doi:https://doi.org/10.1016/j.scitotenv.2020.142721

Matsumura, Y., Yoshikata, K., Kunisaki, S.-i., & Tsuchido, T. (2003). Mode of Bactericidal Action of Silver Zeolite and Its Comparison with That of Silver Nitrate. *Applied and Environmental Microbiology, 69*(7), 4278-4281. doi:10.1128/AEM.69.7.4278-4281.2003

Mavani, K., & Shah, M. (2013a). Synthesis of silver nanoparticles by using sodium borohydride as a reducing agent. *International Journal of Engineering Research & Technology, 2*(3).

Mavani, K., & Shah, M. (2013b). *Synthesis of Silver Nanoparticles by using Sodium Borohydride as a Reducing Agent*.

Maziya, K., Dlamini, B. C., & Malinga, S. P. (2020). Hyperbranched polymer nanofibrous membrane grafted with silver nanoparticles for dual antifouling and antibacterial properties against *Escherichia coli*, *Staphylococcus aureus* and *Pseudomonas aeruginosa*. *Reactive and Functional Polymers, 148*, 104494. doi:https://doi.org/10.1016/j.reactfunctpolym.2020.104494

Mdluli, P. S., Sosibo, N. M., Mashazi, P. N., Nyokong, T., Tshikhudo, R. T., Skepu, A., & van der Lingen, E. (2011). Selective adsorption of PVP on the surface of silver nanoparticles: A molecular dynamics study. *Journal of Molecular Structure, 1004*(1), 131-137. doi:https://doi.org/10.1016/j.molstruc.2011.07.049

Mecha, C., & Pillay, V. L. (2014). Development and evaluation of woven fabric microfiltration membranes impregnated with silver nanoparticles for potable water treatment. *Journal of Membrane Science, 458*, 149-156.

Mecha, C. A., & Pillay, V. L. (2014). Development and evaluation of woven fabric microfiltration membranes impregnated with silver nanoparticles for potable water treatment. *Journal of Membrane Science, 458*, 149-156. doi:https://doi.org/10.1016/j.memsci.2014.02.001

Meng, F.-N., Zhang, M.-Q., Ding, K., Zhang, T., & Gong, Y.-K. (2018). Cell membrane mimetic PVDF microfiltration membrane with enhanced antifouling and separation performance for oil/water mixtures. *Journal of Materials Chemistry A, 6*(7), 3231-3241.

Mer, V., & Dinegar, R. (1950). Theory, production and mechanism of formation of monodispersed hydrosols. *J Am Chem Soc, 72*, 4847-4854.

Méricq, J. P., Mendret, J., Brosillon, S., & Faur, C. (2015). High performance PVDF-TiO2 membranes for water treatment. *Chemical Engineering Science, 123*, 283-291. doi:https://doi.org/10.1016/j.ces.2014.10.047

Meshram, P., Dave, R., Joshi, H., Dharani, G., Kirubagaran, R., & Venugopalan, V. P. (2016). A fence that eats the weed: Alginate lyase immobilization on ultrafiltration membrane for fouling mitigation and flux recovery. *Chemosphere, 165*, 144-151. doi:https://doi.org/10.1016/j.chemosphere.2016.09.017

Mi, B., & Elimelech, M. (2010). Organic fouling of forward osmosis membranes: Fouling reversibility and cleaning without chemical reagents. *Journal of Membrane Science, 348*(1), 337-345. doi:https://doi.org/10.1016/j.memsci.2009.11.021

Minh Dat, N., Linh, V. N. P., Phuong, N. T. L., Quan, L. N., Huong, N. T., Huy, L. A., . . . Hieu, N. H. (2019). The effects of concentration, contact time, and pH value on antibacterial activity of silver nanoparticles decorated reduced graphene oxide. *Materials Technology, 34*(13), 792-799.

Modrzejewska-Sikorska, A., Konował, E., Cichy, A., Nowicki, M., Jesionowski, T., & Milczarek, G. (2017). The effect of silver salts and lignosulfonates in the synthesis of lignosulfonate-stabilized silver nanoparticles. *Journal of Molecular Liquids, 240*(Supplement C), 80-86. doi:https://doi.org/10.1016/j.molliq.2017.05.065

Mohammadi, T., Kohpeyma, A., & Sadrzadeh, M. (2005). Mathematical modeling of flux decline in ultrafiltration. *Desalination, 184*(1-3), 367-375.

Mohanty, M. P., Mudgil, S., & Karmakar, S. (2020). Flood management in India: A focussed review on the current status and future challenges. *International Journal of Disaster Risk Reduction, 49*, 101660. doi:https://doi.org/10.1016/j.ijdrr.2020.101660

Mondal, S., & Wickramasinghe, S. R. (2008). Produced water treatment by nanofiltration and reverse osmosis membranes. *Journal of Membrane Science, 322*(1), 162-170. doi:https://doi.org/10.1016/j.memsci.2008.05.039

Montaser, A., Wassel, A. R., & Al-Shaye'a, O. N. (2019). Synthesis, characterization and antimicrobial activity of Schiff bases from chitosan and salicylaldehyde/TiO2 nanocomposite membrane. *International journal of biological macromolecules, 124*, 802-809.

Moradi, Z., Akhbari, K., Phuruangrat, A., & Costantino, F. (2017). Studies on the relation between the size and dispersion of metallic silver nanoparticles and morphologies of initial silver(I) coordination polymer precursor. *Journal of Molecular Structure, 1133*, 172-178. doi:https://doi.org/10.1016/j.molstruc.2016.12.001

Moskovits, M. (1985). Surface-enhanced spectroscopy. *Reviews of modern physics, 57*(3), 783.

Mozaffarikhah, K., Kargari, A., Tabatabaei, M., Ghanavati, H., & Shirazi, M. M. A. (2017). Membrane treatment of biodiesel wash-water: A sustainable solution for water recycling in biodiesel production process. *Journal of Water Process Engineering, 19*, 331-337. doi:https://doi.org/10.1016/j.jwpe.2017.09.007

Murad, S., & Powles, J. G. (2019). Fluids in Contact with Semi-permeable Membranes *Computational Methods in Surface and Colloid Science* (pp. 775-797): CRC Press.

Murshed, M. F., Aslam, Z., Lewis, R., Chow, C., Wang, D., Drikas, M., & van Leeuwen, J. (2014). Changes in the quality of river water before, during and after a major flood event associated with a La Niña cycle and treatment for drinking purposes. *Journal of Environmental Sciences, 26*(10), 1985-1993. doi:http://dx.doi.org/10.1016/j.jes.2014.08.001

Nady, N., Salem, N., Amer, R., El-Shazly, A., Kandil, S. H., & Hassouna, M. S. E.-D. (2020). Comparison between a conventional anti-biofouling compound and a novel modified low-fouling polyethersulfone ultrafiltration membrane: Bacterial anti-attachment, water quality and productivity. *Membranes, 10*(9), 227.

Nallasamy, P., & Mohan, S. (2005). Vibrational spectroscopic characterization of form II poly (vinylidene fluoride).

Nasir, S., Mataram, A., & Pujiono, E. (2019). Physical and mechanical properties of membrane polyvinilidene flouride with the addition of silver nitrate. *Malaysian Journal of Fundamental and Applied Sciences, 15*(5), 675-678.

Nasrollahi, N., Vatanpour, V., Aber, S., & Mahmoodi, N. M. (2018). Preparation and characterization of a novel polyethersulfone (PES) ultrafiltration membrane modified with a CuO/ZnO nanocomposite to improve permeability and antifouling properties. *Separation and Purification Technology, 192*, 369-382. doi:https://doi.org/10.1016/j.seppur.2017.10.034

Nawfal Dagher, T., Al-Bayssari, C., Diene, S. M., Azar, E., & Rolain, J.-M. (2020). Bacterial infection during wars, conflicts and post-natural disasters in Asia and

the Middle East: a narrative review. *Expert Review of Anti-infective Therapy, 18*(6), 511-529. doi:10.1080/14787210.2020.1750952

Ng, T. S., Ching, Y. C., Awanis, N., Ishenny, N., & Rahman, M. R. (2014). Effect of bleaching condition on thermal properties and UV transmittance of PVA/cellulose biocomposites. *Materials Research Innovations, 18*(sup6), S6-400-S406-404. doi:10.1179/1432891714Z.000000000986

Ngo, Y. H., Li, D., Simon, G. P., & Garnier, G. (2012). Gold nanoparticle–paper as a three-dimensional surface enhanced Raman scattering substrate. *Langmuir, 28*(23), 8782-8790.

Nguyen, T.-T., Adha, R. S., Field, R. W., & Kim, I. S. (2021). Extended performance study of forward osmosis during wastewater reclamation: Quantification of fouling-based concentration polarization effects on the flux decline. *Journal of Membrane Science, 618*, 118755. doi:https://doi.org/10.1016/j.memsci.2020.118755

Nicolais, L., & Carotenuto, G. (2013). *Nanocomposites: In situ synthesis of polymer-embedded nanostructures*: John Wiley & Sons.

Nie, C., Yang, Y., Peng, Z., Cheng, C., Ma, L., & Zhao, C. (2017). Aramid nanofiber as an emerging nanofibrous modifier to enhance ultrafiltration and biological performances of polymeric membranes. *Journal of Membrane Science, 528*, 251-263. doi:https://doi.org/10.1016/j.memsci.2016.12.070

Norizan, N. Z. A., Hassan, N., & Yusoff, M. M. (2021). Strengthening flood resilient development in malaysia through integration of flood risk reduction measures in local plans. *Land Use Policy, 102*, 105178. doi:https://doi.org/10.1016/j.landusepol.2020.105178

Nthunya, L. N., Derese, S., Gutierrez, L., Verliefde, A. R., Mamba, B. B., Barnard, T. G., & Mhlanga, S. D. (2019). Green synthesis of silver nanoparticles using one-pot and microwave-assisted methods and their subsequent embedment on PVDF nanofibre membranes for growth inhibition of mesophilic and thermophilic bacteria. *New Journal of Chemistry, 43*(10), 4168-4180. doi:10.1039/C8NJ06160B

Ozbey-Unal, B., Omwene, P. I., Yagcioglu, M., Balcik-Canbolat, Ç., Karagunduz, A., Keskinler, B., & Dizge, N. (2020). Treatment of organized industrial zone wastewater by microfiltration/reverse osmosis membrane process for water recovery: From lab to pilot scale. *Journal of Water Process Engineering, 38*, 101646. doi:https://doi.org/10.1016/j.jwpe.2020.101646

Pacioni, N. L., Borsarelli, C. D., Rey, V., & Veglia, A. V. (2015). Synthetic routes for the preparation of silver nanoparticles *Silver nanoparticle applications* (pp. 13-46): Springer.

Padaki, M., Murali, R. S., Abdullah, M. S., Misdan, N., Moslehyani, A., Kassim, M., . . . Ismail, A. (2015). Membrane technology enhancement in oil–water separation. A review. *Desalination, 357*, 197-207.

Pagidi, A., Lukka Thuyavan, Y., Arthanareeswaran, G., Ismail, A. F., Jaafar, J., & Paul, D. (2015). Polymeric membrane modification using SPEEK and bentonite for ultrafiltration of dairy wastewater. *Journal of Applied Polymer Science, 132*(21). doi:https://doi.org/10.1002/app.41651

Pal, S., Tak, Y. K., & Song, J. M. (2007). Does the antibacterial activity of silver nanoparticles depend on the shape of the nanoparticle? A study of the gram-negative bacterium *Escherichia coli*. *Applied and environmental microbiology, 73*(6), 1712-1720.

Palencia, M., Rivas, B. L., & Pereira, E. (2009). Metal ion recovery by polymer-enhanced ultrafiltration using poly(vinyl sulfonic acid): Fouling description and membrane–metal ion interaction. *Journal of Membrane Science, 345*(1), 191-200. doi:https://doi.org/10.1016/j.memsci.2009.08.044

Palencia, M., Vera, M., & Rivas, B. L. (2014). Modification of ultrafiltration membranes via interpenetrating polymer networks for removal of boron from aqueous solution. *Journal of Membrane Science, 466*, 192-199. doi:https://doi.org/10.1016/j.memsci.2014.05.003

Pandey, P. K., Kass, P. H., Soupir, M. L., Biswas, S., & Singh, V. P. (2014). Contamination of water resources by pathogenic bacteria. *AMB Express, 4*, 51-51. doi:10.1186/s13568-014-0051-x

Panneerselvam, R., Xiao, L., Waites, K. B., Atkinson, T. P., & Dluhy, R. A. (2018). A rapid and simple chemical method for the preparation of Ag colloids for surface-enhanced Raman spectroscopy using the Ag mirror reaction. *Vibrational Spectroscopy, 98*, 1-7. doi:https://doi.org/10.1016/j.vibspec.2018.06.011

Peeva, P. D., Million, N., & Ulbricht, M. (2012). Factors affecting the sieving behavior of anti-fouling thin-layer cross-linked hydrogel polyethersulfone composite ultrafiltration membranes. *Journal of Membrane Science, 390*, 99-112.

Peiris, R. H., Budman, H., Moresoli, C., & Legge, R. L. (2013). Fouling control and optimization of a drinking water membrane filtration process with real-time model parameter adaptation using fluorescence and permeate flux measurements. *Journal of Process Control, 23*(1), 70-77. doi:https://doi.org/10.1016/j.jprocont.2012.10.001

Peng, Y., & Wu, P. (2004). A two dimensional infrared correlation spectroscopic study on the structure changes of PVDF during the melting process. *Polymer, 45*(15), 5295-5299.

Pentair.com. (2022). Type of membranes and characteristics. The Netherlands: PENTAIR.COM.

Peraza-Castro, M., Sauvage, S., Sánchez-Pérez, J., & Ruiz-Romera, E. (2016). Effect of flood events on transport of suspended sediments, organic matter and particulate metals in a forest watershed in the Basque Country (Northern Spain). *Science of the Total Environment, 569*, 784-797.

Peters, C. D., Rantissi, T., Gitis, V., & Hankins, N. P. (2021). Retention of natural organic matter by ultrafiltration and the mitigation of membrane fouling through pre-treatment, membrane enhancement, and cleaning - A review. *Journal of Water Process Engineering, 44*, 102374. doi:https://doi.org/10.1016/j.jwpe.2021.102374

Piatkovsky, M., Acar, H., Marciel, A. B., Tirrell, M., & Herzberg, M. (2018). A zwitterionic block-copolymer, based on glutamic acid and lysine, reduces the biofouling of UF and RO membranes. *Journal of Membrane Science, 549*, 507-514.

Pimpang, P., Sutham, W., Mangkorntong, N., Mangkorntong, P., & Choopun, S. (2008). Effect of stabilizer on preparation of silver and gold nanoparticle using grinding method. *Chiang Mai J. Sci, 35*, 250-257.

Piñero, S., Camero, S., & Blanco, S. (2017). Silver nanoparticles: Influence of the temperature synthesis on the particles' morphology. *Journal of Physics: Conference Series, 786*(1), 012020.

Pirsaheb, M., Hossein Davood Abadi Farahani, M., Zinadini, S., Zinatizadeh, A. A., Rahimi, M., & Vatanpour, V. (2019). Fabrication of high-performance antibiofouling ultrafiltration membranes with potential application in membrane bioreactors (MBRs) comprising polyethersulfone (PES) and polycitrate-Alumoxane (PC-A). *Separation and Purification Technology, 211*, 618-627. doi:https://doi.org/10.1016/j.seppur.2018.10.041

Polte, J. (2015). Fundamental growth principles of colloidal metal nanoparticles - a new perspective. *CrystEngComm, 17*(36), 6809-6830. doi:10.1039/C5CE01014D

Polte, J. r., Tuaev, X., Wuithschick, M., Fischer, A., Thuenemann, A. F., Rademann, K., . . . Emmerling, F. (2012). Formation mechanism of colloidal silver nanoparticles: analogies and differences to the growth of gold nanoparticles. *Acs Nano, 6*(7), 5791-5802.

Potter, C., Cotts, S., & Wiebke, F. (2017). Materials Characterization by Thermal Analysis (DSC & TGA), Rheology, and Dynamic Mechanical Analysis. *NY Workshops 2017.* Retrieved from http://www.tainstruments.com/wp-content/uploads/Materials_Characterization_Part1.pdf

Pradeep, T., & Anshup. (2009). Noble metal nanoparticles for water purification: A critical review. *Thin Solid Films, 517*(24), 6441-6478. doi:http://dx.doi.org/10.1016/j.tsf.2009.03.195

Premasiri, W. R., Moir, D. T., Klempner, M. S., Krieger, N., Jones, G., & Ziegler, L. D. (2005). Characterization of the Surface Enhanced Raman Scattering (SERS) of Bacteria. *The Journal of Physical Chemistry B, 109*(1), 312-320. doi:10.1021/jp040442n

Quintero-Quiroz, C., Acevedo, N., Zapata-Giraldo, J., Botero, L. E., Quintero, J., Zárate-Triviño, D., . . . Pérez, V. Z. (2019). Optimization of silver nanoparticle synthesis by chemical reduction and evaluation of its antimicrobial and toxic activity. *Biomaterials Research, 23*(1), 27. doi:10.1186/s40824-019-0173-y

Rahimi, Z., Zinatizadeh, A. A., & Zinadini, S. (2019). Membrane bioreactors troubleshooting through the preparation of a high antifouling PVDF ultrafiltration mixed-matrix membrane blended with O-carboxymethyl chitosan-Fe3O4 nanoparticles. *Environmental Technology, 40*(26), 3523-3533. doi:10.1080/09593330.2018.1480665

Rai, M., Yadav, A., & Gade, A. (2009). Silver nanoparticles as a new generation of antimicrobials. *Biotechnology Advances, 27*(1), 76-83. doi:http://dx.doi.org/10.1016/j.biotechadv.2008.09.002

Rai, P., Rai, C., Majumdar, G. C., DasGupta, S., & De, S. (2006). Resistance in series model for ultrafiltration of mosambi (Citrus sinensis (L.) Osbeck) juice in a stirred continuous mode. *Journal of Membrane Science, 283*(1), 116-122. doi:https://doi.org/10.1016/j.memsci.2006.06.018

Ramaswami, S., Behrendt, J., & Otterpohl, R. (2018). Comparison of NF-RO and RO-NF for the treatment of mature landfill leachates: a guide for landfill operators. *Membranes, 8*(2), 17.

Rana, D., Scheier, B., Narbaitz, R. M., Matsuura, T., Tabe, S., Jasim, S. Y., & Khulbe, K. C. (2012). Comparison of cellulose acetate (CA) membrane and novel CA membranes containing surface modifying macromolecules to remove pharmaceutical and personal care product micropollutants from drinking water. *Journal of Membrane Science, 409*, 346-354.

Ravindran, A., Chandran, P., & Khan, S. S. (2013). Biofunctionalized silver nanoparticles: Advances and prospects. *Colloids and Surfaces B: Biointerfaces, 105*, 342-352. doi:https://doi.org/10.1016/j.colsurfb.2012.07.036

Raza, M. A., Kanwal, Z., Rauf, A., Sabri, A. N., Riaz, S., & Naseem, S. (2016). Size- and Shape-Dependent Antibacterial Studies of Silver Nanoparticles Synthesized by Wet Chemical Routes. *Nanomaterials, 6*(4), 74. doi:10.3390/nano6040074

Razdan, U., Joshi, S., & Shah, V. (2003). Novel membrane processes for separation of organics. *Current Science*, 761-771.

Reddivari, M., Chirumamila, R. R., Marchant, R., & Nigam, P. (2001). A Response Surface Approach for the Comparison of Lipase Production by Candida cylindracea Using Two Different Carbon Sources. *Biochemical Engineering Journal, 9*, 17-23. doi:10.1016/S1369-703X(01)00117-6

Reddy, M. V., & Pathak, M. (2018). Sol-gel combustion synthesis of Ag doped CaSiO3: in vitro bioactivity, antibacterial activity and cytocompatibility studies for biomedical applications. *Materials Technology, 33*(1), 38-47.

Ren, J., Li, Z., & Wong, F.-S. (2006). A new method for the prediction of pore size distribution and MWCO of ultrafiltration membranes. *Journal of Membrane Science, 279*(1), 558-569. doi:https://doi.org/10.1016/j.memsci.2005.12.052

Rezaei, H., Ashtiani, F. Z., & Fouladitajar, A. (2011). Effects of operating parameters on fouling mechanism and membrane flux in crossflow microfiltration of whey. *Desalination, 274*(1), 262-271. doi:https://doi.org/10.1016/j.desal.2011.02.015

Rosman, N., Norharyati Wan Salleh, W., Aqilah Mohd Razali, N., Nurain Ahmad, S. Z., Hafiza Ismail, N., Aziz, F., . . . Yusof, N. (2021). Ibuprofen removal through photocatalytic filtration using antifouling PVDF- ZnO/Ag2CO3/Ag2O nanocomposite membrane. *Materials Today: Proceedings, 42*, 69-74. doi:https://doi.org/10.1016/j.matpr.2020.09.476

Rudolph, G., Hermansson, A., Jönsson, A.-S., & Lipnizki, F. (2021). In situ real-time investigations on adsorptive membrane fouling by thermomechanical pulping process water with quartz crystal microbalance with dissipation monitoring (QCM-D). *Separation and Purification Technology, 254*, 117578. doi:https://doi.org/10.1016/j.seppur.2020.117578

Safo, I., Werheid, M., Dosche, C., & Oezaslan, M. (2019). The role of polyvinylpyrrolidone (PVP) as a capping and structure-directing agent in the formation of Pt nanocubes. *Nanoscale Advances, 1*(8), 3095-3106.

Saini, B., Sinha, M. K., & Dash, S. K. (2019). Mitigation of HA, BSA and oil/water emulsion fouling of PVDF Ultrafiltration Membranes by SiO2-g-PEGMA nanoparticles. *Journal of Water Process Engineering, 30*, 100603. doi:https://doi.org/10.1016/j.jwpe.2018.03.018

Salazar-Peláez, M. L., Morgan-Sagastume, J. M., & Noyola, A. (2017). Fouling layer characterization and pore-blocking mechanisms in an UF membrane externally coupled to a UASB reactor. *Water Sa, 43*(4), 573-580.

Samree, K., Srithai, P.-u., Kotchaplai, P., Thuptimdang, P., Painmanakul, P., Hunsom, M., & Sairiam, S. (2020). Enhancing the Antibacterial Properties of PVDF Membrane by Hydrophilic Surface Modification Using Titanium Dioxide and Silver Nanoparticles. *Membranes, 10*(10), 289.

Samtlebe, M., Wagner, N., Neve, H., Heller, K. J., Hinrichs, J., & Atamer, Z. (2015). Application of a membrane technology to remove bacteriophages from whey. *International Dairy Journal, 48*, 38-45. doi:https://doi.org/10.1016/j.idairyj.2014.12.004

Sarkar, P., Bhui, D. K., Bar, H., Sahoo, G. P., De, S. P., & Misra, A. (2009). Synthesis and photophysical study of silver nanoparticles stabilized by unsaturated dicarboxylates. *Journal of Luminescence, 129*(7), 704-709.

Sawada, I., Fachrul, R., Ito, T., Ohmukai, Y., Maruyama, T., & Matsuyama, H. (2012). Development of a hydrophilic polymer membrane containing silver nanoparticles with both organic antifouling and antibacterial properties. *Journal of Membrane Science, 387*, 1-6. doi:http://dx.doi.org/10.1016/j.memsci.2011.06.020

Schroën, C. G. P. H., Roosjen, A., Tang, K., Norde, W., & Boom, R. M. (2010). In situ quantification of membrane foulant accumulation by reflectometry. *Journal of Membrane Science, 362*(1), 453-459. doi:https://doi.org/10.1016/j.memsci.2010.06.066

Sengupta, A., Laucks, M. L., & Davis, E. J. (2005). Surface-enhanced Raman spectroscopy of bacteria and pollen. *Applied spectroscopy, 59*(8), 1016-1023.

Sengur-Tasdemir, R., Urper-Bayram, G. M., Turken, T., Ates-Genceli, E., Tarabara, V. V., & Koyuncu, I. (2021). Hollow fiber nanofiltration membranes for surface water treatment: Performance evaluation at the pilot scale. *Journal of Water Process Engineering, 42*, 102100. doi:https://doi.org/10.1016/j.jwpe.2021.102100

Shanmuganathan, S., Loganathan, P., Kazner, C., Johir, M. A. H., & Vigneswaran, S. (2017). Submerged membrane filtration adsorption hybrid system for the removal of organic micropollutants from a water reclamation plant reverse osmosis concentrate. *Desalination, 401*, 134-141. doi:https://doi.org/10.1016/j.desal.2016.07.048

Shao, S., Li, Y., Jin, T., Liu, W., Shi, D., Wang, J., . . . Li, H. (2020). Biofouling layer maintains low hydraulic resistances and high ammonia removal in the UF process operated at low flux. *Journal of Membrane Science, 596*, 117612. doi:https://doi.org/10.1016/j.memsci.2019.117612

Shao, S., Wang, Y., Shi, D., Zhang, X., Tang, C. Y., Liu, Z., & Li, J. (2018). Biofouling in ultrafiltration process for drinking water treatment and its control by chlorinated-water and pure water backwashing. *Science of the Total Environment, 644*, 306-314.

Shard, A. G. (2014). Detection limits in XPS for more than 6000 binary systems using Al and Mg Kα X-rays. *Surface and Interface Analysis, 46*(3), 175-185. doi:https://doi.org/10.1002/sia.5406

Shen, L., Wang, H., Zhang, Y., Li, R., Fabien, B., Yu, G., . . . Liao, B.-Q. (2018). New strategy of grafting hydroxyethyl acrylate (HEA) via γ ray radiation to modify polyvinylidene fluoride (PVDF) membrane: Thermodynamic mechanisms of the improved antifouling performance. *Separation and Purification Technology, 207*, 83-91. doi:https://doi.org/10.1016/j.seppur.2018.06.044

Smith, V. H., & Schindler, D. W. (2009). Eutrophication science: where do we go from here? *Trends in ecology & evolution, 24*(4), 201-207.

Sondi, I., & Salopek-Sondi, B. (2004). Silver nanoparticles as antimicrobial agent: a case study on *E. coli* as a model for Gram-negative bacteria. *Journal of Colloid and Interface Science, 275*(1), 177-182. doi:http://dx.doi.org/10.1016/j.jcis.2004.02.012

Spadaro, J. A., Berger, T. J., Barranco, S. D., Chapin, S. E., & Becker, R. O. (1974). Antibacterial Effects of Silver Electrodes with Weak Direct Current. *Antimicrobial Agents and Chemotherapy, 6*(5), 637-642.

Sri Abirami Saraswathi, M. S., Rana, D., Divya, K., Gowrishankar, S., & Nagendran, A. (2020). Versatility of hydrophilic and antifouling PVDF ultrafiltration membranes tailored with polyhexanide coated copper oxide nanoparticles. *Polymer Testing, 84*, 106367. doi:https://doi.org/10.1016/j.polymertesting.2020.106367

Stone, D., & Ellis, J. (2008, 26/06/2008). Instrumental Analysis and Calibration. *Stats Tutorial.* Retrieved from

https://sites.chem.utoronto.ca/chemistry/coursenotes/analsci/stats/ConfLevel.html

Sundar, R. S., & Deevi, S. (2006). CO oxidation activity of Cu–CeO2 nano-composite catalysts prepared by laser vaporization and controlled condensation. *Journal of Nanoparticle Research, 8*(3), 497-509. doi:10.1007/s11051-005-9030-0

Surface Water Use in the United States. (2018). *WATER SCIENCE SCHOOL.* Retrieved from https://www.usgs.gov/special-topics/water-science-school/science/surface-water-use-united-states

Suttles, K. M., Eagle, A. J., & McLellan, E. L. (2021). Upstream Solutions to Downstream Problems: Investing in Rural Natural Infrastructure for Water Quality Improvement and Flood Risk Mitigation. *Water, 13*(24), 3579.

Szczygiełda, M., Krajewska, M., Zheng, L., Nghiem, L. D., & Prochaska, K. (2021). Implementation of forward osmosis to concentrate alpha-ketoglutaric acid from fermentation broth: Performance and fouling analysis. *Journal of Membrane Science, 637*, 119593. doi:https://doi.org/10.1016/j.memsci.2021.119593

Taghavizadeh Yazdi, M. E., Hamidi, A., Amiri, M. S., Kazemi Oskuee, R., Hosseini, H. A., Hashemzadeh, A., & Darroudi, M. (2019). Eco-friendly and plant-based synthesis of silver nanoparticles using Allium giganteum and investigation of its bactericidal, cytotoxicity, and photocatalytic effects. *Materials Technology, 34*(8), 490-497.

Tang, L., Huynh, K. A., Fleming, M. L., Larronde-Larretche, M., & Chen, K. L. (2015). Imparting antimicrobial and anti-adhesive properties to polysulfone membranes through modification with silver nanoparticles and polyelectrolyte multilayers. *Journal of Colloid and Interface Science, 451*, 125-133. doi:http://dx.doi.org/10.1016/j.jcis.2015.03.051

Tankhiwale, R., & Bajpai, S. K. (2009). Graft copolymerization onto cellulose-based filter paper and its further development as silver nanoparticles loaded antibacterial food-packaging material. *Colloids and Surfaces B: Biointerfaces, 69*(2), 164-168. doi:https://doi.org/10.1016/j.colsurfb.2008.11.004

Tay, J.-H., Liu, J., & Sun, D. D. (2003). Quantification of membrane fouling using thermogravimetric method. *Journal of Membrane Science, 217*(1), 17-28. doi:https://doi.org/10.1016/S0376-7388(02)00554-9

Teh, D., & Khan, T. (2021). Types, Definition and ClassificationClassificationsof Natural DisastersNatural disasters and Threat LevelThreat levels. In S. Eslamian & F. Eslamian (Eds.), *Handbook of Disaster Risk Reduction for Resilience: New Frameworks for Building Resilience to Disasters* (pp. 27-56). Cham: Springer International Publishing.

Ten Veldhuis, J., Clemens, F., Sterk, G., & Berends, B. (2010). Microbial risks associated with exposure to pathogens in contaminated urban flood water. *Water research, 44*(9), 2910-2918.

Teow, Y. H., Chiah, Y. H., Ho, K. C., & Mahmoudi, E. (2022). Treatment of semiconductor-industry wastewater with the application of ceramic membrane and polymeric membrane. *Journal of Cleaner Production, 337*, 130569. doi:https://doi.org/10.1016/j.jclepro.2022.130569

Thuyavan, Y. L., Anantharaman, N., Arthanareeswaran, G., Ismail, A. F., & Mangalaraja, R. V. (2015). Preparation and characterization of TiO2-sulfonated polymer embedded polyetherimide membranes for effective desalination application. *Desalination, 365*, 355-364. doi:https://doi.org/10.1016/j.desal.2015.03.004

Tiron, L. G., Pintilie, Ș. C., Vlad, M., Birsan, I. G., & Ș, B. (2017). Characterization of Polysulfone Membranes Prepared with Thermally Induced Phase Separation Technique. *IOP Conference Series: Materials Science and Engineering, 209*(1), 012013.

Toh, M. J., Oh, P. C., Chew, T. L., & Ahmad, A. L. (2020). Preparation of polydimethylsiloxane-SiO2/PVDF-HFP mixed matrix membrane of enhanced wetting resistance for membrane gas absorption. *Separation and Purification Technology, 244*, 116543. doi:https://doi.org/10.1016/j.seppur.2020.116543

Tolkach, A., & Kulozik, U. (2006). Transport of whey proteins through 0.1 μm ceramic membrane: phenomena, modelling and consequences for concentration or diafiltration processes. *Desalination (Amsterdam), 199*(1-3), 340-341.

Trigg, M. A., Michaelides, K., Neal, J. C., & Bates, P. D. (2013). Surface water connectivity dynamics of a large scale extreme flood. *Journal of Hydrology, 505*, 138-149. doi:https://doi.org/10.1016/j.jhydrol.2013.09.035

Tsai, H.-Y., Huang, A., soesanto, J. F., Luo, Y.-L., Hsu, T.-Y., Chen, C.-H., . . . Tung, K.-L. (2019). 3D printing design of turbulence promoters in a crossflow microfiltration system for fine particles removal. *Journal of Membrane Science, 573*, 647-656. doi:https://doi.org/10.1016/j.memsci.2018.11.081

Tsarkov, S., Khotimskiy, V., Budd, P. M., Volkov, V., Kukushkina, J., & Volkov, A. (2012). Solvent nanofiltration through high permeability glassy polymers: Effect of polymer and solute nature. *Journal of Membrane Science, 423-424*, 65-72. doi:https://doi.org/10.1016/j.memsci.2012.07.026

Urase, T., Yamamoto, K., & Ohgaki, S. (1994). Effect of pore size distribution of ultrafiltration membranes on virus rejection in crossflow conditions. *Water Science and Technology, 30*(9), 199.

Urase, T., Yamamoto, K., & Ohgaki, S. (1996). Effect of pore structure of membranes and module configuration on virus retention. *Journal of Membrane Science, 115*(1), 21-29.

Van der Bruggen, B., Vandecasteele, C., Van Gestel, T., Doyen, W., & Leysen, R. (2003). A review of pressure‐driven membrane processes in wastewater treatment and drinking water production. *Environmental progress, 22*(1), 46-56.

Vandezande, P., Gevers, L. E., & Vankelecom, I. F. (2008). Solvent resistant nanofiltration: separating on a molecular level. *Chemical Society Reviews, 37*(2), 365-405.

Vijayan, S. R., Santhiyagu, P., Singamuthu, M., Kumari Ahila, N., Jayaraman, R., & Ethiraj, K. (2014). Synthesis and characterization of silver and gold nanoparticles using aqueous extract of seaweed, Turbinaria conoides, and their antimicrofouling activity. *The Scientific World Journal, 2014*.

Villeneuve, W., Bérubé, A., Chamberland, J., Pouliot, Y., Labrie, S., & Doyen, A. (2021). Contribution of biofouling to permeation flux decline and membrane resistance changes during whey ultrafiltration. *International Dairy Journal, 117*, 105010. doi:https://doi.org/10.1016/j.idairyj.2021.105010

Vimbela, G. V., Ngo, S. M., Fraze, C., Yang, L., & Stout, D. A. (2017). Antibacterial properties and toxicity from metallic nanomaterials. *International Journal of Nanomedicine, 12*, 3941-3965. doi:10.2147/IJN.S134526

Vrouwenvelder, H. S., van Paassen, J. A. M., Folmer, H. C., Hofman, J. A. M. H., Nederlof, M. M., & van der Kooij, D. (1998). Biofouling of membranes for drinking water production. *Desalination, 118*(1), 157-166. doi:https://doi.org/10.1016/S0011-9164(98)00116-7

Vuppaladadiyam, A. K., Antunes, E., Sanchez, P. B., Duan, H., & Zhao, M. (2021). Influence of microalgae on synergism during co-pyrolysis with organic waste biomass: A thermogravimetric and kinetic analysis. *Renewable Energy, 167*, 42-55. doi:https://doi.org/10.1016/j.renene.2020.11.039

Waghmode, S., Chavan, P., Kalyankar, V., & Dagade, S. (2013). Synthesis of Silver Nanoparticles Using Triticum aestivum and Its Effect on Peroxide Catalytic Activity and Toxicology. *Journal of Chemistry, 2013*, 5. doi:10.1155/2013/265864

Wang, D.-M., & Lai, J.-Y. (2013). Recent advances in preparation and morphology control of polymeric membranes formed by nonsolvent induced phase separation. *Current Opinion in Chemical Engineering, 2*(2), 229-237. doi:https://doi.org/10.1016/j.coche.2013.04.003

Wang, F., Li, L., Yang, X., You, J., Xu, Y., Wang, H., . . . Gao, G. (2018). Influence of additives in a PVDF-based solid polymer electrolyte on conductivity and Li-ion battery performance. *Sustainable Energy & Fuels, 2*(2), 492-498.

Wang, H.-H., Liu, C.-Y., Wu, S.-B., Liu, N.-W., Peng, C.-Y., Chan, T.-H., . . . Wang, Y.-L. (2006). Highly Raman-Enhancing Substrates Based on Silver Nanoparticle Arrays with Tunable Sub-10 nm Gaps. *Advanced Materials, 18*(4), 491-495. doi:https://doi.org/10.1002/adma.200501875

Wang, K., Amin, K., An, Z., Cai, Z., Chen, H., Chen, H., . . . Gu, J. (2020). Advanced functional polymer materials. *Materials Chemistry Frontiers, 4*(7), 1803-1915.

Wang, N., Li, X., Yang, Y., Zhou, Z., Shang, Y., & Zhuang, X. (2020). Photocatalysis-coagulation to control ultrafiltration membrane fouling caused by natural organic

matter. *Journal of Cleaner Production, 265*, 121790. doi:https://doi.org/10.1016/j.jclepro.2020.121790

Wang, Q., Tang, X., Liang, H., Cheng, W., Li, G., Zhang, Q., . . . Wang, J. (2022). Effects of Filtration Mode on the Performance of Gravity-Driven Membrane (GDM) Filtration: Crossflow Filtration and Dead-End Filtration. *Water, 14*(2), 190.

Wang, Y.-q., Wang, T., Su, Y.-l., Peng, F.-b., Wu, H., & Jiang, Z.-y. (2005). Remarkable Reduction of Irreversible Fouling and Improvement of the Permeation Properties of Poly(ether sulfone) Ultrafiltration Membranes by Blending with Pluronic F127. *Langmuir, 21*(25), 11856-11862. doi:10.1021/la052052d

Wang, Y.-X., Ma, S., Huang, M.-N., Yang, H., Xu, Z.-L., & Xu, Z. (2019). Ag NPs coated PVDF@TiO2 nanofiber membrane prepared by epitaxial growth on TiO2 inter-layer for 4-NP reduction application. *Separation and Purification Technology, 227*, 115700. doi:https://doi.org/10.1016/j.seppur.2019.115700

Winter, J., Barbeau, B., & Bérubé, P. (2017). Nanofiltration and Tight Ultrafiltration Membranes for Natural Organic Matter Removal—Contribution of Fouling and Concentration Polarization to Filtration Resistance. *Membranes, 7*(3), 34.

Wu, J., Du, Y., Wang, C., & Chen, T. (2020). The Detection of a Fluorescent Dye by Surface-Enhanced Fluorescence with the Addition of Silver Nanoparticles and Its Application for the Space Station. *Journal of Nanoscience and Nanotechnology, 20*(5), 3195-3200. doi:10.1166/jnn.2020.17383

Wu, J., Wei, W., Li, S., Zhong, Q., Liu, F., Zheng, J., & Wang, J. (2018). The effect of membrane surface charges on demulsification and fouling resistance during emulsion separation. *Journal of Membrane Science, 563*, 126-133.

Wu, L., Liu, Y., Hu, J., Feng, X., Ma, C., & Wen, C. (2021). Preparation of polyvinylidene fluoride composite ultrafiltration membrane for micro-polluted surface water treatment. *Chemosphere, 284*, 131294. doi:https://doi.org/10.1016/j.chemosphere.2021.131294

Xiao, P., Xiao, F., Wang, D.-s., Qin, T., & He, S.-p. (2012). Investigation of organic foulants behavior on hollow-fiber UF membranes in a drinking water treatment plant. *Separation and Purification Technology, 95*, 109-117. doi:https://doi.org/10.1016/j.seppur.2012.04.028

Xiao, T., Wang, P., Yang, X., Cai, X., & Lu, J. (2015). Fabrication and characterization of novel asymmetric polyvinylidene fluoride (PVDF) membranes by the nonsolvent thermally induced phase separation (NTIPS) method for membrane distillation applications. *Journal of Membrane Science, 489*, 160-174. doi:https://doi.org/10.1016/j.memsci.2015.03.081

Xing, J., Wang, H., Cheng, X., Tang, X., Luo, X., Wang, J., . . . Liang, H. (2018). Application of low-dosage UV/chlorine pre-oxidation for mitigating ultrafiltration (UF) membrane fouling in natural surface water treatment. *Chemical Engineering Journal, 344*, 62-70. doi:https://doi.org/10.1016/j.cej.2018.03.052

Xu, H., Xiao, K., Wang, X., Liang, S., Wei, C., Wen, X., & Huang, X. (2020). Outlining the Roles of Membrane-Foulant and Foulant-Foulant Interactions in Organic Fouling During Microfiltration and Ultrafiltration: A Mini-Review. *Frontiers in Chemistry, 8*(417). doi:10.3389/fchem.2020.00417

Xu, Z., Wu, T., Shi, J., Teng, K., Wang, W., Ma, M., . . . Fan, J. (2016). Photocatalytic antifouling PVDF ultrafiltration membranes based on synergy of graphene oxide and TiO2 for water treatment. *Journal of Membrane Science, 520*, 281-293. doi:https://doi.org/10.1016/j.memsci.2016.07.060

Yang, H.-L., Lin, J. C.-T., & Huang, C. (2009). Application of nanosilver surface modification to RO membrane and spacer for mitigating biofouling in seawater desalination. *Water Research, 43*(15), 3777-3786. doi:http://dx.doi.org/10.1016/j.watres.2009.06.002

Yang, Q., Luo, J., Guo, S., Hang, X., Chen, X., & Wan, Y. (2019). Threshold flux in concentration mode: Fouling control during clarification of molasses by ultrafiltration. *Journal of Membrane Science, 586*, 130-139. doi:https://doi.org/10.1016/j.memsci.2019.05.063

Yang, T., Xiong, H., Liu, F., Yang, Q., Xu, B., & Zhan, C. (2019). Effect of UV/TiO2 pretreatment on fouling alleviation and mechanisms of fouling development in a crossflow filtration process using a ceramic UF membrane. *Chemical Engineering Journal, 358*, 1583-1593. doi:https://doi.org/10.1016/j.cej.2018.10.149

Yee, Y. Y., Ching, Y. C., Rozali, S., Awanis Hashim, N., & Singh, R. (2016). Preparation and Characterization of Poly(lactic Acid)-based Composite Reinforced with Oil Palm Empty Fruit Bunch Fiber and Nanosilica. *2016, 11*(1), 18.

Yin, H., & Yip, A. C. (2017). A review on the production and purification of biomass-derived hydrogen using emerging membrane technologies. *Catalysts, 7*(10), 297.

Yin, J., Yang, Y., Hu, Z., & Deng, B. (2013). Attachment of silver nanoparticles (AgNPs) onto thin-film composite (TFC) membranes through covalent bonding to reduce membrane biofouling. *Journal of Membrane Science, 441*, 73-82. doi:https://doi.org/10.1016/j.memsci.2013.03.060

Yu, L., Yang, Y., Zhang, J., & Yu, Y. (2020). Properties and performance of Ag(I) ion imprinted PVDF-PVA/GO composite membrane: Enhanced permeability, rejection and anti-microbial ability. *Water Cycle, 1*, 121-127. doi:https://doi.org/10.1016/j.watcyc.2020.09.002

Yu, W., Graham, N. J. D., & Fowler, G. D. (2016). Coagulation and oxidation for controlling ultrafiltration membrane fouling in drinking water treatment: Application of ozone at low dose in submerged membrane tank. *Water Research, 95*, 1-10. doi:https://doi.org/10.1016/j.watres.2016.02.063

Yu, Y., Yang, Y., Yu, L., Koh, K. Y., & Chen, J. P. (2021). Modification of polyvinylidene fluoride membrane by silver nanoparticles-graphene oxide hybrid nanosheet for effective membrane biofouling mitigation. *Chemosphere, 268*, 129187. doi:https://doi.org/10.1016/j.chemosphere.2020.129187

Zhang, B., Zhang, R., Huang, D., Shen, Y., Gao, X., & Shi, W. (2020). Membrane fouling in microfiltration of alkali/surfactant/polymer flooding oilfield wastewater: Effect of interactions of key foulants. *Journal of Colloid and Interface Science, 570*, 20-30. doi:https://doi.org/10.1016/j.jcis.2020.02.104

Zhang, D., Liu, X., Wang, X., Yang, X., & Lu, L. (2011). Optical properties of monodispersed silver nanoparticles produced via reverse micelle microemulsion. *Physica B: Condensed Matter, 406*(8), 1389-1394. doi:https://doi.org/10.1016/j.physb.2011.01.035

Zhang, D. Y., Hao, Q., Liu, J., Shi, Y. S., Zhu, J., Su, L., & Wang, Y. (2018). Antifouling polyimide membrane with grafted silver nanoparticles and zwitterion. *Separation and Purification Technology, 192*, 230-239. doi:https://doi.org/10.1016/j.seppur.2017.10.018

Zhang, D. Y., Liu, J., Shi, Y. S., Wang, Y., Liu, H. F., Hu, Q. L., . . . Zhu, J. (2016). Antifouling polyimide membrane with surface-bound silver particles. *Journal of Membrane Science, 516*, 83-93. doi:https://doi.org/10.1016/j.memsci.2016.06.012

Zhang, H., Lu, X., Liu, Z., Ma, Z., Wu, S., Li, Z., . . . Wu, C. (2018). The unidirectional regulatory role of coagulation bath temperature on cross-section radius of the PVDF hollow-fiber membrane. *Journal of Membrane Science, 550*, 9-17. doi:https://doi.org/10.1016/j.memsci.2017.12.059

Zhang, L., Shi, X., Zhao, M., Yin, Z., Zhang, J., Wang, S., . . . Tang, N. (2021). Construction of precisely controllable and stable interface bonding Au-TiO2/PVDF composited membrane for biofouling-resistant properties. *Surfaces and Interfaces, 24*, 101152. doi:https://doi.org/10.1016/j.surfin.2021.101152

Zhang, L., Yu, J. C., Yip, H. Y., Li, Q., Kwong, K. W., Xu, A.-W., & Wong, P. K. (2003). Ambient light reduction strategy to synthesize silver nanoparticles and silver-coated TiO2 with enhanced photocatalytic and bactericidal activities. *Langmuir, 19*(24), 10372-10380.

Zhang, M., Field, R. W., & Zhang, K. (2014). Biogenic silver nanocomposite polyethersulfone UF membranes with antifouling properties. *Journal of Membrane Science, 471*, 274-284. doi:http://dx.doi.org/10.1016/j.memsci.2014.08.021

Zhang, N., Yang, N., Zhang, L., Jiang, B., Sun, Y., Ma, J., . . . Peng, F. (2020). Facile hydrophilic modification of PVDF membrane with Ag/EGCG decorated micro/nanostructural surface for efficient oil-in-water emulsion separation. *Chemical Engineering Journal, 402*, 126200. doi:https://doi.org/10.1016/j.cej.2020.126200

Zhang, S., Acharya, D. P., Tang, X., Zheng, H., Yang, G., Ng, D., & Xie, Z. (2021). Dual Functions of a Au@AgNP-Incorporated Nanocomposite Desalination Membrane with an Enhanced Antifouling Property and Fouling Detection Via Surface-Enhanced Raman Spectroscopy. *ACS Applied Materials & Interfaces, 13*(38), 46202-46212. doi:10.1021/acsami.1c15948

Zhao, J., Han, H., Wang, Q., Yan, C., Li, D., Yang, J., . . . Chen, L. (2019). Hydrophilic and anti-fouling PVDF blend ultrafiltration membranes using polyacryloylmorpholine-based triblock copolymers as amphiphilic modifiers. *Reactive and Functional Polymers, 139*, 92-101. doi:https://doi.org/10.1016/j.reactfunctpolym.2019.03.018

Zhao, Y.-x., Li, P., Li, R.-h., & Li, X.-y. (2019). Direct filtration for the treatment of the coagulated domestic sewage using flat-sheet ceramic membranes. *Chemosphere, 223*, 383-390. doi:https://doi.org/10.1016/j.chemosphere.2019.02.055

Zheng, X., Ernst, M., & Jekel, M. (2009). Identification and quantification of major organic foulants in treated domestic wastewater affecting filterability in dead-end ultrafiltration. *Water Research, 43*(1), 238-244. doi:https://doi.org/10.1016/j.watres.2008.10.011

Zheng, Y., Yu, S., Shuai, S., Zhou, Q., Cheng, Q., Liu, M., & Gao, C. (2013). Color removal and COD reduction of biologically treated textile effluent through submerged filtration using hollow fiber nanofiltration membrane. *Desalination, 314*, 89-95. doi:https://doi.org/10.1016/j.desal.2013.01.004

Zhu, Y., Wei, J., Zhang, H., Liu, K., Kong, Z., Dong, Y., . . . Qin, Z. (2018). Fabrication of composite membrane with adsorption property and its application to the removal of endocrine disrupting compounds during filtration process. *Chemical Engineering Journal, 352*, 53-63. doi:https://doi.org/10.1016/j.cej.2018.06.182

Zhu, Z., & Mhemdi, H. (2016). Dead end ultra-filtration of sugar beet juice expressed from cold electrically pre-treated slices: Effect of membrane polymer on fouling mechanism and permeate quality. *Innovative Food Science & Emerging Technologies, 36*, 75-82. doi:https://doi.org/10.1016/j.ifset.2016.05.016

Zodrow, K., Brunet, L., Mahendra, S., Li, D., Zhang, A., Li, Q., & Alvarez, P. J. J. (2009). Polysulfone ultrafiltration membranes impregnated with silver nanoparticles show improved biofouling resistance and virus removal. *Water Research, 43*(3), 715-723. doi:https://doi.org/10.1016/j.watres.2008.11.014

Zularisam, A. W., Ismail, A. F., & Salim, R. (2006). Behaviours of natural organic matter in membrane filtration for surface water treatment — a review. *Desalination, 194*(1), 211-231. doi:http://dx.doi.org/10.1016/j.desal.2005.10.030

Zuo, J.-H., Wei, C., Cheng, P., Yan, X., Chen, Y., & Lang, W.-Z. (2020). Breakthrough the upperbond of permeability vs. tensile strength of TIPS-prepared PVDF membranes. *Journal of Membrane Science, 604*, 118089. doi:https://doi.org/10.1016/j.memsci.2020.118089